INTERNATIONAL MARS ICE MAPPER MISSION

RECONNAISSANCE / SCIENCE
MEASUREMENT DEFINITION TEAM

Final Report

SUBMITTED TO

ASI | CSA | JAXA | NASA | NSO

August 2022

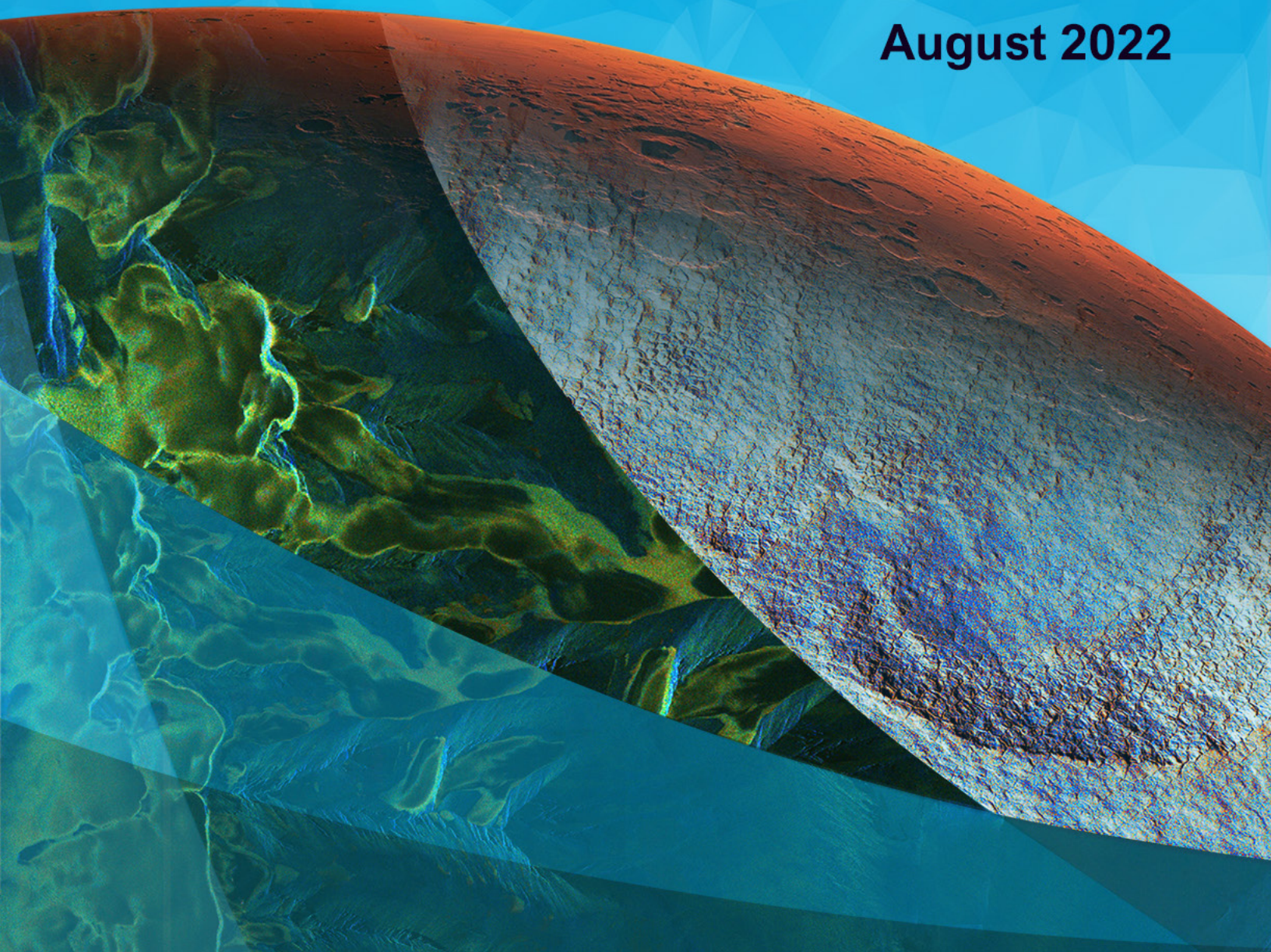

[This page intentionally left blank.]

I-MIM RECONNAISSANCE/SCIENCE MDT PARTICIPANTS

CO-CHAIRS

Michèle	LAVAGNA	Co-Chair	Politecnico di Milano
Jeffrey	PLAUT	Co-Chair	Jet Propulsion Laboratory / California Institute of Technology
Ali	BRAMSON	Assistant Co-Chair	Purdue University

MDT MEMBERS

Oded	AHARONSON	Planetary Science Institute
Robert	ANDERSON	Jet Propulsion Laboratory / California Institute of Technology
Chi	AO	Jet Propulsion Laboratory / California Institute of Technology
Shohei	AOKI	Institute of Space and Astronautical Science (JAXA)
Fabrizio	BERNARDINI	Sapienza University of Rome
Valentin	BICKEL	ETH Zürich
Frances	BUTCHER	University of Sheffield
Shane	BYRNE	Lunar and Planetary Laboratory, University of Arizona
Wendy	CALVIN	University of Nevada, Reno
Michael	DALY	York University
Marco	FERRARI	INAF - Institute for Space Astrophysics and Planetology
Alessandro	FRIGERI	Istituto di Astrofisica e Planetologia Spaziali (IAPS-INAF)
Indujaa	GANESH	University of Arizona
Antonio	GENOVA	Sapienza University of Rome
Matthew	GOLOMBEK	Jet Propulsion Laboratory / California Institute of Technology
John	GRANT	Smithsonian Institution, National Air and Space Museum, Center for Earth and Planetary Studies

Cyril	GRIMA	Institute for Geophysics, University of Texas at Austin
Svein-Erik	HAMRAN	University of Oslo
Patrick	HARKNESS	University of Glasgow
Elise	HARRINGTON	University of Oslo
Shannon	HIBBARD	Jet Propulsion Laboratory / California Institute of Technology
Stephen	HOFFMAN	Aerospace Corporation
Luciano	IESS	Sapienza University of Rome
Takeshi	IMAMURA	Graduate School of Frontier Sciences, University of Tokyo
Atsushi	KUMAMOTO	Tohoku University
Hiroyuki	KUROKAWA	Earth-Life Science Institute, Tokyo Institute of Technology
Daniel	LALICH	Cornell University
Joseph	LEVY	Colgate University
Robert	LILLIS	UC Berkeley Space Sciences Laboratory
Hiroyuki	MAEZAWA	Graduate School of Science, Osaka Prefecture University
Hideaki	MIYAMOTO	University of Tokyo
Michelle	MUNK	NASA - Space Technology Mission Directorate
Hiromu	NAKAGAWA	Tohoku University
Catherine	NEISH	The University of Western Ontario
Stefano	NEROZZI	Lunar and Planetary Laboratory, University of Arizona
Roberto	OROSEI	Istituto Nazionale di Astrofisica, Roma
Gerald (Wes)	PATTERSON	Johns Hopkins University Applied Physics Laboratory
David	PEARCE	Northumbria University at Newcastle
Nathaniel	PUTZIG	Planetary Science Institute
Hannah	SARGEANT	The Open University/University of Central Florida
Kanako	SEKI	University of Tokyo
Yasuhito	SEKINE	Earth-Life Science Institute (ELSI) / Tokyo Institute of Technology
Laurent	SIBILLE	Southeastern Universities Research Association (SURA) / NASA KSC
Isaac	SMITH	York University and Planetary Science Institute
Cassie	STUURMAN	Jet Propulsion Laboratory / California Institute of Technology
Leslie	TAMPPARI	Jet Propulsion Laboratory / California Institute of Technology
Nicolas	THOMAS	University of Bern, Switzerland
Lyle	WHYTE	McGill University

INDEPENDENT ASSESSMENT TEAM (IAT) MEMBERS

Jay	FALKER	Assistant Director for Strategy, NASA GSFC
Enrico	FLAMINI	Professor of Solar System Exploration, D'Annuzio University Pescara-Chieti & President of the International Research School for Planetary Sciences (IRSPS)
James W.	HEAD	Professor, Brown University
Goro	KOMATSU	Research Professor, International Research School of Planetary Sciences, Università d'Annunzio
Ralph	LORENZ	Principal Professional Staff, Johns Hopkins Applied Physics Laboratory
Michael	MISCHNA	Mars Principal Scientist, Mars Exploration Program Office, Jet Propulsion Laboratory / California Institute of Technology

AGENCY / I-MIM MISSION TEAM SUPPORT

Program Executive

NASA	Richard M. Davis

MDT Executive Committee

ASI	Raffaele Mugnuolo
CSA	Tim Haltigin
JAXA	Tomohiro Usui
NASA	Michael S. Kelley

Ex Officio

CSA	Martin Bergeron
NASA	Michael Meyer

Facilitation / Technical Support

CSA	Patrick Plourde, Co-Lead
NASA	Michelle A. Viotti, Co-Lead
ASI	Eleonora Ammannito, Marilena Amoroso
JAXA	Takanori Iwata, Satoru Ozawa
NASA	David Hollibaugh Baker, Rick Saylor

Logistics

NASA	Laura Ratliff, Bob Collom

Additional Acknowledgements / Contributions

ASI	Massimiliano Marcozzi (TASI)
CSA	Geneviève Houde, Lydia Philpott
NASA	Nathan Barba, Chad Edwards, Jim Garvin, Marc Sanchez Nez, Zaid Tofic
US	R. Keith Raney; Gareth Morgan, Matthew Siegler
NSO	Eduard van der Noorda, Rob van Hassel

TABLE OF CONTENTS

1 EXECUTIVE SUMMARY

The International Mars Ice Mapper (I-MIM) mission concept was developed by a multilateral team comprising space agencies from five countries: Canada, Italy, Japan, the Netherlands, and the United States. The primary goal of I-MIM is to map and characterize accessible, near-surface (within the uppermost 10 m) water ice and its overburden in mid-to-low latitudes to support planning for the first potential human surface missions to Mars.

Identifying adequate and accessible water-ice reserves enables the identification of candidate sites for potential scientific discoveries worthy of sending humans. It also enables the identification of water-ice resources to meet human operational needs on the Martian surface. The I-MIM partner Agencies also seek to maximize the mission's return on investment by supporting community-based scientific investigations, as a "supplemental value goal." To refine the mission concept and to define measurements with a set of prescribed tasks, the Agencies assembled a Reconnaissance/Science "Measurement Definition Team" (MDT). This report is the result of the work of the I-MIM MDT. The I-MIM Agency partners provided the MDT with the high-level mission goals, objectives, and the anchor payload: an L-band, polarimetric Synthetic Aperture Radar (SAR) and Sounder.

The Charter directed the MDT to perform three tasks:

TASK 1. Define measurements for the anchor payload that are traceable to requirements-driving Reconnaissance Objectives (ice detection, overburden characterization, and candidate human-site characterization) and ways to optimize the payload(s) for these purposes;

TASK 2. Provide findings on potential high-value, prioritized reconnaissance, science, and engineering augmentations that are synergistic with the anchor payload and might maximize the mission's return on investment within established mission boundary conditions; and,

TASK 3. Prepare a model concept of operations based on findings for Tasks 1 and 2.

OVERALL MDT SUMMARY FINDINGS

- An I-MIM mission will provide a new way to observe Mars, and will acquire essential information to enable human exploration.
- The mission's capabilities provide an opportunity to accomplish unique new science covering a broad range of international science priorities in addition to the primary goal of reconnaissance for human missions.
- Additional instruments could expand the capabilities of I-MIM to undertake high-priority science investigations and fill any gaps in meeting reconnaissance objectives.
- The primary reconnaissance goal can be accomplished in a nominal mission lasting one Mars year. The reconnaissance and science objectives would greatly benefit from an enhancement of data downlink capabilities.
- The Agency partners should continue to pursue development of the I-MIM mission as a key element in the future exploration of Mars.

TASK 1: RECONNAISSANCE OBJECTIVES

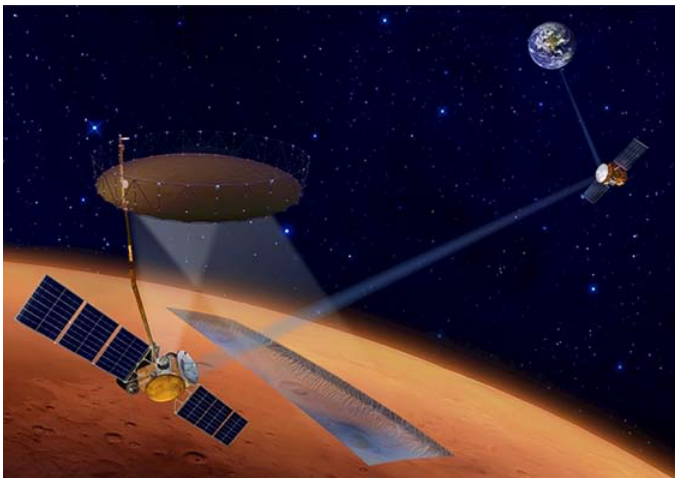

Artist Concept. *Credit: NASA*

FINDING 1. Most of the high-priority reconnaissance objectives can be met with the currently scoped radar instrument.

The MDT identified key parameters related to characteristics of surface or subsurface materials, the knowledge of which is important for advancing the mission reconnaissance goal. The MDT explored these parameters in detail, as summarized in a Reconnaissance Traceability Matrix (RTM).

For those parameters deemed of highest value for the reconnaissance objectives, the MDT found that the anchor radar payload could likely obtain a majority of them. These include:

- the presence/absence of ice in the upper several meters;
- the ice concentration profile with depth (including depth to the top of the ice);
- the lateral extent and continuity of ice;
- ice/rock mixing ratio, density, and strength of the overburden; and,
- surface rock-size distribution.

FINDING 2. The combination of SAR, sounder, and polarimetric capabilities is unique and powerful to accomplish the ice mapping needed to pave the way for the human exploration of Mars.

The anchor payload, as presented to the MDT, is an L-band (930 MHz) radar system that can acquire SAR images (side-looking) in two circular polarizations, and can operate as a nadir sounder, similar in operation to the recent Mars orbital radar sounders MARSIS and SHARAD.

The MDT found that the combination of these capabilities at the selected frequency offers unprecedented capabilities to detect, map, and inventory the ice resources that would be used in a human mission to acquire new science and to access ice for utilization in surface operations.

Along with the polarimetric and repeat-pass capabilities, the synergy of the dual modes of the radar enhances the likelihood of meeting the reconnaissance objectives to locate the ice in three dimensions and to constrain its key characteristics, such as purity.

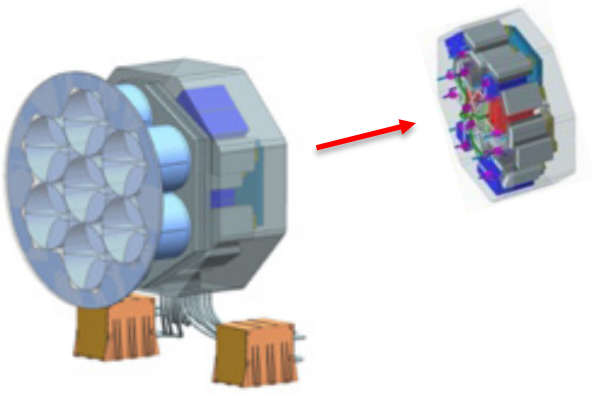

Primary Instrument:
Polarimetric SAR Seven-element Feed Array
Credit: CSA

FINDING 3. The core payload would have a high likelihood of finding ice deposits that could be readily accessed in situ (within the top few meters and not covered with large rocks).

The MDT assessed the likelihood of unambiguous detection of ice under various plausible scenarios of occurrence in the near subsurface (to a depth of 10 m) with the anchor radar payload. It found that the radar system could readily detect and map the mode of ice occurrence that is both likely to be widespread and of interest to human mission planning: ice in the upper few meters with a regolith overburden relatively free of large rocks.

This is a powerful combination of factors: easy to detect, of high interest for future missions, and possibly widespread in occurrence. Other ice deposits (deeper, rougher overburden, etc.) are also of great interest to the scientific community and could be investigated with an additional payload, specifically a nadir sounder operating at VHF (~100 MHz) frequencies.

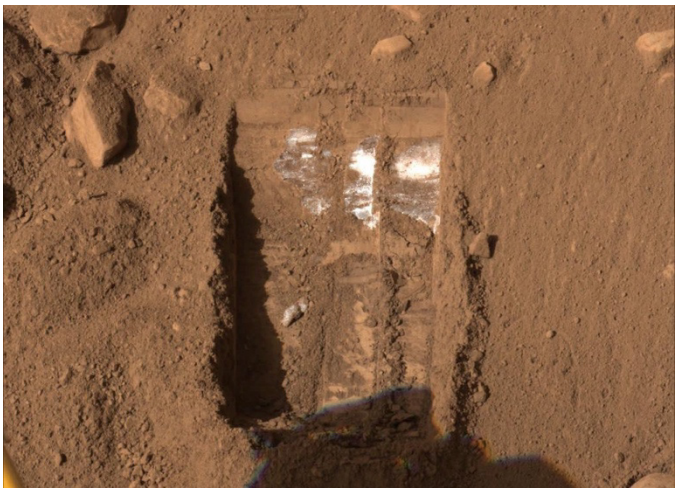

Near-surface ice on Mars; Mars Phoenix Lander. *Credit: NASA/JPL-Caltech/University of Arizona/Texas A&M University*

FINDING 4. Two high-value complementary instruments identified by the MDT could be optimized to aid in achieving the reconnaissance objectives: a VHF sounder and a high-resolution imager with stereo capabilities.

As directed by its Charter, the MDT investigated ways to optimize the instrument payload to accomplish the reconnaissance objectives more fully. Among the many types of instruments and modifications to the radar payload that the MDT considered, two instruments stood out as providing the most value as complements to the L-band radar system: a VHF sounder and a high-resolution imager with stereo capabilities.

- The VHF sounder could fill a remaining gap between the near-surface (several m) sounding of the L-band sounder mode, and the lower boundary of the so-called "blind zone" of SHARAD, which extends to about 20 m. In doing so, the VHF sounder would extend the range of depths that could be investigated, and thus more comprehensively map the ice deposits in the mid-latitude "Reconnaissance Zone" where human exploration would be operationally viable, as well as elsewhere on the planet.
- A high-resolution imager (25 cm/pixel resolution in multiple colors) could provide direct corroboration of ice detections in the vicinity of fresh impacts and ice scarps. Stereo image pairs could be converted to digital elevation models to correlate reflectors with exposed surfaces and contacts for dielectric estimation and to model clutter, as is currently done at coarser resolution with MARSIS and SHARAD using MOLA topography.

TASK 2: SCIENCE OBJECTIVES

FINDING 5. A broad suite of additional high-priority scientific investigations can be accomplished with the anchor radar payload, including multiple themes of interest to the international Mars science community: atmospheric science, geology, and habitability.

The MDT assessed the potential to accomplish additional science investigations beyond those associated with the Reconnaissance Objectives, first using only the anchor radar payload. MDT panels evaluated the science potential in three theme areas aligned with overarching science goals for Mars of the partner Agencies.

The panels found that significant new science investigations would be possible with the anchor radar payload. The Science Traceability Matrix (STM) summarizes these investigations, with assessments of the measurable parameters, resolution needed, and the observational techniques to be applied.

Atmospheric Science

In support of climatology, the anchor radar payload can address surface-atmosphere cycling, recurring slope lineae, and ionospheric irregularities.

Geological Studies

The radar can address many processes acting over various timescales, including present-day activity, the recent past (e.g., volatile cycling over My timescales), and the more distant past. These include such diverse topics as polar processes, mid-latitude ice, volcanism, recent and ancient impacts, landforms such as valley networks, and unique radar terrains such as Medusae Fossae.

Habitability

The radar can contribute to locating ice and brines that may serve as present-day habitable environments, characterizing fluvial or glaciofluvial environments that might have hosted life in the past, and identifying subsurface habitats in the form of voids in the subsurface.

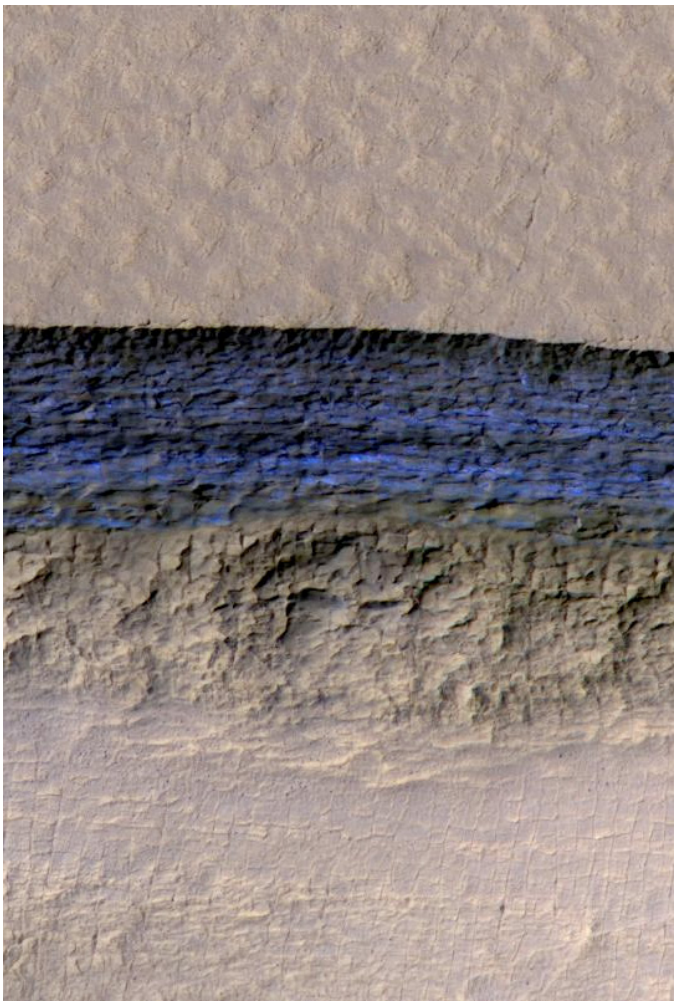

An ice-exposing scarp in the southern midlatitudes of Mars. Blue areas (color-enhanced) show ~80 vertical meters of exposed water ice. *Credit: NASA/JPL-Caltech/University of Arizona*.

FINDING 6. The complementary instruments identified by the MDT for ice reconnaissance (VHF sounder and visible imager) would significantly enhance I-MIM's scientific impact.

The science theme groups examined the additional benefit for science investigations of the complementary instruments identified for ice reconnaissance (VHF sounder and visible imager) in Task 1.

Many investigations would be significantly enhanced or be newly enabled by the addition of these instruments.

- The VHF sounder would enhance investigations of the subsurface in all theme areas and would contribute to the ionospheric irregularities investigation.
- The high-resolution imager would contribute to all theme areas, enhancing such investigations as geomorphology (for habitability and past climate and recent ice-related processes) and ongoing surface changes that may corroborate radar detections, and seasonal volatile exchange.

FINDING 7. I-MIM could increase its scientific impact by making supplemental measurements with additional instruments and/or platforms, which could be optimized to fill remaining high-priority gaps in meeting reconnaissance objectives.

The MDT considered a scenario in which the I-MIM platform(s) could accommodate supplemental science instruments beyond the anchor radar and the previously prioritized complementary instruments for ice reconnaissance. The Task 2 science theme groups identified instruments and associated measurements that would address remaining high-priority gaps in our knowledge of Mars. The MDT identified surface temperature measurements as providing high benefit to both science and ice reconnaissance. For atmospheric studies, additional instruments could target the structure and dynamics of the lower and upper atmosphere and their interconnections. The highest atmospheric priority is the global measurement of winds, with temperature structure, aerosols, water vapor, and mapping of aurora also considered important. Surface compositional information would greatly enhance geological and habitability investigations.

Additional instruments could support scientific studies of a number of ice- and non-ice-related processes on Mars including surface-atmosphere interactions and change detection, among others. Left to right: gullies and recurring slope lineae, high clouds over Gale Crater viewed by the Curiosity rover, polygonal terrain at the ice-rich Phoenix landing site. *Credit: NASA/JPL-Caltech/University of Arizona/MSSS/Texas A&M*

TASK 3: CONCEPT OF OPERATIONS

FINDING 8. The MDT developed a feasible concept of operations for a nominal mission timeframe of one Mars year, split into two phases.

The MDT found that a mission lasting one Mars year, in the proposed ~255 km altitude circular orbit, would be sufficient for accomplishing the reconnaissance objectives, given the anchor radar payload's estimated data production rate and the downlink capabilities provided by the mission concept team prior to the MDT deliberations.

Phase 1. The first 10 months of the mission would be dedicated primarily to acquiring 30 m SAR coverage of the Reconnaissance Zone (RZ). Allocating 80% of the returned data to the 30 m resolution SAR mode would ensure that all useful passes over the RZ can be downlinked during the first 10 months with sufficient margin. The remainder would be available for other modes of operations, such as nadir sounding and high-resolution SAR, and other complementary instrument(s), if provided.

Phase 2. The mission would perform targeted observations to obtain high-resolution SAR imaging and sounding of regions of interest, including new targets identified from the first phase.

FINDING 9. The mission as conceived is achievable within the provided constraints of consumables such as power and data volume, but I-MIM's reconnaissance and science investigations could be more easily and fully accomplished with increased capabilities for downlinking data to Earth, especially if additional instruments are provided.

The MDT found that total data volumes (over a Mars year) were constraining, particularly in the second phase when including the high-resolution SAR modes and potential complementary and supplementary payloads. The Agencies should explore options for increasing downlink capacity in subsequent mission development studies.

> Based on these findings, the MDT concludes that the Agency partners should continue to pursue development of the I-MIM mission as a key element in the future exploration of Mars.

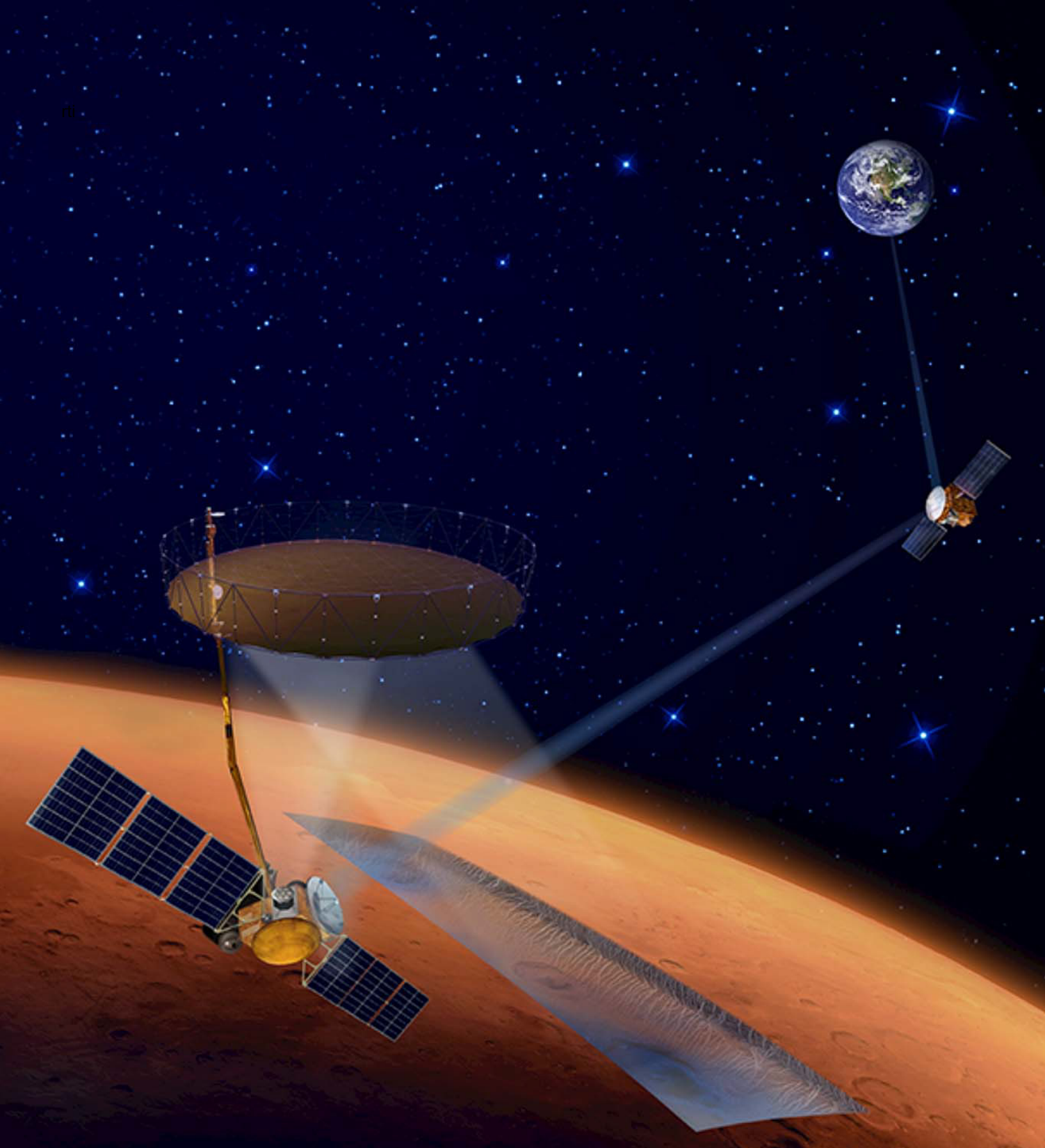

I-MIM's SAR-carrying orbiter in low Mars orbit, sending back high-volume radar data through a conceptual communications relay orbiter in high Mars orbit.

Artist Concept. Credit: NASA

2 I-MIM MISSION OVERVIEW

In January 2021, the Agenzia Spaziale Italiana (ASI), the Canadian Space Agency (CSA), the Japan Aerospace Exploration Agency (JAXA), and National Aeronautics and Space Administration (NASA) signed a joint Statement of Intent (SOI) to establish a multilateral "Concept Team" to assess the potential of an orbital Mars ice-mapping mission, to define their potential roles and responsibilities, and to consider partnership opportunities. The Netherlands Space Office (NSO) subsequently joined the Concept Study.

Conceptually, the International Mars Ice Mapper (I-MIM) mission consists of an orbiter in low Mars orbit (~300 km). It carries an L-band (930 MHz) polarimetric synthetic aperture radar (SAR)/nadir sounder combination to map accessible, near-surface (top 10 m) water ice at Martian midlatitudes – and as close to the equator as possible where human missions are more operationally viable – to support planning for the first human missions to the Martian surface. The partner Agencies have also considered the benefits of an optional high-altitude communications relay capability to support the large volume of data anticipated from the L-band Radar.

As presented to the MDT, the participating Agencies are considering the following contributions:

ASI	Large Deployable Reflector (LDR) antenna, communications subsystems, and potential supplemental payload(s)
CSA	Primary anchor payload, a polarimetric L-band Synthetic Aperture Radar (SAR) and Sounder
JAXA	Spacecraft Bus and potential supplemental payload(s)
NASA[1]	Launch Vehicle, potential Communications Relay capabilities, and potential supplemental payload(s)
NSO	Solar Arrays

The multilateral mission Concept Team operates under a consensus-based process; no single Agency leads, and each has national science communities with common, but not identical, priorities (see Appendix A). Potential Agency contributions are based on those priorities, heritage, expertise, and strategies for both robotic and human exploration. The Agency partners tie their potential I-MIM contributions to their *Artemis Accords* agreements (or, in the case of NSO, its contributions to Orion and other elements), as well as to Agency strategic documents provided to the MDT for traceability, including:

ASI	Documento di Visione Strategica per lo Spazio, 2020–2029
CSA	Canadian Space Exploration – Science and Space Health Priorities for the Next Decade and Beyond
JAXA	JAXA Strategic Mars Exploration Program (JSMEP)
NASA	Origins, Worlds, & Life 2023–2032 Decadal Survey (2022); MEPAG Science Goals (2020); and other relevant MEPAG reports (e.g., ICE-SAG, NEX-SAG, MASWG)

Alignment with these strategic documents is shown in Appendix A.

[1] At the time of this writing, the potential NASA contribution is unclear pending results of Agency and legislative processes, but the multilateral partners (including NASA) unanimously confirmed support for completing the MDT's work for this and/or future mission concept studies.

I-MIM will seek ice-rich locations for the first human home on Mars.

Artist Concept. Credit: NASA

2.1 I-MIM GOALS & OBJECTIVES

For commencing the Concept Study, the Agency partners mutually established the following requirements-driving mission goal and objectives:

RECONNAISSANCE GOAL

The overarching Reconnaissance Mission Goal that enables human exploration by addressing a high-priority knowledge gap is: "to map and characterize accessible, near-surface (within the uppermost 10 m) water ice and its overburden in mid-to-low latitudes to support planning for the first potential human surface missions to Mars."

RECONNAISSANCE OBJECTIVES

The Agency partners have established three Reconnaissance Objectives (RO) that will drive measurement requirements within a region termed the "Reconnaissance Zone" (RZ).[2]

RO-1
Location & Extent of Water Ice

In the Reconnaissance Zone, detect, map, and inventory the spatial distribution and depth-to-ice of water-ice resources in the near surface (top 0–10 m).

RO-2
Accessibility of the Water Ice

In the Reconnaissance Zone, detect, characterize, and map surface/near-surface geotechnical properties (roughness, compactness) to provide a fundamental understanding of the accessibility of water-ice resources (e.g., characterization of the overburden for drilling/ISRU and the structural stability of the terrain for landing/launch, construction, trafficability, and other human-related surface operations).

RO-3
Assessment of Candidate Sites for Human Exploration

Based on analyses of the above surveys of the Reconnaissance Zone, provide detailed high-resolution maps of targeted areas of interest (TAI) that: have adequate (RO-1) and accessible (RO-2) water ice, are as equatorward as possible, and model the potential for human-led surface science and human-class landing and ascent, ISRU, and civil engineering.

[2] Mid-to-low-latitude, low elevation, terrain-favorable areas on Mars where human exploration is likely viable in terms of human-led science potential, in-situ resources, engineering constraints associated with human-class landing/launch and surface operations, civil engineering, and other such factors.

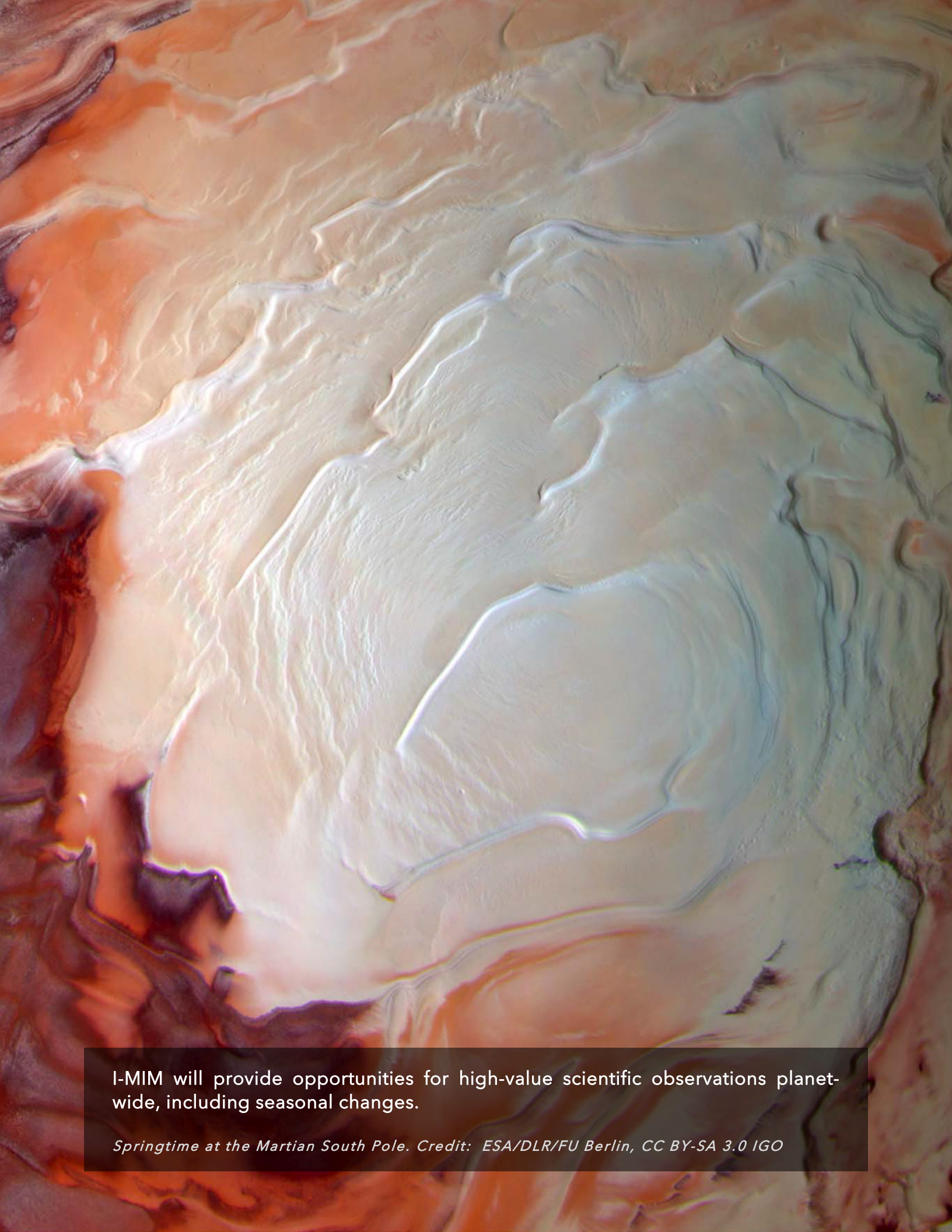

I-MIM will provide opportunities for high-value scientific observations planet-wide, including seasonal changes.

Springtime at the Martian South Pole. Credit: ESA/DLR/FU Berlin, CC BY-SA 3.0 IGO

While focused on reconnaissance for defining their initial engagement in the multilateral Concept Study, the Agency partners have a stated mutual intent to maximize the mission's return on investment to the greatest extent possible within mission boundary conditions.[3] Thus, the partners adopted a "supplemental value goal" with related supplemental science and mission-support objectives.

> **SUPPLEMENTAL VALUE GOAL** As possible, provide *high-value science opportunities* and *high-priority mission-support capabilities* that serve reconnaissance, science, and engineering.

SUPPLEMENTAL VALUE-DRIVEN OBJECTIVES WITHIN BOUNDARY CONDITIONS

Subject to addressing the ROs as overarching priorities that drive the measurement requirements of the L-band anchor payload, the Agency partners established Supplemental Science Objectives (SSO) that maximize its use and Mission Support Objectives (MSO) that further maximize potential returns on investment. None drive mission requirements, but the Agencies are committed to the most benefits possible.

SSO-1
Augmented Water Ice Inventory

Use the anchor payload to extend the detection, mapping, and inventory of shallow water ice to a near-global scale.

SSO-2
Reconnaissance/Science Investigations of Opportunity

Enable reconnaissance/science observations aligned with high priority, international, and multidisciplinary community goals (e.g., Martian climatology and geology, the volatile history of Mars, habitability, search for natural geologic structures for radiation protection, etc.).

MSO-1
Optional Technology Demonstration: High-altitude Communications Relay Orbiter(s)

Provide a dedicated, first-generation, high-altitude Mars Relay Network (MRN) element primarily to support I-MIM's expected high data volume and its delivery at high rates (e.g., raw SAR and sounder data), and, secondarily, to support future Mars missions (including backup support for Mars Sample Return and the testing of a precursor MRN infrastructure that is replenishable, scalable, and interoperable for both robotic and human exploration) *[Note: the MDT did not address this Objective in detail, but assessed the benefits of enhanced downlink data in Task 3.]*

MSO-2
Complementary Payloads for Reconnaissance, Science, & Engineering

Consider additional payloads, rideshares, extended operations, and leverage of capabilities for future human and robotic Mars missions. *[Note: as documented in the RTM and STM (Sections 4.5 and 5.4 respectively), the MDT primarily considered additional payloads that could be added to enhance the mission's reconnaissance and science outcomes, rather than the delivery of those capabilities.]*

As described by the Agencies, the Partners deliberately left the initial supplemental objectives broad to maximize independent input from the international community of scientists and human mission planners – initially through a competitively selected international, multidisciplinary Reconnaissance/Science Measurement Definition Team (MDT) and ultimately through a mission reconnaissance/science team should the mission proceed to formulation.

[3] Boundary conditions include the Reconnaissance Objectives, optimal SAR measurements, cost, timing, mass, power, operational complexity, and partner commitments, among others, as will be articulated to the MDT by the multilateral Concept Team.

2.2 PRIMARY ANCHOR PAYLOAD

Contributed by the CSA, I-MIM's anchor payload is an L-band (930 MHz center frequency) polarimetric radar instrument that uses complementary approaches to inventory the context, extent, location, and potential "resource volume" of buried water-ice deposits on Mars. The agile, dual-mode instrument is capable of measuring aspects of the uppermost several meters of the Martian surface layer using state-of-the-art techniques pioneered on Earth via aircraft (JPL UAVSAR and AirSAR) and space (CSA: Radarsat-1, Radarsat-2, and RADARSAT Constellation Mission; NASA SRTM, SIR-C; JAXA ALOS, etc.).

As presented to the MDT, this potential mission contribution is based on technology readiness given: a prototype of the radar feed; numerical simulations of the radar signal's subsurface scattering behavior in ice-rich environments; and, a RADARSAT-2 demonstration that data-processing techniques, even at high frequency, can enable clearer interpretation of subsurface properties.

In sum, significant preparatory investments over the past several years brought the instrument concept to a level of maturity ready to move to flight.

2.2.1 Instrument Description

The core of the instrument has four main parts:

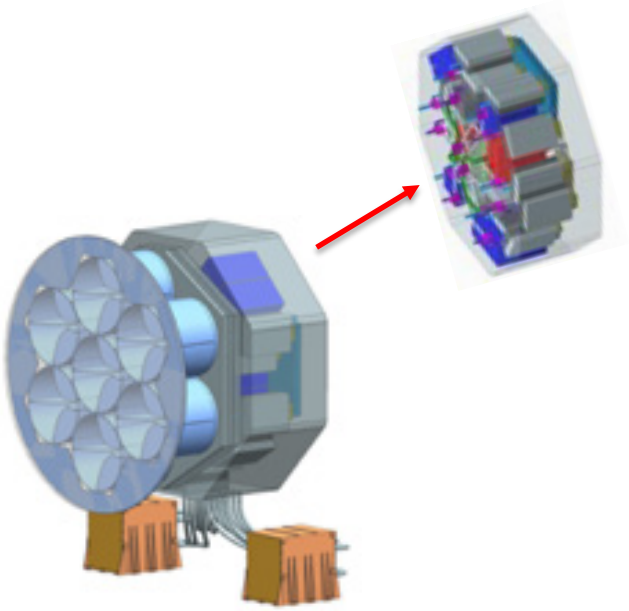

Figure 2.1 Primary Instrument Polarimetric SAR Seven-element Feed Array

Radar Electronics

Receives the parameters that guide the commanded operation (e.g., bandwidth, pulse direction), generates the radio frequency (RF) pulse, receives the radar echo from the target, and converts the returned radar signal into a digital signal that is relayed back to the Earth;

Distributed High Power Amplifier

Takes the generated low-power RF pulse generated by the radar electronics and amplifies it to the levels required to achieve the high sensitivity;

Radiating Element

Radiates the RF pulse toward the reflector mounted on the spacecraft and reciprocally converts the received echo down to a guided RF signal; and,

Distributed Low Noise Amplifier Network

Amplifies the very small received echo to a level suitable for processing by the radar electronics.

The antenna consists of a 7-element circular phased array arranged for circular polarization illuminating an ASI-provided body-fixed Large Deployable Reflector (LDR) mesh with a 6 m effective diameter (Figure 2.2).

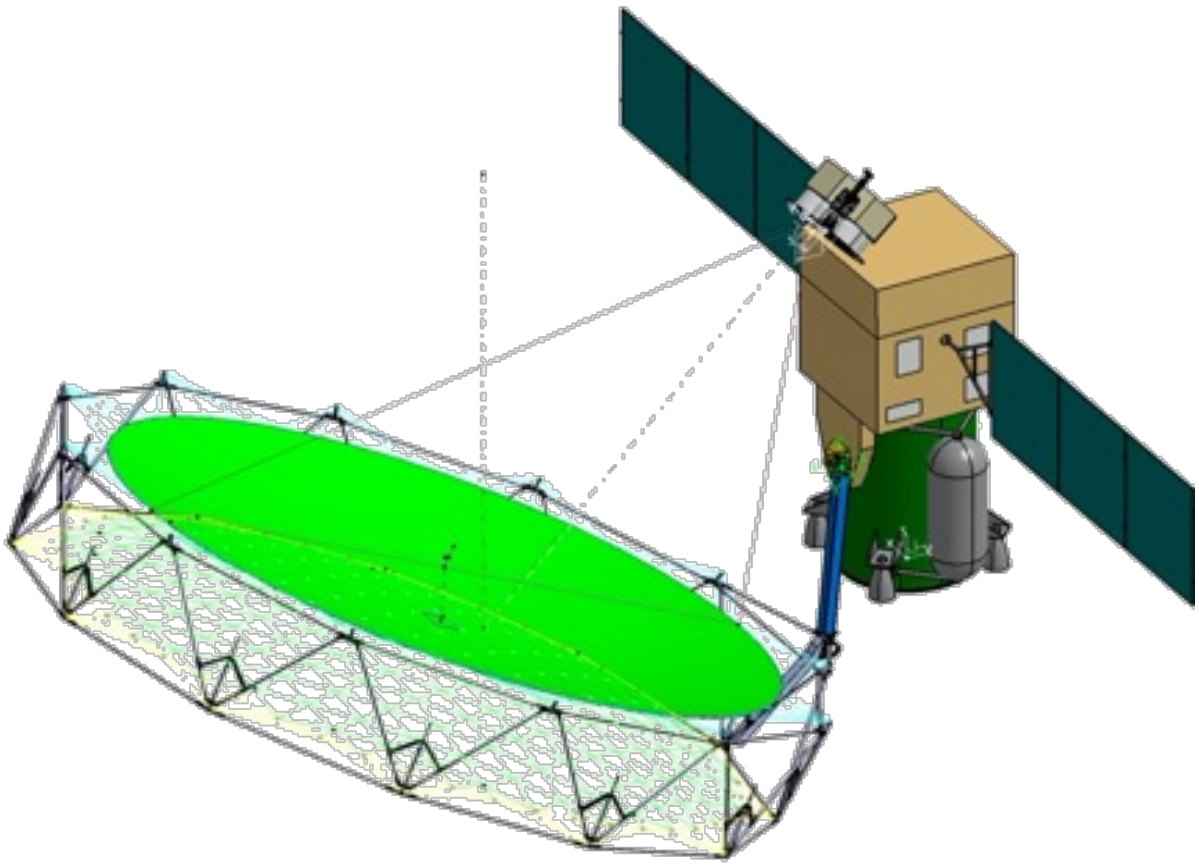

Figure 2.2 ASI-provided LDR with SAR on JAXA-provided Bus

The LDR operates in L-band for the SAR and sounder with a dedicated feed, and in X/Ka-band for communications with an integrated feed. Agency partners chose this configuration because of reduced risk and complexity. The heritage for the X/Ka band communication subsystem is based on extensive ASI experience on transponders/antennas for deep space missions. A 6 m-diameter LDR provides the gain needed to meet the mission objectives. The heritage for the use of an LDR in a radar system has been demonstrated through the Soil Moisture Active Passive (SMAP) mission (Entekhabi et al., 2010; Focardi et al., 2016).

The heritage for the current hardware proposed by ASI for the I-MIM LDR is based on the development efforts and heritage of multiple programs, including the ESA Copernicus Imaging Microwave Radiometer (CIMR) mission (Kilic et al., 2018) and the ESA contract for the development of an "Innovative Scalable Large Deployable Antenna Reflector" (Contu et al., 2019).

Both programs operate in Ka-band with a deployable mesh antenna.

Provided by the mission Concept Team, Table 2.1 shows the high-level radar system parameters.

Table 2.1 Key parameters of I-MIM SAR/nadir Sounder

PROPERTY	VALUE
Center Frequency	930 MHz
Polarization	Hybrid (circular transmit, dual linear reception)
Antenna	6 m deployable mesh (offset-fed reflector)
Sensitivity	−30 dB as NESZ (at 30 m multi-look, side-looking)
RF Bandwidth (RFBW)	10–160 MHz
RF Peak Power	2000 W
Pulse Duration	10–50 μs, selectable
Configuration	Multi-feed offset fed reflector
Operational Modes	Side-looking SAR and Nadir Sounder
Maximum RF Duty Cycle	10%
MODE 1: SIDE-LOOKING SAR	
Swath Width	30 km
Incidence Angle	40–45°, with variable options
Horizontal Resolution (Rg × Az)	5–30 m
Penetration Depth (Typical for Mars)	> 6 m
MODE 2: NADIR SOUNDER	
Vertical Resolution (ranging to ice)	< 1 m
Along-track Spacing	30 m
Across-track Footprint	1.5 km
Along-track Footprint	1.5 km before processing, 450 m after

2.2.2 Instrument Capabilities

I-MIM would be the first orbiting Mars mission to use SAR to explore the surface/subsurface of Mars. The SAR features circular transmit polarization and dual linear receive polarization modes, which enable the use of a "compact polarimetric mode" (CP) to improve interpretation of a variety of subsurface features. The SAR can be operated with a variety of bandwidth and pulse lengths, which can be tailored to optimize the resolution, sensitivity, data rate, and power consumption for each desired operation (Tables 2.2 and 2.3).

The reflector-based array feed design carries the ability to operate as a nadir profiler or sounder as shown in Figure 2.3, as controlled by the spacecraft's roll position.

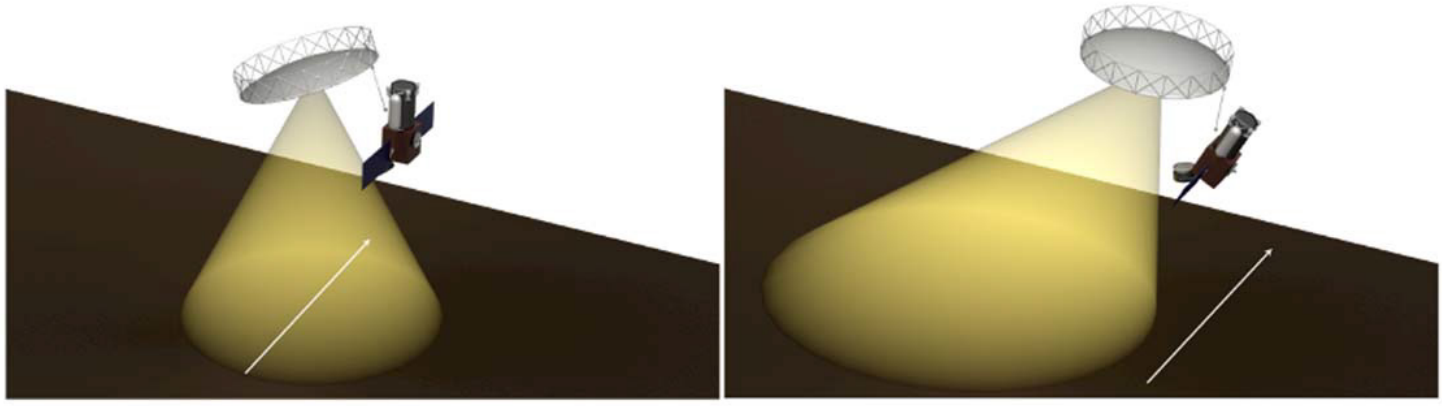

Figure 2.3 (Left) Nadir Sounder Configuration, where the target ground is illuminated at Nadir, directly under the antenna. (Right) Side-looking SAR configuration, where the target ground is illuminated at a certain slant (incidence) angle, resulting in an enlarged swath.

The two modes of operation enable several different approaches to meet mission objectives shown in Tables 2.2 and 2.3.

Mode of Operation 1 Side-looking Polarimetric SAR

As presented to the MDT and shown in Table 2.2, this mode of operation enables four approaches that support I-MIM's reconnaissance measurement needs: baseline reconnaissance-level surveys and high-resolution approaches (SAR imaging, interferometry, and tomography). Initial high-level measurement goals served as a starting point for the MDT in constructing the Task 1 Reconnaissance Traceability Matrix (RTM) and the Task 2 Science Traceability Matrix (STM).

Mode of Operation 2 Nadir-pointing Sounder

As presented to the MDT, this mode of operation enables two approaches that support I-MIM's reconnaissance measurement needs: baseline and repeat-pass nadir SAR sounding (Table 2.3).

Table 2.2 SAR Operation Mode 1: Side-looking Polarimetric SAR

MODE 1: SIDE-LOOKING POLARIMETRIC SAR IMAGING

APPROACH	HORIZONTAL RESOLUTION	HIGH-LEVEL MEASUREMENT GOAL
BASELINE	30 m	Wide-area Detection of Buried Ice
With extremely high sensitivity, this approach can potentially detect buried water ice down to depths as great as, or greater than, ~5 m (depending on the mantling of the Martian regolith and dust on top of, or intermixed with, it, mapping boundaries and associations with other subsurface geologic structures at meso-scales of tens of meters). The polarimetric capability is sensitive to the Coherent Backscatter Opposition Effect (CBOE) (Hapke, 1990; Mishchenko, 1992) allowing more definitive ice detection.		
HIGH-RESOLUTION	3 or 5 m	"Zoom in" on Buried Ice
With particular sensitivity to meter-scale surface and shallowly buried features that impact landing site safety, this approach produces high-resolution maps of the ruggedness of future landing sites in association with near-surface ice to add to the arsenal of data used in the Mars landing site certification process.		
INTERFEROMETRY, REPEAT PASS	5–30 m	Topographic Change Detection
Requiring a repeat pass orbit and precision tracking, the high-resolution Interferometric SAR (InSAR) approach measures the relative change in surface elevation to the centimeter scale. This mode also offers the opportunity of producing topography.		
TOMOGRAPHY, REPEAT PASS	5 m	Delineated Subsurface Layering
With multiple passes over a specific target area, this high-resolution approach shows fine-scale subsurface layering in stacked SAR imagery, characterizes the physical properties of each layer, and distinguishes between ice-poor and ice-rich areas using classical tomographic techniques.		

Table 2.3 Radar Operation Mode 2: Nadir Sounding

MODE 2: NADIR SOUNDING				
APPROACH	ALONG-TRACK SPACING	UNFOCUSED ALONG-TRACK RESOLUTION	VERTICAL RESOLUTION	MEASUREMENT GOAL
BASELINE	30 m	450 m	< 1 m	Depth to Buried Ice Layers
The sub-meter (< 1 m vertical resolution) ranging precision of this sounder approach maximizes the depth of penetrating radar on spatially extensive water-ice layers, distinguishes the depths of distinct subsurface layers (to better than 1 m), characterizes their physical and electrical properties, and provides wavelength-scale roughness profiles (as done for Earth and Venus). The ability to use special ice detection methods known as the Coherent Backscatter Opposition Effect (CBOE) (Hapke, 1990; Mishchenko, 1992) improves definitive detection.				
REPEAT PASS	30 m	450 m	< 1 m	Depth to Buried Ice Layers, Enhanced
While similar to the single-pass baseline sounder approach, three passes over a targeted “corridor” provide an opportunity to mitigate clutter from off-nadir scatterers and increase signal to noise, enhancing near-surface data interpretation in the critical 1–10 m shallow zone.				

Two such profiling sounding radars have previously been sent to Mars. The Shallow Subsurface Radar (SHARAD) (Seu et al., 2007) aboard NASA's Mars Reconnaissance Orbiter (MRO) operates at a center frequency of 20 MHz, enabling detection of subsurface reflectors from approximately 50–2000 m of depth (depending on specific substrates). SHARAD has a bandwidth of 10 MHz that yields a vertical resolution in free space of 15 m. When entering a geologic or icy medium, the resolution improves to 15/sqrt(ε'), where ε' is the dielectric permittivity of the material; however, SHARAD cannot resolve features in the uppermost 15–20 m. The Mars Advanced Radar for Subsurface and Ionosphere Sounding (MARSIS; Jordan et al., 2009) aboard Mars Express (MEX) operates at even lower center frequencies (four channels that span 1.3–5.5 MHz). MARSIS reaches penetration depths of 1–4 km at a vertical resolution of approximately 100 m, depending on ε'.

Thus, I-MIM's nadir sounding mode, with improved vertical resolution and along-track resolution, complements current sounding-radar datasets. Table 2.4 shows a comparison of key parameters between the nadir sounding modes and previous Mars sounding radars (SHARAD and MARSIS).

Table 2.4 Comparison of key parameters of I-MIM Radar Sounder vs MHz-frequency MARSIS and SHARAD sounding radars

MISSION	MRO (NASA)	MARS EXPRESS (ESA)	MARS ICE MAPPER (INTERNATIONAL)
PARAMETER	SHARAD	MARSIS	CURRENT STUDY
Center Frequency	20 MHz	1.3–5.5 MHz	930 MHz
Bandwidth	10 MHz	1 MHz	10–160 MHz
Penetration Depth (Depends on Substrate)	100–2,000 m	2,000–4,000 m	~2–120 m
Wavelength	15 m	60–160 m	0.3 m
Vertical Resolution	8–15 m	150 m	< 1 m
Horizontal Resolution	300–3,000 m	2000+ m	1500 m (unprocessed) 450 m (processed)

3 I-MIM RECONNAISSANCE/SCIENCE MEASUREMENT DEFINITION TEAM (MDT)

3.1 MDT OVERVIEW

As part of its early Concept Study and as a bridge to potential Phase A development, the Partner Agencies competitively selected an international, multidisciplinary, Reconnaissance / Science Measurement Definition Team (MDT). Members are listed at the front of this document, and represent 10 countries and diversity across gender, career stage, and discipline. Per the Agencies, to ensure its mission objectives, the MDT required international experts from the partner Agencies and other nations who collectively have expertise in a variety of domains, including subdisciplines of planetary science, SAR and radar sounding, in situ resource utilization (ISRU), human-class entry, descent and landing (EDL) and ascent, and civil engineering. In selecting members, the Agency partners made a concentrated effort to include early career professionals, recognizing that they will be deeper into their careers at the anticipated time I-MIM would collect data.

To provide an additional level of support to the MDT, the Agency partners also formed an Independent Assessment Team (IAT) comprised of senior international experts in critical disciplines to review MDT progress and outcomes and to provide feedback at relevant intervals. The IAT members are also listed at the beginning of this report. The overall structure of the MDT is shown in Figure 3.1, and a list of members and associated personnel is provided at the beginning of this report.

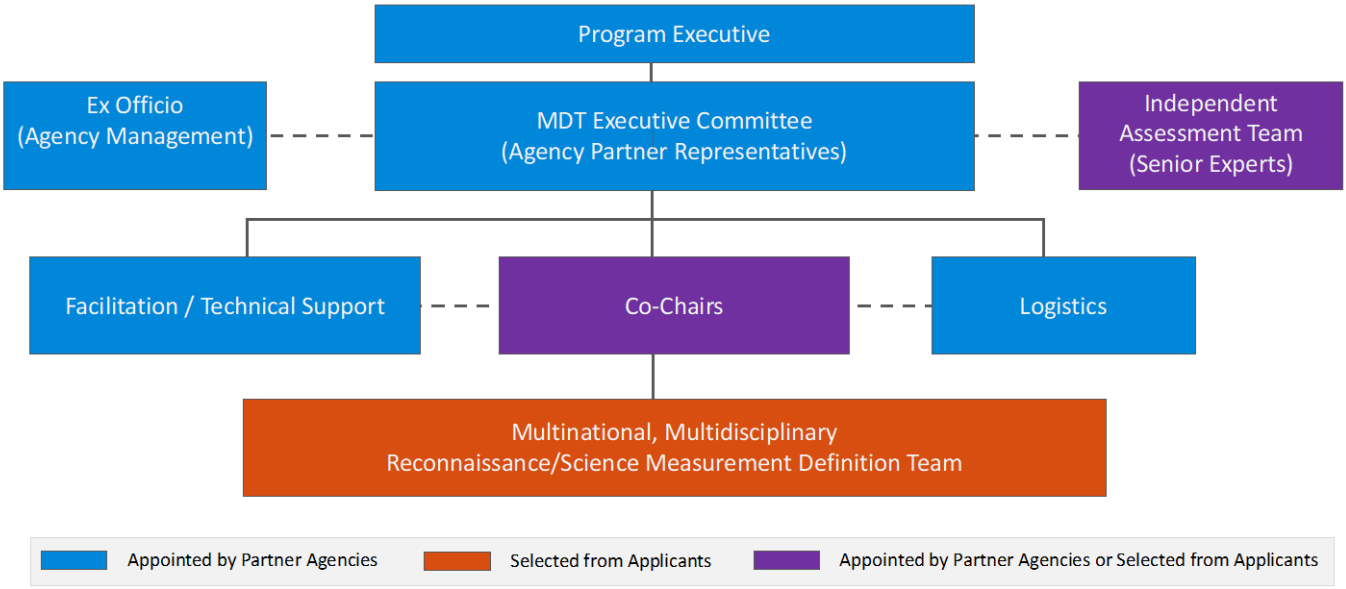

Figure 3.1 MDT Structure

3.2 MDT CHARTERED TASKS

In forming the MDT, the Agency partners sought quantitative, objective, and critical evaluation of the primary anchor payload to ensure that the identified SAR measurement system would optimally meet the mission reconnaissance goal and objectives with instrument-traceable requirements, as well as maximize MDT-identified scientific investigations for the greatest return on investment possible.

The Agencies chartered the MDT to perform three tasks:

1. Define measurements for the anchor payload that are traceable to requirements-driving Reconnaissance Objectives (ice detection, overburden characterization, and candidate human landing-site characterization) and ways to optimize the payload(s) for these purposes;

2. Provide findings on potential high-value, prioritized reconnaissance, science, and engineering augmentations that are synergistic with the anchor payload and might maximize the mission's return on investment within established mission boundary conditions; and,

3. Prepare a model concept of operations based on findings for Tasks 1 and 2.

3.3 ASSUMPTIONS GUIDING MDT FINDINGS

To complete the chartered tasks, the MDT used the following Agency-provided mission assumptions in the Charter to guide MDT Findings:

- The SAR-carrying orbiter ("SARbird") and potential communications relay orbiters ("COMbirds"), would arrive at Mars by 2030 and orbit at ~300 km and ~6000–8000 km respectively. [The baseline mission lifetime requirement is one Mars year (~690 Earth days).
- Note: While the MDT did not formally assess the communications relay option from a detailed technical point of view, it did find that enhanced data-delivery capabilities would enable the addition of MDT-recommended complementary and supplementary payloads, benefitting both of the mission's reconnaissance and science objectives.]
- Mission pre-project activities will provide constraints on spacecraft design and configuration solutions to establish realistic boundary conditions for MDT consideration.
- The anchor payload is a polarimetric Synthetic Aperture Radar (SAR) operating at a center frequency of 930 MHz (L-band), capable of both side-looking and nadir (sounding) measurements.
- Any notional supplemental mission payloads or rideshares would require additional international partner commitments, should be synergistic with the anchor payload and align with reconnaissance, science, and mission-support objectives, and must not interfere with the measurement capabilities of the primary (SAR) instrument in accommodation and operations.

The mission Concept Team also provided additional, more detailed technical information as needed by the MDT.

3.4 MDT PROCESS

As presented by the Agencies, the MDT process differs from traditional mission Science Definition Teams (SDT) in that the Agency partners pre-defined the high-level mission goals, objectives, the anchor payload, and other hardware contributions for the Concept Study on the basis of shared future strategies for Mars exploration, expertise, technology readiness levels, and the likelihood of available funding within the Partners' individual programs. The MDT followed a process for Tasks 1 and 2 shown in Figure 3.2.

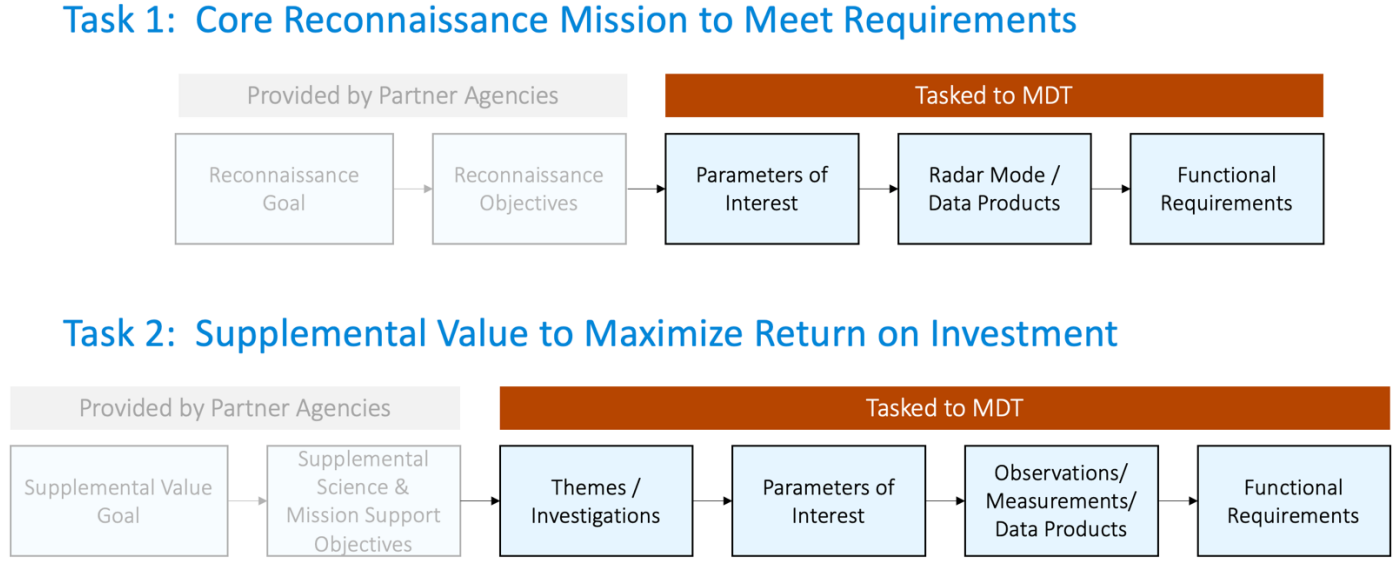

Figure 3.2 MDT Process Overview

Meetings were conducted through video-conferencing, with all plenary and individual group sessions recorded for review by any member not able to attend a given session. The MDT also maintained an ongoing online chat area for open discussion, widely available for asynchronous review and participation by members. The Co-Chairs requested that certain team members act as Subgroup leads, who then organized the content-targeted discussions and the synthesis of those inputs and outcomes. With the participation of the Subgroup leads, the Co-Chairs presented these evolving products at regular intervals through the plenary sessions. The MDT also utilized collaborative online writing and editing tools, with open opportunities for further discussions and revisions.

Since the IAT also engaged at key intervals to provide independent feedback helpful to the process, the Co-Chairs shared their IAT briefing presentations on the MDT's progress and products with the full MDT to enable members' inputs into high-level communications about the MDT's products. These same opportunities applied to an interim presentation made to the Mars Exploration Program Analysis Group (MEPAG) in May, 2022, which relied heavily on the consensus-based outputs of the Task 1 and Task 2 subgroups. The MDT had full access to feedback from the IAT for revisions to their ongoing work and eventual conclusions. At the plenary sessions, the Co-Chairs made a concerted effort to focus the MDT on the language of the findings to capture any nuances from their more detailed subgroup activities and, ultimately, for consensus. Utilizing the available online collaboration tools previously mentioned, MDT members then had open access to iterative versions of the preliminary drafts of the full final report, collated from the contributions of each subgroup. The Co-Chairs then completed the final draft for production, coordination, and dissemination by the partner Agencies, through the MDT Executive Committee.

Following review of the near final draft of the MDT final report, the IAT's final report to the Agency stakeholders stated:

> *"The IAT commends, in the highest terms, the efforts of the MDT to produce such a comprehensive document that confirms the efficacy of the primary anchor payload to achieving the proposed I-MIM mission reconnaissance goals, lays out augmentations to the anchor payload to both complement and supplement the science and reconnaissance goals of the mission, and establishes a basic concept of operations for a such a mission."*

Details on the three-part process used by the MDT to achieve this comprehensive assessment of chartered tasks follow.

Task 1 Process

MDT members divided into three groups (Figure 3.3) according to the three reconnaissance objectives (in brief: ice detection, overburden characterization, and studies of viable candidate sites for human exploration). Representatives with requisite expertise from all three groups formed two additional groups: radar and human mission planning. These two groups interacted to ensure the instrument was capable of making measurements traceable to the reconnaissance objectives and that the measurements addressed the needs of human mission planners for architecture studies and initial data leading toward human landing site certification. From the Task 1 analysis and construction of a Reconnaissance Traceability Matrix (RTM), the MDT reached consensus on two priority complementary instruments that, if implemented, would increase the robustness of the radar data interpretations and improve the mission's ability to meet its requirements-driving reconnaissance objectives.

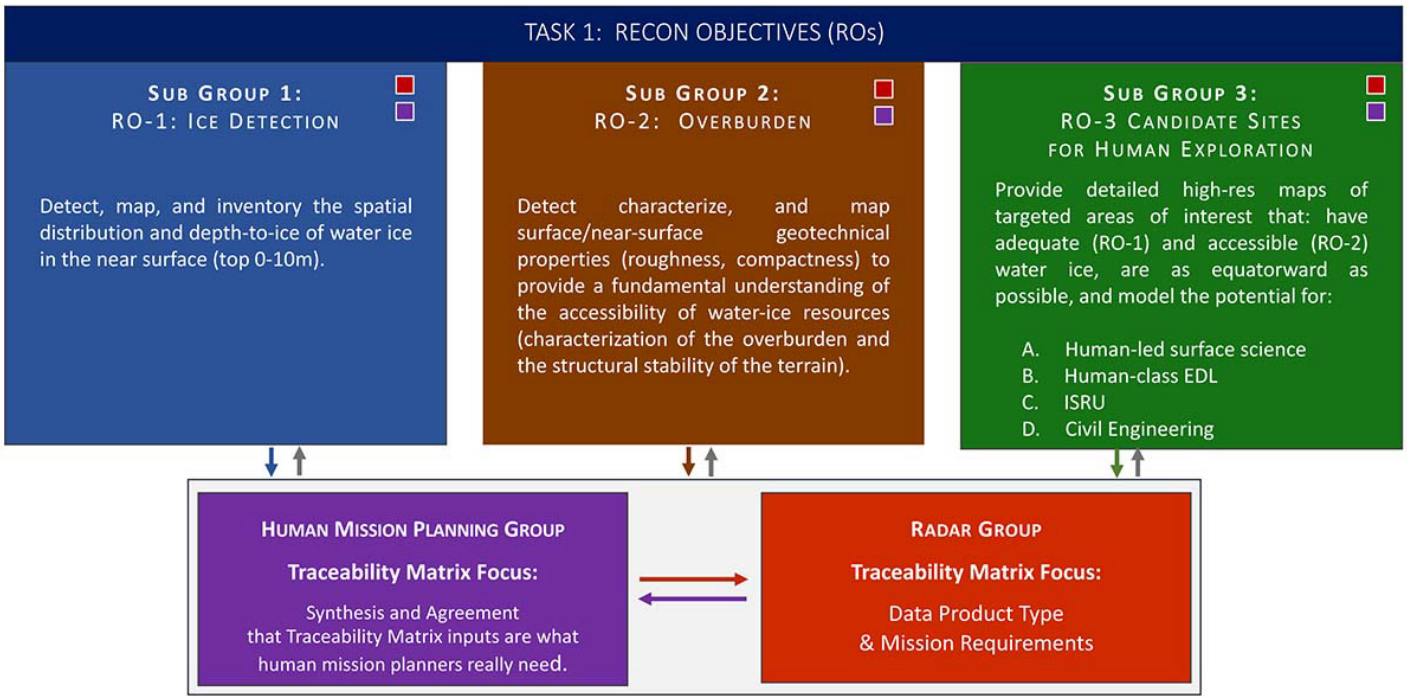

Figure 3.3 MDT Structure to Address Task 1

Task 2 Process

For Task 2, the MDT members divided into three groups according to the following broad science themes: Atmosphere, Geology, and Habitability (Figure 3.4).

Task 2 teams considered supplemental science possibilities, first assuming the primary anchor payload only, then considering complementary instruments with an MDT consensus on their prioritization to meet reconnaissance objectives from Task 1, and finally exploring additional payloads that would maximize return on investment further, within mission boundary conditions (e.g., accommodated either onboard the I-MIM orbiter or as piggybacks/rideshares). Out of the Task 2 analysis, representatives with requisite radar expertise interacted to create a Science Traceability Matrix (STM).

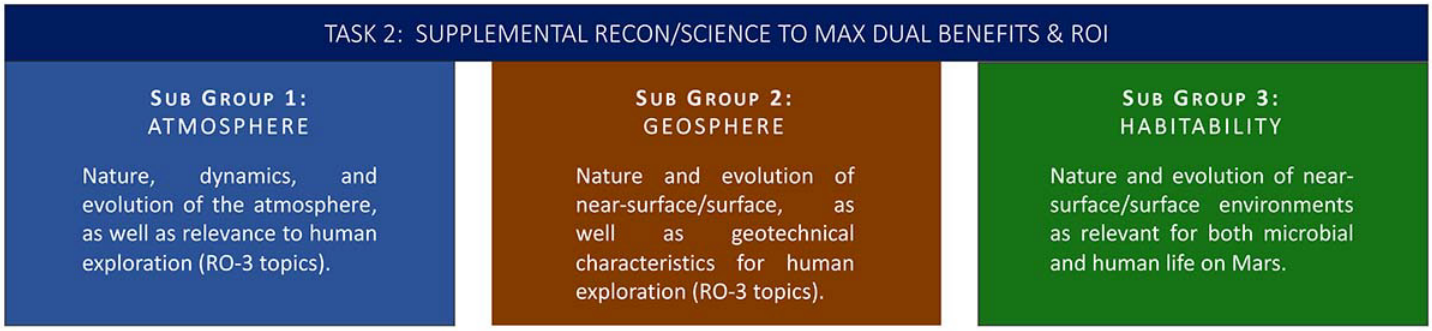

Figure 3.4 MDT Structure to Address Task 2

Note: In this report, “complementary” instruments refer to those identified to complete the Task 1 reconnaissance objectives, and “supplementary” instruments refer to those identified to accomplish additional science per Task 2.

Task 3 Process

MDT members developed a draft Concept of Operations (ConOps) based on Task 1 and Task 2 findings and traceability matrices. Per the MDT Charter, the first priority was optimizing the ConOps for meeting requirements-driving reconnaissance objectives, with a focus on the anchor instrument. Designing a ConOps to maximize opportunities for scientific investigations only using the SAR followed, then consideration of complementary and other payloads as in Task 2.

As described by the Agency partners, this process allows the multilateral Agencies to understand budget, accommodations, and other implications for:

- the design of a threshold mission based only on the anchor radar payload;
- the design of a baseline mission based on the addition of potential high-priority complementary payload(s) identified by the MDT and validated by consensus; and,
- the potential for other augmentations of high value to the international community (science and human mission planners), including instruments, communications relay capabilities, and the means of delivering more mass to Mars, as described by the supplemental science and mission-support objectives.

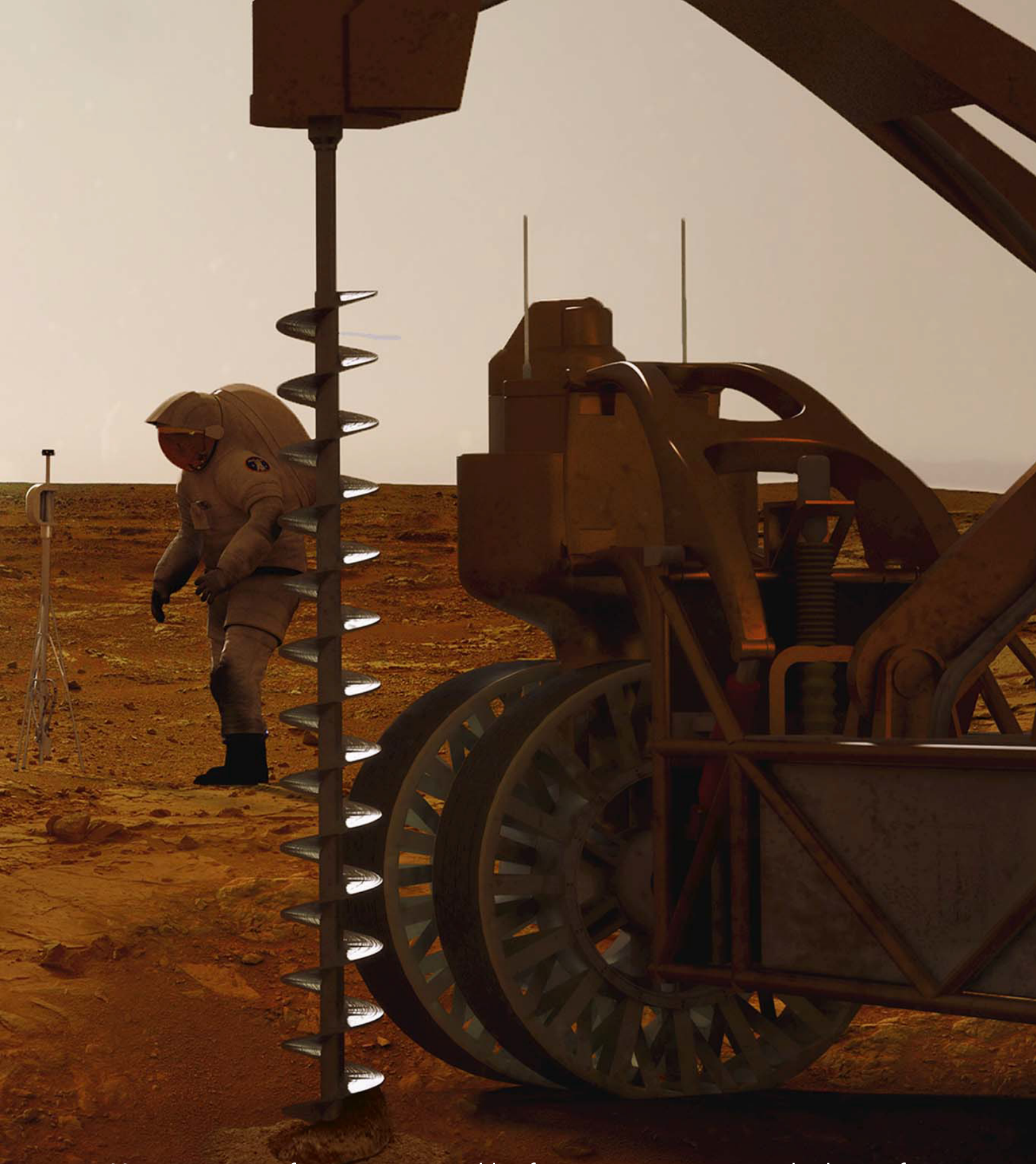

Mapping near-surface water ice enables future astronauts to sample the ice for science and use it as a local resource for surface operations, including producing propellant for the return trip to Earth.

Artist Concept. Credit: NASA Langley Advanced Concepts Lab/Analytical Mechanics Associates

4 TECHNICAL ANALYSIS: RECONNAISSANCE OBJECTIVES

> The Charter directed the MDT to develop measurement requirements to pursue the overarching Reconnaissance Goal: "to map and characterize accessible (within the uppermost 10m) subsurface water ice and its overburden in mid-to-low latitudes to support planning for the first potential human surface missions to Mars."

The Charter further defined the three Reconnaissance Objectives (ROs) that drive the measurement requirements for the Reconnaissance Goal (see Section 2.1). The MDT referred to this consideration of the mission reconnaissance goal and objectives as MDT Task 1. Based on expertise and cross-fertilization (cross-disciplinary, cross-national, career-level, and other factors), the MDT formed three groups targeting the Reconnaissance Objectives:

RO-1 Tasked with determining the measurements required to detect, map, and inventory the spatial distribution and depth-to-ice of water-ice in the near surface (top 0–10 m). Included 17 members.

RO-2 Tasked with determining the measurements required to detect, characterize, and map the surface/near-surface geotechnical properties (roughness, compactness) to provide a fundamental understanding of the accessibility of water-ice resources (characterization of the overburden and the structural stability of the terrain). Included 17 members.

RO-3 Tasked with determining the measurements required to provide detailed high-resolution maps of targeted areas of interest that have adequate and accessible water-ice, are as equatorward as possible, and model the potential for human-led surface science, human-class EDL, ISRU, and civil engineering. Included 15 members.

These RO groups included members from two additional MDT groups, including:

Human Mission Planning (HMP) Group

- Tasked with providing input to the RO groups regarding measurements specifically required for human mission planning. Included 9 members.

Radar Group

- Tasked with providing input to the RO groups regarding radar capabilities and measurements needed to support radar data collection. Included 17 members.

The RO groups' efforts built around the concept of key "parameters." In this context, the MDT defined a parameter as a characteristic of surface or subsurface materials, the knowledge of which was important for advancing the reconnaissance objectives of the mission. The parameters are intended to be measurable to some degree, by some method, with a focus on those that could be constrained by the radar anchor payload (L-band SAR and Sounder). Other key parameters may be only partly (or not at all) constrained by such a radar; the MDT noted these and explored alternative methods to obtain them.

For each identified parameter, the groups developed a definition; a rationale for constraining the parameter (why is it important in the context of the mission goals?); the needed scale, resolution and/or accuracy; and, the priority/value of the parameter (high, medium, or low). In addition, the groups assessed the capability of the radar to obtain the parameter (is the radar necessary and/or sufficient to obtain it?); which radar modes would be applied; and, what functional requirements would be placed on the radar to study this parameter. Most of the adopted parameters require the application of algorithms or other data-analysis methodology to convert an instrumental measurement into a constraint on a material or geometric property of the surface/subsurface.

The RO, HMP, and Radar Groups therefore described the expected methodology to be used, including any key assumptions or models (existing or to-be-developed). In many cases, the MDT found that fully constraining a parameter to the desired level would require more than a single type of measurement. For example, several of the parameters associated with the configuration of ground ice could be partly constrained by polarimetric SAR imaging, but would benefit strongly from additional observations from a sounder or topographic sensor. The groups identified any parameters that needed a complementary observation not provided by the anchor radar payload.

The cumulative collection of such parameters, and the complementary tools that could be used to constrain them, formed the basis of the MDT consensus recommendation of complementary payloads useful for achieving the Reconnaissance goal and objectives.

In the following sections, the parameters identified by each of the RO groups are described, along with details of the rationale, importance, capability of payload elements, and analysis methodologies. These results form the basis of the Reconnaissance Traceability Matrix (RTM; Section 4.5). The RTM captures in abbreviated form the complete list of key parameters identified in Task 1, along with short descriptions of their characteristics.

4.1 RO-1: LOCATION AND EXTENT OF WATER ICE

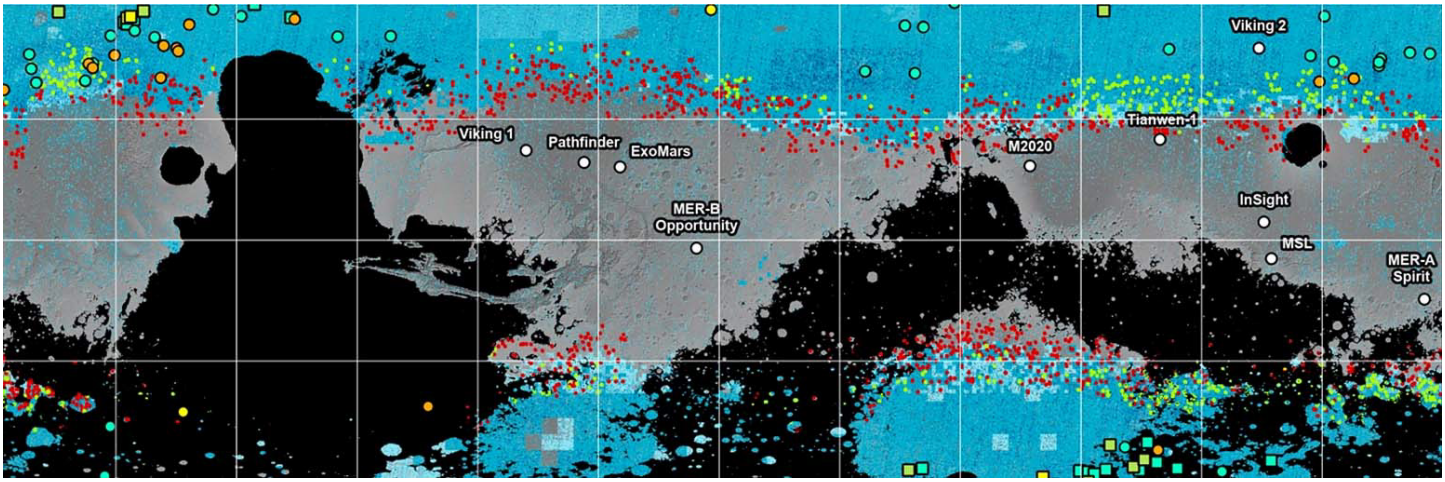

Potential Midlatitude Ice on Mars (aqua areas). *Credit: NASA/JPL-Caltech/Mars SWIM Team*

The objective of the RO-1 Group was to determine what parameters are needed in order to detect, map, and inventory the spatial distribution and depth of water ice in the upper 10 meters of the Martian subsurface that could be used as a potential water-ice resource and support ice science within the Reconnaissance Zone. The RO-1 Group established 6 top-level parameters (Table 4.1) to address this objective and refined these into more specific sub-parameters that the team used to define measurements aligned with the top-level parameters. Selection of parameters aimed to close the current knowledge gap of where ice exists within the upper 10 m of the subsurface.

Table 4.1 Top-level parameters and relationship to RO-1 charge

	RO-1 PARAMETERS	RO-1 RELATIONSHIP	RTM
1.	Ice Presence/Absence	Ice Detection	1
2.	Ice Concentration Profile with Depth	Ice Inventory	2.1A & 2.1B, 2.2, 2.3, 2.4, 2.5, 4.1A, 4.1B
3.	Lateral Extent & Continuity of Ice	Ice Spatial Distribution	3.1, 3.2
4.	Non-ice Component Properties	Ice Inventory	4.2, 4.1C, 5.4
5.	Overburden/Surface Properties	Ice Inventory	5.1, 6.1, 6.2, 6.3, 6.4A-E
6.	Other Science Parameters	Ice Inventory	7.1, 7.3, 7.4

4.1.1 Scientific/Technical Basis for RO-1 Parameters

In the last ~3 billion years, the climate of Mars has been cold and dry. Water present at the surface and near surface has mostly been in the form of ice, and ice stability has been driven by orbital variations analogous to Milankovitch cycles on Earth (e.g., Head et al. 2003; Laskar et al. 2002). In Mars' current obliquity (i.e., the tilt of the rotational axis), ice is only stable on the surface at (and near) the poles, as kilometers-thick ice caps with a combined volume similar to the Greenland ice sheet (Smith et al. 2001a). However, in the last decade, aided by the high-resolution data and continuous monitoring by spacecraft missions by NASA, ESA, and other space Agencies, substantial evidence has emerged supporting the presence of abundant ice buried across the mid latitudes of Mars. Growing evidence suggests that much of this ice may be relatively widespread, concentrated (low amounts of lithic impurities), extend very near to the surface, and occur at lower latitudes than previously thought (in some regions of the northern hemisphere, as low as ~35°; e.g., Figure 4.1), potentially providing a large in situ resource for future human explorers to Mars. Additionally, the ice is of interest scientifically, as a comprehensive understanding of the distribution and nature of this ice would place constraints on Mars' climate history and total water budget. Sampling by human missions (e.g., NASA First Ice Cores from Mars Report, 2021) would enable analyses of environmental records within the ice and the search for habitable environments and life.

Several direct detections of this ice have been made in the last ~15 years. In 2008, NASA's Phoenix lander excavated both pore-filling (ice which fills into the pore spaces of regolith) and excess (massive ice exceeding the pore space of the regolith) ice in the upper centimeters of the surface at 68°N (Figure 4.2a; Mellon et al., 2009; Smith et al., 2009). Cameras onboard NASA's Mars Reconnaissance Orbiter (MRO) spacecraft have imaged sites where a meteorite happened to impact Mars' surface in between two images being acquired; at some mid-latitude sites, such impacts exposed nearly-lithic-free ice (<10% dust by volume) under less than a meter of debris (Figure 4.2b) (Byrne et al., 2009; Dundas et al., 2014, 2021). More recently, in both hemispheres, cliffs have been found (Figure 4.2c) that expose thick (~100 m) deposits of ice (Dundas et al. 2018, 2021). Additionally, numerous geomorphological features, such as polygonal and

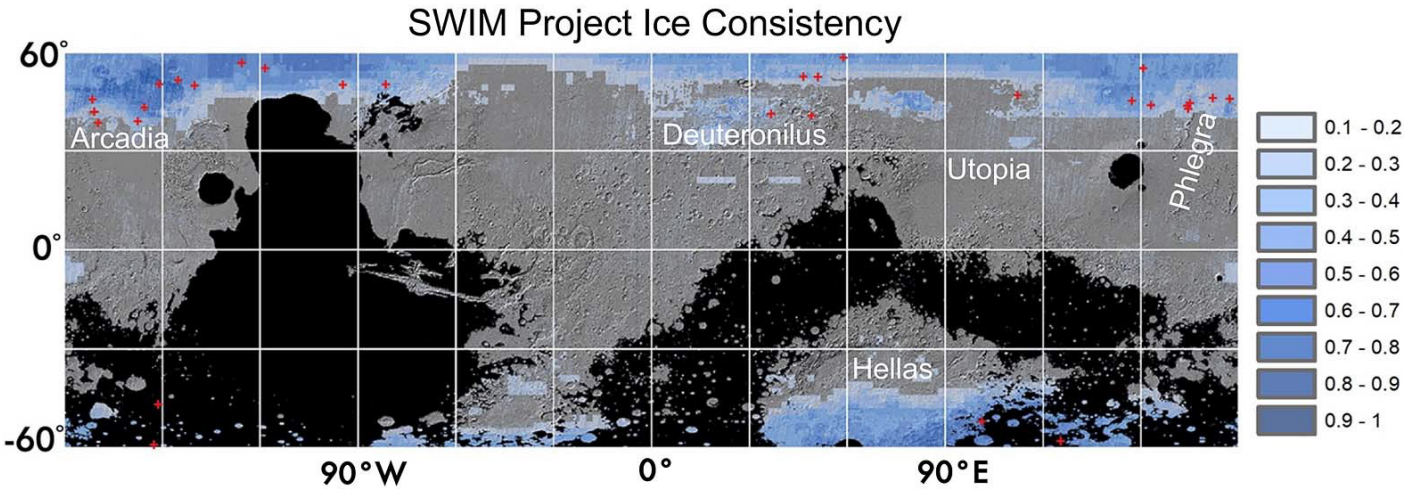

Figure 4.1 SWIM map of total ice consistency from multiple datasets (darker blue indicates that multiple remote sensing datasets are more consistent with presence of ice) within 60 degrees of the equator. Red + symbols represent locations of ice-exposing impacts. Basemap is MOLA shaded relief and black masks indicate elevations above +1 km. Figure adapted from Putzig and Morgan, et al. 2022. An update to this map is forthcoming after release of this I-MIM MDT report and will be available at the SWIM Project website (swim.psi.edu).

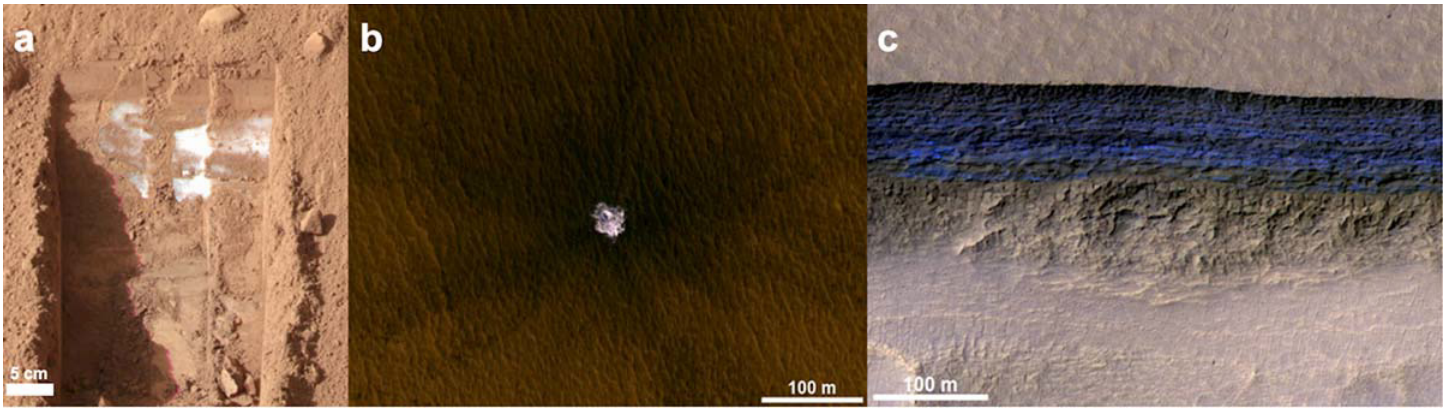

Figure 4.2 Recently discovered sites on Mars that expose buried ice in the mid-latitudes: a) Ice exposed by trench dug by the Phoenix lander at 68°N; b) New impact crater at 44°N that exposes and excavates nearly pure ice, c) Icy cliff site at 56°S that exposes ~100 m thick ice. *Credit: NASA/JPL-Caltech/UArizona*

thermokarstic terrains (Seibert and Kargel, 2001; Costard and Kargel, 1995; Mangold et al., 2004) and the Latitude-Dependent Mantle (LDM; a meters-to-tens-of-meters-thick layered deposit that drapes topography; Kreslavsky and Head, 2002; Schon et al., 2009) suggest a recent and/or present-day excess ice-rich subsurface across the mid latitudes. However, the specific properties of the ice and its vertical and horizontal distribution in the subsurface are poorly constrained from imaging datasets alone.

The presence of shallow ice is consistent with several geophysical remote-sensing datasets. For example, data from the Mars Odyssey Neutron Spectrometer (MONS) show the near subsurface (upper ~meter) of the mid latitudes in both hemispheres to be hydrogen-rich, which has been attributed to the presence of water ice (Feldman et al., 2011; Wilson et al., 2018; Pathare et al., 2018). Detections consistent with excess ice in the upper meter typically occur at latitudes greater than ~55°N/S (Pathare et al., 2018), which coincides approximately with the latitudinal onset of polygonized terrain imaged by high-resolution cameras, interpreted as having formed by thermal contraction cracking of ice-rich materials in the shallow subsurface (e.g., Mangold et al., 2004). More equatorward (<55°N/S) shallow ice is still detected in the upper meter, but typically in smaller volume percentages, perhaps reflecting the progressive deepening of the zone of predicted ice stability towards the lower mid latitudes and removal of destabilized ice from the near surface. That is in broad agreement with geomorphic evidence for the progressive dissection of the LDM towards the lowest latitudes of its distribution (e.g., Kreslavsky and Head, 2002; Head et al., 2003). However, regions exist where excess ice detections from neutron spectrometry extend to relatively low latitudes (e.g., in Arcadia Planitia) (Pathare et al. 2018). Additionally, thermal infrared sensing – by instruments such as the Thermal Emission Imaging System (THEMIS), Thermal Emission Spectrometer (TES), and Mars Climate Sounder (MCS) – is consistent with abundant shallow ice, for example, detecting ice to latitudes as low as ~35°N in Deuteronilus Mensae (e.g., Piqueux et al., 2019). However, these techniques are only sensitive to the properties of the very shallow (upper ~meter) subsurface, and therefore cannot provide information regarding deeper or thicker ice deposits (Figure 4.3). Sensing of deeper and thicker ice becomes particularly important towards the lower mid latitudes, where the theoretical depth of the thermal stability of subsurface ice deepens beyond ~1 m. Additionally, these techniques generally have large spatial footprints on the surface and are sensing regional-scale bulk properties, rather than capturing the local-scale variability that is expected within the shallow ice and that would be necessary for characterizing candidate sites for human exploration.

Radar can sense deeper into the subsurface (e.g., Figure 4.4); the Shallow Radar (SHARAD) ground-penetrating-radar instrument onboard MRO has detected subsurface interfaces attributed to the

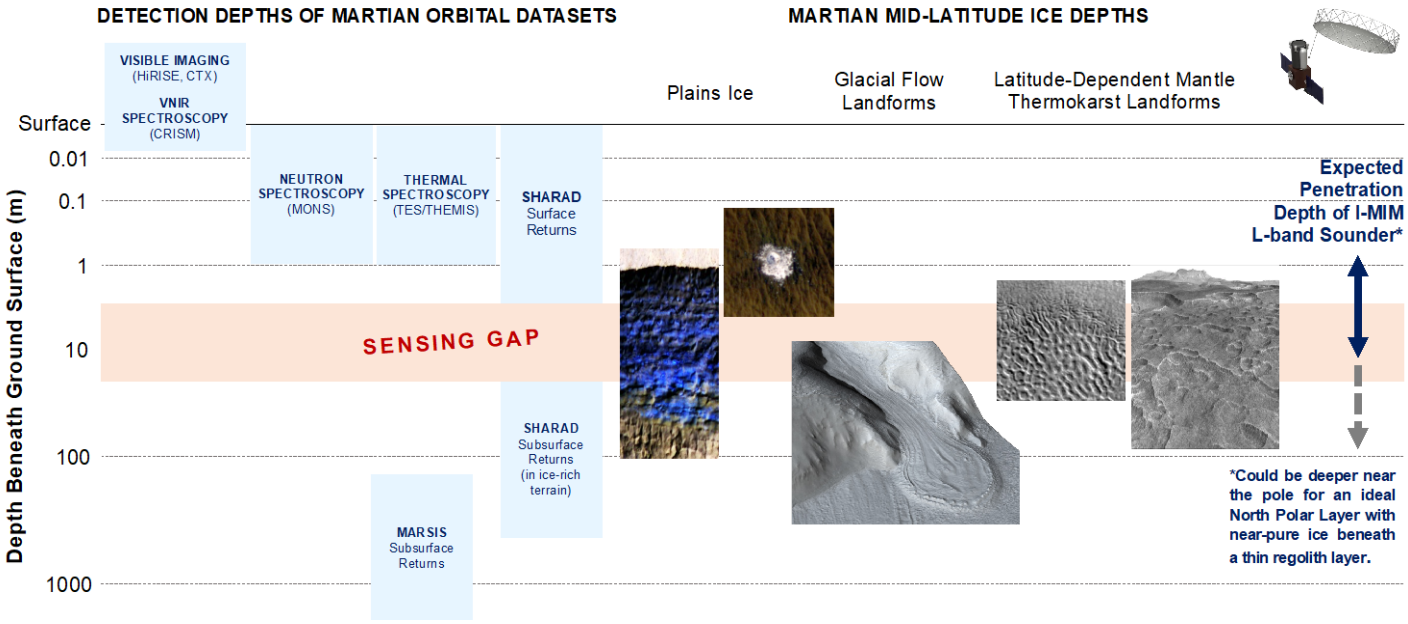

Figure 4.3 A vertical sensing gap in remote sensing datasets at Mars occurs at the meters to tens of meters depths, which are depths of importance for various icy landscapes in the mid latitudes.

bottom of broad, excess ice sheets across the plains regions of Arcadia Planitia (Bramson et al., 2015) and Utopia Planitia (Stuurman et al., 2016). These units are tens of meters to a hundred meters thick, and likely covered by a fine, insulating dust layer (often referred to as a "lag deposit") that is thought to have accumulated from dust, originally in the ice matrix, that gets left behind during sublimation of the upper portion of the ice during climatic periods of ice instability (e.g., Schorghofer, 2007; Levrard et al., 2007). Studies of signal attenuation suggest that the bulk of the unit sensed by the deeper subsurface reflectors must have on the order of tens of percent lithics present within the ice (Campbell and Morgan, 2018), which is in line with recent updates to the dielectric permittivity inferred from combining SHARAD subsurface reflections with topographic measurements (Morgan et al., 2021). Despite these capabilities of SHARAD, its spatial footprint and vertical resolution in the subsurface is not suited to detecting subsurface interfaces – including the top boundary of the ice in the subsurface – within relatively thin and/or shallow (10s m) deposits in the mid latitudes. The surface echo of SHARAD can provide constraints on the density of the upper several meters of the surface. In many places across the mid latitudes, this surface reflectivity analysis suggests low-density material, but this technique cannot uniquely distinguish between low-density ice or lithics with high porosity.

SHARAD subsurface sounding has detected the beds of many 'viscous flow features' (VFFs), which are mid-latitude morphologic features up to hundreds of meters thick and tens of kilometers long (Holt et al., 2008; Plaut et al., 2009; Petersen et al., 2018). VFFs are now widely interpreted as debris-covered glaciers deposited by snowfall during periods of higher planetary spin-axis obliquity (e.g., Head et al., 2005). They occur in various topographic settings across Mars' mid latitudes (e.g., Souness et al., 2012; Levy et al., 2014). VFFs that occupy large, wide valleys are termed 'lineated valley fills' (LVFs) (Squyres, 1978, 1979); those that occupy smaller, high-relief valleys (e.g., in mountainous or cratered terrain) are termed 'glacier-like forms' (GLFs) (Hubbard et al., 2011); VFFs that fill impact craters are termed 'concentric crater fills' (CCFs) (Squyres, 1979); and, VFFs that are topographically unconfined and extend across plains (e.g., away from mountainsides or valley outlets) are termed 'lobate debris aprons' (LDAs) (Squyres, 1978).

Analysis of SHARAD data (e.g., Figure 4.4) overcame a decades-long impasse on the ice contents of VFFs (e.g., Squyres, 1978, 1979; Luchitta, 1984; Colaprete

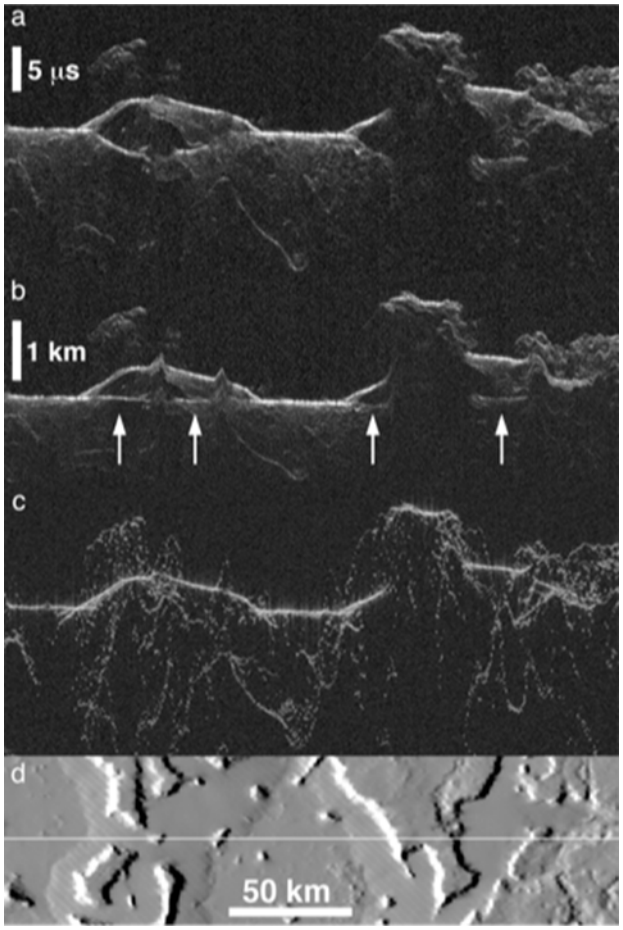

Figure 4.4 SHARAD radar sounding analysis over LDAs located near 39.1°N, 24.2°E. a) SHARAD observation 719502, with time delay as vertical axis and distance along the spacecraft track as the horizontal axis (North to the right). The brightness of each pixel indicates echo power; b) The same radargram as in (a), depth-corrected with a subsurface dielectric constant of 3.2 (pure water ice), which causes the basal interfaces (white arrows) associated with the LDAs to become coplanar with adjacent surrounding valley floor; (c) Simulation of radargram based on topography to show expected off-nadir topographic echoes (radar "clutter"); and (d) MOLA topography along the ground track. (Figure from Plaut et al., 2009).

and Jakosky, 1998; Mangold et al., 2002; Head et al., 2005), and it is now well understood that LDAs have ice contents up to 90% by volume (Holt et al., 2008; Plaut et al., 2009; Petersen et al., 2018) and provide the most confident detections of subsurface glacier-like ice outside of the polar regions.

In some regions such as Deuteronilus Mensae, Phlegra Montes, and Arcadia Planitia, shallow ice detections overlap with VFF distributions (e.g., Piqueux et al., 2019; Pathare et al., 2018). In some locations, fresh impacts into VFFs have exhumed shallow ice, which could source from the top of the glacial ice or from smaller (albeit still substantial) ice lenses within the debris cover (Dundas et al., 2021). To date, the contact between the debris cover and glacial ice within VFFs has not been detected; it likely occurs within the 0–15 m depth zone where SHARAD cannot resolve subsurface interfaces. As relatively low-latitude, high-purity (low lithic content) glacial ice deposits, VFFs could be of interest for ISRU (e.g., Hoffman et al. 2017; Baker and Carter 2019a). Better constraints are needed on the depth to ice, its spatial variations, and the nature of the covering material.

Recent efforts to integrate the datasets and techniques mentioned above attempt to address the outstanding questions that remain surrounding the distribution, properties, and accessibility of mid-latitude ice. These include studies across swaths of the northern plains regions (Orgel et al., 2019; Ramsdale et al., 2019; Séjourné et al., 2019), as well as large areas of the entire mid-to-low latitudes of both hemispheres (Morgan et al., 2021; Putzig and Morgan et al., 2022, In Press). However, the currently available datasets have been pushed to their limits, as a critical sensing gap (Figure 4.3) exists between the shallow remote-sensing techniques (including SHARAD surface returns) and the depths that can be sensed by subsurface returns from the SHARAD (15–25 MHz; 15 m wavelength) and MARSIS (1.3–5.0 MHz; 60–160 m wavelength) radar sounders.

Each sub-parameter below builds a sequential refinement in understanding the inventory and distribution of ice in the subsurface. At a minimum, ice presence/absence is a "must-have" value to meet RO-1. To inventory the ice within the Reconnaissance Zone successfully, the vertical distribution of ice must be determined, ideally at multiple locations, so that the spatial variability in ice content and depth can be determined.

Determining the non-ice components of ice-rich subsurface regions is next in priority to distinguish usable ice from non-usable ice (e.g., ice with solutes or particulate matter in it, which would increase the

processing costs to a point at which it would not be feasible to utilize it). Understanding intermixed non-ice components will also help distinguish accessible ice from inaccessible ice that is contained in lithic materials through which it would be difficult to mine. Finally, the additional science parameters would provide added return on investment by increasing the science return from I-MIM by helping to distinguish between major competing hypotheses related to the origin of ice in the Martian subsurface and the climate history recorded in those ice deposits.

RO-1 Parameter 1 – Ice Presence/Absence (RTM 1)

Locating subsurface ice deposits is the focus of the I-MIM mission, supporting the identification of ice-rich candidate locations for human-led ice science, human-class ascent, ISRU, civil engineering, and other surface operations. It also supports investigation-based science (Section 5.0) by addressing the water inventory, climate, and volatile-cycling evolution of Mars. This top-level parameter has a binary value where ice is either present or absent within the footprint and detection limits of the I-MIM sensor suite. Thus, Parameter 1 does not contain any sub-parameters; it simply provides targeted assessment of subsurface ice presence, expanding from the geophysical/geomorphological confidence maps from the Mars SWIM project (Morgan et al., 2021; Putzig and Morgan et al., 2022 In Press) and landform-focused geomorphic mapping (e.g., Levy et al., 2009; Mangold, 2005) or grid-mapping (Ramsdale et al., 2019; Séjourné et al., 2019) of ice-related landforms. Determining ice presence meets RO-1 Ice Detection and will determine the most equatorward ice deposits in the Reconnaissance Zone.

RO-1 Parameter 2 – Concentration Profile with Depth

To meet RO-1 Inventory of Near-surface Ice in the RZ, ice concentration with depth defines the vertical distribution of ice in the Martian subsurface. Based on prior radar, geomorphology, and modeling studies, ground ice on Mars may be present in a wide variety of configurations, including pore ice (ice present in voids between sediment grains or within bedrock voids) and excess ice (ice exceeding sediment pore space, either as veins, wedges, buried glacier ice, or snowfall, etc.). It may also be layered as a consequence of its emplacement history.

This parameter assists in identifying accessible ice across the RZ, as well as its most equatorward locations. It supports the identification of candidate sites for human exploration and characterizing them for human-led science (e.g., ice sampling/coring) and of potentially stable ground for landing and infrastructure emplacement, ISRU, civil engineering, and other life-support needs. To maximize science benefits, it also informs an understanding of mid-latitude ice stability under current and past climate conditions and provides insight into ice origin.

RO-1 2.1 (RTM 2.1A & 2.1B) Depth to the Top of the Ice

While surface water-ice is present perennially at the Martian poles and seasonally at high latitudes (Boynton et al., 2002; Feldman et al., 2004; Zuber et al., 1998), ice within the RZ (nominally between 25° and 40° latitude) is expected only beneath overlying sediment or rock. Burial of ice at depth limits the penetration of the annual thermal wave and keeps the ice from warming to the frost-point temperature, at which point it would sublimate and diffuse out of the soil column (Mellon and Jakosky, 1993; Schorghofer and Aharonson, 2005). Ice is only expected within the zone of thermal stability; however, ice may not be present within the subsurface zone of stability at a given location based on its depositional and removal history. In the uppermost 10 m of the soil column, heat flux is dominated by thermal diffusion from insolation, rather than upwelling geothermal heat, producing a limit to ice stability in the upper portion of the soil column that is set by atmospheric temperature and humidity and the thermal diffusivity of the overburden.

The depth in the subsurface that never reaches above this annual average frost-point temperature defines the top of the zone of ice stability and the depth at which ice is predicted to be present (Mellon et al., 2004), largely a function of latitude, albedo, thermal inertia, and insolation. This depth forms an ice-bearing or ice-cemented horizon analogous to the ice-table in terrestrial permafrost environments (Bockheim et al., 2007; McKay, 2009). Ice could be present at shallower depths over geologically short timescales if diffusively disconnected from the atmosphere by overlying materials.

RO-1 2.2 (RTM 2.2) Thickness of Ice in the Upper 10 m

Coupled with the depth to the top of the ice, this parameter identifies the thickness of subsurface ice and defines the depth range over which it is present. Ice may extend tens to hundreds of meters deeper than the upper 10 m reconnaissance depth in some locations (e.g., Holt et al. 2008; Plaut et al., 2009; Conway and Balme, 2014; Bramson et al., 2015; Stuurman et al., 2016; Dundas et al., 2018), or may be present in thinner mantles or lenses of up to a few meters thickness (Head et al., 2003; Schon et al., 2009). Determining the depth range over which ice is present can constrain its depositional history and distinguish between diffusive and depositional models for ice emplacement, and can also help constrain the amount of ice available for ISRU.

RO-1 2.3 (RTM 2.3) Nature of Ice/Overburden Transition

This parameter characterizes how ice-free subsurface material becomes ice-rich approaching the ice table. Transitions may be abrupt, with ice-free sediment transitioning directly to excess ice or pore-filling ice, as observed at the contacts with buried ice sheets beneath the Phoenix lander (Smith et al., 2009) and in contacts with pore-filling ice observed in Phoenix lander trenches (Mellon et al., 2009). Alternatively, the transition may be gradational, with sediment slowly increasing in ice content towards saturation and/or excess ice. Determining the nature of the ice/overburden contact would help distinguish between ablational contacts (where sublimation removes excess ice in the subsurface) and depositional contacts in which ice is being deposited in pore space as a consequence of vapor transport.

RO-1 2.4 (RTM 2.4) Integrated Ice Mass in the 10 m Subsurface Column

This parameter encompasses a mass estimate of ice in the RZ as a column abundance, which includes the starting and stopping depths of the ice, the ice/rock mixing ratio, the vertical distribution of that ice/rock mixing ratio, and the void space present in ice-rich domains. Determining the total mass of ice in the upper 10 m of the subsurface is the final step in inventorying the stock of ice available for ice sampling, ISRU, civil engineering, and other purposes at a location on the Martian surface, and constrains the water ice inventory of the near-surface environment.

RO-1 2.5 (RTM 2.5) Ice Porosity

This parameter identifies the fraction of void space within ice-dominated domains in the subsurface. Ice can be present in several configurations, from high-porosity, vapor-emplaced frost or hoar (e.g., Fisher, 2005) or snowfall, to compact, low-porosity ice that has undergone snow metamorphism, compaction, or densification with or without melt phases and/or recrystallization, as occurs in terrestrial firn.

Surface snow and ice (on Earth) range in density from ~100 kg/m^3 (porosity up to ~90%) to ~900 kg/m^3 (porosity approaching 0), so knowing the porosity of ice-rich domains would help determine the expected yield from ice ISRU processes and the relevance of the deposits to human-led ice sampling, while also providing insight into ice geotechnical properties for planning surface operations. Useful thresholds for porosity/density determination might be >30% (frost and snow), 10–30% (firn or otherwise densified snow), and <10% (compact ice bodies).

For high-value science described in Section 5.0, it would also help distinguish between ice emplacement and evolutionary processes. Ice emplaced within the last 2–4 million years is unlikely to have experienced widespread active (thawed) layer formation (Kreslavsky et al., 2008), and, as a consequence, is unlikely to have been concentrated by liquid water movement through soil. Older ices may have undergone more extensive thermal processing, firnification, etc.

RO-1 2.6 (RTM 4.1A) Ice/Rock Mixing Ratio

This parameter determines the volume percentage of subsurface ice. Ice can be present in pore spaces between sediment or rock grains (i.e., pore ice), constituting a volume fraction up to the porosity of the host lithic material, or can exceed the porosity of the substrate (i.e., excess ice) as either ice lenses or massive ice bodies (French, 2013). Ice-rock mixing ratio defines the "grade" of ice as an ISRU resource and provides key insight into its depositional history, distinguishing pore-filling vapor mechanisms from excess-ice-forming precipitation and burial mechanisms, including snowfall burial and glacial ice emplacement, etc.

RO-1 2.7 (RTM 4.1B) Layering of Ice

This parameter determines the vertical zonation of ice in the upper 10 m of the RZ. Ice could be continuous below the ice table, or could be present in one or multiple layers of interbedded ice and lithic material (Schon et al., 2009).

Varying lithic content in ice-dominated portions of the subsurface could relate to the depositional history of the ice, while sediment-rich bands in the subsurface could be related to debris entrainment and ice flow processes or sublimation lag formation during periods of ice destabilization.

RO-1 Parameter 3 – Lateral Extent & Continuity Of Ice

This parameter aims to understand the spatial distribution and lateral heterogeneity of ice deposits within the upper 10 m of the subsurface across the RZ. This parameter addresses the thinning or thickening, shallowing or deepening, and starting or stopping of ice-containing layers across the RZ. This information is important for inventorying ice, locating ice boundaries, understanding climate change and ice preservation processes, inferring ice origin, estimating infrastructure stability, and determining ISRU locations and the traverse distances between these sites. Several hypotheses for the origin of mid-latitude ice deposits exist, and there is evidence that multiple mechanisms have operated. They include: burial of ice deposited by airfall (Dundas et al., 2018; Head et al., 2003), vapor deposition of pore ice (Mellon and Jakosky, 1993), or ice lens formation via vapor emplacement (Fisher, 2005). Airfall deposits have the potential to be the thickest and most homogenous, with vapor-phase emplacement likely to include vertical and lateral heterogeneities at scales ranging from centimeters (differences between rocks and ice lenses) to hundreds of kilometers (e.g., variability associated with surface energy balance).

RO-1 3.1 (RTM 3.1) Spatial Continuity of Ice (Patchiness)

While the *stability* of ice within the Martian subsurface is controlled by latitude, albedo, thermal inertia, and insolation, the *presence* of ice within that zone of stability is a function of the history of atmospheric and geological processes active at that site over time (Schorghofer, 2007). Patchiness in ice presence near the limits of ice stability may result from differences in original emplacement or in evolution via heterogeneity of overburden thermal properties, slopes, or albedo (Putzig and Mellon, 2007a).

Ice distribution and thickness in the vicinity of impact craters and ejecta may vary as a result of differences in ejecta porosity, distance from the center of the crater, or thermal history (Heet et al., 2009).

RO-1 3.2 (RTM 3.2) Probability Distribution of Ice Presence as a Function of Distance

After determining the column distribution of ice at multiple locations (applying sub-parameters from RO-1 Parameter 2 to multiple sites in Sub-parameter 3.1), the probability of identifying subsurface ice of a given concentration can be determined for the region around any potential landing/launch site or other areas of interest in the vicinity (e.g., locations of interest for science, ISRU, civil engineering, and other infrastructure emplacement).

RO-1 Parameter 4 – Non-Ice Component Properties

Non-ice components can affect our ability to detect and to quantify ice, can affect the effective utilization of ice as a resource, can alter the potential habitability of the ice, and can change the thermal behavior and strength of ice. These effects have direct implications for ice inventory, ground stability, ISRU, and astrobiology. Additionally, non-ice components (i.e., lithics, solute, or air) affect technology choices for future extraction. Non-ice components may also provide information about the origin, history, or habitability potential of subsurface ice.

RO-1 4.1 (RTM 4.2) Salts/Solutes in Ice or Ice Matrix

The presence of salts and solutes in ice or in the ice matrix directly affects the usability of ice as an ISRU resource, and may generate potentially habitable brine droplets or lenses. Although solutes are largely excluded from water ice during the freezing process, dissolved salts commonly concentrate between ice grains along crystal boundaries. Solutes may freeze-concentrate to produce brines (saturated solutions) that could remain unfrozen at temperatures approaching those present in the upper 10 m of the Martian subsurface (Davila et al., 2010; Möhlmann, 2011). Chloride and perchlorate salts are present across the Martian surface and may be common in ices in contact with sediments (Hecht et al., 2009; Leask et al., 2018; Osterloo et al., 2008).

RO-1 4.2 (RTM 4.1C) Grain Size Distribution of Lithics in Ice

In terrestrial permafrost environments, sediment grain size plays a large role in active (thawed) layer water transport, vapor diffusion, and the generation of unfrozen water droplets via matric potential (French, 2013). Fine-grained sediments (i.e., clay- to silt-sized particles) inhibit vapor and water flow by decreasing permeability. They simultaneously promote the growth of segregation ice during the freezing of water-saturated sediments by driving cryosuction as a consequence of strong capillary rise/matric potential in fine-grained sediments. Fine-grained sediments can also maintain unfrozen water droplets to temperatures well below freezing due to matric forces generated by silicate-water bonding (French, 2013). Materials hosting ground ice on Mars are likely to comprise fine-grained and larger (boulder-to-cobble-sized) lithic materials in spatially varying mixing ratios. Observations suggest that some lithics exist within buried glacial ice on Mars (Butcher et al., 2021; Dundas et al., 2018), and large lithic fragments have also been observed on and within the debris cover (Baker and Carter, 2019a; Levy et al., 2021). Lithics may also exist in lower-latitude, near-surface ice deposits on Mars, potentially in higher volume fractions due to ice-removal processes.

RO-1 4.3 (RTM 5.4) Presence of Steeply-dipping Debris/Dust Layers

Steeply dipping bands interpreted as dust/debris-rich layers have been directly observed in mid-latitude VFFs (e.g., putative debris-covered glaciers; Butcher et al., 2021) and in ice-exposing cliffs (Dundas et al., 2018). In addition, indirect observations of boulder clusters across debris-covered glaciers at middle and high latitudes are inferred to indicate the presence of internal debris bands (Levy et al., 2021). This finding suggests

that internal debris layers may be common in ice-rich, debris-covered, glacier landforms that are otherwise low in lithic content. These debris bands are either too thin or too steeply dipping to be detected by SHARAD (Holt et al., 2008; Plaut et al., 2009), but need to be identified to avoid intersecting them when accessing ice. Thus, identification of steeply-inclined debris bands is an important step in inventorying near-surface ice, as debris layers may affect the accessibility of otherwise highly concentrated ice deposits.

RO-1 Parameter 5 – Overburden/Surface Properties

The properties of materials overlying subsurface ice bear directly on the stability, depth, concentration, origin, and preservation of that ice, which together makes assessing this parameter an important step in understanding the vertical and horizontal distribution of ice across the RZ.

RO-1 5.1 (RTM 6.1 & 6.2) Lithology of Surface Cover

Determining the grain size distribution, lithology, and composition of the material overlying ice will help determine whether the ice is in equilibrium with current climate conditions or is a relict of past climate conditions that has not yet equilibrated. This can occur when surface materials have low permeability or thermal/albedo properties that limit warming of the subsurface or that limit diffusive exchange of water vapor out of lithic materials (Kowalewski et al., 2006). The presence of large lithic material (e.g., surface boulders) can increase heat flux into the subsurface, deepening the ice table (Sizemore et al., 2010).

RO-1 5.2 (RTM 6.4B-E) Surface Roughness

Microtopography at the surface of ice-rich units increases roughness and shadowing, which can reduce heat flux into the subsurface, and which can also be used as a morphological indicator of ground-ice presence (e.g., the presence of diagnostic landforms or slopes exceeding the angle of repose). Surface roughness also alters atmospheric exchange with subsurface ice (Kowalewski et al., 2012). In addition, surface roughness generated by the topography of fine-grained sediments or the presence of large clasts can scatter radar energy away from ice-rich units, limiting the detectability of underlying ice (Petersen et al., 2018). For those reasons, measurement of surface roughness at height scales comparable to radar wavelengths are needed in order to understand uncertainty associated with non-detections of basal reflectors.

RO-1 5.3 (RTM 5.1) Thermal Properties of Overburden

Thermal inertia largely governs the penetration of the annual thermal wave into the subsurface and determines the depth beneath which ice will be stable relative to the atmospheric frost-point temperature (Putzig et al., 2005). Thermal properties aid in inventorying ice by determining how close ice at a given depth is to equilibrium and how changes to the overburden thickness affect the longevity of the ice against sublimation. For ice present within one annual thermal skin depth of the surface, thermal inertia measurements can detect ice (e.g., Bandfield, 2007) that may be too shallow to detect using the sounder.

RO-1 5.4 (RTM 6.3 & 6.4A-C) Surface Morphology/Local Slopes

A wide variety of landforms including thermal contraction crack polygons, scalloped depressions, expanded/terraced craters, and scarps have been used directly or indirectly to infer the presence of ground ice within the upper 10 m of the subsurface on Mars (Dundas et al., 2018; Hibbard et al., 2021; Levy et al., 2009; Mangold, 2005; Mellon, 1997; Mustard et al., 2001; Viola et al., 2015; Bramson et al., 2015; Zanetti et al., 2010). Intact or presently forming landforms provide strong morphological evidence for

ice presence within the annual thermal wave depth of the subsurface because landforms such as thermal-contraction- crack polygons require high tensile stresses resulting from rapid (shallow) cooling to form. They only form where ice cements sediments or is present as excess ice beneath those sediments, providing cohesion to form brittle fractures.

RO-1 Parameter 6 – Other Science Parameters

These parameters provide additional insight into RO-1 ice inventory efforts by providing constraints on the formation and evolution of subsurface ice. Different formation mechanisms (e.g., precipitation of ice particles versus direct frost emplacement) may inform predictions about ice concentrations at depths greater than 10 m or may be useful in interpreting the regional spatial extent of ice distributions.

RO-1 6.1 (RTM 7.1) Subsurface Temperature Profile

The subsurface temperature profile determines the stability of ground ice, as well as constrains the water activity of any brines in contact with that ground ice (Koop, 2002). The current temperature profile largely controls the spatial and vertical distribution of subsurface ice, including depth to ice beneath the seasonal thermal wave and active layer. Under current conditions, discordance between the presence of subsurface ice and the temperature profile and predicted thermal stability may suggest emplacement under different climate regimes and at disequilibrium with the present climate. Temperature profiles are sensitive to properties of the shallow subsurface materials. Ice, and other high thermal inertia materials, within the thermal skin depth will absorb, store, and releases energy throughout the year. The presence and depth of these materials affects the amplitude and timing of annual temperature curves at the surface and subsurface compared to porous and/or ice-free thermal inertia materials (e.g., Bandfield, 2007; Piqueux et al., 2019).

RO-1 6.2 (RTM 7.3) Ice Grain Size

Ice-grain size provides insight into ice thermal and depositional history. Ice bodies with larger grain sizes have a greater volume to surface-area ratio, decreasing the effects of solute concentration at ice-grain margins. The ice-crystal size, shape, and orientation are directly related to the processes controlling ice emplacement, such as the direction and speed of the freezing or ice-crystal growth process. These characteristics may help to distinguish between ice types and genesis, including segregated ice, open-cavity ice (e.g., vapor diffusion), or buried ice (e.g., snowpack or glacial) (French, 2013).

RO-1 6.3 (RTM 7.4) Surface Frost Thickness, Extent, & Composition

Seasonal and episodic surface water-ice frosts can reverse vapor gradients for near-surface ice bodies, enhancing their stability against sublimation and increasing their persistence, even when average temperature and relative humidity conditions might result in their destabilization and removal (Kowalewski et al., 2012; Lacelle et al., 2013; McKay, 2009; Williams et al., 2018).

Frost duration can also be used as an indirect measure of ice presence in the subsurface and can provide additional lines of evidence for estimating the depth to the top of the ice table (Vincendon et al., 2010).

4.1.2 Methodology to Constrain the Parameters

Existing radar sounder and SAR methodologies could be used to constrain many of the parameters described above using the core I-MIM payload. Methods to constrain several of the top-level parameters follow.

To constrain broadly ice presence/absence (RO-1 Parameter 1), SAR and sounder observations can be used in concert. SAR observations would be a primary determining measurement over wide spatial areas. The circular polarization ratio is an established measurement to identify bodies of ice that have some inclusions, either as fractures, pore space, or internal scatterers. Values of CPR between 1 and 2 are in the range for bodies of ice, whereas values ≥2 are more indicative of blocky surface materials, and values <1 are smoother and are inferred to lack ice bodies (Campbell, 2016).

This method works best if the ice is two or more wavelengths thick and within the top 2–5 m of the subsurface, depending on the overburden. For the CPR, surface characteristics derived from stereo imagery can help differentiate between blocky surfaces that cause high CPR and ice bodies. Recent work has shown that examination of same-sense vs. opposite-sense polarimetric SAR data products can robustly characterize the presence of ice with ≳20% impurity content, at the sensing depth of the system (Rivera-Valentín et al., 2022). Sounder observations can be used to support ice-presence identification based on CPR surveys. For example, sounder reflections from dielectric permittivity contrasts would be used to identify ice bodies, and ice compositions could be confirmed based on two-way radar travel times, if additional information is available about the thickness of a unit. Alternatively, if the ice is within one wavelength of the surface, the surface power return can be used to calculate the dielectric permittivity, which is a strong determinant of near-surface ice content.

In order to constrain ice presence/absence using the core payload, several models would be needed to interpret the radar data. For SAR observations, models are needed to deconvolve roughness and dielectric properties (Grima et al., 2012, 2014a). Polarization ratios have a very robust measurement-to-interpretation pathway (Slade et al., 1992; Harmon et al., 2001; Black et al., 2001a, 2001b; Grima et al., 2012) and can be complemented by new techniques such as polarization decomposition (e.g., m-chi) (Raney et al., 2012, 2019). Ice detection via sounding requires a model of the geologic structure with depth that can be related to any observed dielectric permittivity interfaces. This is very robust where reflectors are present and the thicknesses of the layers are measurable (Nunes et al., 2011; Bramson et al., 2015; Stuurman et al., 2016), although in practice this relies on an assumption that the interface/layering in topography is also associated with the interface in dielectric properties causing the radar reflector. In areas where the geologic profile with depth is unknown, constraints on subsurface properties can be obtained by measuring the loss of radar energy between reflectors and/or inverting for the dielectric permittivity by depth, correcting the radargrams to plausible geologic forms (e.g., geologic strata are often assumed to be flat and continuous) (Holt et al., 2008, Plaut et al., 2009).

RO-1 Parameter 2 (Ice Concentration Profile with Depth) can be constrained using both sounder and SAR methods as well. SAR tomography can be used to infer the structure of the subsurface units. Sounding (below 20 cm depth for L-band) can measure ice concentration with depth using rate of loss of reflection from dielectric interfaces (Grima et al., 2009; Campbell et al., 2008; Campbell and Morgan, 2018).

As with RO-1 Parameter 1, ice-concentration-profile interpretations would be model-dependent. Near-nadir sounding plus SAR produces a robust roughness-reflectivity deconvolution that correlates with ice-profile structure, and which surface return power complements. Sounding is limited to knowledge of dielectric permittivity and the wavelength of radar. Surface reflectivity from sounding can be used to

determine dielectric permittivity in the upper two wavelengths of the subsurface, but models of surface roughness and scattering characteristics at sounder wavelength are needed (Grima et al., 2012).

To constrain the lateral extent and continuity of ice (RO-1 Parameter 3), SAR observations can use CPR from polarimetric radar to produce maps of the horizontal extent of ice deposits. Measurements need to be regional in scale (e.g., 30 m spatial resolution over wide swaths), could be targeted by landform, and could be generalized from higher resolution SAR observations (e.g., 5 m spatial resolution). Tomography from repeated SAR observations could help identify subsurface interfaces associated with ice deposits. Subsequently, the SAR sounding mode can be used as a follow-up of SAR observations that reveal CPR signatures compatible with ice to identify and measure the continuity of subsurface reflectors associated with ice deposits.

Ultimately, regional ice detection will require a SWIM-like analysis of the congruence of parameters, and not a single interpretive model. Models of penetration depth of radar at various wavelengths and in various substrates are needed to guarantee that polarimetric radar can be used to interpret returns from the top 10 m of the subsurface.

To determine non-ice component properties (RO-1 Parameter 4), sounder observations could be used (in particular, attenuation and loss tangent measurements, split chirp methods). Split chirp gives the attenuation at two frequency ranges, providing sufficient information to calculate the loss tangent (Campbell and Morgan, 2018). Interpreting sounder data related to complex geological systems requires an understanding of dielectric contributions from multiple phases. Three-phase (ice, rock, air) mixing models (e.g., Bramson et al., 2015; Stillman et al., 2010) exist; however, multi-phase models including salts must be developed. A need also exists to determine specular and non-specular surface-reflection characteristics and to develop sounder propagation/reflection models.

4.1.3 High-Value Complementary Data to Address RTM Parameters

None of the top-level RO-1 parameters require complementary data, but several would be enhanced or disambiguated by complementary observations such as the following:

High-resolution Stereo Imaging

SAR/SAR Sounder ice detection in RO-1 Parameter 1 could be corroborated by spectroscopic/color-filter imaging of fresh, ice-exposing impacts at High Resolution Imaging Science Experiment (HiRISE; McEwen et al., 2007) scale resolution, although it is worth noting that fresh impacts are typically first detected by Context Camera (CTX; Malin et al., 2007)-class imagers with broader mapping swaths, from which HiRISE observations have been targeted. Ice presence and vertical structure (e.g., layering) could also be better determined with a surface topography model from stereo imagery to correlate reflectors with exposed surfaces/material contacts and to model clutter (1 m vertical resolution, 1 m horizontal resolution). Importantly, HiRISE-scale-resolution stereo imaging could be used to identify blocky surfaces and thus disambiguate high CPR signals. Reducing image resolution to 50 cm or 1 m per pixel would degrade elevation model roughness calculations, potentially beyond the point at which they could be used for disambiguation.

Thermal Infrared (TIR) Spectrometer

Concurrent thermal infrared measurements of surface temperature could be used to complement depth-to-ice-table measurements. Detailed measurements of surface temperature that show spatial variation of thermal inertia can be used to infer ice depth for shallowly-buried ice at high (~60°N) latitude based on the increased thermal inertia of ice-rich sediments

under ice-free sediments (Bandfield, 2007; Bandfield and Feldman, 2008). This technique works when ice is present within the annual thermal skin depth, but would not be feasible for ice buried deeply (e.g., in the lower ~5–10 m of the reconnaissance depth). Accordingly, concurrent TIR measurements at THEMIS-comparable spatial resolution in the RZ could assist in the identification and depth determination for anomalously, shallowly buried ice; for example, ice on cold, pole-facing slopes or ice that is out of equilibrium (e.g., due to impact excavation or mass wasting) and is undergoing removal by sublimation.

VHF Sounder

A VHF sounder would enable detection of reflectors associated with ice deposits buried under materials too thick and/or too lossy for an L-band sounder. If both L-band and VHF sounders detect subsurface reflectors, then the presence and thus continuity of water ice could be determined by analysis of the frequency-dependent dielectric permittivity of subsurface materials.

4.2 RO-2: CHARACTERIZATION OF THE OVERBURDEN

Icy Scarp in the Southern Midlatitudes. *Credit: NASA/JPL-Caltech/UArizona*

The RO-2 Group discussed the parameters and associated measurements required to establish the geotechnical properties of the rock and regolith, or overburden, overlying any ice at a site (e.g., thickness, load-bearing, etc.). The objective of the RO-2 Group was to define the parameters necessary for defining the accessibility of water-ice in the Reconnaissance Zone, including those necessary for detecting, characterizing, and mapping near-surface geotechnical properties that constrain whether the surface is likely suitable for landing, infrastructure, operations, and mining of ice resources (Bussey and Hoffman et al., 2016; Polsgrove et al., 2016; Hoffman et al., 2017). The group also considered parameters and measurements that could constrain the geologic evolution of the overburden as related to the origin of underlying ice and the uppermost Martian surface.

The group began by introducing various parameters that could be relevant to the objective and quickly focused on discussion of the accuracy of associated measurements necessary to establish the occurrence, origin, and material properties/nature of the overburden. Emphasis was placed on defining a robust list of necessary parameters. These included parameter descriptions, units, and geospatial accuracy required meet RO-2 objectives, and the way in which these parameters tied to specific objectives (landing, habitat, trafficability, and/or ice access and mining concerns). The group established measurement requirements for each parameter, but placed less emphasis on definitions of absolute metrics. This strategy allowed the group to get feedback from the Radar and Human Mission Planning (HMP) groups on whether the intent of each parameter was clear and how realistic measurement capabilities of the I-MIM radar could satisfy the parameter requirements. Collaborating with the Radar and HMP groups also helped to establish the degree of overlap with parameters defined by the RO-1 and RO-3 groups.

In addition to considering which parameters could be directly measured by the I-MIM radar, the group considered additional measurements that could be addressed by additional (non-radar) payloads that were either required or highly desired prior to human landings. These measurements are listed as separate potential contributions to the mission payload and are discussed as such.

4.2.1 Scientific/Technical Basis for RO-2 Parameters

In RO-2 Group discussions, it became apparent that most parameters fell within three broad groups related to understanding the:

1. Nature of the Overburden Surface;
2. Thickness of the Overburden; and,
3. Stratigraphic and Structural Character and Complexity of the Overburden.

In considering the necessity of a minimum acceptable threshold for a parameter's mission criticality, the group ultimately decided to capitalize on its assembled expertise to include all possible parameters regardless of necessity to I-MIM in order to provide potential outcomes for other future potential Mars missions. The HMP and Radar groups took in the RO parameter inputs, considered associated measurement capabilities versus requirements, and integrated their findings into the RTM. The individual parameters defined by RO-2 are discussed in the order listed above, with references to the RTM for additional details. The Parameters and Sub-Parameters for RO-2 are discussed in order below, beginning with those related to understanding the nature of overburden surface, followed by those related to overburden thickness, and then overburden stratigraphy and structure. The subsequent section focuses on the radar and/or other measurements that can constrain these parameters.

Table 4.2 Top-level Parameters and Sub-parameters and their Relationship to RO-2 Charge

RO-2 PARAMETERS & SUB-PARAMETERS		RO-2 RELATIONSHIP	RTM
1.	**Nature of the Overburden Surface**	Compactness/Roughness	–
1.1	Character of the Overburden Surface	Compactness/Roughness	5.3
1.2	Surface Rock Distribution	Roughness	6.1
1.3	Surface Topography	Roughness	6.4
1.4	Composition & Hydration State of the Surface	Compactness	2.6, 4.1, 4.2, 4.3
2.	**Thickness of the Overburden**	Compactness	2.1
3.	**Character & Complexity of the Overburden**	Compactness	–
3.1	Structure & Stratigraphy of the Overburden	Compactness	5.4
3.2	Porosity of the Overburden	Compactness	5.2, 5.3B
3.3	Strength/Hardness of the Overburden	Compactness	5.3C
3.4	Rock Distribution	Compactness	6.1
3.5	Number & Nature of Interbeds	Compactness	5.4
3.6	Orientation of the Overbeds	Compactness	2.4, 5.4

RO-2 Parameter 1 – Nature of the Overburden

Threshold parameters regarding the nature of the overburden surface are critical for assessing whether a surface is suitable for landing, operations, and mining, and help to establish the necessary engineering requirements on associated systems (Golombek et al., 2003a, 2003b, 2012a, 2012b, 2017, 2018; Grant et al., 2004, 2011, 2018). These include knowledge of the degree to which a surface is load-bearing, as well as an understanding of the rock distribution on the surface and surface slopes at 5-m, 10-m, and km-length scales (Polsgrove et al., 2017; Trent et al., 2021). Baseline parameters include knowledge of the composition and/or hydration state of the surface and an understanding of local atmospheric conditions at a site (Trent, et al., 2021). Parameters related to the nature of the overburden surface emphasize information required for landing and operating on the surface of Mars, often with less direct relevance or benefit to advancing ice science (Toups et al., 2016; Polsgrove et al., 2017). However, they closely correspond with the scientific investigations defined by the Geosphere group (see Section 5.3).

RO-2 1.1 (RTM 5.3) Character of the Overburden Surface

Parameters related to the character of the overburden surface are important for a range of both operations and ice-science reasons (Golombek et al., 2003a, 2003b, 2012a, 2012b, 2017, 2018; Grant et al., 2004, 2011, 2018). Understanding the degree to which a candidate surface is load-bearing at a scale of 10s of meters laterally is fundamental to ensuring landing can occur safely. For example, it is important to understand how much material on the surface will be excavated when landing, whether the surface can support a landed spacecraft, infrastructure, and equipment of the scale needed to deliver and support humans on Mars. Data regarding whether a surface is load-bearing would ideally be presented in pascal units accurate to within ~10% of reality and may be related to the average/bulk density of the overburden.

RO-2 1.2 (RTM 6.1) Surface Rock Distribution

Knowledge of the surface rock distribution is required for factors ranging from constraining lander tolerance to expected landing and traverse hazards (or finding a suitable location where rock size-abundance is below tolerance limits) to assessing mobility capabilities to the siting of habitats. It is also an important constraint on the design of the mining system that will need to remove and or access beneath any surface rocks (Golombek et al., 2003b, 2012b, 2017, 2018; Grant et al., 2004, 2011, 2018). The surface rock distribution can also cause scattering of the radar signal (Mouginot et al., 2010; Grima et al., 2012) and limit the depth to which underlying ice can be detected. It is therefore important for understanding the setting at locales where ice may occur but not be detected in the radar data. The expected tolerance of landing and operating systems dictates that knowledge of size-frequency for rocks >30 cm within ~5% of actual abundance is required, as is knowledge of the variability in the distribution over length scales of 10s of meters.

RO-2 1.3 (RTM 6.4) Surface Topography

Accurate knowledge of surface topography, or the distribution of local slopes or roughness, is needed at 5-m, 10-m, and km-length scales, mostly to ensure that the surface is suitable for landing, constructing habitats, and operations (Golombek et al., 2003b, 2012b, 2017, 2018; Grant et al., 2004, 2011, 2018; Toups et al., 2016).

The limits on the various acceptable values are not yet known, as the tolerance of the landing craft and other hardware to surface relief have not yet been defined. As an example, however, the landing craft may need to target a circle on order of 100 m across (Craig et al., 2015), within which differences in relief of more than a meter, and slopes of more than a few degrees over 5–10 m lengthscales, are likely unacceptable (Polsgrove et al., 2017).

RO-2 1.4 (RTM 2.6, 4.1, 4.2, 4.3) Surface Composition & Hydration State

Baseline parameters related to the nature of the overburden surface include knowledge of the composition and/or hydration state of the surface and an understanding of local atmospheric conditions in the vicinity of a candidate landing site (Golombek et al., 2003b, 2012b, 2017, 2018; Grant et al., 2004, 2011, 2018). The former is primarily related to ice science and understanding how the surface compositional properties relate to the varying occurrence of ice that can help in understanding the formation and evolution of the near-surface materials.

RO-2 Parameter 2 – Thickness of the Overburden

For parameters related to the thickness of the overburden, the RO-2 Group considered a threshold of knowledge must include overburden thickness variations within the upper 10 m of the subsurface (with an emphasis on the upper 5 meters due to accessibility concerns), as well as the nature of the overburden-to-ice contact (e.g., topology, gradational vs. abrupt) (Hoffman et al., 2017). The RO-2 Group considered as baseline knowledge an understanding of overburden thickness, and therefore depth to the overburden-to-ice contact, where it exceeds 10 meters from the surface. These parameters are important for both operations and mining (i.e., accessibility) concerns, as well as ice science related to the origin and evolution of the ice deposits over time (Baker and Carter, 2019a; Morgan et al., 2021; Putzig and Morgan et al., 2022 In Press).

RO-2 2.1 (RTM 2.1) Thickness of the Overburden

Parameters related to overburden thickness are extremely important (Morgan et al., 2021; Putzig et al., 2019, 2022). Constraining the thickness of the overburden up to 10 m over a candidate ice resource (to within 50–100 cm actual thickness and ~100 m footprints laterally) is critical to understanding how and whether the ice is accessible. Several aspects to overburden thickness are important to understand: an overburden-to-ice transition in the uppermost 0.5 m, which is a “blind zone” to the anchor radar; the thickness and the way in which it varies from 0.5 m to 10 m depth; and, whether the overburden thickness can be constrained in locations where it exceeds 10 m. In addition, the abruptness and topology along the overburden-to-ice transition is a reflection of where ice may be locally shallow and more accessible and holds important information on the emplacement and modification of the ice deposit over time. Accordingly, the RO-2 Group focused mainly on measurements of overburden thickness up to 10 m, with an emphasis on achieving measurements to 5 meters that may represent the depth of accessible ice. Both the topology and the abruptness of the overburden-to-ice contact are considered threshold parameters. Overall, this set of parameters is important for both operations and mining (accessibility) concerns, as well as ice science related to the origin and evolution of the ice deposits over time.

RO-2 Parameter 3 – Character & Complexity of the Overburden

Parameters required for understanding the stratigraphic and structural character and complexity of the overburden include knowledge of the average overburden porosity/density, strength (hardness), the distribution of rocks >10 cm, number and expression of any interbeds, and the occurrence and thickness of any capping airfall deposits (e.g., that represent unique dust and integrity issues relative to other materials; see Grant et al., 2010). Parameters that are considered important, but not necessarily required, include knowledge of the orientation of any interbeds within the overburden and whether ice lenses may lie above the depth to any mineable ice that could be more accessible and whose occurrence and nature could help understand the evolution of the near-surface ice deposit. The stratigraphy

and structure of the overburden is important for understanding what may be encountered in the near surface while accessing water ice, which will influence the design of the mining operations equipment. The stratigraphy and structure also reflect the basic first-order geologic evolution of a site, providing knowledge that can be used to understand the origin of any ice that may be present below the overburden relative to the long-term history of the near surface (e.g., Squyres et al., 2004; Grotzinger et al., 2014, 2015).

RO-2 3.1 (RTM 5.4) Overburden Structure & Stratigraphy

Multiple parameters are important for constraining the stratigraphic and structural character and complexity of the overburden, particularly its homogeneity (e.g., determining if pore-filling ice is present or if there are low-porosity zones that might pose hazards to mining) and evolution, as well as how accessible the underlying ice might be (Morgan et al., 2021; Putzig and Morgan et al., 2022 In Press). The threshold parameters of average overburden porosity; strength (hardness); rock distribution in the overburden >10 cm in diameter; number of interbeds (if any); and, the occurrence and thickness of any capping airfall deposits (e.g., Grant and Schultz, 1990) are all critical for defining the capabilities that the mining equipment must have to access and harvest the ice. Parameters considered important, but baseline, include knowledge of the orientation of any interbeds within the overburden and whether ice lenses exist above the ice-table that could be more accessible than ice at depth and whose occurrence and nature could help in understanding the evolution of the near-surface water-ice deposit (Morgan et al., 2021; Putzig and Morgan et al., 2022 In Press).

RO-2 3.2 (RTM 5.2 & 5.3B) Porosity of the Overburden

Knowledge of the overburden porosity or density is desired to within 10% or 0.1 gm/cm-cubed of the actual value over tens of meters laterally in areas where ice is detected in the subsurface. The value is important for factors ranging from knowing the character and suitability of the near surface at landing to understanding the stability of mining trenches and whether the overburden can be used in construction materials. Moreover, if substantial pore-filling ice is present, the overburden may be considered a mineable ice deposit.

RO-2 3.3 (RTM 5.3C) Overburden Strength/Hardness

The strength or hardness of the overburden closely relates to porosity and load-bearing properties and should be constrained to within 10% of real values as measured in Pascals over 10 m lateral footprints. Hardness is directly related to the ease and associated design of mining equipment and how durable the surface is to landing and operations. Moreover, ice-science studies require access to the ice which will be significantly influenced by the strength of the overburden.

RO-2 3.4 (RTM 6.1) Rock Distribution within the Overburden

The distribution of rocks >10 cm within the overburden imparts important capability requirements on mining access tools and can provide clues to the origin of the overburden. For example, if many large rocks are present, then mining equipment will not likely be able to avoid them and will need to be designed to penetrate or remove them. If the rocks are confined to discrete horizons or are in the vicinity of an impact crater, then they might be related to ejecta emplacement that could both hinder ice access and inform the persistence (due to deeper burial) of an ice deposit in a particular location. Although the wavelength of the I-MIM radar makes it best suited to understanding the distribution of rocks 0.3 m and larger, both within and on the overburden, known aspects of rock-size-frequency distributions enable fairly reliable extrapolation to smaller sizes.

RO-2 3.5 (RTM 5.4) Number & Nature of Interbeds

The number and nature of interbeds within the overburden are important for understanding the age and emplacement processes of any underlying ice deposits, especially when they can be tied to surface outcrops that can be imaged and otherwise remotely explored. They are also critical for understanding whether a bed, or beds, with properties significantly different from the bulk overburden could impede access to underlying ice. A mantling layer of low-density non-water or carbon-dioxide ice air-fall deposits could be considered part of the stratigraphy and would pose a hazard to landing and operations. Disruption of fine-grained particles could create a health hazard to humans on the surface. Therefore, if such materials are present, it is important to know whether they are of a fine veneer or represent thicker materials whose properties may preclude landing at a particular site.

Ideally, the depth and extent of any beds within, or air-fall material on, the overburden should be known to within 1 m vertically and over horizontal distances of 10s to 100s of meters. Any of the strata noted could help to preserve an ice deposit and/or pose a serious challenge to landing and operations related to ice access. As result, knowledge of the occurrence of such layers to within 1 m vertical resolution across footprints of 10 m laterally is important.

RO-2 3.6 (RTM 2.4 & 5.4) Orientation of Interbeds

Finally, the orientation (to within several degrees of actual) of any overburden interbeds and/or the identification of ice lenses (meters thick and 100s of meters laterally) within the overburden could identify locations where ice could be mined with relative ease as compared to deposits more deeply buried or protected by deeper, more resistant rock beds. The orientation of any strata also has implications for the geologic evolution of the overburden. For example, dipping beds can help in understanding the transport direction of responsible emplacement mechanisms (e.g., ice-flow, aeolian, volcanic, or aqueous) or whether they uniformly drape underlying topography (e.g., ash or airfall).

4.2.2 Methodology to Constrain the Parameters

A variety of different measurements acquired using both SAR and sounder modes of the I-MIM radar can help constrain the character of the overburden surface (RO-2 Parameter 1.1). To evaluate the load-bearing capacity of the overburden at any site, both sounder and SAR measurements (e.g., surface reflectivity, polarization) can be used to determine shallow subsurface structure and density. These measurements would include evaluating dielectric permittivity, polarization, and stokes parameters, combined with radargrams, reflector coefficients, and circular polarization ratio (CPR). Additional data from thermal-imagers to evaluate dust cover and thickness, as well as information on albedo and morphology from imaging systems (mono and/or hyperspectral), can help support or confirm interpretations drawn from the radar data; some of these data are in-hand for various locations on Mars.

To constrain the surface rock distribution (RO-2 Parameter 1.2), I-MIM SAR-derived roughness, CPR, SAR tomography, and sounder reflectivity can all provide complementary information on rock sizes ≥30 cm and could be augmented by high-resolution image data, thermal inertia, or albedo data. Some of these data exist as HiRISE data for some portions of the Martian surface.

For surface topography and the distribution of local slopes or roughness (RO-2 Parameter 1.3), the I-MIM SAR and nadir reflectometry could provide key insights to constraining these values, bolstering existing data for some locations based on high-resolution stereo imaging (e.g., CTX, CaSSIS, HiRISE) and topography (e.g., MOLA, HRSC stereo). Alternatively, a high-resolution stereo imager carried on the I-MIM spacecraft could collect data that

satisfies this requirement in conjunction with the radar measurements.

Baseline parameters related to the composition and/or hydration state of the surface (RO-2 Parameter 1.4) and local atmospheric conditions likely cannot be achieved using measurements from the I-MIM radar. Instead, multi- or hyperspectral data is necessary to satisfy the measurements related to this parameter. Existing data could suffice in some locales (e.g., CRISM). As this parameter is mostly related to ice science and would require an additional payload element to satisfy, the RO-2 Group considered it a baseline parameter. Accurate modeling and understanding of the atmosphere at any landing site on Mars are requirements to ensure safe access to the surface and will likely require unique data sets collected using non-I-MIM orbital assets. Nevertheless, the historical importance (from prior landed missions) of having detailed atmospheric data for understanding accessibility of a landing site cannot be overstated and is included herein as a baseline parameter to ensure it is properly considered in the future.

A variety of measurements can also help constrain parameters related to the thickness of the overburden (RO-2 Parameter 2). Sounding and SAR tomography can be used to constrain the overburden thickness to depths of ~5 m and perhaps as deep as ~10 m, if assumptions are made regarding the dielectric properties. Establishing the abruptness and relief of the overburden-to-ice contact may be accomplished via a combination of multi-frequency (split chirp) sounding and SAR tomography. A caveat is that the InSAR requires well localized repeat passes and return of Single Look Complex (SLC) data (Massonnet and Feigl, 1998; Zhou et al., 2009). Constraints on overburden thicknesses less than 0.5 m and greater than 10 m (thickness would preclude ice access) are beyond the means of the anchor payload to measure, and would likely require alternate instruments to be carried on the I-MIM orbiter. For overburden thickness less than 0.5 m, neutron and gamma ray data and/or thermal inertia data could be useful and could draw from existing data sets. Understanding thickness of the overburden where it exceeds 10 meters depth and the topology or relief on the underlying overburden-to-ice contact could be measured via a longer wavelength sounder.

The I-MIM radar can also make measurements capable of understanding many of the parameters related to stratigraphic character and complexity (RO-2 Parameter 3.1). It is likely that a combined approach using both SAR and sounder investigations can help constrain porosity/density (RO-2 Parameter 3.2) using dielectric mixing models and SAR subsurface/volume scattering models that may be improved during future surface deployment of GPR or by using corner reflectors associated with a lander for absolute signal calibration (Grima et al., 2012, 2014b).

Both SAR and sounder modes of the I-MIM radar can provide proxy information related to hardness (RO-2 Parameter 3.3), using many of the same measurements for understanding the load-bearing and porosity parameters. Example measurements include knowledge of the dielectric permittivity, polarization, and stokes parameters, combined with radargrams, reflector coefficients, and CPR. Data obtained or derived from other measurements (e.g., thermal inertia, albedo, and high-resolution imaging of outcrops exposed in shallow craters) can also shed light on the hardness of the overburden. Nevertheless, precise constraints may require future surface investigations.

For the distribution of rocks in the overburden (RO-2 Parameter 3.4), many of the same radar measurements relevant to understanding the surface rock distribution can be used, including measurements of SAR roughness, CPR, and SAR tomography, coupled with high-resolution imaging data of outcrops, crater walls, and crater morphology (some exist; some would likely need to be acquired) should be able to satisfy the parameter.

The I-MIM radar should be able to help understand the number and nature of overburden interbeds (RO-2 Parameter 3.5). For example, using the radar in sounder mode coupled with sounder propagation/reflection models should achieve the

necessary resolution of interbeds within the overburden, though resolving multiple, closely spaced, and or thin beds (relative to the radar wavelength) may be problematic. The 10 m lateral requirement of the parameter could require InSAR and tomography with precise position control and knowledge during repeat passes and single-look-coherent radar data. High-resolution imaging of the surface could reveal muted morphologies indicative of the presence of a mantling air-fall deposit and provide some information on likely thickness based on the scale of expected versus identifiable features. Imaging of the overburden cross-section as exposed in craters or fractures could further help constrain the number and expression of stratigraphy and help with mapping the presence and thickness of air-fall materials. The same methods used to characterize the occurrence of interbeds could be used to evaluate the orientation of any beds, but detection of ice lenses would require detailed sounding (perhaps augmented by the addition of a VHF sounder) and/or polarimetric SAR (PolSAR). CPR could help distinguish between rocky and ice-rich lenses, but may not have sufficient information to constrain the depth at which they occur.

4.2.3 Radar Functional Requirements to Constrain the Parameters

It is clear from the preceding discussion and review of the RTM that a large majority of the RO-2 parameters related to understanding the geotechnical properties of the overburden can be completely or at least partially addressed via realistic performance expectations of the radar measurements made by the I-MIM anchor payload. Most of the measurements related to the threshold and baseline parameters appear achievable, including the most fundamental measurement of the thickness, and general character of, the overburden to at least 5 meters and perhaps up to 10 meters depth.

Additional parameters likely achievable with the model anchor radar payload performance include:

- understanding the rock distribution on and beneath the surface;
- definition of local surface slopes and surface roughness;
- characterization of overburden stratigraphy (if present);
- characterization of the regolith-to-ice contact; and,
- regolith porosity, overburden strength, and detection of ice lenses of possible ISRU potential.

4.2.4 High-Value Complementary Data to Address RTM Parameter

While the core payload meets a majority of parameters established by the RO-2 Group, it may be difficult to achieve several threshold parameters using the I-MIM radar, including the overburden strength and the degree to which the surface is load-bearing within the stated measurements ultimately needed by human mission planners, and (to a lesser degree) measure of the local surface relief and slopes at <10 m scale (Polsgrove et al., 2017). With the exception of the load-bearing parameter, however, most of these may be satisfied by existing or new stereo image data (e.g., HiRISE, CaSSIS) that has been or can be acquired during later missions, including landed deployment of ground penetrating radar and/or other instruments on the surface.

While the I-MIM radar cannot achieve parameters related to the composition of the overburden and characterization of local atmospheric conditions above a candidate landing site, past missions have

satisfied them using a variety of measurements/ interpretations (e.g., CRISM and MCS, respectively) and are included herein primarily for completeness.

Finally, most of the parameters addressed completely or even incompletely by I-MIM radar measurements could be improved and/or refined via interpretation of data from an orbiting HiRISE-to CaSSIS-scale stereo imager. While data from the named orbiting imagers continues to be collected and almost certainly covers some of the future identified ice deposits, it is equally likely that the unknown distribution of the ice means that many areas will not have been imaged. Such image data in tandem with the radar would help constrain interpretations by providing independent corroboration of radar-derived values (e.g., imaging of outcrops in crater walls, surface slopes from stereo data). The RO-2 Group deems to be of high value the modification of the anchor radar payload (including lower frequencies and/or a complementary VHF sounder that would enable interrogation of the overburden at greater depths) or other existing techniques and data sets (e.g., multispectral, thermal IR, atmospheric sounding).

4.3 RO-3: CANDIDATE HUMAN SITE ASSESSMENT

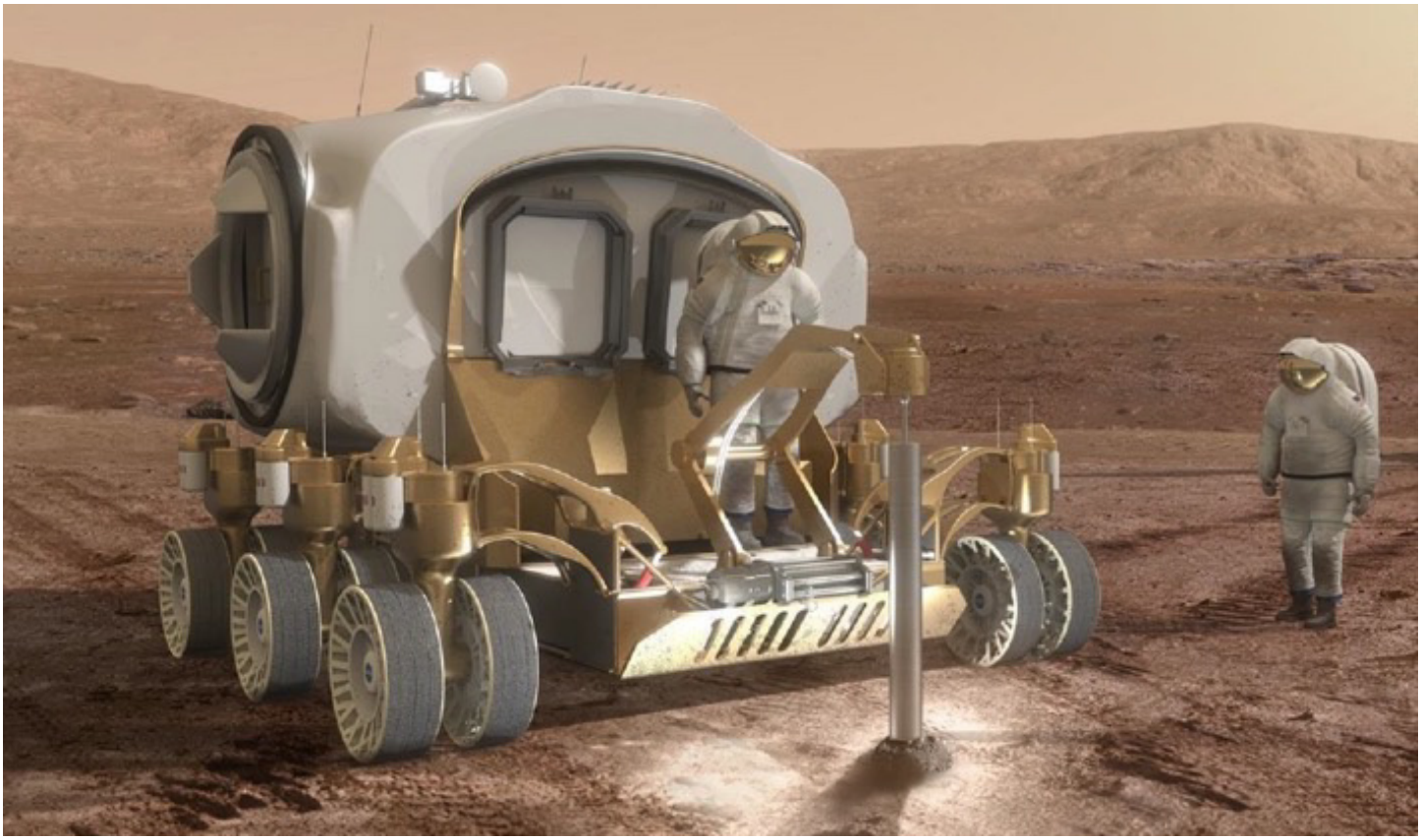

Artist Concept of Astronauts accessing near-surface water ice. *Credit: NASA*

The objective of the RO-3 Group was to provide information about the measurements human mission planners would need to characterize candidate locations for human exploration, contributing to the eventual selection and certification of sites for future human missions. Per the MDT Charter, Reconnaissance Objective 3 (RO-3) is to:

> *"provide detailed high-resolution maps of targeted areas of interest that: have adequate (RO-1) and accessible (RO-2) water-ice, are as equatorward as possible, and model the potential for human-led surface science, human-class EDL (entry, descent and landing), ISRU (in situ resource utilization), and civil engineering."*

For the purpose of this task, the term "targeted areas of interest" (TAI) refers to the area of coverage necessary to characterize candidate locations for human missions, as described by the ConOps plan in Section 6.0.

In considering measurements needed by human mission planners, the RO-3 Group provided rationales for the RO-1 and RO-2 parameters described in Sections 4.1 and 4.2, as shown in the RTM in Section 4.5. The RO-3 Team organized its contributions using the four focus areas in RO-3:

- Human-led Surface Science;
- Human-class EDL (entry, descent and landing);
- ISRU (in situ resource utilization); and,
- Civil Engineering.

Given the need for many orbital and surface measurements to select and to eventually certify a location for the scale and complexity of one or more human missions, the RO-3 Group found that a tiered landing site selection strategy is appropriate. Because the presence of ice at middle to low latitudes is central to human missions, the I-MIM payload provides a critical first step in identifying and characterizing these deposits from orbit.

The radar payload provides important first-order characterization of the overburden, rock abundance, ice thickness, extent, purity, and subsurface stratigraphy. Data returned from I-MIM would provide an important first step in identifying particularly attractive locations for the first human mission(s) (Beaty et al., 2016).

The I-MIM mission could include, or be followed up with, orbital high- and medium-resolution stereo imaging targeted to initial candidate sites for human exploration identified from analysis of I-MIM data. These orbital images would provide basemaps for more detailed mission planning to locate the best places for conducting scientific expeditions and emplacing the habitat, launch and landing pads, ISRU, power generation, and the roads that connect all of these elements. Long-term environmental monitoring stations could be sent to the top few candidate sites to provide detailed information that can only be acquired from the surface. Data from these surface assets could then be used to select the final location(s) for the first human mission(s) to the surface of Mars.

The RTM (Section 4.5) displays RO-3 articulated human-mission-planning needs as rationales for the RO-1 and RO-2 Parameters and Sub-Parameters.

4.3.1 Scientific/Technical Basis for RO-3 Measurements

A significant factor in RO-3 Group considerations was the scale of the human missions being considered for Mars, as provided to the MDT. The reference case for a human mission sequence included four to eight 50–70 MT landers (roughly the size of a two-story house), with precision landing (100 m-diameter landing areas) within an area to set up a human habitat, a power generation station, a launch pad, several landing pads, an ice mining and extraction operation, and the civil engineering infrastructure (roads, cables, etc.) that links them together (NASA 2021, 2022; Bussey and Hoffman et al., 2016; Toups et al., 2016; Hoffman et al., 2017; Polsgrove et al., 2017). The scale of these missions and the requirements needed to fulfill their needs places the level of data and knowledge far beyond anything considered for landing-site requirements for robotic missions to Mars and far beyond the requirements for the level of human “flags and footprints” Apollo missions to the Moon.

In this regard, although evaluating landing-site safety requirements for a 50 MT spacecraft might be able to be done with orbital data (as has been the case for all robotic landers to Mars), setting up a mining operation and constructing a small settlement on the surface of Mars requires information on a scale that cannot be determined solely from orbit (Beaty et al., 2016). As a result, a significant number of requirements to fulfill those necessary for the scale of the human missions to Mars being considered will require in situ investigations by ground-based and airborne assets in addition to orbiters. Accordingly, a tiered site selection effort that begins with orbital information and subsequently proceeds to landed and mobile robotic assets with drills should be considered.

The scale of potential human missions to Mars (as provided to the MDT) also makes it clear that the centerpiece of characterizing potential locations for human exploration is the water-ice needed to support the in situ production of propellant needed to return to Earth, and other human-habitation needs (Hoffman et al., 2017). As a result, the characterization of the ice depth, thickness, and purity and overburden that are central to the RO-1 and RO-2 Group investigations are also required for RO-3 Group investigations. The details of the spatial extent, depth to ice, purity, any layering, and thickness of the ice, as well as the

characteristics of the overburden, are necessary to begin looking for locations to land/launch, construct a continuously operated human-exploration site, prepare a water-ice mining operation, as well as high-priority human-led surface investigations such as ice sampling and coring for climatology and astrobiology (per the reference case provided by the Partner Agencies, including the First Ice Cores from Mars Report, 2021). Consequently, RO-3 views the main results of the I-MIM mission as an appropriate first step in beginning to search for, locate and characterize candidate sites for human exploration.

4.3.2 Methodology

The RO-3 Group had collective expertise in landing site selection, human mission planning, radar measurements, civil engineering, ice-related science, and analog field experience. RO-3 Group members with expertise in these fields gave individual presentations, followed by group discussion.

The charter for RO-3 was to

"provide detailed high-resolution maps of targeted areas of interest that: have adequate (RO-1) and accessible (RO-2) water-ice, are as equatorward as possible, and model the potential for four key areas:

- RO-3A, Human-led Surface (Ice) Science;
- RO3-B, Human-class Landing and Launch;
- RO-3C, ISRU (water ice in situ resource utilization); and,
- RO-3D, Civil Engineering."

4.3.3 RO-3 Parameters for Characterizing Candidate Sites for Human Exploration

The RO-3 Group contributed rationales for the parameters based on the four RO-3 focus areas. Individual requirements are referenced to the composite table of parameters used by all three groups. Observations that can and cannot be met by the I-MIM payload are identified. Both orbital and surface measurements are considered where more information may be needed.

RO-3A: CHARACTERIZING CANDIDATE SITES FOR HUMAN-LED SURFACE SCIENCE

Per guidance from the Agency partners (including the guiding First Ice Cores from Mars Report, 2021), the RO-3 Group focused on human-led ice science on the surface rather than all science that humans could pursue. The leading I-MIM science questions are related to the origin of the ice, the climatic implications, and astrobiology. These investigations require clean access to the ice (not contaminated by humans or equipment) and the desire to observe the stratigraphy of the ice, which would require the ability to acquire cores and a cold laboratory and storage facility with analytic instruments. It is clear that human-led ice science would need, a priori, a well characterized surface and subsurface stratigraphy.

However, it was not obvious that any other observations clearly stood out that would be required. As a result, the RO-3 Group identified no obvious separate requirements on the landing site other than sufficient characterization of the surface, ice, and subsurface stratigraphy to design access and acquire samples needed for these types of investigations.

RO-3B: CHARACTERIZING CANDIDATE SITES FOR HUMAN-CLASS LANDING & LAUNCH

Delivering spacecraft from the top of the atmosphere to the surface is one of the riskiest parts of human exploration, with significant uncertainties. I-MIM has the potential to remove knowledge gaps that would help human mission planners design approaches for safe landings. To date, no launches from the surface of Mars have yet been achieved, though the first is in planning with the Mars Sample Return campaign. A major challenge for both landing and launch is the size of human-class vehicles (on the order of 50–70 MT each). Not only would landing and ascent eject regolith at high velocities, potentially damaging other surface infrastructure, engine jets could fluidize sub-surface ice, creating craters that could significantly affect stability.

Artist Concept of a human-class ascent from the Martian surface (based on lunar model). *Credit: NASA*

For robotic landed missions to Mars, landing-site selection efforts have relied on remote-sensing data; ground truth information from previous landing sites; and, models to address engineering constraints, science objectives and planetary-protection requirements. The types of available information, and the fidelity and means of addressing the requirements and objectives in the post-Viking era, has improved dramatically from the selection of the Mars Pathfinder landing site, which had little new data beyond that provided by Viking 20 years earlier (Golombek et al., 1997). For the Mars Exploration Rover and initial Phoenix landing site selections, Mars Global Surveyor provided remote-sensing data (e.g., Golombek et al., 2003a). The final Phoenix, Mars Science Laboratory, InSight, and Mars 2020 Rover landing site selections (e.g., Golombek et al., 2012a, 2017) used medium-class (e.g., CTX) and high-resolution (HiRISE) images and spectral information from Mars Reconnaissance Orbiter to predict accurately surface characteristics important for safely landing the spacecraft (e.g., Golombek et al., 2005, 2008a, 2020a).

Overall, the characteristics and physical properties of surface materials at the landing sites have compared favorably with their orbital imaging and thermophysical properties (e.g., Christensen and Moore, 1992; Golombek et al., 2008a), which has substantially aided landing-site selection. Neutron, thermal, visible and near-infrared imagers and spectrometers (e.g., Grant et al., 2004, 2011, 2018; Arvidson et al., 2008) have also accurately predicted the materials present at the surface for investigation by landers and rovers to address their science objectives. Landing-site selection efforts also adequately addressed planetary protection requirements using available remote sensing data (e.g., Golombek et al., 2017).

While the experience with robotic craft offers a great deal to human mission planning, more knowledge is needed for safe pinpoint landings, hazard detection and avoidance (e.g., slopes, rocks etc.), and the load-bearing nature of the surface. All of these also inform the civil engineering that may be needed to prepare the site (e.g., construction of a landing/launch pad).

RO-3B TOPIC 1 EDL & Landing Ellipse

Human-class entry, descent and landing (EDL) includes aero-maneuvering and terrain relative navigation (TRN) to land in a 100 m-diameter landing circle (Polsgrove et al., 2016). The landing site must be below 0 km Mars Orbiter Laser Altimeter (MOLA) elevation (Smith et al., 2001a) to have sufficient atmosphere to slow the spacecraft during EDL (RTM 6.4b). Landing a 50 MT spacecraft requires large retrorockets with substantial thrust that will significantly erode unconsolidated or poorly consolidated material creating craters. Landing on bedrock or a surface with less than 0.1–0.2 m of regolith is preferred (Polsgrove et al., 2016). The surface must be load-bearing to support the 50 MT lander (RTM 5.3). Surface slope must be less than 15° at the scale of the lander (~10 m) and rover (~1–3 m) (RTM 6.4) and rocks and relief must be less than 0.3 m for landing stability and trafficability (RTM 6.1). The lander will use sensors and thrusters to avoid hazards during final descent, but the selected landing site must have hazard-free areas to find a safe touchdown location. If smooth, flat, load-bearing bedrock cannot be found, then launch and landing pads may need to be constructed. For thermal management and to reduce thrust needed to launch, the landing site should be as close to the equator as possible.

Precision landing a spacecraft on Mars requires carefully constructed basemaps in the cartographic frame (i.e., with respect to other surface features). Spacecraft in flight, however, are controlled in inertial space and during approach to Mars must be targeted to an entry point such that EDL will take it to the selected landing site. For Mars, the cartographic frame is provided by the Mars Orbital Laser Altimeter (MOLA; Smith et al., 2001a) binned DEM at 463 m/pixel. Because the Mars Global Surveyor spacecraft was tracked from Earth while MOLA was operating, the uncertainty between the cartographic and inertial frames is around 100–300 m (Arvidson et al., 2004a, 2004b; Golombek et al., 2020b). The MOLA cartographic frame is a positive east planetocentric coordinate system referenced to the International Astronomical Union / International Association of Geodesy, IAU/IAG 2000 frame (Archinal et al., 2018; Abalakin et al., 2002). Landing in a 100 m-diameter location in the cartographic frame requires TRN, which allows the spacecraft to use one or more orthographically controlled images (maps) of the landing site produced from orbital data to compare with images acquired during descent. This technique allows the spacecraft to "fly out" the cartographic-inertial uncertainty. TRN for the Mars 2020 landing system used an orthographic image compiled from four different 6 m/pixel Context Camera (CTX) stereo pairs (Malin et al., 2007). Landing in a 100 m-diameter circle will likely require a number of orthographically controlled TRN images of the surface over progressively decreasing areas with progressively increasing resolution that may vary from ~10 m/pixel to ~1 m/pixel. TRN orthoimages can be acquired by orbital cameras and produced well before launch. This need sets the requirement for multiple stereo images of the landing site at medium and high resolution to produce orthoimages at this scale (0.25–6 m/pixel).

RO-3B TOPIC 2 Slopes

Slopes within the landing circle must be <15° at the scale of the lander (~10 m) for touchdown stability and at the scale of rovers (~1–3 m) for trafficability (RTM 6.4B). Stereo HiRISE images at 0.25 m/pixel (McEwen et al., 2007) can produce digital elevation models (DEMs) with 1 m elevation postings (e.g., Kirk et al., 2008; Fergason et al., 2017). Stereo CTX images at 6 m/pixel can produce DEMs with ~20 m elevation postings (Fergason et al., 2017). This sets the requirement for 0.25 m/pixel stereo imaging of the landing site (RTM 6.4C).

RO-3B TOPIC 3 Rocks

Rocks that are larger than 0.3 m in diameter are generally considered a concern for Mars lander clearances (RTM 6.1). Most rocks on Mars are hemispheres, so a 0.3 m-diameter rock would be about 15 cm high. Relief of this amount over the scale

of the lander feet (1–2 m) would also be a concern. Prior to HiRISE images, the risk to landing on rocks of a given size were constrained by using thermal differencing estimates of rock abundance (total area covered by >~0.15 m diameter rocks; Christensen, 1986; Nowicki and Christensen, 2007) and size-frequency distribution models based on the Viking landing sites, rocky locations on Earth, and fracture and fragmentation models (Golombek and Rapp, 1997; Golombek et al., 2003b). With the advent of HiRISE images, individual rocks could be resolved from orbit and machine vision algorithms were developed that segment shadows from the image and fit ellipses to the shadows and cylinders to the rocks to (±1 pixel) measure accurately rock diameter and height for rocks greater than 1.5 m diameter (Golombek et al., 2008b). Rock size-frequency distributions measured in HiRISE images were then extrapolated along model curves to estimate accurately the number of rocks at smaller diameters (0.7–1 m diameter for Phoenix, Mars Science Laboratory, InSight and Mars 2020 Rover; Golombek et al., 2008b, 2012b, 2017). Note however, that relatively moderate extrapolation from rock diameters of 1.5 m to 0.7–1 m did not include large uncertainties and have been accurate. Human landing sites with few rocks >0.3 m diameter would likely have no rocks visible in HiRISE images, so it would be difficult to estimate quantitatively the rock abundance. For this reason, landing sites being considered for the Mars Sample Return lander currently under development, which can tolerate rocks as high as 0.19 m (0.38 m diameter), are located in areas where no rocks can be seen in HiRISE and require surface images from the Mars 2020 rover to measure rocks and certify the landing site.

Polarized radar backscatter expected from the core payload can detect areas with a high or low abundance of ~0.3 m diameter rocks (e.g., Neish et al., 2017a; Neish et al., 2021) (RTM 5.4b). These data provide qualitative estimates of rock abundance (e.g., high, medium or low) at a scale similar in size to the radar wavelength. Directly imaging rocks 0.3 m diameter and 0.15 m high from orbit would require stereo images with a resolution of ~5 cm/pixel, which would be very difficult from orbit. Examination of the InSight and Mars 2020 Rover and Ingenuity images does indicate that around 25% of rocks at the scale of HiRISE pixels can be detected and that relatively featureless, rock free areas in HiRISE do have very low rock abundance (Golombek et al., 2021, 2022; Brooks et al., 2022). As a result, it might be possible initially to select potential human landing sites based on their rock-free appearance in HiRISE (or a similar follow-up high-resolution imager) and their low rock abundance in radar backscatter, which could be followed up with surface or helicopter images at higher resolution in following missions to measure rocks <0.3 m diameter.

RO-3B
TOPIC 4 Bearing Capacity

The landing site for a 50 MT lander must have a bearing capacity that can support the lander (RTM 5.3). In addition, the retrorockets used to slow the vehicle will likely remove substantial thicknesses of loosely consolidated regolith and generate shallow craters beneath the lander (surface disturbance has occurred for all landers with retrorockets that fired near the surface). These craters could be large enough to affect the stability of the lander. As a result, the preference is to have the spacecraft land on strong bedrock that would restrict erosion of the substrate. Unfortunately, most of the mid-latitude ice deposits are in regions with relatively low to moderate thermal inertia (Putzig and Mellon, 2007b) and thus are covered by soils with low cohesion (Christensen and Moore, 1992; Golombek et al., 2008a) that would be easily mobilized by large retrorockets. If erosion of soil turns out to be a problem, landing pads (and launch pads) would need to be constructed. Although some information about the cohesion of soil can be inferred from orbital thermal inertia measurements, construction of landing and launch pads would fall into the civil engineering category discussed later, and would likely require in situ surface measurements of the chemistry, mineralogy and geotechnical properties of soils to make a strongly bonded surface material such as concrete for launch and landing pads.

RO-3 C: CHARACTERIZING CANDIDATE SITES FOR ICE-RELATED ISRU

In Situ Resource Utilization (ISRU) involves accessing, extracting, and processing water from ice to make it usable for human needs on Mars. Uses include propellant, life support, construction, mining, manufacturing, and eventually, agriculture. Substantial deposits of ice are needed to support human missions. As an example, 68 tons of water would support a crew of 4 during a 500-day mission (Hoffman et al., 2017).

ISRU is, in essence, the equivalent of setting up a mining and extraction process, which typically requires detailed information about overburden material properties, ice content and purity, and its mapped subsurface location and extent.

The I-MIM anchor radar payload is designed to obtain a first order orbital assessment of much of this information and is included in the results of Groups RO-1 and RO-2. However, it is highly unlikely that orbital remote sensing data by itself would be sufficient to design an ice extraction and mining technique and process. It is more likely that subsequent surface landers and/or rovers would be needed to provide the detailed information required (Beaty et al., 2016).

Nevertheless, the I-MIM radar payload could identify the location, distribution, and extent of ice deposits, as well as information about purity and overburden properties that would provide an excellent first step in identifying appropriate potential landing sites for ISRU and human-led ice science.

RO-3C
TOPIC 5 Nature of the Ice Deposit

Basic information about the ice deposit is needed to set up an ice extraction and mining operations. While the RTM details ISRU needs where relevant, the following are key points:

- The location and spatial extent of the ice deposit and surface topography must be known to decide where to locate the mine (RTM 1, 3).
- The overburden and ice deposits must be resolved to ~100 m spatial scale with a depth resolution of 1 m (RTM 3.1, 3.2).
- The mining extraction technique would depend on the depth and thickness (i.e., isopach maps), density, voids, purity and layering of the ice deposit (RTM 2, 4).
- The depth to the top of the ice deposit should be known to within 10s of cm, purity to within 5–10%, voids at the 10 cm scale, and the extent, frequency, and depth of layers within the ice to within ~10 cm (RTM 2.1, 2.5, 4.1).
- Impurities in the ice affect the extraction technique, so knowledge about the mineralogy, chemistry, and grain size of lithics or other impurities is needed, as is the presence of any bubbles, phase changes, or liquids (RTM 4.1, 4.2).
- Detailed information about impurities almost certainly requires in situ access to the ice via removal of overburden and/or drilling.
- Detailed information is needed about the overburden as it affects the mining operation and extraction technique (RTM 5). Isopach maps of overburden thickness and variations over the spatial extent of the ice deposit are needed to spatial scales of 10s of m and thickness to ~10 cm (RTM 2.1A).
- Detailed grain size frequency information from m to μm is needed along with the mineralogy and geochemistry of the overburden (RTM 5, 6.2). Although the I-MIM payload will provide orbital information relevant to this (RTM 5), detailed information will require in situ surface measurements.

RO-3 D: CHARACTERIZING CANDIDATE SITES FOR CIVIL ENGINEERING

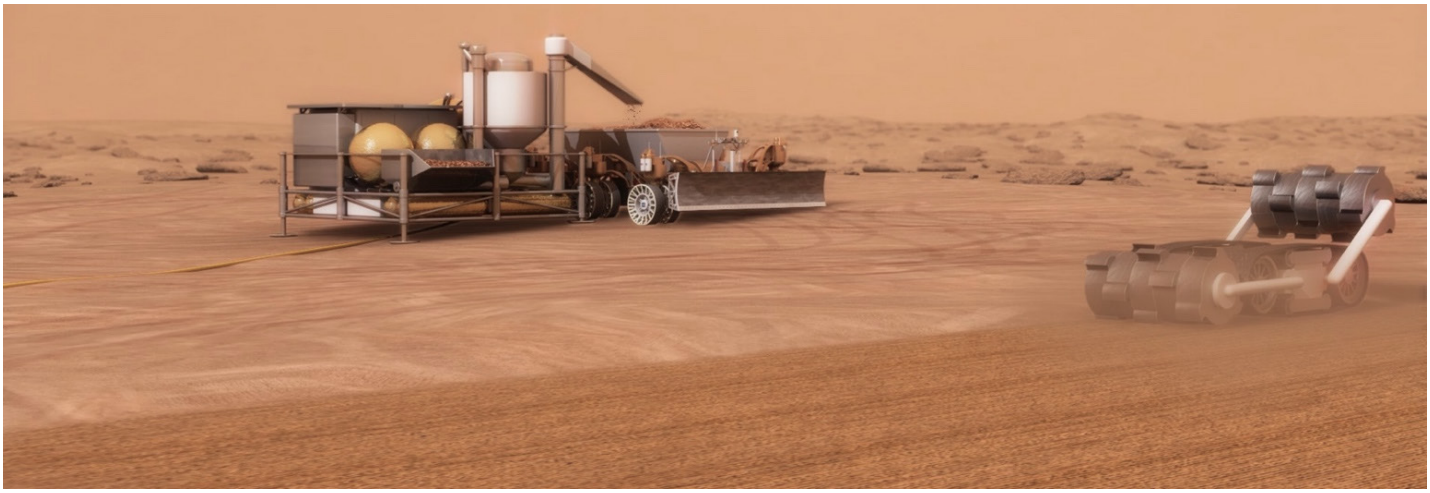

Artist Concept of Civil Engineering on Mars. *Credit: NASA*

Civil engineering considerations are an important component of the human mission scenarios presented to the MDT. In addition to the likely need to construct launch and landing pads and to set up an ISRU operation, other infrastructure (e.g., habitats, laboratories, power stations and roads) must also be constructed (Sibille et al, 2021). As for ISRU, although the I-MIM payload will provide important basic geotechnical information about the overburden and soils (RTM 5), the kinds of detailed information needed to construct habitats, landing pads and berms, a power station, and roads will almost certainly require in situ measurements.

Needs for characterizing candidate locations for civil-engineering fall into several categories: surface topography and slope, surface materials, subsurface stratigraphy, and surface environment. Topography and slope are clearly important for locating landing elements and constructing roads and must be known at least to the length scale of landers and rovers (down to ~1 m). Stereo images at 0.25 m/pixel would enable DEMs at a 1 m scale (RTM 6.4). Knowledge of surface material mineralogy and chemistry, density, permeability, shear strength parameters (including cohesion and angle of internal friction), grain size distribution, and rock type are all required for designing and building structures with surface materials (RTM 5.2, 5.3, 6.2). Some of this information can be constrained from orbital measurements. For example, thermal inertia can constrain particle size and cohesion, L-band radar measurements can constrain the density of rocks ~0.3 m in diameter, and spectral information may provide some information about surface mineralogy. Measurements of 0.2 m diameter rocks would require images with resolution of ~3–4 cm/pixel, which would be difficult from orbit.

Grain-size distribution would require surface measurements (microscope), and detailed information about material mineralogy, geochemistry, and material geotechnical properties would also require surface measurements. Information about the regolith thickness and layering in the subsurface down to 1–5 m is required to build habitats, launch and landing pads, roads, foundations and walls (RTM 5).

The I-MIM radar payload would provide preliminary information. It would need to be followed up with in situ Ground Penetrating Radar, cores, drill holes, and penetrometers to retrieve the necessary data at spatial scales of <1 m and depths of ~10 cm. Finally, the construction, operation, and management of surface landed elements and any possible hazard mitigation requires detailed knowledge of the surface environment over extended periods of time. Environmental monitoring of weather, radiation, impacts, seismicity, seasonal changes (climate, ice), aeolian changes, and mass wasting would require long term surface elements (RTM 8).

4.3.4 High Value Complementary Data to Address RO-3

In assessing observations by the anchor radar payload, the RO-3 team identified complementary instruments that would enhance the capabilities of I-MIM to identify and characterize potential candidate sites for human .

High-resolution Stereo Imaging

Orbital observations that are important for characterizing candidate locations for the class of human missions being considered should include high-resolution imaging. Stereo images at HiRISE class (~0.25 m/pixel) are needed for all of the input considerations to the RO-3 Group, including human-led surface science, landing and launch pads, ISRU, and civil engineering. Existing HiRISE stereo images cover only a small fraction of the Martian surface (a few %). For an actual human-class site selection and certification effort, it will be difficult to cover the areas being considered for human-class missions with the existing HiRISE instrument (e.g., as provided to the MDT as a reference case, a 100-km radius area allowing astronauts to explore beyond the immediate habitation area, yet stay within an acceptable range of it). As a result, whether as part of I-MIM or another future mission, a replacement for a HIRISE-class imager is ultimately required for human mission planning and eventual site certification.

Medium-resolution Stereo Imaging

Medium-resolution stereo imaging at ~6 m/pixel may be required to create TRN maps an orthoimages required for pinpoint landing. Medium-resolution images may be satisfied by existing CTX stereo images or higher-resolution images can be downsampled to create these.

Additional High-value Orbital Observations

Additional orbiting mineralogy or geochemistry observations and thermal observations that get at thermophysical properties (e.g., particle size, cohesion, and rock abundance) would also be helpful, particularly if they are at higher resolutions than previous observations.

Additional High-value Surface Observations

Surface observations ultimately required for ISRU and civil engineering (i.e., constructing launch and landing pads, including berms) involve detailed observations of the regolith, ice, and subsurface stratigraphy at spatial scales that cannot be achieved from orbit.

Surface observations by rovers on subsurface stratigraphy (e.g., GPR, cores), surface chemistry and mineralogy (e.g., in situ and laboratory instruments), soil grain-size-frequency distribution (e.g., microscope) and physical properties (density and soil mechanics, e.g., penetrometers). Airborne assets could provide very high-resolution stereo images at resolutions smaller than 10 cm/pixel. Finally, environmental monitoring stations could acquire long records of surface weather, radiation, seismicity and surface changes.

4.4 COMPLEMENTARY PAYLOADS

While the partner Agencies have not determined whether augmentations beyond the anchor radar payload are possible, they chartered the MDT to consider high-priority augmentations that might improve the mission's ability to meet its Reconnaissance Goal and Objectives. The MDT conducted an activity to prioritize additional payloads that would strengthen I-MIM's ability to meet its Reconnaissance Goal and Objectives ("Complementary Payloads"). Complementary Payloads increase the accuracy/interpretation of the SAR results and/or lead to the certification of candidate (accessible, ice-rich) locations for human exploration. This activity focused on relevance to the measurement requirements/ reconnaissance objectives, not the extent to which it might be feasible from an engineering, cost, or other perspective, which was outside the scope of the MDT and thus provided to the partner Agencies for future potential trade-space studies.

4.4.1 Complementary Payloads Considered

Per Table 4.3, the MDT organized the following complementary payloads into four categories. Team members voted for and prioritized at least one, and up to three, instruments, to assess the additional capabilities relevant to achieving the Reconnaissance Objectives outlined in the MDT Charter. The breakdown of results is shown in Figure 4.5 and Table 4.4.

Table 4.3 Payloads Considered for Prioritization

RADAR MODIFICATIONS/ AUGMENTATIONS	CAMERAS (EXAMPLE CLASS)	SPECTRAL SENSORS	OTHER
VHF Sounder (30–300 MHz)	**Hi-res Imager** (HiRISE; ~10s cm resolution)	**Thermal Spectrometer**	**Surface Investigation**
P-band Sounder (250–500 MHz)	**Medium-res Imager** (CTX/CaSSIS; ~5–10m resolution)	**VIS-IR Spectrometer**	**Neutron & Gamma Ray Spectrometer**
C-band Sounder (4–8 GHz)	**Low-res Imager** (e.g., 10s m or more resolution)	**Albedo** (Camera or Spectrometer)	**Altimeter**
Passive Radiometry	**Stereo Imagery** (hi res: HiRISE; ~1 m resolution)		**Other** (Not Listed Above)
	Stereo Imagery (med res: CTX/CaSSIS scale; ~10s m resolution)		
	Stereo Imagery (low res; ~100 m or more resolution)		

The response rate among I-MIM MDT members was 60%. Results and findings of this activity are provided below.

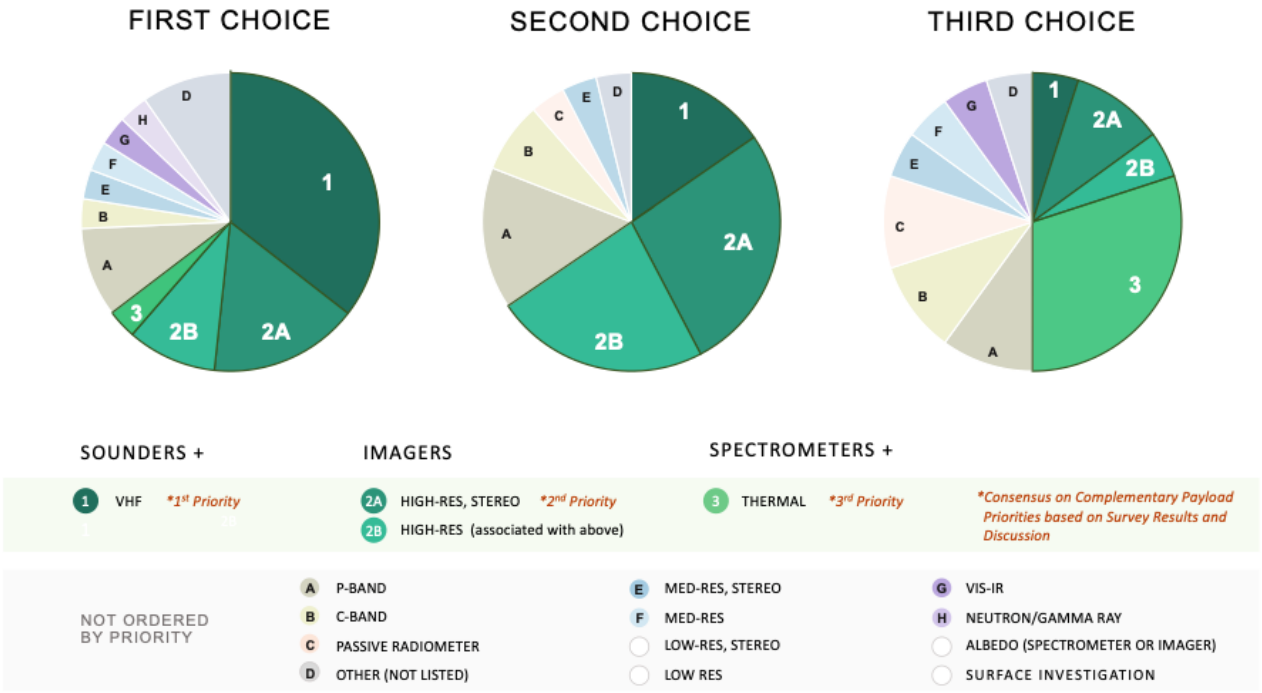

Figure 4.5 Pie charts showing the breakdown of responses for highest priority Complementary Payloads.

Table 4.4 Detailed breakdown of results of the Complementary Payload prioritization

FIRST CHOICE (31 RESPONSES)		SECOND CHOICE (26 RESPONSES)		THIRD CHOICE (20 RESPONSES)	
1. Sounder – VHF	35.5%	1. Imager – Hi-res, Stereo	26.9%	1. Spectrometer – Thermal	30%
2. Imager – Hi-res, Stereo	16.1%	2. Imager – Hi-res	23.1%	2. Imager – Hi-res, Stereo	10%
3. Imager – Hi-res	9.7%	3. Sounder – VHF	15.4%	3. Passive Radiometer	10%
4. Sounder – P-band	9.7%	4. Sounder – P-band	15.4%	4. Sounder – P-band	10%
5. Spectrometer – VIS-IR	3.2%	5. Passive Radiometer	7.7%	5. Sounder – C-band:	10%
6. Spectrometer – Thermal	3.2%	6. Imager – Med-res, Stereo	3.8%	6. Sounder – VHF	5%
7. Imager – Med-res, Stereo	3.2%	7. Spectrometer – VIS-IR	3.8%	7. Imager – Hi-res, Stereo	5%
8. Imager – Med-res	3.2%	8. *Other – Not Listed: Abstention due to stated lack of expertise across instruments.*	*3.8%*	8. VIS-IR Spectrometer:	5%
9. Sounder – C-band	3.2%			9. Imager – Med-res, Stereo	5%
10. Neutron/Gamma Ray Spec:	3.2%			10. Imager – Med-res	5%
11. *Other – not listed: Surface Impactor, Gravimeter, Abstention due to stated lack of expertise across instruments.*	*9.7%*			11. *Other – Not Listed: Temperature Measurements*	*5%*

4.4.2 Complementary Payloads Findings

A VHF/P-band Sounder (~30–300 MHz) is the highest priority payload for potential augmentation. VHF and P-band sounders were considered a single candidate, due to overlap in frequency, operation and capabilities. A close second priority payload for potential augmentation is a high-resolution imager (HiRISE-class; 10s cm spatial resolution) with stereo capabilities. A thermal spectrometer emerged as third highest priority, and a few other instruments (Vis-IR spectrometer, C-band sounder, passive radiometry, and neutron/gamma ray spectrometer) also received votes.

The MDT decided to include considerations of the top two complementary payloads in Task 2 and Task 3 deliberations.

4.4.3 High-Priority Complementary Payload Descriptions

MODEL VHF SOUNDER

The MDT determined that the addition of a second radar sounder that operates at VHF (~100 MHz) frequencies would strongly complement the anchor L-band radar system by acquiring additional information on the nature of the surface and subsurface. Such a sounding radar would fill a gap in frequency coverage between I-MIM's L-band (930 MHz) and MRO's SHARAD (20 MHz) instruments. This gap also corresponds to a sensing gap in depth of sounding within SHARAD's "blind zone" (from the surface to ~20 m depth) and below the upper 5–10 m expected to be penetrated by the I-MIM sounder (see Figure 4.3).

This gap is a key area, as the connections between near-surface ice and ice at 10s of meters depth are poorly understood. Some areas in the upper 10 m will not likely be amenable to penetration at L-band, but will be at VHF. This potential augmentation would enable a more complete inventory and characterization of buried ice, both in the RZ and more globally. Compared to SHARAD, the higher VHF frequency would allow a wider radar bandwidth, which results in finer range (depth) resolution, again intermediate between the L-band sounder and SHARAD.

Longer radar wavelengths are generally less susceptible to scattering by objects such as rocks, cracks and voids. In areas of greater surficial (or buried) roughness, a VHF signal will scatter less than an L-band signal and thus will be more likely to detect subsurface interfaces. Viscous flow features, such as the debris-covered glaciers shown by SHARAD to be covered by massive ice would likely be more amenable to sounding at VHF than at L-band; a VHF sounder has the potential to measure the thickness of the debris cover over many of these ice-rich landforms.

A detailed description of a possible design for a VHF sounder is provided in the Concept of Operations section 6.4. Briefly, the instrument would operate in a similar fashion to SHARAD and MARSIS, sending a frequency modulated ("chirp") pulse toward nadir and capturing the reflected signals at a rate of several hundred to 1000 pulses per second. The partner Agencies would need to determine operational integration with the rest of the payload. In support of RO-3, observations would be primarily aimed at Targeted Areas of Interest (TAI; see Section 6) for evaluation of the characteristics of subsurface ice deposits and suitability for human exploration.

MODEL HIGH-RESOLUTION IMAGER WITH STEREO CAPABILITIES

The MDT determined high-resolution color imaging (and derived stereo topography) to be an important potential augmentation payload for addressing gaps in the anchor radar's ability to meet I-MIM reconnaissance objectives. Direct observations of exposed mid-latitude ice layers and ice-exposing impacts can confirm the presence of icy deposits. Measurements of thermal contraction polygons can, in conjunction with models, determine ice depth. Blocky surfaces and buried ice may both produce high radar CPR signals that high-resolution images can disambiguate. Stereo topography in conjunction with radar sounding of buried ice interfaces can constrain bulk dielectric properties. High-resolution imaging also plays a key role in enabling future exploration. Landing-site safety is determined by roughness and rockiness. Images at decimeter-scale resolutions are required to characterize adequately the abundance of meter-scale boulders, and stereo products (with meter-scale resolution) are necessary to characterize small scale slopes.

Although it has imaged less than 4% of Mars, the investigations listed above have already benefited from HiRISE data (three colors; 1 µrad IFOV; 25–30 cm/pixel from an MRO-like orbit) and further progress requires an imaging system at least this capable. However, increases in resolution must be matched by increases in the diffraction-limited HiRISE optics (e.g., 5 cm resolution requires a primary mirror 2.5 m in size). Thus, resolutions significantly higher than HiRISE cannot likely be accommodated onboard an orbiter where the radar system is the main priority.

The MDT finds that the current HiRISE-class optical performance with enhanced color capability represents the best strategy for advancing I-MIM's reconnaissance and science goals. Optically, such a system might resemble HiRISE with a 50 cm aspheric primary mirror (leading to 1 µrad IFOV at visible wavelengths); sub-pixel distortion over a field of view >1 degree; and a modulation transfer function of ~30% at Nyquist. Modern CMOS detectors can improve considerably on the HiRISE CCDs, allowing for several minutes of continuous imaging (versus <10 s on HiRISE) and color coverage across the entire field of view (only the central 20% was covered by HiRISE).

Color bands (up to four) should be chosen to provide continuation with the HiRISE bands so changes may be detected, as well as inclusion of a band at shorter wavelengths to characterize atmospheric haze. Time-delay integration (TDI) remains necessary to attain sufficient signal-to-noise ratios (SNRs) and drives stringent pointing stability requirements of <0.2 µrad of crosstrack drift over 9.5 msec (128 image lines). High quantum efficiency CMOS detectors with 128 lines of TDI can reach SNRs in a panchromatic filter exceeding 200 over typical Mars terrain and with better radiometric accuracy than CCDs.

Such an instrument can generate several Gbs of 12-bit data per second and so reduction to 8-bit and lossy compression would be necessary to return data of imaged terrain. Stereo coverage is expected to be asynchronous with instrument pointing controlled by spacecraft rolls.

4.5 RECONNAISSANCE TRACEABILITY MATRIX (RTM)

FORMULATION OF THE RTM

In fulfilling Task 1, each RO Group created a list of parameters with descriptions, units, accuracy, and linkages to RO-3 criteria (human-led ice science, human-class landing/launch, ISRU, and civil engineering) to ensure traceability to the requirements-driving reconnaissance objectives and to specific human mission planning (HMP) needs. The RO Groups considered the necessity of a minimum acceptable threshold for a parameter to be considered worthwhile or critical to the mission. Ultimately, the RO Groups included all possible parameters discussed to capture a fuller suite of human-mission-planning measurement

needs, even those beyond the scope of I-MIM (e.g., surface measurements not possible from orbit). By doing so, the work of the MDT and the collective expertise of its members can inform other future Mars mission planning. The final RTM has a total of 46 parameters that are organized into 7 categories:

1. Ice Presence and Concentration
2. Lateral Extent and Continuity of Ice
3. Non-ice Constituents in the Matrix
4. Overburden Properties
5. Surface Characteristics
6. Post-landing Science
7. Long-term HMP “Nice-to-Haves"

The RO Groups considered additional payloads that would improve the accurate interpretation of SAR data and/or address each parameter more fully. The MDT then ranked the parameters based on relevance to the tasked objective for each RO Group, and established measurement requirements for each parameter. The MDT considered accuracy and resolution necessary for each measurement to characterize each parameter. The MDT also identified critical models needed for radar interpretation, where applicable for each measurement.

The HMP and Radar Groups had the responsibility for compiling RO group outputs and developing an integrated Reconnaissance Traceability Matrix (RTM) that summarized results of Task 1 discussions. The Radar Group ensured the anchor payload would be capable of making the desired measurement, while the HMP Group had the responsibility for confirming that the measurements matched their needs. This multidisciplinary group developed a template for a final RTM that served as a guide for the following work. They then appended input from each RO into one large spreadsheet that retained the traceability and prioritization from the original discussions and RO reports. This document was sent to the HMP group to look for overlap among parameters. The MDT initially identified a total of 50 parameters in the combined table of parameters with abundant overlap across the three RO documents. Additionally, each RO Group contributed unique parameters, including 5 from RO-1, 4 from RO-2, 12 from RO-3, and 3 from HMP.

Together, the HMP and Radar groups identified redundant parameters or those that could be effectively combined. The HMP Group then completed priority rankings (high, moderate, or low) and rationales for each parameter, traceable to the Reconnaissance Goal and Objective and based on input from the RO Groups. Expert members of the HMP group provided individual rankings of each parameter according to each of the four RO-3 criteria.

An average of the priorities across these four HMP criteria resulted in the overall priority ranking for each parameter. The HMP Group then sent the compiled table to the Radar Group to review and assess the radar functionality. The Radar Group determined whether the primary anchor payload could sufficiently make the measurement, what mode and/or band would be necessary to collect the measurement at the specified accuracy and resolution, and what models would be needed to interpret the radar data. They also made determinations as to whether additional measurements, possibly from alternate instruments, would be necessary. The HMP and Radar Groups then sent the RTM draft to the entire MDT for review. In this stage, the MDT further merged parameters with enough overlap in measurements and accuracy.

The following sections of the Reconnaissance Traceability Matrix (RTM) are organized for readability and accessibility.

The original spreadsheet is available at https://science.nasa.gov/researchers/ice-mapper-measurement-definition-team for those wishing to view the content without page breaks.

The content is the same.

RO-1 WHERE IS THE HUMAN-ACCESSIBLE ICE ON MARS?

1. ICE PRESENCE

PARAMETER	SUB-PARAMETER	RO-3 LINKS: HUMAN MISSION PLANNING RATIONALES FOR PRIORITY RANKING	SCALE/RESOLUTION/ ACCURACY	RO-1 & RO-2 LINKS	PRIORITY OF MEASUREMENT TO HMP							RADAR MODES	RADAR FUNCTIONAL REQUIREMENTS	MODELS NEEDED
					OVERALL	ICE SCI	LAND/ LAUNCH	ISRU	CIV ENG	RADAR NECESS -ARY?	RADAR SUF-FICIENT?			
1 Ice Presence/ Absence	–	**A focus of the I-MIM mission.**	▪ ~100 m resolution ▪ up to km resolution **ISRU Planning** ▪ 1 km resolution	RO-1 P1	H	H	H	H	H	Y	Y	SAR/ Sounder	**SAR** ▪ Single Look Coherent (SLC) returned SAR data. Orbital control sufficient to enable InSAR ▪ Instrument design should provide NESZ sufficient for the measurement, TBD in Phase A **Sounder** ▪ 160 MHz bandwidth ▪ Sufficient SNR for the measurement, TBD in Phase A	CPR and m-chi polarization decomposition to distinguish ice from blocky terrain

RO-1 WHERE IS THE HUMAN-ACCESSIBLE ICE ON MARS?

2. ICE CONCENTRATION (1 of 2 Pages)

PARAMETER	SUB-PARAMETER	RO-3 LINKS: HUMAN MISSION PLANNING RATIONALES FOR PRIORITY RANKING	SCALE/RESOLUTION/ ACCURACY	RO-1 & RO-2 LINKS	PRIORITY OF MEASUREMENT TO HMP							RADAR MODES	RADAR FUNCTIONAL REQUIREMENTS	MODELS NEEDED
					OVERALL	ICE SCI	LAND/ LAUNCH	ISRU	CIV ENG	RADAR NECESS -ARY?	RADAR SUF-FICIENT?			
2.1 Depth to Top of Ice Table	2.1A Overburden/ Ice Transition Depth Below 0.5 m	**HUMAN-LED ICE SCIENCE** ▪ Identify most equatorward place for human-led surface science ▪ Understand mid-latitude ice stability under current climate conditions ▪ Inventory water ice **HUMAN-CLASS LANDING/LAUNCH** ▪ Determine how much soil exists to excavate before melting ice on landing **ISRU** ▪ Design ice-access equipment and select ISRU site **CIVIL ENGINEERING** ▪ Determine presence of ice that affects ground stability ▪ Define exclusion zones for landing/launch pads, habitats, & power sources	**ICE SCI** ▪ cm to m **H-C L/L** ▪ ±20–50 cm **ISRU** ▪ within ±1 m **CE** ▪ ±20–50 cm	RO-1 P2.1 RO-2 P2.1	H	H	H	H	H	Y	Y/M	Sounder/ InSAR Tomography	**SAR** ▪ Single Look Coherent (SLC) returned SAR data. Orbital control sufficient to enable InSAR ▪ Instrument design should provide NESZ sufficient for the measurement, TBD in Phase A **Sounder** ▪ 160 MHz bandwidth ▪ Sufficient SNR for the measurement, TBD in Phase A	Assumptions about Overburden ε'
	2.1B Overburden/ Ice Transition Depth to 0.5 m	Same as for 2.1A	Same as for 2.1A	RO-1 P2.1 RO-2 P2.1	H	H	H	H	H	N	N	-	-	Existing Instruments Can Make These Measurements
2.2 Thickness of Ice in Upper 10 m	–	**HUMAN-LED ICE SCIENCE** ▪ Inventory ice ▪ Determine total mass/distribution ▪ Understand mid-latitude ice stability under current and past climate conditions **HUMAN-CLASS LANDING/LAUNCH** ▪ Understand surface stability for landing and infrastructure **ISRU** ▪ Determine if ISRU will be viable at a location ▪ Assist in choosing among viable sites **CIVIL ENGINEERING** ▪ Determine seasonal ground stability for construction planning (road bases, foundations, piles, & landing/launch pads)	**H-C L/L & ISRU** ▪ 0.5 m Vertical Resolution **CE** ±20–50 cm (CE)	RO-1 P2.2	H	H	H	H	H	Y	Y/M	Sounder	**Sounder** ▪ 160 MHz bandwidth ▪ Sufficient SNR for measurement, TBD in Phase A	Radar Sounder Propagation/ Reflection Model
2.3 Integrated Ice Mass in Column of 10 m	–	**HUMAN-LED ICE SCIENCE** ▪ Decipher between crystalline vs non-crystalline and/or pore-filling vs. massive ice (i.e., differing ice densities), which can provide information on past and current climate/ice stability and insight into ice origin **HUMAN-CLASS LANDING/LAUNCH** ▪ [nature of the top 5 m for landing; may be lower priority if characterized by all of the other measurements] **ISRU** ▪ Assist in identifying a site that maximizes the amount of water that can be extracted **CIVIL ENGINEERING** ▪ Inform strength-related properties and mass-wasting potential of subsurface	**ISRU** ▪ Volumetric fraction of the non-ice component within 10% accuracy **CE** ▪ Volumetric and density estimates of the ice body	RO-1 P2.3	H	H	M	H	H	Y	Y/M	Sounder	**Sounder** ▪ 160 MHz bandwidth ▪ Sufficient SNR to accommodate this measurement, TBD in Phase A	–

RO-1 WHERE IS THE HUMAN-ACCESSIBLE ICE ON MARS?

2. ICE CONCENTRATION (2 of 2 Pages)

PARAMETER	SUB-PARAMETER	RO-3 LINKS: HUMAN MISSION PLANNING RATIONALES FOR PRIORITY RANKING	SCALE/RESOLUTION/ ACCURACY	RO-1 & RO-2 LINKS	PRIORITY OF MEASUREMENT TO HMP							RADAR MODES	RADAR FUNCTIONAL REQUIREMENTS	MODELS NEEDED
					OVERALL	ICE SCI	LAND/ LAUNCH	ISRU	CIV ENG	RADAR NECESS -ARY?	RADAR SUF-FICIENT?			
2.4 Nature of Ice/ Overburden Transition	–	**HUMAN-LED ICE SCIENCE** ▪ Provide insight into ice history, origin, and redistribution processes ▪ Infer whether the 'top of ice table' seen in other measurements is the true depth to the main ice deposit (or, where massive ice has diffused upwards into the overburden to create pore-filling ice over massive ice) **HUMAN-CLASS LANDING/LAUNCH** ▪ Determine stability for landing (priority also dependent on lateral extent) **ISRU** ▪ Determine the type and quantity of ISRU equipment based on the depth and sharpness/abruptness of the transition from overburden to ice **CIVIL ENGINEERING** ▪ Understand ground stability	**ISRU** ▪ Multi-frequency sounding, 1°m vertical/ 100 m horizontal (for variability studies). **CE** ▪ Tomography from sounder data, 1 m vertical / 10 m horizontal. ▪ 0.5 m scale (abrupt or gradual) ▪ ±20–50 cm	RO-1 P2.4 RO-2 P3.6	H	H	H	H	H	Y	Y/M	Sounder/ InSAR Tomography	**SAR** ▪ Single Look Coherent (SLC) returned SAR data. Orbital control sufficient to enable InSAR ▪ Instrument design should provide NESZ sufficient for the measurement, TBD in Phase A **Sounder** ▪ 160 MHz bandwidth ▪ Sufficient SNR for the measurement, TBD in Phase A	Assumptions about Overburden ε'
2.5 Ice Porosity	–	**HUMAN-LED ICE SCIENCE** ▪ Inventory ice ▪ Determine total mass/distribution ▪ Understand mid-latitude ice stability under current and past climate conditions **HUMAN-CLASS LANDING/LAUNCH** ▪ Understand surface stability for landing and infrastructure **ISRU** ▪ Determine if ISRU will be viable at a location ▪ Assist in choosing among viable sites **CIVIL ENGINEERING** ▪ Determine seasonal ground stability for construction planning (road bases, foundations, piles, and landing/launch pads)	▪ 1 m vertical resolution ▪ volumetric fraction of the non-ice component to 10% accuracy	RO-1 P2.5	H	H	H	H	H	Y	Y/M	Sounder	**Sounder** ▪ 160 MHz bandwidth ▪ Sufficient SNR for the measurement, TBD in Phase A	Radar Sounder Propagation/ Reflection Model
2.6 Ice Lenses in Overburden	–	**HUMAN-LED ICE SCIENCE** ▪ Determine: – ice origin (e.g., buried snowpack or glacial ice have very different implications for extracting climate info – atmospheric gas samples probably would have leaked out of a porous snowpack), – the potential fragility of samples (will they crumble when drilled/extracted?), and – the porosity of the ice given it affects ice mass and concentration, and thus informs where to sample to determine ice metamorphism processes/timeline **HUMAN-CLASS LANDING/LAUNCH** ▪ Determine: stability for landing **ISRU** ▪ Understand ways to extract and process ice-bearing material **CIVIL ENGINEERING** ▪ Understand ground stability over time if volatiles liberate (don't need to know accurately early on)	–	RO-2 P1.4	H	H	M	H	H	Y	Y/M	Sounder	**Sounder** ▪ 160 MHz bandwidth ▪ Sufficient SNR for this measurement, TBD in Phase A	–

RO-1 WHERE IS THE HUMAN-ACCESSIBLE ICE ON MARS?

3. LATERAL EXTENT & CONTINUITY OF ICE

PARAMETER	SUB-PARAMETER	RO-3 LINKS: HUMAN MISSION PLANNING RATIONALES FOR PRIORITY RANKING	SCALE/RESOLUTION/ ACCURACY	RO-1 & RO-2 LINKS	PRIORITY OF MEASUREMENT TO HMP							RADAR MODES	RADAR FUNCTIONAL REQUIREMENTS	MODELS NEEDED
					OVERALL	ICE SCI	LAND/ LAUNCH	ISRU	CIV ENG	RADAR NECESS-ARY?	RADAR SUF-FICIENT?			
3.1 Spatial Continuity of Ice (Patchiness)	–	**GENERAL** ▪ Need map of ice deposits. ▪ Measurements must be regional in scale (SAR) and could be targeted by landform and generalized for spotlight/sounding **HUMAN-LED ICE SCIENCE** ▪ Inventory ice, to locate ice boundary, and to understand climate change, ice origin, and preservation processes **HUMAN-CLASS LANDING/LAUNCH** ▪ Help select 100 m landing spots within 5 km "region" **ISRU** ▪ Seek sites that maximize the amount of water that can be extracted from the minimum number of access points (e.g., drill holes) **CIVIL ENGINEERING** ▪ Inform strength-related properties and mass wasting potential of subsurface (stability)	**ISRU** ▪ 20% knowledge at 100 m × 100 m spot, yields 20 m final resolution after processing **CE** ▪ Lateral extent needs to be known at each resolved layer (±20–50 cm as stated above) to build the 3D deposit map	RO-1 P3.1	H	H	H	H	H	Y	Y/M	SAR with Follow-up by Sounder	**SAR** ▪ Full Polarization information returned; ▪ Instrument design should provide NESZ sufficient for the measurement, TBD in Phase A **Sounder** ▪ 160 MHz bandwidth ▪ Sufficient SNR for this measurement, TBD in Phase A	Penetration Depth of Radar at Various Wavelengths in Various Substrates
3.2 Horizontal Extent of Ice	–	**GENERAL** ▪ Useful for horizontal distribution of ice within 5 km radius of landing site **HUMAN-LED ICE SCIENCE** ▪ Inventory ice ▪ Locate the ice boundary ▪ Understand climate change, ice origin, and preservation processes **HUMAN-CLASS LANDING/LAUNCH** ▪ Indicate relative safety of landing spots, especially if no ice-free landing spots **ISRU** ▪ Minimize traverse distance (but considered with several other "economic" factors when choosing a site) **CIVIL ENGINEERING** ▪ Inform strength-related properties and mass wasting potential of subsurface (stability) for landing/launch and infrastructure emplacement	**ISRU** ▪ 20% knowledge at 100 m × 100 m spot, yields 20 m final resolution after processing ▪ 1 km Scale (probability of sufficient ice is within 1 km of landing site, or 2 km from landing site, or 3 km from landing site, etc.) ▪ Local: 5 m resolution within a 5 km radius	RO-1 P3.2	M	H	L	M	H	Y	Y	SAR with Follow-up by Sounder	–	Penetration Depth of Radar at Various Wavelengths in Various Substrates Probability Distribution of Ice Presence as a Function of Distance from Any Surface Point (e.g., LZ)

RO-1 WHERE IS THE HUMAN-ACCESSIBLE ICE ON MARS?

4. NON-ICE CONSTITUENTS IN THE MATRIX (1 of 2)

PARAMETER	SUB-PARAMETER	RO-3 LINKS: HUMAN MISSION PLANNING RATIONALES FOR PRIORITY RANKING	SCALE/RESOLUTION/ ACCURACY	RO-1 & RO-2 LINKS	PRIORITY OF MEASUREMENT TO HMP							RADAR MODES	RADAR FUNCTIONAL REQUIREMENTS	MODELS NEEDED
					OVERALL	ICE SCI	LAND/ LAUNCH	ISRU	CIV ENG	RADAR NECESS -ARY?	RADAR SUF-FICIENT?			
4.1 Rocks in Ice or Ice Matrix	4.1A Ice/rock Mixing Ratio	**HUMAN-LED ICE SCIENCE** ▪ Test hypotheses regarding ice origin ▪ Provide information on what tools to brin ▪ Perform climate science **HUMAN-CLASS LANDING/LAUNCH** ▪ Help select 100 m landing spots within 5 km "region" **ISRU** ▪ Help determine hardness of material and, therefore, the difficulty in accessing and extracting ice-bearing material **CIVIL ENGINEERING** ▪ Plan infrastructure emplacement ▪ Understand ground stability, modeling needs, structural capabilities, & types of building materials	**ISRU/CE** ▪ 1 m vertical resolution ▪ volumetric fraction of the non-ice compo-nent to 10% accuracy	RO-1 2.6 RO-2 1.4	H	H	H	H	H	Y	Y	Sounder with Split Chirp	**Sounder** ▪ 160 MHz bandwidth ▪ Sufficient SNR for this measurement, TBD in Phase A; some observations with no onboard range compres-sion	Need to determine specular and non-specular surface reflection characteristics
	4.1B Layering of Lithics in Ice - Thickness & Frequency	**HUMAN-LED ICE SCIENCE** ▪ Identify interesting sites with layering useful for climate science (e.g., seasonal climate dynamics/ changes) **HUMAN-CLASS LANDING/LAUNCH** ▪ Help select 100 m landing spots within 5 km "region" **ISRU** ▪ Identify sites with the fewest layers/most ice that can be extracted ▪ Determine the type and quantity of ISRU equipment needed **CIVIL ENGINEERING** ▪ Inform strength-related properties and mass wasting potential of subsurface	**ISRU** ▪ 0.5 m vertical resolution **CE** ▪ ±20–50 cm	RO-1 2.7 RO-2 1.4	H	M	H	M/H	H	Y	Y/M	Sounder / InSAR Tomography	**SAR** ▪ Single Look Coherent (SLC) returned SAR data. ▪ Orbital control sufficient to enable InSAR ▪ Instrument design should provide NESZ sufficient for the measurement, TBD in Phase A **Sounder** ▪ 160 MHz bandwidth; Sufficient SNR for this measurement, TBD in Phase A	Radar Sounder Propagation/ Reflection Model
	4.1C Grain Size Distribution of Lithics in Ice Cannot be obtained from orbit.	**HUMAN-LED ICE SCIENCE** ▪ Understand tools to bring ▪ Understand ice/rock-mixing ratio, ice origin and/or reworking, and habitability potential (can get thin films of water at ice-rock contacts at <<0C, + rocks can be a nutrient source) **HUMAN-CLASS LANDING/LAUNCH** ▪ [may not matter, assuming landing is not on ice] **ISRU** ▪ Determine the appropriate methods for separating dissolved solids as part of ISRU design (and if melting the ice simply separates the lithic content and settles it to the bottom) **CIVIL ENGINEERING** ▪ Understand thermal behavior and strength of ice and to plan excavation/stabilization technology and operations	▪ Quantitative assessment of scattering within ice-layers ▪ 0.1–1 m boulder sizes ▪ 2.5 cm scale (e.g., fraction less than 2.5 cm dia, fraction between 2.5 and 5.0 cm dia, etc.) (and see 5.1a?)	RO-1 4.2 RO-2 1.4	M	M/L	L	M	M	Y	N	SAR & Sounder	**Sounder** ▪ 160 MHz bandwidth; Sufficient SNR for this measurement, TBD in Phase A; some observations with no onboard range compression	Need to determine specular and non-specular surface reflection characteristics.

RO-1 WHERE IS THE HUMAN-ACCESSIBLE ICE ON MARS?

4. NON-ICE CONSTITUENTS IN THE MATRIX (2 of 2)

PARAMETER	SUB-PARAMETER	RO-3 LINKS: HUMAN MISSION PLANNING RATIONALES FOR PRIORITY RANKING	SCALE/RESOLUTION/ ACCURACY	RO-1 & RO-2 LINKS	PRIORITY OF MEASUREMENT TO HMP: OVERALL	ICE SCI	LAND/ LAUNCH	ISRU	CIV ENG	RADAR NECESS-ARY?	RADAR SUF-FICIENT?	RADAR MODES	RADAR FUNCTIONAL REQUIREMENTS	MODELS NEEDED
4.2 Solutes in Ice or Ice Matrix	–	**HUMAN-LED ICE SCIENCE** ▪ Plan science (habitability, climate); solutes could drastically alter the melting point, which would affect whether sampling methods produce liquid water that could overprint natural melt signatures **HUMAN-CLASS LANDING/LAUNCH** ▪ Determine the way in which surface chemistry will affect landing plume effects **ISRU** ▪ Know the nature of impurities in advance in order to determine the appropriate methods for separating solutes in ISRU system design **CIVIL ENGINEERING** ▪ Infer thermal behavior, strength of ice, and subsurface stability	▪ 1 m vertical resolution ▪ Volumetric fraction of the non-ice component within 20% accuracy	RO-1 4.1 RO-2 1.4	M	M/H	M	M/H	M	Y	Y	Sounder	**Sounder** ▪ 160 MHz bandwidth; Sufficient SNR for this measurement, TBD in Phase A; some observations with no onboard range compression	–
4.3 Presence of Liquids	–	**HUMAN-LED ICE SCIENCE** ▪ Investigate climate, astrobiology, and geology, but not necessary to inventory ice ▪ Know at/near melt conditions because sampling techniques could induce artificial melting and potentially overprint natural signatures **HUMAN-CLASS LANDING/LAUNCH** ▪ Know stability of landing surface and resistance to thermal/pressure input from plumes **ISRU** ▪ Understand how they could affect the separation/purification process selected **CIVIL ENGINEERING** ▪ Infer thermal behavior, mass wasting potential, strength of ice and subsurface stability	▪ Stratigraphy of top 10 m with 1 m vertical resolution, 100 m horizontal resolution ▪ High dynamic range for assessing reflection strength **ISRU** ▪ Need to resolve a minimum of 1 m (i.e., must detect liquid lenses ≥ 1 m thick) at a confidence interval of at least 80%	RO-2 1.4	M	M/L	H	M/L	H	Y	Y	Sounder	**Sounder** ▪ 160 MHz bandwidth; Sufficient for this measurement, TBD in Phase A; some observations with no onboard range compression	–
4.4 Orientation of Lithic Layers in Ice Parameter cannot be obtained from orbit.	–	**HUMAN-LED ICE SCIENCE** ▪ Know layer tilt, which is important for modification history and configuration of climate record within ice ▪ Inform on source regions (science interest) of lithic samples outcropping at surface **HUMAN-CLASS LANDING/LAUNCH** ▪ [may not matter, assuming not landing on ice] **ISRU** ▪ Design top-side equipment for excavating/drilling to reach ice layers ▪ Determine appropriate equipment for actual ice extraction (See also HMP sub parameter 2.6) Also similar rationale as CE **CIVIL ENGINEERING** ▪ Understand thermal behavior, and strength of ice and to plan excavation and stabilization technology and operations	▪ Stratigraphy of top 10 m with 0.5 m vertical resolution, 100 m horizontal resolution **ISRU** ▪ Layer thickness at 0.10 m resolution	-	M	M	L	M	M	Y	N	Sounder/ InSAR Tomography	**SAR** ▪ Single Look Coherent (SLC) returned SAR data ▪ Orbital control sufficient to enable **InSAR** ▪ Instrument design should provide NESZ sufficient for the measurement, TBD in Phase A **Sounder** ▪ 160 MHz bandwidth; Sufficient SNR for this measurement, TBD in Phase A	–

RO-2 CAN REGIONS OF HUMAN-ACCESSIBLE ICE SUPPORT SURFACE OPERATIONS?

5. OVERBURDEN PROPERTIES (1 of 3)

					PRIORITY OF MEASUREMENT TO HMP									
PARAMETER	SUB-PARAMETER	RO-3 LINKS: HUMAN MISSION PLANNING RATIONALES FOR PRIORITY RANKING	SCALE/RESOLUTION / ACCURACY	RO-1 & RO-2 LINKS	OVERALL	ICE SCI	LAND/ LAUNCH	ISRU	CIV ENG	RADAR NECESS -ARY?	RADAR SUF-FICIENT?	RADAR MODES	RADAR FUNCTIONAL REQUIREMENTS	MODELS NEEDED
5.1 Thermal Properties of Overburden (Thermal Inertia)	–	**HUMAN-LED ICE SCIENCE** ▪ Know contribution of buried ice to thermal signature in conjunction with depth ▪ Know thermal variations to understand ice-flow history (climatology/climate record preservation/source regions of potential samples) **HUMAN-CLASS LANDING/LAUNCH** ▪ Find bedrock and understand its depth **ISRU** ▪ Determine site selection for ISRU-related activities (likely a major factor on par with the quality of the ice deposit) **CIVIL ENGINEERING** ▪ Detect buried rock masses	ICE SCI cm to m H-C L/L ±20–50 cm ISRU within ±1 m CE ±20–50 cm	RO-1 5.3	H	M	H	H	H	Y	Y/M	Passive Mode	▪ Large bandwidth for multiple channels ▪ Nadir pointing; no onboard processing to maintain full bandwidth	Assumptions about Overburden ε'
5.2 Density of Overburden	–	**HUMAN-LED ICE SCIENCE** ▪ Identify candidate sites for human- or robot-led investigations **HUMAN-CLASS LANDING/LAUNCH** ▪ Model surface materials for designing safe landing systems **ISRU** ▪ Design top-side equipment and understand the appropriate drilling or excavation equipment to use **CIVIL ENGINEERING** ▪ Understand the density, with angle of friction permeability, of the overburden	▪ 10 m spatial resolution ▪ 0.1 g/cm^3 resolution, inverted from 10% accuracy of density	RO-2 3.2	H	L	H	M/H	H	Y	Y	SAR	▪ 160 MHz bandwidth ▪ Sufficient SNR for this measurement, TBD in Phase A ▪ Some observations with no onboard range compression	–

RO-2 CAN REGIONS OF HUMAN-ACCESSIBLE ICE SUPPORT SURFACE OPERATIONS?

5. OVERBURDEN PROPERTIES (2 of 3)

PARAMETER	SUB-PARAMETER	RO-3 LINKS: HUMAN MISSION PLANNING RATIONALES FOR PRIORITY RANKING	SCALE/RESOLUTION/ ACCURACY	RO-1 & RO-2 LINKS	PRIORITY OF MEASUREMENT TO HMP							RADAR MODES	RADAR FUNCTIONAL REQUIREMENTS	MODELS NEEDED
					OVERALL	ICE SCI	LAND/ LAUNCH	ISRU	CIV ENG	RADAR NECESS-ARY?	RADAR SUF-FICIENT?			
5.3 Strength of Overburden	5.3A Load-bearing Capacity of Overburden	**HUMAN-LED ICE SCIENCE** ▪ Identify candidate sites for human- or robot-led investigations **HUMAN-CLASS LANDING/LAUNCH** ▪ Model surface materials for designing safe landing systems **ISRU** ▪ Design top-side equipment and understand the appropriate drilling or excavation equipment to use **CIVIL ENGINEERING** ▪ Determine needs for landing/launch preparations	▪ 10 m spatial resolution ▪ Pascals, derived from density of overburden that is known to 10% accuracy	RO-2 1.1	H	L	H	M/H	H	Y	Y	SAR	▪ Full Polarization information returned; Instrument design should provide NESZ sufficient for the measurement, TBD in Phase A ▪ 160 MHz bandwidth; Sufficient SNR for this measurement, TBD in Phase A; some observations with no onboard range compression	–
	5.3B Average/Bulk Porosity of Overburden	**HUMAN-LED ICE SCIENCE** ▪ Determine if pore-filling ice or volatile exchange between surface and subsurface is likely **HUMAN-CLASS LANDING/LAUNCH** ▪ Model materials on which human-class landers would land to mitigate cratering by descent engines and support lander mass **ISRU** ▪ Design top-side equipment ▪ Determine the appropriate drilling or excavation equipment to use **CIVIL ENGINEERING** ▪ Understand the density, strength, and permeability of the overburden to plan excavation/stabilization technology and operations and surface materials for construction	▪ 10 m spatial resolution ▪ 10% accuracy inverted from density	RO-2 1.1 RO-2 3.2	H	L	H	M/H	H	Y	Y	SAR	▪ Same as for 5.3A	–
	5.3C Hardness of Overburden	**HUMAN-LED ICE SCIENCE** ▪ Understand accessibility of ice for sampling **HUMAN-CLASS LANDING/LAUNCH** ▪ Model materials on which human-class landers would land to mitigate cratering by descent engines and support lander mass **ISRU** ▪ Determine top-side equipment design and drilling or excavation equipment to use **CIVIL ENGINEERING** ▪ Plan excavation/stabilization technology and operations and surface materials for construction	▪ 10 m spatial resolution ▪ Pascals, derived from density of overburden that is known to 10% accuracy	RO-2 1.1 RO-2 3.3	H	L	H	M/H	H	Y	Y	SAR	▪ Same as for 5.3A	–
	5.3D Surface Soil/Regolith Angle of Internal Friction	**SUBPARAMETERS CANNOT BE OBTAINED FROM ORBIT.** **HUMAN-CLASS LAUNCH/LANDING, ISRU, & CIVIL ENGINEERING** ▪ Evaluate the environmental impacts on the subsurface and surface caused by the human mission activities (infiltration/permeation of rocket engine gases, habitat or ISRU effluents, wastes)	▪ Information derived from determination of soil type if possible from orbit ▪ Actual data needed is shear strength vs. applied stress measured by surface equipment	RO-2 1.1	H	L	H	H	H	Y	Y	SAR	**SAR** ▪ Full Polarization information returned; Instrument design should provide NESZ sufficient to accommodate the measurement, TBD in Phase A	–
	5.3E Surface Soil/ Regolith Permeability	▪ Same as for 5.3D	▪ Information derived from determination of soil type if possible from orbit ▪ Actual measurements through surface equipment	RO-2 1.1	L	L	L	M	L	Y	M	SAR	**SAR** ▪ Same as for 5.3D	–

RO-2 CAN REGIONS OF HUMAN-ACCESSIBLE ICE SUPPORT SURFACE OPERATIONS?

5. OVERBURDEN PROPERTIES (3 of 3)

PARAMETER	SUB-PARAMETER	RO-3 LINKS: HUMAN MISSION PLANNING RATIONALES FOR PRIORITY RANKING	SCALE/RESOLUTION/ ACCURACY	RO-1 & RO-2 LINKS	PRIORITY OF MEASUREMENT TO HMP							RADAR MODES	RADAR FUNCTIONAL REQUIREMENTS	MODELS NEEDED
					OVERALL	ICE SCI	LAND/ LAUNCH	ISRU	CIV ENG	RADAR NECESS -ARY?	RADAR SUF-FICIENT?			
5.4 Stratigraphy/ Interbedding	–	**HUMAN-LED ICE SCIENCE** ▪ Support science (climate, depositional environment, frost action cryoturbation) **HUMAN-CLASS LANDING/LAUNCH** ▪ Model the surface materials at the landing spots **ISRU** ▪ Design top-side drilling or excavation equipment **CIVIL ENGINEERING** ▪ Plan excavation/stabilization technology and operations and surface materials for construction	▪ Sensitivity to 0.3 m rocks ▪ 10 m spatial resolution	RO-1 4.3 RO-2 3.1 RO-2 3.5 RO-2 3.6	H	L	H	M/H	H	Y	Y	SAR	**SAR** ▪ Full Polarization information returned; Instrument design should provide NESZ sufficient to accommodate the measurement, TBD in Phase A	–
5.5 Depth to Bedrock	–	**HUMAN-CLASS LANDING/LAUNCH** ▪ Determine ability of surface material to mitigate cratering by descent engines and to support lander mass **CIVIL ENGINEERING** ▪ Understand soil stability and make load-bearing estimates	▪ Sensitivity to 0.3 m rocks ▪ 10 m spatial resolution	–	H	L	H	H	H	Y	Y	SAR	**SAR** ▪ Same as for 5.4	–

RO-2 CAN REGIONS OF HUMAN-ACCESSIBLE ICE SUPPORT SURFACE OPERATIONS?

6. SURFACE CHARACTERISTICS (1 of 2)

PARAMETER	SUB-PARAMETER	RO-3 LINKS: HUMAN MISSION PLANNING RATIONALES FOR PRIORITY RANKING	SCALE/RESOLUTION/ ACCURACY	RO-1 & RO-2 LINKS	PRIORITY OF MEASUREMENT TO HMP							RADAR MODES	RADAR FUNCTIONAL REQUIREMENTS	MODELS NEEDED
					OVERALL	ICE SCI	LAND/ LAUNCH	ISRU	CIV ENG	RADAR NECESS -ARY?	RADAR SUF-FICIENT?			
6.1 Surface Rock Size Distribution	–	**HUMAN-LED ICE SCIENCE** ▪ Provide limits on detectability of underlying ice and information on ice origin and history **HUMAN-CLASS LANDING/LAUNCH** ▪ Know particle size and bulk density in order to predict crater depth and what is jettisoned from landing/ascent ▪ Understand general lander tolerance (hazard detection sensors have 7.5 cm/px resolution and map 100 m × 100 m area in 2 seconds) **ISRU** ▪ Design top-side drilling or excavation equipment **CIVIL ENGINEERING** ▪ Plan excavation and stabilization technology and operations ▪ Know surface materials for construction ▪ Understand trafficability	▪ Sensitivity to 0.3 m rocks ▪ 10 m spatial resolution **The following must be made from the surface:** ▪ <1 cm (dust) to boulders with a 2.5 cm diameter fraction size above 2.5 cm (e.g., 0–1 cm, 1–2.5 cm, 2.5–5 cm, 5–7.5 cm, etc.)	RO-1 5.1 RO-2 1.2 RO-2 3.4	H	L	H	M/H	H	Y	Y	SAR	**SAR** ▪ Full Polarization information returned; Instrument design should provide NESZ sufficient to accommodate the measurement, TBD in Phase A	–
6.2 Lithology of Surface Cover	–	**HUMAN-LED ICE SCIENCE** ▪ Determine places for scientific investigation **HUMAN-CLASS LANDING/LAUNCH** ▪ Know particle size and bulk density to predict crater depth and what is jettisoned from landing/ascent ▪ Know general lander tolerance (hazard detection sensors have 7.5 cm/px resolution and map 100 m × 100 m area in 2 seconds) **ISRU** ▪ Design top-side drilling or excavation equipment **CIVIL ENGINEERING** ▪ Design excavation/ stabilization technology and operations ▪ Know available surface materials for construction ▪ Understand trafficability	▪ λ = 0.3-5 µm; Band depth Rb(I)/Rc(I) (accuracy 1%) ▪ Band Area ▪ Spectral Slope (ΔR/Δλ) ▪ Band ratio ▪ Map of the spatial variability of some selected ▪ spectral properties across the landing site over multiple 1 km^2 areas ▪ Orbital 0.25 m/pixel imaging, later ~3 cm/pixel to identify rocks/features 20 cm ▪ Reflectivity/Scattering <1dB precision/ accuracy	RO-1 5.1	H	L	H	M/H	H	Y	N	SAR Reflectivity from Sounder Mode	**Sounder** ▪ with Split Chirp	Spectral Models Backscattering Models for Permittivity/ Roughness Deconvolution
6.3 Surface Morphology	–	**HUMAN-LED ICE SCIENCE** ▪ Locate the scientifically interesting sites for ice sampling using surface morphology in conjunction with radar, elevation, and topographic data (Ice may be closer to the surface on steep pole-facing slopes at lower latitudes) **HUMAN-CLASS LANDING/LAUNCH** ▪ Select safe landing spots (done by hazard detection system if no other info) ▪ Understand depositional/erosional processes dominating the landing area (e.g., aeolian erosion, ice sublimation, etc.) **ISRU** ▪ Design top-side drilling or excavation equipment; Likely a major factor in site selection on par with the quality of the ice deposit **CIVIL ENGINEERING** ▪ Plan surface CE operations ▪ Understand mass wasting potential ▪ Make landing/ launch preparations	▪ 1 m spatial resolution for imagery ▪ 5 m SAR resolution	RO-1 5.4 RO-2 1.3	H	H	M	M/H	H	Y	N	SAR	**SAR** ▪ Full Polarization information returned; Instrument design should provide NESZ sufficient to accommodate the measurement, TBD in Phase A	–

RO-2 CAN REGIONS OF HUMAN-ACCESSIBLE ICE SUPPORT SURFACE OPERATIONS?

6. SURFACE CHARACTERISTICS (2 of 2)

PARAMETER	SUB-PARAMETER	RO-3 LINKS: HUMAN MISSION PLANNING RATIONALES FOR PRIORITY RANKING	SCALE/RESOLUTION/ ACCURACY	RO-1 & RO-2 LINKS	PRIORITY OF MEASUREMENT TO HMP							RADAR MODES	RADAR FUNCTIONAL REQUIREMENTS	MODELS NEEDED
					OVERALL	ICE SCI	LAND/ LAUNCH	ISRU	CIV ENG	RADAR NECESS -ARY?	RADAR SUF-FICIENT?			
6.4 Surface Topography &Texture	6.4A* Roughness at 30 cm length scales	**HUMAN-LED ICE SCIENCE** ▪ Identify bands (layers) of potential lithics outcropping at surface at sub-imaging scales ▪ Infer grain size/blocky material and potential sorting **HUMAN-CLASS LANDING/LAUNCH** ▪ Select safe landing spots **ISRU** ▪ Design topside equipment **CIVIL ENGINEERING** ▪ Understand trafficability	▪ Local: 0.075 m to get 0.30 m final resolution ▪ Radar backscatter provides quantitative roughness information from 10 cm to 1 m	RO-1 5.4	H	H	M	M/H	H	Y	Y	SAR, Nadir Reflectometry	**SAR** ▪ Single Look Coherent (SLC) returned SAR data; Instrument design should provide NESZ sufficient for the measurement, TBD in Phase A **Sounder** ▪ 60 MHz bandwidth; Sufficient SNR for this measurement, TBD in Phase A	Backscattering Models
	6.4B Elevation	**HUMAN-LED ICE SCIENCE** ▪ Account for atmospheric pressure in science investigations **HUMAN-CLASS LANDING/LAUNCH** ▪ Inform Terrain Relative Navigation **ISRU** ▪ Account for atmospheric pressure **CIVIL ENGINEERING** ▪ Understand trafficability and the location of landed elements	–	RO-1 5.2 RO-1 5.4	H	H	M	M/H	H	N	N	InSAR & Tomography	**SAR** ▪ SLC returned SAR data. Orbital control sufficient to enable InSAR; Instrument design should provide NESZ sufficient for the measurement, TBD in Phase A **Sounder** ▪ 160 MHz bandwidth; Sufficient SNR for this measurement, TBD in Phase A	–
	6.4C* Roughness at 1 m length scales	**HUMAN-LED ICE SCIENCE** ▪ Develop a topography model needed for interpreting subsurface reflectors ▪ Locate accessible ice closer to the surface on steep pole-facing slopes at lower latitudes **HUMAN-CLASS LANDING/LAUNCH** ▪ Select safe landing spots **ISRU** ▪ Design topside equipment **CIVIL ENGINEERING** ▪ Understand trafficability	▪ Local: 0.25 m to get 1 m final resolution	RO-1 5.2 RO-1 5.4	M	M	M	L	M	N	N	–	–	–
	6.4D* Roughness at 10 m length scales	**HUMAN-LED ICE SCIENCE** ▪ To produce a topography model for interpreting subsurface reflectors and to identify accessible ice closer to the surface (more on steep pole-facing slopes at lower latitudes **HUMAN-CLASS LANDING/LAUNCH** ▪ Find safe landing spots ▪ Potentially model winds at landing sites. **ISRU** ▪ Design topside equipment	▪ Local: 2.5 m resolution	RO-1 5.2	M/L	M	M	L	L	N	N	–	–	–
	6.4E* Roughness at 100 m length scales	**HUMAN-CLASS LANDING/LAUNCH** ▪ Find safe landing spots (100 m circle) ▪ Provide 1st-order pre-reconnaissance at global scale for descent radar spoofing ▪ Potentially provide information for modelling winds at landing sites	▪ Local: 25 m resolution	RO-1 5.2	L	L	M	L	L	Y	Y	SAR/ Altimeter	▪ Same as for 6.4A	–
	6.4F RMS Slope at 1 km length scales	REFERRED TO TASK 2	▪ Global: 250 m resolution	–	L	L	M	L	L	Y	Y	–	▪ Same as for 6.4A	–

* Note 6.A, C, D, E: Relevant roughness sub-parameters are RMS slope, RMS height, Hurst exponent(s).

WHAT ADDITIONAL ICE SCIENCE IS POSSIBLE?

7. POST-LANDING MARS ICE-RELATED SCIENCE

PARAMETER	SUB-PARAMETER	RO-3 LINKS: HUMAN MISSION PLANNING RATIONALES FOR PRIORITY RANKING	SCALE/RESOLUTION/ ACCURACY	RO-1 & RO-2 LINKS	PRIORITY OF MEASUREMENT TO HMP							RADAR MODES	RADAR FUNCTIONAL REQUIREMENTS	MODELS NEEDED
					OVERALL	ICE SCI	LAND/ LAUNCH	ISRU	CIV ENG	RADAR NECESS-ARY?	RADAR SUF-FICIENT?			
7.1 Ice Emplacement	–	HUMAN-LED ICE SCIENCE ▪ Support science (climate, astrobio)	–	RO-1 6.1	L	M	L	L	L	–	–	–	–	–
7.2 Ice Age	–	REFERRED TO TASK 2	Not needed for reconnaissance.	–	L	M	L	L	L	–	–	–	–	–
7.3 Ice/Snow/Firn Grain Size & Density	–	HUMAN-LED ICE SCIENCE ▪ Support science (climate, astrobio) and know what tools to bring HUMAN-CLASS LANDING/LAUNCH ▪ Understand surface stability (if in upper 10 cm) ISRU ▪ Understand ice access and extraction method to use CIVIL ENGINEERING ▪ Understand surface preparation (e.g., leveling for equipment placement), reshaping (e.g., constructing roads and berms), and excavation	–	RO-1 6.2	M	M	M	M/H	M/H	–	–	–	–	–
7.4 Surface Frost Thickness, Extent, Seasonality, Composition	–	HUMAN-LED ICE SCIENCE ▪ Understand current climate and to inventory ice HUMAN-CLASS LANDING/LAUNCH ▪ Low, depending on thermal and insolation properties within a specific landing site CIVIL ENGINEERING ▪ Understand surface preparation (e.g., leveling for equipment placement), reshaping (e.g., constructing roads and berms), and excavation	–	RO-1 6.3	L	M/L	L	L	M/H	–	–	–	–	–
7.5 Temperature Profile	–	REFERRED TO TASK 2	–	–	L	L	L	L	L	–	–	–	–	–
7.6 Surface Environment	–	REFERRED TO TASK 2	–	–	M	M	M	L	L	–	–	–	–	–
7.7 Subsurface Diurnal or Seasonal Ice/Ice-soil Mixtures	–	HUMAN-LED ICE SCIENCE ▪ Inventory ice, to understand depth to ice samples, and to support climate science HUMAN-CLASS LANDING/LAUNCH, ISRU, & CIVIL ENGINEERING ▪ Know if it is present and its subsurface structure to understand surface stability	▪ 0.5 m vertical resolution ▪ lateral scale of landing zone area (100s of meter scale) ▪ 10 m horizontal resolution (finest res needed)	–	M	M/L	M	M	M	–	–	–	–	–
7.8 Presence/ Volume of Methane Clatherates	–	REFERRED TO TASK 2	–	–	L	L	L	L	L	–	–	–	–	–

Long-term "Nice to Haves" for Human Mission Planning

8. OVERBURDEN PROPERTIES

PARAMETER	SUB-PARAMETER	RO-3 LINKS: HUMAN MISSION PLANNING RATIONALES FOR PRIORITY RANKING	SCALE/RESOLUTION/ ACCURACY	RO-1 & RO-2 LINKS	PRIORITY OF MEASUREMENT TO HMP							RADAR MODES	RADAR FUNCTIONAL REQUIREMENTS	MODELS NEEDED
					OVERALL	ICE SCI	LAND/ LAUNCH	ISRU	CIV ENG	RADAR NECESS -ARY?	RADAR SUF- FICIENT?			
8.1 Surface Seismicity	–	**CIVIL ENGINEERING** ▪ Provide radar evidence of seismic activity by measuring displacement and mass wasting features after an event (SAR interferometry)	▪ presence/ absence primary ▪ 10s of cm displacement in surface elevation	–	L	L	L	L	M	–	–	–	–	–
8.2 Surface Impact Rate	–	**CIVIL ENGINEERING** ▪ Determine risk and building design criteria based on information on frequency of impacts by meteors of threshold size	**CE** ▪ detection impacts of 10 cm objects per year	–	L	L	L	L	L	–	–	–	–	–
8.3 Surface Rock Fracture Toughness	–	**HUMAN-CLASS LANDING/LAUNCH** ▪ Determine ability of surface to resist thermal stress of descent engines and to support lander mass; may be one of the best ways **CIVIL ENGINEERING** ▪ Plan engineering of drilling and comminution equipment to access subsurface or to create construction materials ▪ Determine strength, which can be can be obtained partially from mineralogy. but requires in-situ measurements (e.g., for compression & tensile strength/abrasivity)	▪ Should be derived for a number of individual boulders + on outcrops, for all present materials	–	M	L	H	M	M/L	–	–	–	–	–

Long-term "Nice to Haves" for Human Mission Planning

9. POST-LANDING ENVIRONMENTAL SCIENCE FOR HUMAN MISSION PLANNING

PARAMETER	SUB-PARAMETER	RO-3 LINKS: HUMAN MISSION PLANNING RATIONALES FOR PRIORITY RANKING	SCALE/RESOLUTION/ ACCURACY	RO-1 & RO-2 LINKS	PRIORITY OF MEASUREMENT TO HMP							RADAR MODES	RADAR FUNCTIONAL REQUIREMENTS	MODELS NEEDED
					OVERALL	ICE SCI	LAND/ LAUNCH	ISRU	CIV ENG	RADAR NECESS -ARY?	RADAR SUF-FICIENT?			
9.1 Degree of Mass Wasting	–	**CIVIL ENGINEERING** ▪ Indicate potential seismicity, potential direct hazards to infrastructure ▪ Derive geologic samples from elevated sites (could facilitate access to the subsurface)	▪ 0.25 m horizontal resolution (for small mass wasting = rockfalls) ▪ 5 m horizontal for large(r) mass wasting = slope streaks/ granular flows ▪ long temporal baseline (years) and as high imaging frequency as possible (week to months)	-	L	L	L	L	H	–	–	–	–	–
9.2 Aeolian Changes	–	**CIVIL ENGINEERING** ▪ Understand changes in dust deposition in a given area to determine risks for surface ops and CE activities on a seasonal timescale		-	M	L	L	M	H	–	–	–	–	–

RTM NOTES

P1 Ice Presence / Absence

- Ice detection can include detection of the top of the ice table, the base of ice-rich deposits, or some volume of ice within the subsurface.
- Ice detection interpretations may result from a preponderance of evidence from multiple sources.

P2.1A Overburden/Ice Transition Depth Below 0.5 m

InSAR

- Requires tight repeat passes and good position knowledge
- Requires the return of Single Look Complex (SLC) data
- Assumes surface doesn't scatter all of the energy from the sounder, yielding a null result; important information for deciding on a human-class landing site.

SAR/Sounder

- Sounding (below 20 cm) measured using reflection from dielectric interfaces + reflector time delay, CPR + model Imaging
- High-resolution imager + stereo for ice-exposing impact depth/diameter and exposed ice on cliffs/slopes

P2.1B Overburden/Ice Transition Depth to 0.5 m (Referred to Considerations of Potential Augmentations)

- Thermal Inertia, Geomorphology, Neutron & Gamma Ray Spectrometer needed
- Thermal spectrometer TI measurements and modeling for depth to ice in upper 10s of cm; TI maps
- High-resolution imager + stereo for ice-exposing impact depth/diameter, and exposed ice on cliffs/slopes

P2.2 Thickness of Ice in Upper 10 m

- Priority also dependent on lateral extent.

P2.3 Integrated Ice Mass in Column of 10 m

- No additional requirements besides nadir pointing

P2.4 Nature of Ice/Overburden Transition

- InSAR requires tight repeat passes, good position knowledge, & the return of SLC data
- Split chirp requires no new hardware, but must return un-processed data
- Sounder doesn't have fine-scale horizontal resolution
- InSAR can provide constraints at finer horizontal resolutions
- SAR CPR ice detection, combined with an absence of ice table reflections from the Sounder, would be interpreted as gradational contact
- Multi-frequency sounding and SAR tomography from sounder data possibly needed
- If < 30 cm from surface, then neutron spectrometer + models can help
- Thermal inertia + models could derive a slope for a gradational contact

P2.5 Ice Porosity

- Split chirp gives the attenuation at two frequency ranges, providing sufficient information to calculate the loss tangent
- Dielectric permittivity from 2-way travel time (sounding) and loss tangent
- Requires basal reflection and topography

P2.6 Ice Lenses in Overburden

- Ice lenses defined as well-oriented horizontal lenses alternating with soil layers between surface and ice cement or massive ice

PolSAR

- Can identify spatially non-contiguous units at fine horizontal resolution, but not depth

SAR/Sounder

- Backscatter, CPR

High-resolution Imaging

- High-latitude outcrops (Dundas papers)

P3.1 Spatial Continuity of Ice (Patchiness)

- SWIM-like congruence of parameters. Measurements need to be regional in scale (SAR) and could be targeted by landform and generalized for spotlight/sounding. Map of deposits.
- No additional requirements

P3.2 Horizontal Extent of Ice

- No additional requirements

P4.1A Ice/Rock Mixing Ratio

- Sounder reflectivity can be used as a proxy for dust content.
- Split chirp gives the attenuation at two frequency ranges, providing sufficient information to calculate the loss tangent
- SAR/Sounder: Dielectric permittivity from 2-way travel time (sounding) and loss tangent. Requires basal reflection and topography

P4.1B Layering of Lithics in Ice - Thickness & Frequency

- Layers caused by differing lithic content. Lithics refer to any grain size. Sounder doesn't have fine-scale horizontal resolution
- InSAR can provide constraints at finer horizontal resolutions.
- InSAR requires tight repeat passes, good position knowledge, and the return of Single Look Coherent (SLC) data

P4.1C Grain Size Distribution of Lithics in Ice

- SAR/Sounder: Scattering from within ice-rich layers; split chirp for loss tangent
- Cannot be completed from orbit – ground-based mission is required

P4.2 Solutes in Ice or Ice Matrix

- Split chirp gives the attenuation at two frequency ranges, providing sufficient information to calculate the loss tangent
- Split chirp requires no new hardware but additionally signals generated by the instrument

P4.3 Presence of Liquids

- Plausible liquids that can exist on Mars are mono-layers thick and unlikely to have enhanced radar returns
- No additional requirements, unlikely to be completed from orbit

P4.4 Orientation of Lithic Layers in Ice

- Layers caused by differing lithic content. Lithics refer to any grain size.
- InSAR requires tight repeat passes and good position knowledge. This also requires the return of Single Look Coherent (SLC) data. Layer thickness at 0.1 m resolution requires ground-based GPR.
- 0.10 m resolution for layer definition is more than previous target of ±20–50 cm
- Imaging (high res): imaging for surface boulder detection, HiRISE-scale topography for plane-fitting
- Imaging (low res): imaging for surface structure detection

P5.1 Thermal Properties of Overburden (Thermal Inertia)

- Would require Passive Radiometer mode. Improvement could be had with second set of frequencies, potentially C-band radar also in passive mode
- Team lists thermal inertia as a way to infer other parameters; it is not clear that thermal inertia itself is a needed parameter
- Passive radiometry measurement
- Thermal emission spectroscopy

P5.2 Density of the Overburden

- While separate parameters, load-bearing capacity, density, porosity, and hardness are intimately related. Load-bearing capacity, hardness of overburden, surface soil/regolith angle of internal friction and regolith permeability can be derived from average/bulk porosity and density of overburden by analysis. Beyond constraints for load-bearing capacity based on the need to land and traverse, it isn't clear what the resolution requirements are for these parameters, or even how some of them would be defined and derived.
- Calibrated Surface Reflection, either by ground-based knowledge (e.g., RIMFAX) or by known corner reflector positioned with a lander

SAR/Sounder

- Dielectric permittivity; split chirp for loss tangent

Other

- Thermal inertia
- Neutron spectroscopy

P5.3A Load-bearing Capacity of Overburden

- While all are separate parameters, load-bearing capacity, density, porosity, and hardness are intimately related. Load-bearing capacity, hardness of overburden, surface soil/regolith angle of internal friction and regolith permeability can be derived from average/bulk porosity and density of overburden by analysis. Beyond constraints for load-bearing capacity based on the need to land and traverse, it isn't clear what the resolution requirements are for these parameters, or even how some of them would be defined and derived.
- Additional instruments may be necessary (Thermal Imager, Thermal Inertia (>100 tiu), Albedo (<0.25), HiRes Imager). May require surface investigation.

P5.3B Average/Bulk Porosity of Overburden

- Porosity includes air-, water-, or ice-filled
- While separate parameters, load-bearing capacity, density, porosity, and hardness are intimately related. Load-bearing capacity, hardness of overburden, surface soil/regolith angle of internal friction and regolith permeability can be derived from average/bulk porosity and density of overburden by analysis. Beyond constraints for load-bearing capacity based on the need to land and traverse, it isn't clear what the resolution requirements are for these parameters, or even how some of them would be defined and derived.
- Calibrated surface reflection, either by ground-based knowledge (e.g., RIMFAX) or by known corner reflector positioned with a lander

SAR/Sounder

- Dielectric permittivity, reflector coefficients, scattering, CPR; split chirp for loss tangent

High-resolution imaging

- Craters/outcrops exposing shallowest few m

P5.3C Hardness of Overburden

- While separate parameters, load-bearing capacity, density, porosity, and hardness are intimately related. Load-bearing capacity, hardness of overburden, surface soil/regolith angle of internal friction and regolith permeability can be derived from average/bulk porosity and density of overburden by analysis. Beyond constraints for load-bearing capacity based on the need to land and traverse, it isn't clear what the resolution requirements are for these parameters, or even how some of them would be defined and derived.

SAR/Sounder

- Dielectric permittivity, CPR

Other

- Thermal IR
- Additional instruments may be necessary (Thermal Imager, Spectrometer etc.)

P5.3D Surface Soil/Regolith Angle of Internal Friction & P5.3E Surface Soil/Regolith Permeability

- While separate parameters, load-bearing capacity, density, porosity, and hardness are intimately related
- Load-bearing capacity, hardness of overburden, surface soil/regolith angle of internal friction and regolith permeability can be derived from average/bulk porosity and density of overburden by analysis.
- Beyond constraints for load-bearing capacity based on the need to land and traverse, it isn't clear what the resolution requirements are for these parameters, or even how some of them would be defined and derived.

P5.4 Stratigraphy/Interbedding

- 1 meter vertical resolution requires nothing additional; 10 m spatial resolution and stratigraphy requires InSAR and Tomography with precise position knowledge, repeat passes, and SLC.
- Thin layers in the overburden could affect drilling capability
- May not be able to see layers if dielectric contrasts are not strong enough
- SAR/Sounder: Polarimetric SAR data (to 1–10 m depths), reflector coefficients
- High resolution imagery, crater morphology, GPR
- May require surface investigation (cores, drills, penotrometers)

P5.5 Depth to Bedrock

- A non-ice property intended to capture properties of the surface and near-surface
- No additional requirements for depths to 10 m

P6.1 Surface Rock Size Distribution

- Additional requirements for information below 10 cm could be provided by a thermal imager or ground-based measurements
- SAR/Sounder: SAR roughness, CPR, SAR Tomography
- High-resolution imaging, crater morphology
- Thermal inertia
- Albedo
- VIS-IR imaging spectrometer

P6.2 Lithology of Surface Cover

- Might require further discussion for an irreducible list of sub-parameters
- 1dB accuracy is common for sounder, better might be required for SAR
- SAR/Sounder Signal Stability & Absolute Calibration
- SAR/Sounder: SAR roughness, CPR, SAR Tomography
- High-resolution imaging, crater morphology
- Thermal Inertia
- Albedo
- VIS-IR imaging Spectrometer

P6.3 Surface Morphology

- It is possible that the radar won't provide measurements for small-scale morphology, but it can provide complementary data at slightly lower resolution
- SAR images can provide morphology information that is complementary to visual images at lower resolution
- High-resolution imaging, DTMs
- SAR topography/backscatter, roughness

P6.4A Roughness at 30 cm Length Scales

- Signal Sensitivity; Stability; Dynamic Range
- DTMs, SAR roughness, CPR

P6.4B Elevation

- High-resolution stereo imagery to reach 5 m horizontal resolution. InSAR tomography can do some of this, but not perfectly
- Request from RO group for decimetric resolution would preclude global coverage

P6.4C Roughness at 1 m Length Scales & P6.4D Roughness at 10 m Length Scales

- Stereo-imagery; DTMs
- SAR Roughness
- CPR

P6.4E Roughness at 100 m Length Scales & P6.4F RMS Slope at 1 km Length Scales

- Stereoradargrammetry and/or Altimetry Mode
- DTMs
- SAR Roughness
- CPR

4.6 SUMMARY OF RECONNAISSANCE OBJECTIVES & TRACEABILITY

The MDT Charter directed the Team to develop measurement requirements to pursue the overarching I-MIM Reconnaissance Goal:

> *"to map and characterize accessible (within the uppermost 10 m) subsurface water ice and its overburden in mid-to-low latitudes to support planning for the first potential human surface missions to Mars."*

The MDT groups studied the three pre-defined Reconnaissance Objectives (ROs): RO-1 Ice Mapping; RO-2 Geotechnical and Overburden Characterization; and RO-3 Characterizing Candidate Sites for Human Exploration. For each RO, the groups identified key characteristics of the surface or subsurface materials ("parameters"), the knowledge of which advances the reconnaissance goal of the mission. These parameters, and the details associated with them, are summarized in the RTM. These include the rationale for the parameter, the priority/value, the scales of needed measurements, and the capability of the radar to obtain the parameter. If additional capabilities or instruments were needed, the MDT identified and included them in the discussion and RTM. The MDT identified two instrument types as providing the best complementarity to the anchor radar payload to achieve the ROs: a VHF sounder and a high-resolution imager with stereo capabilities.

For RO-1, to map and inventory near-surface water ice, the MDT deemed the anchor radar payload both necessary and sufficient to fulfill the knowledge of many of the high-priority parameters, such as the presence or absence of ice, depth to the ice table, thickness of ice in the upper 10 m, ice porosity, ice/rock mixing ratio, and lateral continuity of the ice. The MDT found several high-priority parameters to be more fully constrained with (or in some cases, to require) observations from the identified complementary payloads.

Many of the parameters identified as critical to characterizing the overburden for addressing RO-2 are also necessary for characterizing candidate sites for human exploration (RO-3), so the MDT considered them together. The anchor radar payload was again found to be both necessary and sufficient to fulfill the knowledge of many of the high-priority parameters concerning the overburden and other surface characteristics. These include surface rock-size distribution, roughness at 30 cm scales, and the density, load capacity, bulk porosity, and hardness of the overburden. The MDT noted limitations of the anchor radar payload to achieve several high-priority parameters such as elevation and topography, roughness at 1–10 m scales, thermal properties, and lithology. The MDT identified how the complementary payloads or other instruments could contribute to constraining these parameters.

The RO-3 group found that data returned from I-MIM would provide an important first step in identifying particularly attractive locations for the first human mission(s), as part of a tiered site selection strategy. RO-3 assessed the capabilities of the anchor radar payload to constrain key parameters related to four areas of human mission planning: human-led surface science, human-class launch and landing, ISRU, and civil engineering. The RTM summarizes the rationale and importance of the identified parameters to each of these areas. The MDT found the anchor radar payload met a significant number of the parameters.

Given the need for many orbital and surface measurements to select and eventually to certify one or more locations for the scale and complexity of human missions, the MDT notes that additional instruments on both orbital and landed robotic spacecraft would likely be needed to characterize fully and certify the safety and suitability of candidate sites for human exploration.

Example of a synthetic aperture radar image over the Antarctica Dry Valleys, which has known buried ice deposits. Yellow indicates an area of potential ice (both exposed and subsurface), and blue indicates return from the surface.

Credit: RADARSAT Constellation Mission Imagery © Government of Canada (2022). RADARSAT is an official mark of the Canadian Space Agency.

5 TECHNICAL ANALYSIS: SCIENCE OBJECTIVES

The primary driving motivation for the I-MIM mission concept is reconnaissance of ice to prepare for human missions to Mars. However, the international Agency partners and the MDT recognize that a scientific payload tailored to locate and characterize ice deposits for humans could also be used to address many scientific questions about Mars. The MDT's second major task was to assess the range of scientific investigations that could be conducted with the anchor payload (L-band SAR and Sounder).

As described in this section, the team assessed the value added to scientific investigations if one or both complementary instruments identified in Task 1 (VHF sounder and high-resolution stereo-capable imager) accompanied the anchor payload. The MDT also examined options for supplemental instruments that could provide synergistic or augmented capabilities to address outstanding scientific questions. For Task 2, the MDT again formed three subgroups with the following scientific themes:

- ATMOSPHERE Atmospheric processes and dynamics, past and present, as well as atmosphere-surface interactions and ionospheric phenomena. Included 14 members.
- GEOSPHERE Investigations of geologic processes currently active, active in the recent past (such as climate cycles), and in the ancient past. Included 16 members.
- HABITABILITY Investigations that enable the search for past and present habitable environments, and that enhance the protection of Martian and terrestrial life. Included 18 members.

These theme areas reflect the priorities of the partner Agencies (see Appendix A). For example, they are similar to Science Goals I–III of the Mars Exploration Program Analysis Group (MEPAG, 2020).

The following sections present science investigations that could be undertaken with I-MIM for each of the theme areas. The descriptions include background on the current state of knowledge relevant to the investigations, and an assessment of the potential contributions of I-MIM to advancing this state. The potential contributions of the anchor radar payload, the complementary instruments from Task 1, and any possible supplemental instruments are presented.

The results of these assessments are summarized in the Science Traceability Matrix (STM) shown in Section 5.4. Analogous to the Reconnaissance Traceability Matrix (RTM) presented in the previous section, the STM traces the investigations from their driving thematic goal, through the measurable parameters, the resolution and accuracy required, and the needed instrumental capabilities.

5.1 SUPPLEMENTAL SCIENCE: ATMOSPHERE THEME

The I-MIM platform provides a unique opportunity to address key outstanding questions regarding connections within and between Mars' dynamic climate regions, from shallow subsurface volatiles, through the lower atmospheric circulation structure, to emissions and atmospheric escape from the thermosphere and ionosphere, out to the space-weather environment (Figure 5.1). The associated scientific topics identified by the MDT Atmosphere Group are linked to high-priority science investigations of the partner Agencies (e.g., NASA MEPAG Goals 2 and 4; JAXA JMSEP). The anchor payload by itself can address important questions regarding volatile cycling between the shallow subsurface and near-surface environment, as well as characterize variability in the ionosphere.

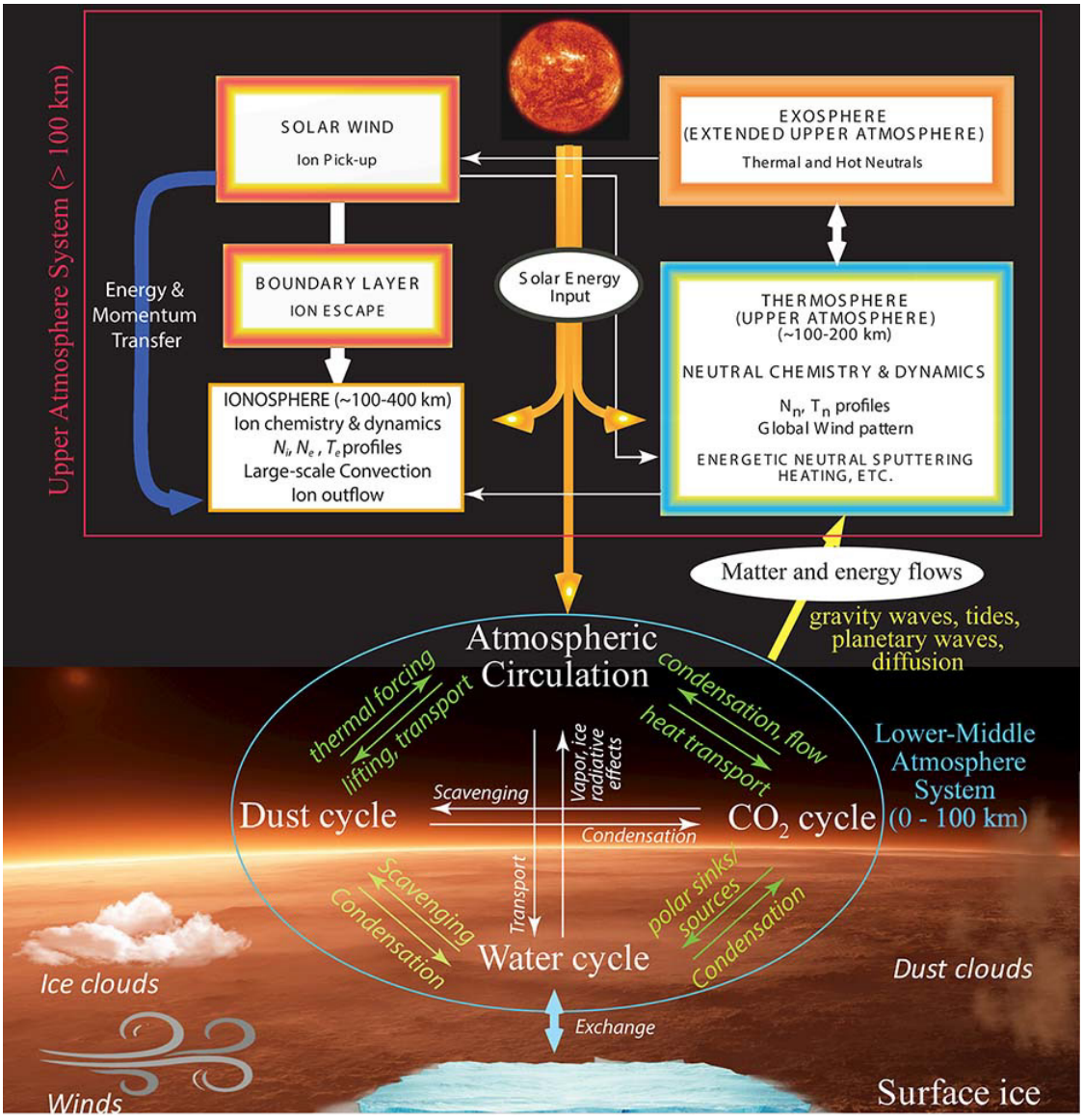

Figure 5.1 Schematic of some of the many expected connections within and between Mars' diverse climate domains. The I-MIM platform is well-suited to host payloads to conduct key investigations to unveil these connections and elucidate Mars' unique climate system and processes.

High-priority augmentations could further improve these investigations: a VHF radar sounder would improve ionospheric measurements and contribute to the fine characterization of the polar layered deposits, while a high-resolution stereo imager would provide important context to radar sounder measurements of both recurring slope lineae and polar layered deposits. As considered by the Atmosphere Group, additional supplemental payloads on the primary orbiter could finally elucidate Mars' atmospheric circulation and radiative balance by making 3D maps of temperature, water vapor, aerosols, and (crucially for the first time) vector wind. Further payloads could fill an important gap in our understanding of the ionosphere by mapping out electron precipitation, airglow, and the escape of water-bearing ions. To accommodate supplemental payloads, a high-altitude SEP communications relay orbiter (MSO-1) could host much-needed continuous weather and space weather monitoring, while a possible lander could provide key measurements constraining Mars' past climate, as well as ground truth orbital measurements (MSO-2). Many of the climate-related measurements and instruments discussed in this section were originally envisioned as part of the MOSAIC mission concept (described in significantly more detail by Lillis et al., 2021) studied in advance of the U.S. 2023–2032 Decadal Survey of Planetary Science and as the MACO (Mars Aqueous-environment and space Climate Orbiter) mission concept selected as large-scale research project #96 of Master Plan 2020 by the Science Council of Japan (SCJ), which corresponds to the second step of JSMEP.

As shown in the Science Traceability Matrix (Section 5.4), the MDT Task 2 Atmosphere Group established two organizing science themes related to the Martian atmosphere and climatology: 1) Surface-Atmosphere Interactions and 2) Atmospheric and Aeronomic Structure and Processes. The Atmosphere Group identified 5 Subtopics that represent priority investigations under each theme. Those that can be addressed by the primary anchor payload are shown in bold below. Additional high-value investigations that could maximize the mission's return on investment are identified (in *italics*) as supplemental payloads that would maximize the mission's return on investment.

Table 5.1 Overview of Atmosphere Group High-priority Science Topics

TASK 1 ATMOSPHERE GROUP – HIGH-PRIORITY SCIENCE TOPICS	
ATMO TOPIC 1	**Surface-Atmosphere Interactions**
ATMO 1.1	Surface/subsurface Volatile Inventory and Variability
ATMO 1.2	Recurring Slope Lineae
ATMO 1.3	*Near-surface Atmospheric Conditions*
ATMO TOPIC 2	**Atmospheric and Aeronomic Structure & Processes**
ATMO 2.1	Ionospheric Irregularities +Space Weather & Crustal Magnetic Field Effects on the Upper Atmosphere
ATMO 2.2	*Atmospheric Structure & Dynamics, Vertical Coupling, & Loss to Space*

KEY: Addressed by the anchor payload. *Addressed through potential augmentation.*

Per the STM, the I-MIM primary anchor payload makes measurements relevant to understanding key aspects of surface/subsurface/atmosphere interaction, recurring slope lineae, and ionospheric irregularities. In particular, its measurements of radar backscatter and reflection power can be used to probe near-surface structure and composition, including seasonal ice thickness, near-surface ice abundance, and depth to the ice table. In addition, plasma-induced frequency-dependent phase changes can be used to probe ionospheric irregularities that can disrupt communication and positioning signals.

Scientific foundations for each are summarized below, as are the ways in which the L-band SAR/SAR Sounder measurements enable key investigations, and the potential for complementary and supplementary payloads.

5.1.1 ATMOSPHERE GROUP: Scientific Foundations & Payloads

Learning more about surface-atmosphere interactions and the structure and processes of the Martian atmosphere is fundamental to understanding the climate history of Mars; whether, when, and how long conditions may have been favorable for microbial life; comparisons to the evolution of our home planet Earth and similar worlds in our solar system and beyond; and, the environmental conditions future robotic and human explorers will encounter. I-MIM has the potential to reveal much more about Mars as a system, linking the as-yet unexplored near-surface cryosphere with the atmosphere to reveal both short-term and long-term cycles that define Martian weather and climate. The following provides the scientific foundations for each topic identified by the Atmosphere Group, and describes I-MIM's potential contributions to addressing gaps in the current state of knowledge with the core, complementary, and/or supplementary payloads.

ATMOSPHERE SCIENCE TOPIC 1

SURFACE-ATMOSPHERE INTERACTIONS

Modern Mars is not a static planet. Volatiles, including H_2O and CO_2, are exchanged between the subsurface, surface, and atmosphere over diurnal, seasonal, and longer-term time scales (e.g. Head et al., 2003; Byrne et al., 2008; Calvin et al., 2015). In particular, large amounts of volatiles cycle between the polar region and lower latitudes through the atmosphere, resulting in dramatic changes to surface conditions and atmospheric conditions over time (e.g. Newman et al., 2005; Levrard et al., 2007; Phillips et al., 2011).

Understanding the volumes and geographical distribution of volatiles on Mars, as well as the processes responsible for volatile cycling and how they feed back upon one another, is critical for understanding the planet's global climate system (e.g., MEPAG Goals Document).

While the importance of volatile cycling on Mars is clear, large knowledge gaps remain. For example, it is well known that large amounts of both H_2O and CO_2 are seasonally deposited on the surface in the polar regions (Calvin et al., 2015; Piqueux et al., 2015). However, the volume of those deposits, their spatial variability, and how they evolve throughout the year is difficult to constrain given existing data. Up to ~1/3 of the Martian atmosphere condenses out at the poles during winter, being deposited as a dusty, porous CO_2 ice seasonal cap that extend down to the mid latitudes (Kieffer and Titus, 2001; Schorghofer and Edgett 2006). In some areas, the underlying older northern residual ice cap (a meters-thick deposit of water ice) is exposed in the summer, while other areas retain the seasonal frost and may be actively accumulating it (Calvin and Titus 2008). These observations demonstrate much temporal and spatial variability in the behavior of seasonal volatiles and their interaction with older volatiles and terrain.

In the North (but not the South), an annulus of water frost is also deposited seasonally (Wagstaff et al. 2008), which highlights hemispheric differences in volatile behavior that remain poorly understood. The retreat of this seasonal water-ice annulus may contribute to the majority of the total increase in atmospheric water vapor that occurs in the time leading up to seasonal CO_2 cap recession (Jakosky and Farmer 1982). Meanwhile, in the Southern hemisphere, the CO_2 ice sinters into a transparent solid slab throughout the winter. The base gets heated in the Spring, generating pressurized CO_2 jets that release fans of dust and create radial channels called araneiforms (e.g., Kieffer et al. 2006). Evidence of both accumulation and ablation of the Southern residual ice cap exists, but the secular changes to the mass balance of CO_2 ice at seasonal and longer timescales, and at different spatial scales, is still unknown.

Multiple datasets also confirm the likely presence of near-surface water ice throughout the Martian high and mid latitudes (Morgan et al., 2021), but the relative concentration of ice, its depth below the surface, and its geographical distribution all remain largely unknown. Without more detailed knowledge of those parameters, it is difficult to say how the ground ice may interact with the atmosphere, or even to determine the total volume of H_2O available for exchange over various timescales. Beyond seasonal variations, evidence suggests the polar ice caps record changes in relative ice and dust accumulation at the poles over much longer (kyr to Myr) timescales (Toon et al., 1980; Cutts and Lewis, 1982; Putzig et al., 2009; Hvidberg et al., 2012). In effect, the polar layered deposits may serve as a global climate record, similar to ice sheets on Earth. Volatile reservoirs at different latitudes are expected to exchange with each other over these longer timescales. Ice that has been building the polar cap likely comes from water vapor that was lost from lower latitude reservoirs as they became unstable. Therefore, knowledge of ice volumes, deposition/sublimation rates, and scales of water-vapor transport for any volatile reservoir (whether buried mid-latitude ice or ice in the polar layered deposits) will aid in interpreting the entire system and connecting what occurs at short timescales to longer-scale processes. Layers are observed on multiple vertical scales (from tens of centimeters in high-resolution images to tens-to-hundreds of meters in SHARAD and MARSIS radar-sounding subsurface reflectors), but still lacking is a clear connection between visible layers and layers (or packets of layers) that cause the radar reflectors. Overall, the link between layer formation, atmospheric processes, and orbital forcing-induced changes to the Martian system has remained elusive, rendering the record difficult, if not impossible, to interpret.

Recent observations with the ExoMars Trace Gas Orbiter (TGO) have captured the transport of water vapor in the upper atmosphere and emerging from the detached layer into the gas phase (Vandaele et al., 2019; Aoki et al., 2019; Villanueva et al., 2021). These observations suggest the importance of comprehensively monitoring water-vapor circulation in all seasons (including the dust-storm season) on a global scale (including day and night regions) and in the lower, middle, and upper atmosphere. This comprehensive study would reveal new insights about the interaction process among the water-vapor buffers of the polar cap, surface layer, and ice clouds; the detached layers with the atmosphere via condensation and sublimation (Villanueva et al., 2015; Aoki et al., 2015); and, vicissitudes of the atmospheric environment and climate of Mars.

To elucidate the processes that control the exchange of water and dust between the atmosphere and the surface, simultaneous observations of wind, temperature, water vapor, and atmospheric dust in the boundary layer are crucial. In-situ measurements of water vapor by a tunable laser spectrometer, combined with meteorological observations, would clarify the diurnal cycle of water condensation/evaporation near the surface. The relationship between the temporal variations of wind speed and dust measured by an in-situ meteorological package would clarify the threshold wind speed for dust lifting. Such measurements can fill the gap between the subsurface radar sounding and the submillimeter sounding at higher altitudes.

ATMO 1.1
Surface/Subsurface Volatile Inventory & Variability

Central to the investigation of surface-atmosphere interactions on Mars is characterizing the inventory of H_2O and CO_2 in the Martian surface and near-subsurface environment and its variability on diurnal and seasonal timescales. This topic includes seasonal water and CO_2 ice cap thickness, near-surface ice abundance, depth to the ice table, and characterizations of polar layered deposits, snowfall, and ice-related surface deformation.

CORE PAYLOAD

The anchor payload's ability to constrain near-surface ice abundance and properties helps shed light on the role and timescales for volatile emplacement and evolution (i.e., pore-filling versus snowfall, diffusive exchange through the regolith, seasonal processes, etc.). The I-MIM radar may be able to detect ground frost during certain times of year, plus InSAR phase differences may be used to detect changes in frost. The Mars Orbiter Laser Altimeter (MOLA) topography revealed latitude-dependent changes in elevation due to seasonal CO_2 processes on the order of tens of centimeters (at mid-to-high latitudes) to ~1.5–2 m (winter at latitudes poleward of 80°N) (Smith et al., 2001b; Aharonson et al., 2004; Xiao et al., 2022).

Variations in elevation may be of sufficient magnitude to be detectable as changes to the I-MIM surface reflectivity (in sounder mode) or the backscatter polarization properties (in SAR mode). Seasonal frost deposition begins around autumn equinox, reaching a maximum around spring equinox before retreating back to a minimum by summer solstice. Repeat measurements at a few locations throughout the mid to polar latitudes at intervals of Ls of ~20° can provide new temporal and spatial measurements of surface changes due to seasonal frost. InSAR with 1 cm sensitivity to vertical surface deformation would allow measurements of surface changes due to volatiles throughout the year.

Constraining the volatile inventory is a cross-disciplinary investigation, and the parameters needed to do so overlap those of the geosphere- and habitability-related investigations considered by the MDT. The I-MIM L-band radar measurements with vertical resolution of <1 m would provide a new scale of measurements of the polar layered deposits, which would help bridge the gap between the scales of layers seen in visible images and those of the lower frequency radar sounder data currently available.

The parameters needed for this investigation of the PLD are the same as those needed for the GEO 2.1 investigation. The parameters required for constraining the subsurface volatile inventory (both the near-surface ice abundance and depth to the ice table) are the same as those required for the GEO 2.2 and HAB 1.2 investigations. To reduce redundancy, the Atmosphere Group does not further address these investigations, but notes their crosscutting value.

HIGH-PRIORITY, POTENTIAL COMPLEMENTARY PAYLOAD OPTIONS

High-Resolution Stereo Imager

A high-resolution imager can provide important context to radar sounder measurements of polar layered deposits. For example, imagery can support interpretations of sounder data that measure the stratigraphic record, also known as the climate archive, of the polar layered deposits. HiRISE images show layers to ~1 meter in thickness, but current orbital sounding can only resolve ~ 10 meters vertically (McEwen et al., 2007; Seu et al., 2007).

VHF Sounder

The L-band sounder, a mode of the anchor payload, and a wide-band VHF sounder will both have ≥10x better vertical resolution than SHARAD, comparable to the best optical imagery available at present. Both of these instruments would support interpretations of radar observations that are currently ambiguous about the cause of reflections (Lalich et al., 2019). Despite optical imagery only being useful at exposed outcrops, the VHF sounder would nonetheless be useful for probing deeper into the PLDs than the L-band, with a gain of several hundred meters.

ATMO 1.2
Recurring Slope Lineae

Recurring slope lineae (RSL) are one of the most enigmatic features of the Martian surface, appearing as lengthening streaks on steep slopes that reappear each year during the warm seasons and fade during the cold seasons (McEwen et al., 2011). RSL are narrow (0.5–5 m) but long (>50 m), and occur as a group of ~100 in a single RSL site (McEwen et al., 2011, 2014; Stillman et al., 2014). The RSL sites are mainly located in four primary RSL regions (Stillman et al., 2014). Liquid water and brine have been proposed as the flowing material on RSL (the wet origin; McEwen et al., 2011, 2014; Grimm et al., 2017; Stillman et al., 2014, 2016, 2017) or as a trigger of the granular flow (the hybrid origin, e.g., melting and boiling; Massé et al., 2016; Raack et al., 2017), while other studies have proposed that RSL are not associated with water (the dry origin; Dundas et al., 2017; Dundas, 2020; Schmidt et al., 2017; Schaefer et al., 2019).

As these RSL formation mechanisms involve cycling of water vapor/ice (Kurokawa et al., 2022), dust (Dundas et al., 2017), or both, unveiling RSL origins is important for understanding the modern Martian climate system. Moreover, if RSL are triggered by subsurface ice, aquifers, or both (Abotalib and Heggy, 2019), I-MIM could obtain an indication of past Martian climate conditions, which deposited and preserved subsurface water reservoirs at these mid-to-low latitudes.

In order to understand the formation mechanism(s) of RSL and relevance to volatile and dust cycling, the Atmosphere Group aimed to constrain:

i. Surface and Subsurface Materials;
ii. Surface Topography Change with Time; and,
iii. Local Atmospheric Moisture Content.

While previous attempts to unveil the formation mechanism(s) of RSL chiefly relied on visible camera images taken by the HiRISE camera on Mars Reconnaissance Orbiter (MRO), the I-MIM radar would be able to acquire unique constraints on i and ii. A high-resolution imager, an MDT-identified high-priority payload, would support these radar observations. A potential demonstration lander would, if sent to RSL regions, be able to constrain iii.

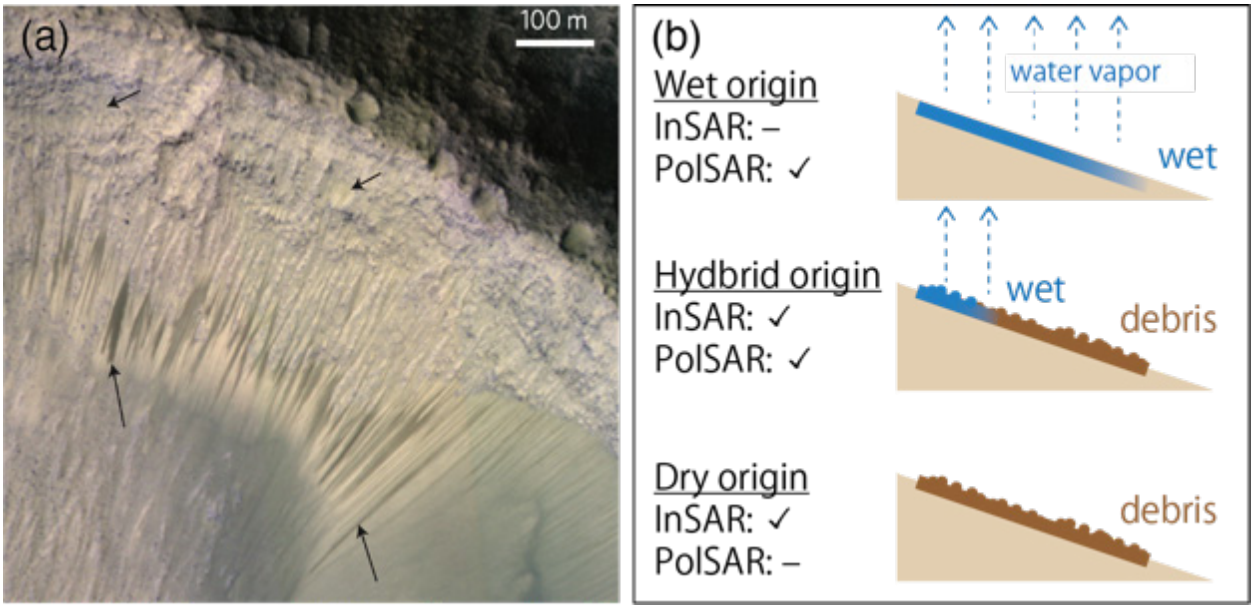

Figure 5.2 (a) A typical image of an RSL site when RSL are active. Adapted from McEwen et al. (2014). (b) Three categories of possible RSL formation mechanisms. Wet origin: RSL are water/brine flow and detectable by PolSAR. Hybrid origin: RSL are debris flow triggered by water and detectable by both InSAR and PolSAR. Dry origin: RSL are debris flow triggered by water-free mechanisms and detectable with InSAR.

CORE PAYLOAD: HIGH-RES APPROACHES

Three RSL-related investigations could be accomplished using the primary anchor payload:

1. To constrain subsurface water-ice content, SAR tomography, sounder mode observations, or both would indicate whether RSL regions have subsurface water reservoirs that trigger and sustain RSL activity. The spotlight mode is needed to resolve a single RSL. However, because numerous RSL that appear in a single RSL site likely share their water reservoir (in the case of the wet origin), even 30 m resolution mode observations would be sufficient for this purpose.
2. To detect possible changes in topography caused by RSL debris flow, which InSAR images of the surface can detect by measuring line-of-sight RSL changes. The I-MIM radar's spotlight mode can provide 0.5–5 m resolution (the widths of RSL), which is necessary given the horizontal scale of the topographic change is identical to that of (visible) RSL.
3. To constrain the nature of surface materials, most importantly whether they are dry or wet, which can be distinguished by combining InSAR and PolSAR approaches. Dry granular flow (the dry origin) is visible only using InSAR, while liquid flow (the wet origin) is visible only using PolSAR. Wet granular flow (the hybrid origin) is visible in both. Sounder observations might also constrain whether the surface is wet or not, but PolSAR would be desirable. Note that the reflected intensity of surface echo can be used to detect the water content, although the relation is not simply linear. The radar's 30 m-resolution observations can constrain the surface materials of RSL sites and regions.

Steep slope angles of RSL (typically ~30°; McEwen et al. 2011) may cause cluttering; the I-MIM team should evaluated the I-MIM radar further for RSL observations.

HIGH-PRIORITY, POTENTIAL COMPLEMENTARY PAYLOAD OPTIONS

High-Resolution Stereo Imager

Although HiRISE on MRO has obtained high-resolution images of RSL, simultaneous observations with a high-resolution imager would augment the radar studies. The imager could identify RSL activity by observing visible albedo changes, while both stereo imagery (made into digital terrain models) and InSAR and PolSAR approaches could detect any topographic changes. The latter could detect any subsurface water reservoirs associated with the activity as well.

OTHER POTENTIAL SUPPLEMENTAL PAYLOADS OF INTEREST

TIR Imager

Thermal infrared (TIR) imagers have measured surface temperatures of RSL-active regions (Stillman et al., 2014, 2016, 2017). The correlation between RSL activity and surface temperature is a basic property for understanding their formation mechanism(s). Along with existing data, simultaneous TIR observations at sufficiently high spatial resolution (5–10 m) along with the radar observations would help determine if RSL activity could be associated with melting water ice or brine formation.

ATMO 1.3 Near-Surface (Lowest Scale Height) Atmospheric Conditions

Together with radar measurements of the ice-cap thickness and the near-surface ice table, monitoring the surface temperature, dust, ice, and water abundances, and winds in the lowest scale height would help quantify the surface-atmosphere cycling of volatiles. Measuring D/H ratios could aid in understanding water condensation/sublimation processes through time. Further, measuring these same quantities above the boundary layer (described in 2.2.A, below) would help reveal the modern-day transport of volatiles and aerosols leading to a better understanding of the timescales for emplacement and preservation of ice around the planet.

OTHER POTENTIAL SUPPLEMENTAL PAYLOADS OF INTEREST

Meteorological Package on Potential Demo Lander, If Implemented

Another key issue related to Atmosphere Topic 1 is the extent to which heat exchanges occur between the atmosphere and the surface. Thus, the following lander-hosted measurements are desired: solar radiation, thermal radiation, temperature, pressure on the surface (required accuracy: < 1Pa), in-situ dust number density, and wind velocity.

Tunable Laser Spectrometer on Potential Demo Lander, If Implemented

The significance of water exchange and its role in the long-term atmospheric evolution of the subsurface (regolith) and atmosphere are poorly understood due to a lack of high-accuracy, daytime-relative, humidity measurements (e.g., Martinez et al., 2017; Polkko et al., 2022) at non-polar locations. A humidity sensor on the Curiosity rover implied a significant local time variation of water-vapor-volume mixing ratio at Gale Crater. However, the derived volume-mixing ratio has large uncertainty due to low humidity in daytime (Savijärvi et al., 2016). A tunable laser spectrometer is a relatively small, light, simple instrument that could perform in-situ measurements of gas abundances with high sensitivity. A tunable laser spectrometer on the Curiosity rover (Mahaffy et al. 2012) provided many new insights, such as detection of high-variability methane abundances (Webster et al., 2015) and the isotopic ratio of carbon dioxide (Webster et al., 2013). However, that instrument was not optimized for water-vapor measurements. A similar instrument optimized to measure water-vapor abundances on the surface could be flown (e.g., Rodin et al., 2020) to identify water exchange between the regolith and the atmosphere, which is key for understanding volatiles, as well as RSL, atmospheric structure, coupling, and loss to space. It could also measure the diurnal variation of D/H in water vapor, which can constrain the origin of its observed diurnal variation (Hu, 2019). Remote-sensing observations from orbit (e.g., by a submillimeter sounder) could measure water vapor in the planetary boundary layer (PBL) with 2–3 km vertical resolution. In-situ measurements of water vapor on the surface by a lander/rover platform, if implemented by the Agency partners, could characterize surface-atmosphere interactions, supplementing I-MIM and other remote-sensing observations.

TIR Spectrometer

A nadir-pointed TIR spectrometer can measure surface temperature. These measurements would be important to quantifying the surface-atmosphere cycling of volatiles. Prior missions have made such measurements and would be supplement measurements made by the anchor payload.

TIR Atmospheric Limb Sounder

See 2.2.A below.

NIR Spectrometer

A highly compact near-IR spectrometer could measure surface pressure from low Mars and areostationary orbits. Observing the NIR spectrum from 1000 to 2400 nm at 6 nm resolution to resolve fully the CO_2 band structure in reflected sunlight, it collects the necessary information to correct for the effects of variability in surface albedo/composition and broadband aerosol absorption/scattering. From this information, column abundance of CO_2 can then be retrieved to obtain surface pressure (Toigo et al., 2013) at a resolution of < 1 km from low orbit or <40 km from an areostationary orbit, where it may be slewed along with other instruments observing the disk.

Submillimeter Sounder

The D/H ratio in water is a good proxy for both water exchange between subsurface reservoirs and the atmosphere and the sublimation-condensation process (e.g., Aoki et al., 2015; Villanueva et al., 2015). Submillimeter-wave (submm) (0.3–1 THz) heterodyne spectroscopy would provide a powerful tool for measuring surface temperature, H_2O, and

HDO/H_2O. (For submm capabilities providing atmospheric vertical water-vapor profiles, temperatures, and vector winds, see 2.2.A below).

Doppler Lidar

See 2.2.A below.

ATMOSPHERE SCIENCE TOPIC 2
ATMOSPHERIC AND AERONOMIC STRUCTURE & PROCESSES

The I-MIM platform has the potential to host payloads that can transform our understanding of the Martian atmosphere and climate system, from the near-surface planetary boundary layer up through the mesosphere, thermosphere, ionosphere, exosphere, and magnetosphere. As described in the MOSAIC concept (Lillis et al., 2021), the more atmospheric variables measured simultaneously, the greater the improvement in understanding processes responsible for the circulation of matter and energy within and between Mars' dynamic and diverse climate domains.

The anchor payload would characterize ionospheric irregularities that can disrupt communication and future potential GPS signals. The mission would benefit from significant improvements in accuracy if a VHF sounder accompanied the core payload. Additional payloads on the main polar orbiter would have the potential to transform our understanding of atmospheric structure, dynamics, vertical coupling, and loss to space. The first-ever systematic, remote-sensing of the wind in the lower atmosphere (below 150 km) would provide the greatest scientific return, especially if combined with measurements of temperature, water vapor, and aerosol abundance.

The recently discovered unexpected rapid transport of water vapor to the middle atmosphere (~70 km altitude) during dust storms (e.g., Fedorova et al., 2020; Chaffin et al., 2021) can shed a new light on the atmospheric evolution of water and escape to space. The direct transport of water vapor to the middle and upper atmosphere significantly accelerates the water-loss rate to space and may be responsible for major water loss from Mars. However, the gap of continuous observations in the upper atmosphere (thermosphere and ionosphere) and between the middle atmosphere to the resultant corona makes our understanding highly model-dependent. The orbit of the I-MIM orbiter is ideal to fill the gap by capturing both solar and dust-event responses, as well as seasonal variations.

ATMO 2.1
Ionospheric Irregularities, Space Weather, & Crustal Magnetic Field Effects on the Upper Atmosphere

IONOSPHERIC IRREGULARITIES

It is well known that ionospheric irregularities cause distortions of L-band SAR images on Earth (Sato et al., 2021). In order to remove ionospheric noise from SAR images, it is necessary to understand and characterize ionospheric irregularities. Measuring the horizontal scales and amplitudes of ionospheric irregularities is important for understanding the dynamics of Mars' upper atmosphere and its response to space-weather activity. In addition, these irregularities cause disruptions to surface-orbit communications including future potential global positioning (GPS) systems that might be envisioned for Mars.

Agency partner strategic documents (e.g., MEPAG; JSMEP goals documents) identify ionospheric structure and dynamics and their influences from both below and above as priority areas of investigation. L-band SAR images measure total electron content (TEC). While past radars including MARSIS (Safaeinili et al., 2007) and SHARAD (Campbell et al., 2014) have measured TEC, it is valuable to extend the TEC climate record into the 2030s. TEC measurements by the anchor payload could be augmented by measurements of variables in processes driving these irregularities, such as high-energy electron precipitation from above and atmospheric wave activity from below (i.e., dayglow imaging).

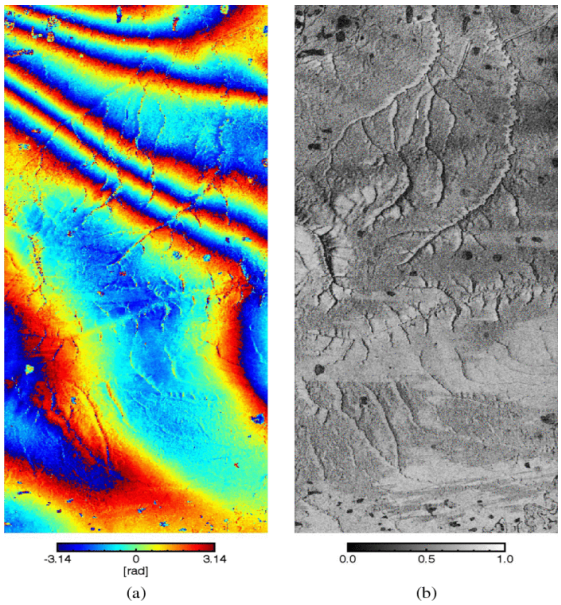

Figure 5.3 An example of ionospheric irregularities caused by aurora activity observed by ALOS (Advanced Land Observing Satellite) L-band synthetic aperture radar (SAR) at Earth. (a) Interferogram as phase changes and (b) coherence with azimuth and range lengths of 66 and 28 km, respectively (adopted from Gomba et al., (2016).

SPACE WEATHER

Human exploration of the Moon and Mars introduces new challenges for space-weather research and operations. Enhancement of capabilities for the characterization and forecasting of the space-radiation environment outside of the protection of Earth's atmosphere and intrinsic magnetic field is a timely and important research subject, as it will be vital to protect astronauts exploring Mars.

Understanding of the magnetic structure and variations around the planet provides essential information to assess the space-radiation environment.

To infer the radiation environments on the surface of Mars, critical knowledge includes: (a) the distribution of open magnetic field lines connected to the surface resulting from magnetic reconnection between the crustal and solar-wind fields; and, (b) the portion of these open field regions over the entire surface of Mars. These parameters directly determine the peak altitude and geographic distribution of auroral emission that arises from the penetration of energetic particles. Conversely, by taking a 2D image of the Martian aurora (e.g., Schneider et al., 2021), it is possible to visualize the distribution of the penetrating energetic particles. The combination of auroral imaging and measurements of solar energetic particles would allow us to characterize the energetic particle environment from the surface to the upper atmosphere of Mars. The comparison of northern and southern hemispheres would enable investigations of the global effects of intrinsic magnetic fields of crustal origin. In particular, it is likely that atmospheric escape rates are directly controlled by variations in the penetration depth of solar-wind magnetic fields in the presence or absence of intrinsic magnetic fields.

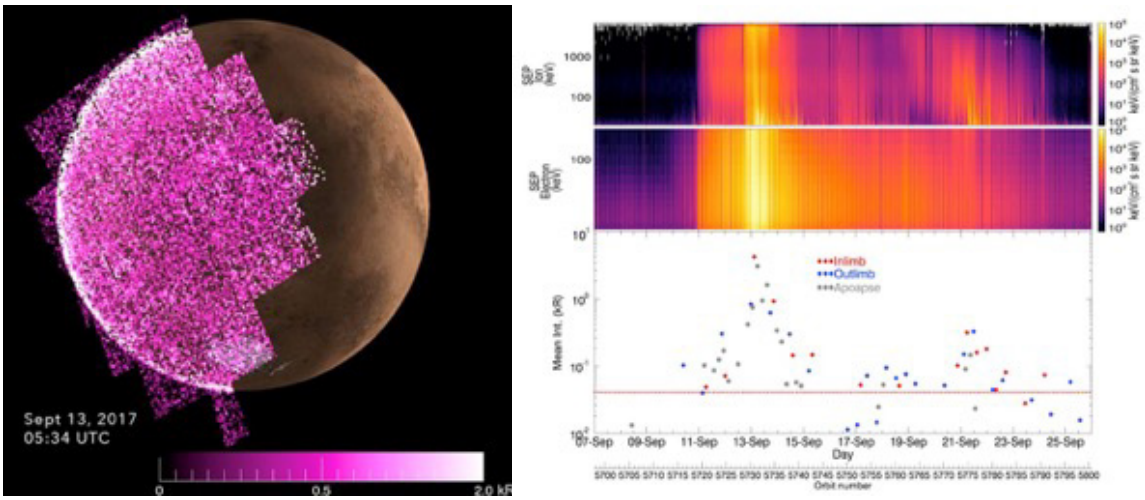

Figure 5.4 Ultraviolet diffuse aurorae image of Mars (left) at the peak of September 2017 space weather event, globally spanning Mars' nightside. The right panel shows the timeline of diffuse auroral detections and precipitating solar energetic particles (SEPs) populations. The primary auroral brightening correlates well with SEPs (Schneider et al., 2018).

CRUSTAL MAGNETIC FIELD EFFECTS ON THE UPPER ATMOSPHERE

Mars does not possess a global intrinsic magnetic field and the space environment around Mars is very different from that of Earth. Despite the lack of a global magnetic field in the present day, Mars has remanent crustal magnetic fields, indicating that ancient Mars once had a strong intrinsic magnetic field (e.g., Weiss et al., 2008). Planetary magnetic fields can either suppress or enhance the atmospheric loss of water to space (e.g., Sakata et al., 2020; Sakai et al., 2021), and understanding the space environment during extreme solar events is also relevant to elucidate the past atmosphere.

Martian crustal magnetic fields have a large hemispheric asymmetry and strong fields only exist in the southern hemisphere (e.g., Langlais et al., 2019) (Figure 5.5). High-cadence observations of both northern and southern hemispheres with the ~2-hour orbital period of the I-MIM orbiter could enable comparisons of regions with and without crustal magnetic fields under similar external solar conditions. Since the I-MIM orbiter would continuously stay in the direct source region of water and atmospheric loss to space around 300 km altitude, the comparison provides crucial information for assessing the effects of crustal magnetic fields, not only on the space-radiation environment at Mars but also on atmospheric escape.

Although the crustal magnetic fields are stable on human timescales, the changing solar conditions and resultant complex interaction between the solar wind and planetary atmosphere/magnetic fields facilitates the dynamically changing space environment around Mars (e.g., Lee et al., 2018). Solar energetic electrons precipitate along magnetic field lines into the upper atmosphere of Mars, with a highly complex magnetic field structure (Jolitz et al., 2021). The pattern of energetic electron precipitation is reflected in maps of Martian diffuse aurora (Schneider et al., 2015), providing potentially groundbreaking observational tools for understanding crustal magnetic field effects on the space-radiation environment around Mars.

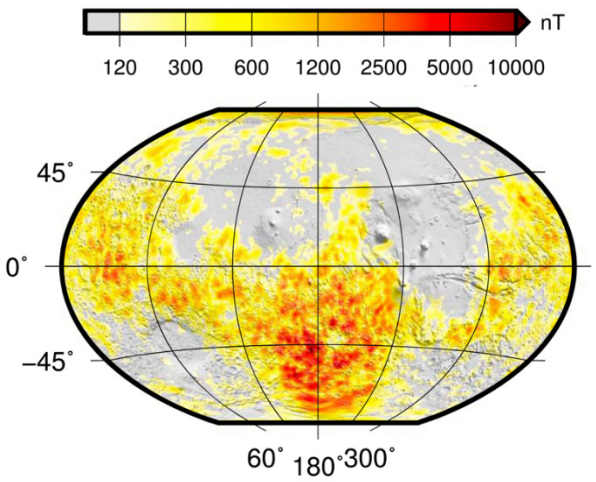

Figure 5.5 Spatial distribution of Martian crustal magnetic fields at the surface (adopted from Langlais et al., 2019)

I-MIM's roughly 300 km-altitude, high-inclination orbit is suitable for clarifying the effects of crustal magnetic fields on space-radiation environments and resultant effects on atmospheric escape. Two measurements are of particular interest: (a) observationally clarify the dependence of atmospheric composition and escape on crustal magnetic fields; and, (b) compare Mars aurora over the northern (no significant crustal magnetic fields) and southern (strong magnetic field) hemispheres. For the first investigation of interest, the orbiter could obtain in-situ horizontal 2D maps of the magnetic field, O+ outflow/downflow, and ion composition in the ionosphere. For the second, important observations are altitude profiles of aurora emissions, electron precipitation, and magnetic field strength and direction in the northern and southern hemispheres and their time variations.

CORE PAYLOAD

The phase shift of InSAR can be used to determine total electron content (TEC) in the Martian ionosphere. TEC is expected to respond to both influences from above (solar EUV and electron precipitation), as well as gravity and planetary waves from below, leading to ionospheric irregularities. In terms of ionospheric density and ionospheric irregularities, two effects of the ionosphere on radio-wave propagation are phase advance of the carrier and rotation of the polarization angle (Faraday rotation). The former is proportional to the total electron

content experienced by the radio wave, and the latter is related to the magnetic field strength along the propagation direction and TEC. Several methods can be used to determine and remove ionospheric TEC effects from InSAR data (e.g., Gomba et al., 2016; Furuya et al., 2017). For example, in addition to the main band, a Phased Array-type L-band Synthetic Aperture Radar-3 (PALSAR-3) onboard ALOS-4 would provide a split-band of 1294.5 MHz ±5 MHz to reduce ionospheric effects (Motohka et al., 2019). Adding onboard signal processing functions for ionospheric correction by splitting the bandwidth would not require large additional resources and would enable calibration of ionospheric effects in the InSAR data. Adoption of a similar method for the SAR onboard I-MIM may be worth consideration.

HIGH-PRIORITY, POTENTIAL COMPLEMENTARY PAYLOAD OPTIONS

VHF Sounder

The 2D structure of ionospheric irregularities (TEC variations) could be obtained by split-band observation using L-band InSAR. If VHF SAR with the same horizontal resolution is added, derivation of lower or more accurate TEC at each pixel could be attained by utilizing large frequency differences.

OTHER POTENTIAL SUPPLEMENTAL PAYLOADS OF INTEREST

Radio Occultation

The frequency shift of radio waves passing through the Martian ionosphere could provide ionospheric density profiles, providing important altitude-dependent information complementary to the InSAR's altitude-integrated TEC measurements. While radio occultations with Earth can be useful, inter-spacecraft radio links could provide significantly better coverage (Lillis et al., 2021).

UV/Visible Imager

A 2D UV/visible image of the Martian aurora could be used to visualize the distribution of penetrating energetic particles. Continuous observations at the same altitude would unambiguously differentiate the effects of lower atmospheric activities such as dust storms and gravity waves; solar activities including solar extreme events; and, crustal magnetic fields mainly localized in the southern hemisphere. A dayglow imager (limb and nadir imaging at 297 nm and/or 557.7 nm) could provide the 2D structure of the atmospheric wave activities independently from SAR and might help calibrate out ionospheric interference in SAR data. In order to understand the upward transport of energy from the lower atmosphere, suitable measurements of the effects of the upward propagation of gravity waves are needed. Such measurements could be made by dayglow imaging at CO_2 UVD (and/or O5577) emission with nadir and limb geometries, ranging 10–20,000 Rayleigh with accuracy 10 R. Such an instrument would also be capable of characterizing aurora on the nightside caused by the precipitation of electrons.

Energetic Particle Detector & Electron Analyzer

High-energy electron precipitation from space is one important source of ionization that can cause the structure of, and irregularities in, ionospheric densities. Electron precipitation measurements by an energetic particle detector and electron analyzer covering the energy range of 0.01–200 keV could help in understanding the mechanisms behind the formation of the irregularities. A simple lightweight energetic particle detector on the primary orbiter could measure electrons from 10 to 200 keV. These particles deposit their energy between ~40 km and ~100 km in the Martian atmosphere, often causing radar blackouts (Sanchez-Cano et al., 2019), and are thus important to characterize as a primary source of energy input to the Martian middle and upper atmosphere. An electron electrostatic analyzer (ESA) on the primary orbiter could characterize the population of precipitating electrons (i.e., 0.02–5 keV) that causes most ionization in the nightside upper atmosphere, and is thus primarily responsible for the highly dynamic and patchy nightside ionosphere. This ionosphere may interfere with communication and

positioning signals. In order to elucidate effects of solar activities (solar flares and CMEs) and related particle precipitation on water and atmospheric loss to space, observations of solar energetic particles and an electron precipitation map resulting from electron detectors covering energy of 0.02–200 keV would be suitable.

Ion Mass Spectrometer

See 2.2.A below.

Retarding Potential Analyzer (RPA) and Ion Drift Meter

See 2.2.B below.

Magnetometer

Magnetic fields guide the motion of electrons and ions within Mars' induced hybrid magnetosphere. A 3-axis vector magnetometer with the range of ±2000 nT with accuracy 0.5 nT per-axis on the primary orbiter would thus provide important context for measurements of ions and electrons.

Space Weather Package on Potential High-altitude or Areostationary Relay Orbiter, If Implemented

The source region of atmospheric loss to space is known to be highly affected by severe solar events such as solar flares and interplanetary coronal mass ejections (ICMEs) (e.g., Jakosky et al., 2015). Continuous solar radiation, upstream solar wind, and interplanetary magnetic field (IMF) monitoring are essential elements for space-weather research and operation. A high-altitude platform hosting a solar-wind ion analyzer, magnetometer, solar EUV monitor, and (desired) solar energetic particle monitor could make these measurements in a package <8 kg. These measurements are more useful if at least one high-altitude platform is outside the Martian bow shock in the upstream solar wind, as noted in the MOSAIC concept (Lillis et al., 2021).

ATMO 2.2
Structure, Dynamics, Vertical Coupling, & Loss to Space

It is almost certain that Mars once had a wet and warm climate with the presence of liquid water on the surface. Where/how has such a large amount of water gone? Recent studies show that it is partially lost to space, driven by the short-term variation of the climate in the lower atmosphere (e.g., Chaffin et al., 2021). Thus, coupling between lower and upper atmosphere (in particular the vertical transport of water), is important for understanding the water history on Mars. The lower atmosphere (ATMO TOPIC 2.2.A) and the upper atmosphere (ATMO TOPIC 2.2.B) are treated separately below.

ATMO 2.2.A – Lower Atmosphere

These lower atmosphere measurements could be combined with in-situ wind, temperature, and composition measurements around 300 km to understand the role of vertical atmospheric coupling in the loss of volatiles to space. Measurement of isotopic ratios of O, H, C, and N in this region would provide a breakthrough in understanding atmospheric evolution by constraining all important mass fractionation factors (i.e., the degree to which lighter isotopes escape more easily). Internal atmospheric gravity waves are recognized as an important part of the regional coupling between the lower and upper atmosphere. An airglow measurement is suited to measuring the key parameters of these waves and complements observations up to 120–140 km altitude.

Last, the role of surface-atmosphere interactions (Atmosphere Topic 1) in long-term water history is not understood. If implemented by the Agency partners, a tunable-laser spectrometer on a potential lander/rover could make a key measurement: continuous monitoring of atmospheric water vapor abundance on the surface to constrain water exchange between subsurface (regolith) and atmosphere.

Core Payload

N/A.

To address atmospheric structure, vertical coupling, and loss to space, the systematic vertical profiling of vector winds and water vapor is the highest priority. A variety of instrument concepts could advance these measurement goals (e.g., Tamppari et al., 2018; 2022).

OTHER POTENTIAL SUPPLEMENTAL PAYLOADS OF INTEREST

Submillimeter Sounder

Submm sounding (0.3 – > 1 THz frequency region) observations, especially from a near-circular orbit, can systematically profile the atmosphere, yielding measurements of temperature, vector wind, water vapor and its isotopologues, and various other trace gases. These daily, globally sampled profiles would provide new and unique information furthering the study of the water cycle, weather and climate, and vertical coupling within the atmosphere.

This instrument type has high-frequency resolution, which enables observations of trace molecules in the upper atmosphere, as well as observations of the wind field by Doppler velocity. In addition, because of its longer wavelength compared to infrared, it is less susceptible to absorption and scattering by dust.

Therefore, it is possible to observe the target species, including water vapor, even during dust storms. Also, since it does not need a background light source like the Sun, it can be used for observations at any time, day or night, on Mars.

When observing the atmosphere from a near-circular orbit allowing multiple orbits per Martian day, submm limb sounding and nadir observations would provide information necessary to create seasonal 3D (altitude, longitude, latitude) maps of winds, temperature, and trace gases, including volume mixing ratios of water vapor, HDO, and O_3. By having two views (either rapid scanning of the atmosphere for different look angles or two antennas), the native line-of-sight winds can be used to produce vector wind fields.

The detectable molecules (those with a dipole moment) as well as the altitude range, vertical resolution, and precision achievable for various frequency regions between 0.3 - ~1 THz are shown in Read et al., (2018) and reproduced in Figures 5.6 and 5.7. These results depend somewhat on seasons (e.g., abundance of water vapor or dust-induced warming of the atmosphere), tangent altitude, band selection, and integration time.

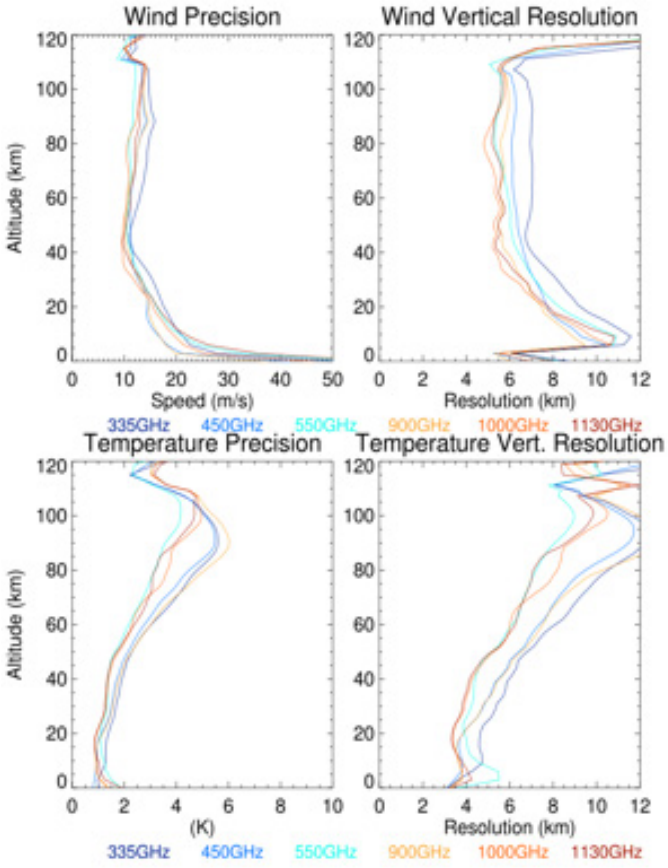

Figure 5.6 Wind and temperature estimated single-profile precisions for a variety of frequency ranges. Reproduced from Read et al. (2018).

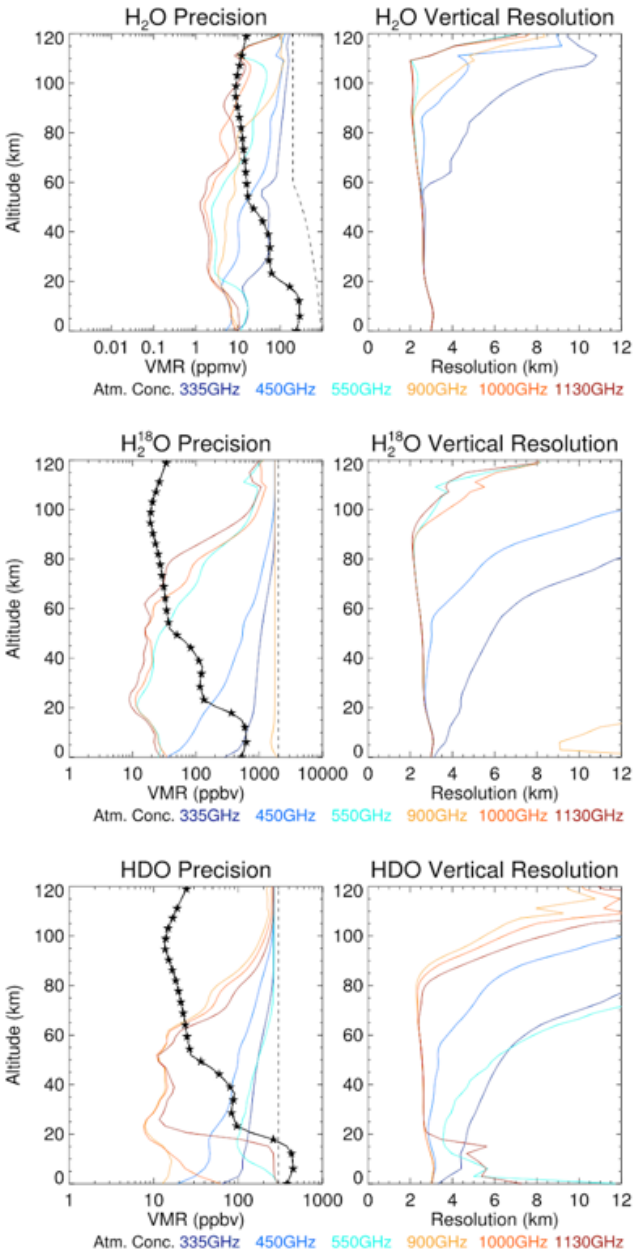

Figure 5.7 Water, $H_2{}^{18}O$, and HDO estimated single-profile precisions for a variety of frequency ranges. The black, starred line gives the assumed concentration profile. The dashed, black line is the assumed a priori uncertainty. Reproduced from Read et al. (2018).

Doppler Lidar

A lidar instrument could measure the vertical profile of line-of-sight winds in the lower atmosphere, making use of the backscatter of dust aerosols. One example is the MARLI instrument under development (Abshire et al., 2022), which is envisioned to fly on an orbiter in a near-circular orbit, oriented 30 deg off-nadir in the cross-track direction.

It would measure vertical profiles of atmospheric dust (aerosol backscatter), water-ice (via cross-polarized backscatter), line-of-sight winds (via aerosol doppler shift), and line-of-sight distance to the surface. The performance of MARLI has been estimated using extinction profiles, scaled to the MARLI wavelength of 1064 nm, from the MRO Mars Climate Sounder instrument (MCS; McCleese et al., 2007; Kleinböhl et al., 2011, 2017). Performance estimates are shown in Figures 5.8 and 5.9.

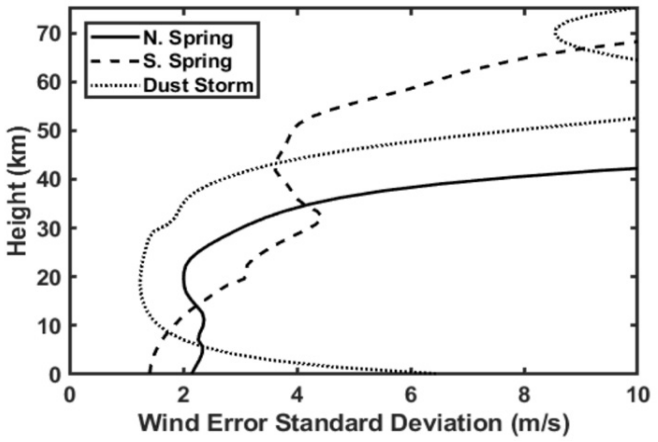

Figure 5.8 Estimated RMS wind speed uncertainty averaged over 2 deg latitude and 2 km vertical bins, assuming a horizontal wind speed of 18 m/s in the cross-track direction.

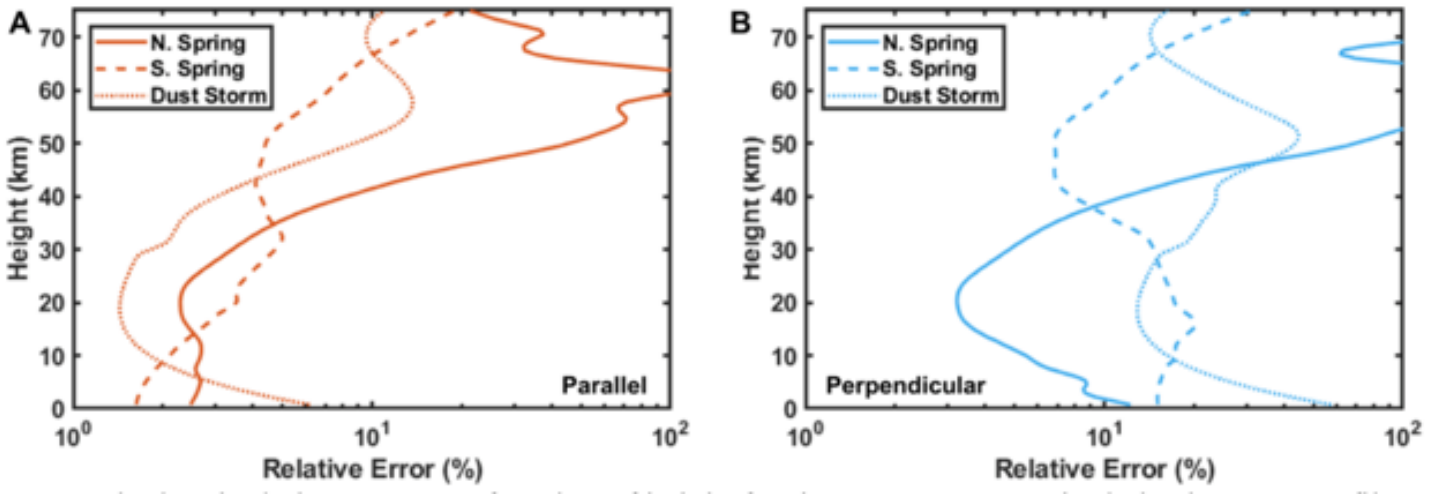

Figure 5.9 Relative error estimates for the parallel and cross-polarized backscatter measurements (A and B, respectively), used for dust and water-ice aerosol profile retrievals. This assumes 2 deg latitude and 2 km altitude bins.

Thermal Infrared Atmospheric Imager

This technique could provide wind data from an orbital platform in a near-circular orbit (e.g., the Mars Doppler Wind and Temperature Sounder, MDWTS, currently under development). This instrument uses gas-cell radiometers (Banfield et al., 2022; Colaprete et al., 2022). Accuracy estimates are < 5 m/s over an altitude range of ~5–120 km with <5 km vertical resolution. With a fixed (non-scanning system), such an instrument would measure both zonal and meridional winds with 10 km horizontal spacing.

TIR Atmospheric Limb Sounder

Because systematic vertical profiles of aerosols are also high priority in providing key information about what forces the atmospheric temperature and wind response, an infrared limb sounder similar to the currently operating MRO MCS experiment (Kleinböhl et al., 2016) would be beneficial. Such an instrument could also measure the vertical profiles of temperature and water vapor (Figure 5.10). While other methods could achieve vertical profiles of water vapor (e.g., the submm sounder discussed above) and ongoing measurements such as the solar occultation measurements (e.g., ACS and NOMAD on TGO; Belyaev et al., 2021; Aoki et al., 2019), an infrared profiler technique with its important supplementary aerosol measurements would naturally complement the envisioned wind measurements.

It would be able to provide water-vapor vertical profiles over ~13 orbits per day, yielding systematic global coverage from near-surface to 30 km, with < 10 ppm below 20 km altitude (Figure 5.10). It could also provide surface temperature as well as the vertical profiles mentioned above, all with current technology enabling improved vertical resolution especially in the boundary layer. The measurement of aerosols would complement the wind measurements by identifying the forcing of the atmosphere.

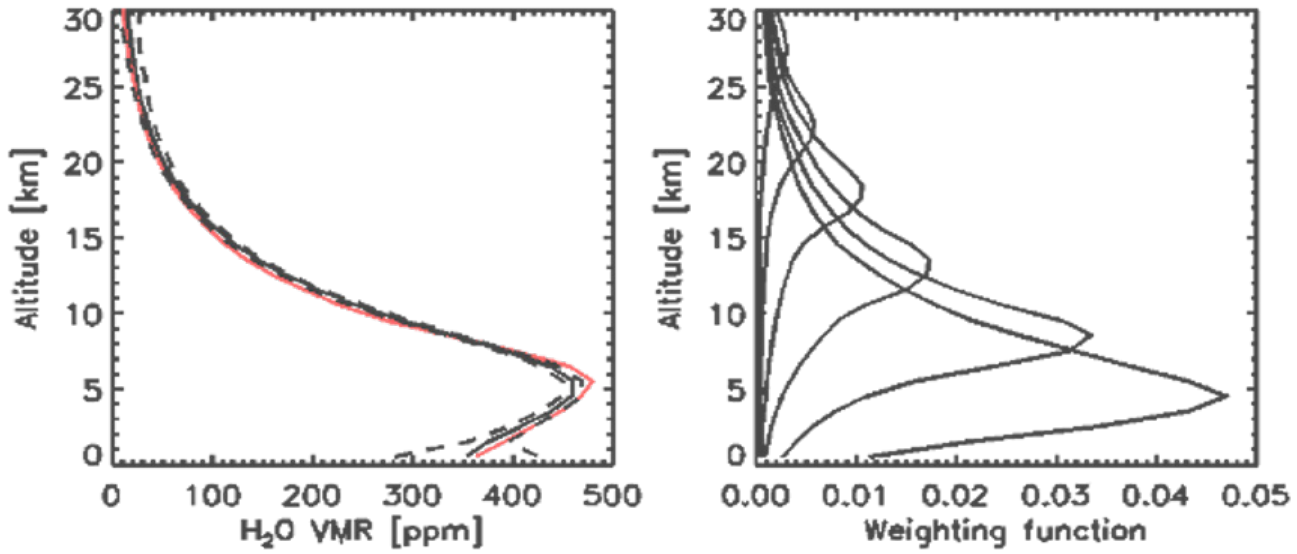

Figure 5.10 Simulated water-vapor retrieval for a limb measurement in the far infrared from an instrument such as the Advanced Mars Climate Sounder (AMCS). (Left) The retrieval profile is in black, with dashed lines giving error bars. The red profile is the true water-vapor profile. This simulation uses the current MCS detector geometry. (Right) Vertical response functions (weighting functions) for the simulated retrieval. The simulation still uses the current MCS detector geometry. However, AMCS would have higher vertical resolution enabled by modified detector geometry, which provides a weighting function distribution with three weighting functions in the lowest scale height.

Meteorological Package on High-altitude or Areostationary Orbiter, if Implemented.

A high-altitude platform allows for synoptic monitoring of mesoscale and regional-scale conditions in the lower atmosphere. A lightweight instrumentation package (<7 kg) consisting of a NIR spectrometer, mini-TIR spectrometer, and lightweight visible camera could measure dust and ice optical depth, water vapor and ozone column abundance, and altitude profiles of temperature up to 50 km, across all seasons and times of day. Optimally, four small areostationary platforms would allow for continuous lower atmosphere monitoring over most latitudes (Lillis et al., 2021).

Meteorological Package on Demo Lander, if Implemented

One of the big unsolved issues is the mechanism of how dust lifts into the atmosphere. Since dust is the major heat source, this fundamental information would help define the vertical structure of the atmosphere. This mechanism can be investigated by the simultaneous in-situ measurements of dust number density (required accuracy: < $10^6/m^3$), wind velocity (required accuracy: < 1m/s), and pressure (required accuracy: < 1Pa) on the surface.

ATMO TOPIC 2.2.B – Upper Atmosphere

An understanding of the upward transport of water/water-related species to the source altitude of atmospheric escape (i.e., exobase for neutrals and upper ionosphere for the ionized atmosphere) is essential for understanding water and volatile loss to space. Completing the investigation of the vertical transport of water molecules and other species from the surface to the upper atmosphere requires observations of the main ionospheric water-related ions (separation of CO_2 and H_2O related species) simultaneously with O+ and O2+ inflow and outflow fluxes, along with lower atmospheric wind and water vapor described above.

Understanding the escape history of the Martian atmosphere is strengthened by measurements of isotopic ratios in the upper atmosphere. Heavier isotopes are more difficult to remove from the atmosphere by processes such as sputtering (e.g., Jakosky, 2019). Thus, comparison of isotopic ratios at

the surface and in the upper atmosphere can effectively anchor models of isotope-dependent atmospheric escape and thus constrain possible climate histories.

A high-resolution ion/neutral mass spectrometer (HRMS) on the primary radar-carrying orbiter could make key measurements to elucidate Mars' atmosphere. Determination of the fractionation factors combined with noble gas isotope compositions in the lower atmosphere would enable estimation of the mass of Mars' past atmosphere and support studies of climate evolution.

At minimum, important measurements would constrain ^{20}Ne (the major isotope) abundance within a factor of three uncertainty, which corresponds to uncertainty estimates of ^{22}Ne measurements by the Viking lander (Owen et al. 1977; Figure 5.11).

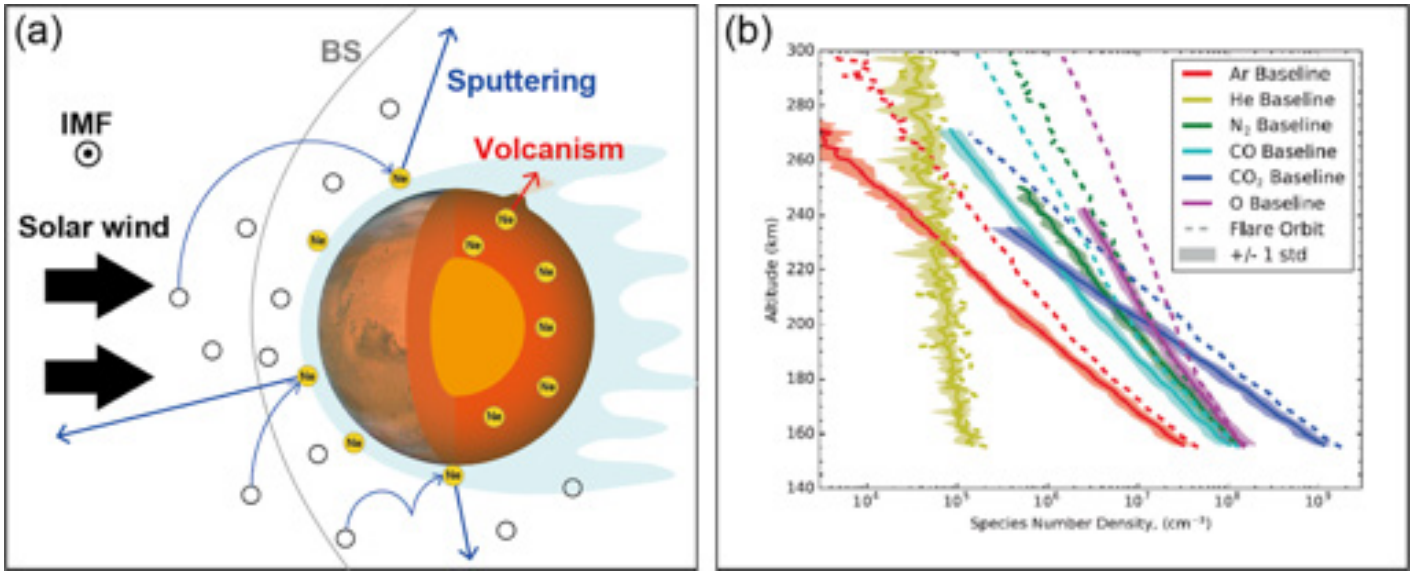

Figure 5.11 (a) A schematic image of Mars' atmospheric Ne in a balance between sputtering loss and volcanic degassing. Its abundance and isotopic ratio are the target for the measurements with the mass spectrometer onboard any potential demonstration lander, if implemented. (b) The number densities of neutral species in Mars' upper atmosphere for the average (solid lines) and flare-affected (dashed lines) conditions (Adapted from Cramer et al., 2020). The mass-dependent fractionation with the altitude causes isotopic fractionation for noble gases upon sputtering, which can be directly measured by HRMS onboard the I-MIM orbiter.

Fully constraining ^{20}Ne abundance within a factor of two an ^{20}Ne/^{22}Ne ratio with an uncertainty less than 10% would be sufficient for elucidating the source of Ne (captured solar nebula/solar-wind-implanted dust or chondritic building blocks; Kurokawa et al., 2021; Figure 5.12). Additional constraints on the ^{20}Ne/^{22}Ne ratio with the uncertainty less than 1% would distinguish between two possible Ne origins with similar (but not identical) isotope ratios: captured solar nebula and solar-wind-implanted dust. Identifying the origin of Ne requires the isotopic fractionation factor of Ne escape, which could be constrained by an HRMS.

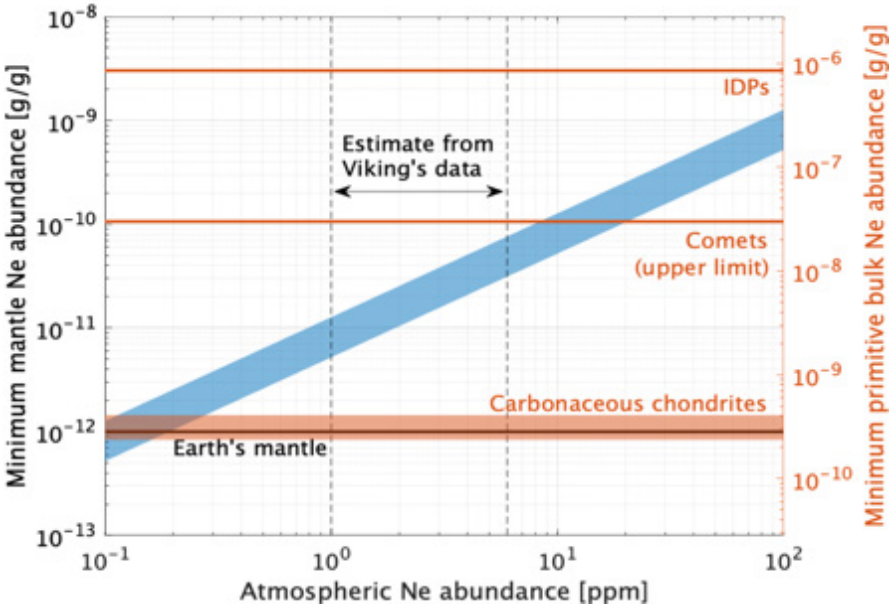

Figure 5.12 Minimum estimates for mantle (left axis) and primitive bulk (right axis) Ne abundances as a function of that of atmospheric Ne (blue area). The balance between the atmospheric loss and volcanic supply is assumed. The range of the blue area comes from the uncertainty in the elemental fractionation factor of sputtering. Dashed lines denote the range of atmospheric Ne abundance estimated from Viking data (Owen et al., 1977). Earth's bulk mantle Ne abundance (Marty, 2012) is shown for comparison to the Martian mantle value (left axis). Orange lines are Ne abundances in possible sources to compare with the Martian primitive bulk value (right axis). Carbonaceous chondrites: Marty (2012). Comets: Rubin et al. (2018). IDPs: Flynn (1997). Adapted from Kurokawa et al. (2021).

OTHER POTENTIAL SUPPLEMENTAL PAYLOADS OF INTEREST

UV & Visible Imager

To understand energetic transport from the lower atmosphere, dayglow imaging at CO_2^+ UVD (and/or O5577) emission with nadir and limb geometries, ranging 10–20,000 Rayleigh with accuracy 10 R is suitable for measuring the key parameters of internal atmospheric gravity waves.

Retarding Potential Analyzer (RPA) & Ion Drift Meter

Investigations on the effects of lower atmosphere variation (e.g., dust storms) on atmospheric escape could benefit from an in-situ horizontal 2D map of O+ outflow/downflow in the ionosphere, obtained through a combination of an IDM (ion drift meter) with a vertical velocity accuracy of less than 20 m/s and ion composition (M/dM > 40) observations. Based on the model I-MIM orbit, the expected density range to be observed is 100–105 cm^{-3}.

Ion Mass Spectrometer

Understanding the upward transport of water/water-related species to the source altitude of atmospheric escape (i.e., exobase for neutrals and upper ionosphere for ionized atmosphere) is essential to understanding water and volatile loss to space).

To complete the investigation of vertical transport of water molecules and other species from the surface to the upper atmosphere, simultaneous observations of the vertical profiles of the main ionospheric water-related ions (separation of CO_2 and H_2O related species) and of lower atmospheric wind and water vapor is necessary. To separate CO_2 and H_2O related species, in-situ high-resolution measurements of ion composition with M/dM > 3000 in the density range of > 103 cm^{-3} is required, along with accurate ion temperature observations in the range of 300–20000 K per the model I-MIM orbit.

OTHER POTENTIAL SUPPLEMENTAL PAYLOADS OF INTEREST

UV & Visible Imager

To understand energetic transport from the lower atmosphere, dayglow imaging at CO_2^+ UVD (and/or O5577) emission with nadir and limb geometries, ranging 10–20,000 Rayleigh with accuracy 10 R is suitable for measuring the key parameters of internal atmospheric gravity waves.

Retarding Potential Analyzer (RPA) & Ion Drift Meter

Investigations on the effects of lower atmosphere variation (e.g., dust storms) on atmospheric escape could benefit from an in-situ horizontal 2D map of O+ outflow/downflow in the ionosphere, obtained through a combination of an IDM (ion drift meter) with a vertical velocity accuracy of less than 20 m/s and ion composition (M/dM > 40) observations. Based on the model I-MIM orbit, the expected density range to be observed is 100–105 cm^{-3}.

Ion Mass Spectrometer

Understanding the upward transport of water/water-related species to the source altitude of atmospheric escape (i.e., exobase for neutrals and upper ionosphere for ionized atmosphere) is essential to understanding water and volatile loss to space). To complete the investigation of vertical transport of water molecules and other species from the surface to the upper atmosphere, simultaneous observations of the vertical profiles of the main ionospheric water-related ions (separation of CO_2 and H_2O related species) and of lower atmospheric wind and water vapor is necessary. To separate CO_2 and H_2O related species, in-situ high-resolution measurements of ion composition with M/dM > 3000 in the density range of > 103 cm^{-3} is required, along with accurate ion temperature observations in the range of 300–20000 K per the model I-MIM orbit.

High-Resolution Mass Spectrometer (HRMS)

One target for HRMS observations is to measure escaping Ar isotopes, which would provide estimates for fractionation factors of species that escape via sputtering: namely, noble gases. HRMS's high mass resolution (m/dm > 3000) would enable direct observations of different Ar isotopes. Lower orbits (e.g., down to ~170 km) are desired for measurements of Ar isotope compositions in the upper atmosphere within reasonable integration time.

Ne-MS Instrument on a Potential Demo Lander, if Implemented

The goal for Ne-MS measurements is to measure elemental and isotopic abundance of Ne, both of which constrain the mantle volatile content, which in turn controls atmospheric evolution via volcanic degassing and informs the primitive atmospheric content through accretion and magma-ocean modeling.

The primary scientific goal would be to constrain ^{20}Ne abundance within a factor of two and $^{20}Ne/^{22}Ne$ ratio, with an uncertainty of less than 10%, which is sufficient for elucidating the source of Ne (captured solar nebula/solar-wind-implanted dust or chondritic building blocks; Kurokawa et al., 2021), and better than that measured by Viking (Owen et al., 1977). Constraining the $^{20}Ne/^{22}Ne$ ratio with an uncertainty of less than 1% would distinguish between two possible Ne origins that show similar (but not identical) isotope ratios: captured solar nebula and solar-wind-implanted dust. Identifying the origin of Ne requires the isotopic fractionation factor of Ne escape, which could be constrained by HRMS on an orbiter.

5.1.2 Summary for the Atmosphere Theme

I-MIM's primary anchor payload can address three major atmospheric science topics of interest to Agency partners (e.g., per the 2023–2032 U.S. Decadal Survey, MEPAG Goals Document, JMSEP document): surface/subsurface volatile inventory and variability, recurring slope lineae, and upper atmospheric processes, especially ionospheric irregularities. Atmospheric science would benefit from either or both of the MDT-identified complementary payloads. The addition of a high-resolution imager as a potential complementary payload would address the inventory of surface/subsurface volatiles and variability and would contribute to understanding recurring slope lineae. The addition of the VHF Sounder as a complementary payload would also contribute to understanding surface/subsurface volatiles and would additionally contribute to investigating ionospheric irregularities.

Several supplemental payloads could make measurements to address these and other atmospheric and aeronomic structure and processes that are of great interest to the international science community, as detailed in the STM. They would contribute vital information about past and present climatology, weather, and space weather, and contribute crosscutting data relevant to geology, habitability, and reconnaissance topics described elsewhere in this report. However, the MDT recognizes that resources are finite and stakeholders often must choose between several highly recommended payload options. Thus, the Atmosphere Group prioritized potential supplemental payloads:

Priority 1 Submillimeter Sounder

This instrument has the highest priority for two main reasons. First, it is a highly versatile instrument capable of measuring the vertical profiles of many atmospheric variables, including temperature, pressure, water vapor, and wind. Second, winds have never been measured systematically throughout the lower atmosphere and have consistently ranked as the number one atmospheric measurement priority in the last two NASA Decadal Surveys of Planetary Science. The instrument provides crucial information for Atmosphere Topics 1.3 and 2.2.

Priority 2a TIR Atmospheric Limb Sounder

A TIR Spectrometer has second priority, tied with the UV/VIS imager below. This instrument type would measure the vertical profiles of dust and water-ice aerosols in the atmosphere, along with vertical profiles of temperature, water vapor, all as a function of pressure. Measurement of the dust and water-ice aerosols provides the forcing of the atmosphere that would cause temperature changes and result in wind fields, and relevant to Atmosphere Topics 1.2 and 1.3.

Priority 2b UV and VIS Imager

With the same priority as TIR, this instrument can provide 2D maps of the airglow and aurora, and provide essential information relevant to Atmosphere Topic 2.1. The I-MIM orbiter is suited to new measurements of spatial distributions of TEC, atmospheric wave activities, and energy inputs from space. This instrument is important to JSMEP's primary focus (space weather and climate), as well as key questions in the 2023–2032 U.S. Decadal Survey for Planetary Science and Astrobiology and MEPAG Goal II A4.2 (neutrals, ions & aerosols in the upper atmosphere and magnetosphere).

Priority of Other Instruments

The priority among other instruments [the electron analyzer, energetic particle detector, RPA&IDM, magnetometer, high-resolution ion composition spectrometer] depends on which higher priority instrument the I-MIM orbiter would carry, given the importance of simultaneous observations with those instruments. If the Sub-mm or TIR instrument is onboard, the RPA&IDM and high-resolution ion composition spectrometer would have highest priority. If the UV+VIS imager is onboard, the space-weather-related instrument package would have higher priority.

Polygonal and other terrain shapes indicate widespread mid-latitude near-surface ice, likely associated with a buried glacier in Arcadia Planitia.

Credit: NASA/JPL-Caltech/UArizona

5.2 SUPPLEMENTAL SCIENCE: GEOSPHERE THEME

The surfaces of terrestrial planetary bodies are modified by impact cratering, volcanism, tectonics and weathering processes (i.e., aeolian, fluvial, glacial, etc.). Decades of science conducted at Mars, using remotely-sensed and in-situ data, have shown that the nature and evolution of these processes have a dynamic history. These data have provided a global perspective of Mars at spatial scales as small as 10s of cm at the surface and for depth scales of meters to 10s of meters in the subsurface. Localized in-situ data (e.g., Phoenix, InSight, Perseverance) of the upper meter of the Martian regolith have shown how crucial information in the near subsurface (1–10 m) is for telling the story of Mars' dynamic geologic history. I-MIM will bridge a gap in these data by providing capability to observe the upper meter(s) of the surface at regional-to-global scales. The Geosphere Group aimed to build a foundation for addressing a variety of important science objectives related to understanding the geologic history of Mars. As shown in the Science Traceability Matrix (Section 5.4) and in Table 5.2 below, the MDT Geosphere Group established three organizing topics that categorize processes that have shaped: (1) the present day, (2) the recent past, and (3) the more distant past. These relative timeframes broadly correspond to the depth scales and penetration depths achievable with the I-MIM core payload. Each topic is further divided into subtopics related to processes of scientific interest active in those relative timeframes. Regolith properties, as a subtopic of interest, was not included here because it was extensively covered in Section 4.2.

The topics are all addressed with the core payload, but can be significantly expanded upon with the addition of other payload elements (as described below). The subtopics of this theme all complement or supplement the Reconnaissance Objectives (ROs) and have relevance to future human exploration and science goals defined by the community.

Table 5.2 Overview of Atmosphere Group High-priority Science Topics

TASK 2 GEOSPHERE GROUP – HIGH-PRIORITY SCIENCE TOPICS	
GEO TOPIC 1	**Processes that Shape the Present**
GEO 1.1	Mobile Sediments, Mass Wasting, and Seasonal Change
GEO 1.2	Flowing Ice
GEO 1.3	Present Cratering Rates
GEO TOPIC 2	**Processes that Shape the Recent Past**
GEO 2.1	Polar Deposits
GEO 2.2	Mid-latitude Ice
GEO 2.3	Recent Volcanism
GEO TOPIC 3	**Processes that Shape the More Distant Past**
GEO 3.1	Crater Ejecta Emplacement and Degradation
GEO 3.2	Sedimentation and Stratigraphy
GEO 3.3	Unique Radar Terrains
GEO 3.4	Noachian Climate & Ice

5.2.1 GEOSPHERE GROUP: Scientific Foundations & Payloads

GEOSPHERE SCIENCE TOPIC 1

PROCESSES THAT SHAPE THE PRESENT DAY

GEO 1.1
Mobile Sediments, Mass Wasting, & Seasonal Change

Sediment mobility on Mars is epitomized by the migration of dunes and ripples across its surface. Confirmation of current dune and ripple motion was only possible with the acquisition of high-resolution (sub-meter) images by MRO's HiRISE camera (Bridges et al., 2013). Since that initial confirmation, bedform motions of up to several meters per year have been observed in many locations across Mars (Chojnacki et al., 2019; Silvestro et al., 2020). Studies of currently active sand motion on Mars are relevant to fields such as global and regional sediment cycles, agents of geomorphologic change and near-surface wind regimes as climate indicators.

The surface of Mars is subject to active weathering and erosion in an extremely arid and cold present-day climate. In regions with sufficient surface relief and inclination, material can be displaced downslope from gravitational forces (i.e., via mass wasting).

Mass wasting processes on present-day Mars produce a large variety of geomorphic expressions, including avalanches of polar ice and dust (Russell et al., 2008; Schorghofer et al., 2002), rockfalls (Roberts et al., 2012), slope streaks (Aharonson et al., 2003; Schorghofer et al., 2007), recurring slope lineae (Dundas et al., 2017; Stillman et al., 2020), and landslides (Crosta et al., 2018) that are often linked with seasonal changes (Figure 5.13). The type, magnitude, and frequency of mass wasting is controlled by numerous endo- and exogenic, long- and short-term drivers, including impacts (Kumar et al., 2019), tectonic activity (Roberts et al., 2012), and thermal fatigue (Tesson et al., 2020). Therefore, the analysis of mass wasting features can provide key information about the historic and present-day drivers of landscape evolution.

Seasonal frost caps also drive repeatable surface change and mobilize sediment. Thick seasonal CO_2 caps (up to 1 m) at high Martian latitudes can undergo rapid grain growth, and sublimate from below, leading to the formation of dendritic araneiform surface channels (Portyankina et al., 2017; Hansen et al., 2010) and jets of CO_2 gas entraining debris that form dark fans (Kieffer et al. 2006; Piqueux et al., 2003; Thomas et al., 2010). At lower latitudes seasonal CO_2 frost is thinner, but still commonly results in the mobilization of sediment in present day gullies both on dunes (Diniega et al., 2010; 2013; 2019; 2021) and crater walls (Dundas et al. 2010; 2012; 2019; 2021).

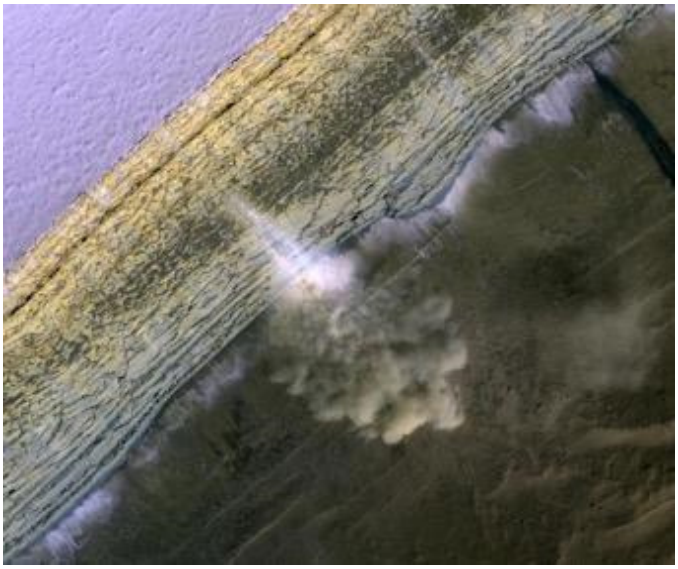

Figure 5.13 Example of present-day surface activity: An avalanche in progress at a steep high-relief north polar scarp (HiRISE image ESP_016228_2650). Such scarps are also possible sites of ice flow.

Residual ice caps (CO_2 at the southern pole and H_2O at the northern pole) show changes with season and

interannually. The extent of high-albedo water ice in the north polar residual cap varies from year to year (Byrne et al., 2008). The south polar residual ice cap varies in thickness up to 10 m and contains numerous pits and linear troughs that reach an underlying water ice layer (Byrne and Ingersoll, 2003; Titus et al., 2003). Repeat imaging shows these pits to expand by meters per year through sublimation, with a bright upper layer being undercut and collapsing inward (Thomas et al., 2009; 2013; 2016; 2020). A thicker buried CO_2 deposit at the south pole (Phillips et al., 2011; Bierson et al. 2016) accumulated and deflated in multiple episodes over 100s of kyr (Buhler et al., 2020) and likely flowed appreciably (Smith et al., 2022). Continued study of seasonal and residual cap evolution can expand understanding of the interplay between frost deposition, evolution, and sublimation, as well as surface-atmosphere dust and volatile exchange occurring on Mars today.

GEO 1.2
Flowing Ice

Deformation of icy deposits (or lack thereof) yields Deformation of icy deposits (or lack thereof) yields constraints on internal temperatures, bulk thermal state, and, therefore, mass balance, surface temperatures and ice history. Steep high-relief polar cliffs would have optimal conditions for flow and finite-element models have suggested flow rates that exceed mass wasting rates (Sori et al., 2016; Fanara et al., 2020), making these sites of particular interest for further analysis. Mid-latitude viscous flow features (VFFs), including lobate debris aprons (LDA), concentric crater fill (CCF), and lineated valley fill (LVF), are interpreted to be debris-covered glaciers (e.g., Holt et al., 2008; Plaut et al., 2009; Petersen et al., 2018) and exhibit clear morphological evidence of extensive ice deformation and flow (e.g., Head et al., 2010), despite theoretical expectations of much lower deformation rates suggested to be at the mm to sub-mm scale per year under various Late Amazonian conditions (Fastook and Head, 2014).

Present-day flow rates of mid-latitude glaciers have been suggested to be at the sub-mm scale per year (Sori et al., 2016; 2017). In addition, glacial flow of atmospherically deposited CO_2 ice at the polar layered deposits is evident by numerous geomorphic features (e.g., topographic contours, crevasses and compressive ridges), all of which resemble features observed on terrestrial glaciers (Smith et al., 2022). Models suggest these polar CO_2 glaciers presently flow at a ~1/3 reduced rate from higher flow periods in the past > 400 kyr that may have ranged between 0 and 0.65 m/year (Smith et al., 2022).

GEO 1.3
Present Cratering Rates

The crater production rate on Mars is central to constraining the timescales and dates of geological activity, including those contributing to ice deposition in the recent past. Extrapolations of lunar crater production rates to Mars (Hartmann, 2005) have been used to date terrain, but these methods are unreliable for small or young areas which contain only small craters. The small crater production rate at Mars is best constrained by spacecraft observations (Malin et al., 2006; Daubar et al., 2013; 2019), but can be difficult to reconcile with lunar extrapolations (Hartmann and Daubar, 2017). The size-frequency distribution of small craters observed on the Moon has a much steeper power law exponent than that of Mars (Speyerer et al., 2016; Daubar et al., 2013) despite expectations that they are derived from a common impactor population. Thus, refining the production rate of small craters on Mars through direct observation is a topic whose importance spans much of the inner Solar System.

Statistical uncertainties in the crater production rate are improved by detection of additional craters over longer time baselines. Currently, impacts can only be detected in images covering large expanses of dusty terrain and, even in these regions, it is uncertain if all imaged impacts are recognizable. Seasonal variation in the impact rate is also expected (JeongAhn and Malhotra, 2015), but not reported in observations. Therefore, additional detection and observations of impact craters will help minimize statistical uncertainty.

GEOSPHERE SCIENCE TOPIC 1

PAYLOADS

CORE PAYLOAD

I-MIM's core payload is capable of collecting Interferometric Synthetic Aperture Radar (InSAR) data (see Section 2.2.1). InSAR is commonly used on Earth to observe present-day surface changes. It leverages phase differences in an interferogram to detect surface changes as small as ~1/10 of the transmitted wavelength (~2 cm for L-band) (Zebker et al., 1996). This information is uniquely suited for addressing present-day active processes acting on scales of centimeters to meters. InSAR data have been used to address a wide variety of active terrestrial geologic processes, including: dune migration (Havivi et al., 2018), mass wasting (Delaloye et al., 2010; Kang et al., 2017; Rouyet et al., 2019), seasonal changes (Rouyet et al., 2019), and glacial flow (Gray et al., 1998; Leinss and Bernhard, 2021). Constraining rates of surface change related to sediment mobility, mass wasting, seasonal cycles, and glacial flow on Mars would provide key information about the historic and present-day drivers of landscape evolution.

Constraining the crater production rate on Mars with observations of present-day cratering is important for understanding the ages and timescales of geological activity in the present and the past. This subtopic cannot be directly addressed with the I-MIM core payload. Adding a high-resolution imager and thermal IR imaging spectrometer would provide a means of obtaining that information (as described below).

HIGH-PRIORITY, POTENTIAL COMPLEMENTARY PAYLOAD OPTIONS

High-Resolution Stereo Imager

The inclusion of a high-resolution stereo imager on the I-MIM orbiter would significantly augment the capabilities of the core payload to address active geological processes on Mars. HiRISE image data of features and processes acting at scales of 10s of cm exist as far back as 2006. Re-imaging them at comparable resolution during the I-MIM mission could take advantage of an especially long-time baseline (approximately 25 years).

Detection of new craters requires repeat coverage of large areas at resolutions of at least 10s of meters, while accurate diameter measurements require follow-up imaging at resolutions of 10s of cm. The former data may be provided by a low-resolution camera or single band observations from an imaging spectrometer, while the latter data come from a high-resolution camera.

Subsurface excavation by new impacts has also revealed buried clean ice at latitudes as low as 35°N. These sparse tests of ice presence can be enabled by the addition of color capability to high-resolution imaging. Rapid follow-up between excavation and high-resolution imaging is required to detect excavated ice as sublimation reduces its diagnostic color and brightness.

OTHER POTENTIAL SUPPLEMENTAL PAYLOADS OF INTEREST

VIS-IR SPECTROMETER

In concert with a high-resolution imager, a spectrometer with a spatial resolution of 10s of meters would provide a crucial context imaging capability that is necessary to address present-day cratering rates.

C-BAND SAR

The addition of a C-band SAR would provide an InSAR capability at wavelength scales that would be sensitive to surface changes of less than a centimeter. This capability would be highly complementary to the core payload (L-band) data collected to address present-day activity.

GEOSPHERE SCIENCE TOPIC 2
PROCESSES THAT SHAPE THE RECENT PAST

GEO 2.1
Polar Deposits (PLD & CO_2 Ice)

Thick, buried, CO_2 ice deposits at the south pole are thought to record atmospheric collapse dated to 100s of kyr (Phillips et al., 2011; Bierson et al., 2016). Internal layering may reflect periods of CO_2 ice loss with associated recharge of the atmosphere (Buhler et al., 2020; 2021; Alwarda and Smith, 2021). A complex history of accumulation/sublimation (Buhler et al., 2020; 2021) coupled with ice flow (Smith et al., 2022) have controlled the history of this deposit and its stratigraphy, and current flow rates are important observations that can be made with radar sounding and InSAR, respectively.

Layered water-ice deposits have long been thought to record climate history on Mars. The North Polar Layered Deposits (NPLD) stratigraphy is thought to record environmental conditions over the past ~4–5 Myr (e.g., Levrard et al., 2007; Hvidberg et al. 2012; Becerra et al., 2017), while some mid-latitude ice deposits and the South PLD record environmental conditions 10s to 100s of Myr in the past (Viola et al., 2015; Herkenhoff and Plaut, 2000; Becerra et al., 2019; Sori et al., 2022), with ice loss that persists to the present (Bramson et al., 2017).

GEO 2.2
Mid-Latitude Ice

Shallow ice is now known to be almost ubiquitous beneath roughly one third of the Martian surface (Morgan et al., 2021; Putzig and Morgan et al., 2022, in Press). Polygons (Mellon, 1997; Mellon et al., 2014), neutron spectrometer data (Feldmann et al., 2002; Pathare et al., 2018) and seasonal thermal behavior (Bandfield, 2007; Piqueux et al. 2019) indicate the presence of ground ice in the upper decimeters to ~meter of the subsurface. This ice may fill regolith pores and diffuse into or out of the ground in response to short-term (100 kyr) climatic variations (e.g., Schorghofer and Aharonson, 2005; Schorghofer and Forget, 2012; Chamberlain and Boynton, 2007). However, there is also evidence that ice exceeds the available pore space (i.e., excess ice) in many locations and has a low lithic content. For example, the Phoenix lander uncovered a mix of excess and pore-filing ice at its landing site (Smith et al., 2009). Ice-exposing impacts have also exposed and excavated excess ice at dozens of mid-latitude sites (Byrne et al., 2009; Dundas et al., 2021) suggesting that excess subsurface ice is common. Some gamma-ray and neutron spectrometer data also suggest ice content in the 60–90% range at shallow depths over broad areas (Boynton et al., 2002; Pathare et al., 2018). Additionally, viscous flow features (VFFs) are spread widely across the surface, and are interpreted as debris-covered glaciers (ice contents up to 90% by volume) on the basis of SHARAD radar data (Holt et al. 2008; Plaut et al. 2009; Petersen et al. 2018). They are expected to have thicker and coarser overburden than the plains deposits (Petersen et al., 2018), but the purity of their ice content has been more confidently constrained with SHARAD.

Several lines of evidence now suggest that thick accumulations of excess ice are also common in the northern plains poleward of 40°N (Dundas et al., 2021). Radar reflections in Arcadia (Bramson et al. 2015) and Utopia (Stuurman et al., 2016) Planitia indicate extensive decameters-thick ice sheets [but see Campbell & Morgan (2018), for consideration of how radar losses may affect ice content.] Thermokarst features such as expanded craters (Viola et al. 2015) and scalloped depressions (Lefort et al., 2010) are explained by incomplete removal of excess ice (Dundas et al., 2015) over ten meters in thickness. Ice-exposing scarps have decameters of relief (Dundas et al., 2020) and indicate that in places, this excess ice is continuous up to near-surface depths. Utilizing these multiple datasets and observations together have supported an ice-rich near-surface across the mid-latitudes (e.g., Hibbard et al., 2021; Morgan et al., 2021).

GEO 2.3
Recent Volcanism

Volcanism has significantly shaped the surface of Mars and the identification of very young (< 10 Ma) volcanic products (Jaeger et al., 2010; Horvath et al., 2021) and possible related seismic activity (Giardini et al, 2020; Kedar et al., 2021) argues that it may be an ongoing process. A variety of fresh lava flows are found across its surface, featuring a diverse array of surface textures and morphologies. Some of the volcanic features observed within Mid-Late Amazonian volcanic terrain exhibit extremely bright radar returns within Arecibo S-band SAR image data, suggesting a very blocky surface (Harmon et al., 2012). However, the origin of this extreme roughness is presently unknown, with no obvious terrestrial analogues (Rodriguez Sanchez-Vahamonde and Neish, 2021). SHARAD and MARSIS detections of these regions have revealed stacks of buried lava flows built up over time from multiple eruptive sources (Morgan et al., 2015; Ganesh et al., 2020; Shoemaker et al., 2022), burying the pre-existing terrain including outflow channels (Morgan et al., 2013).

Thick dust cover over the majority of Amazonian volcanic terrains has greatly restricted geochemical analysis of Martian lava flows. Dielectric analysis of sounder data provides an alternative means to constrain volcanic composition and compare the properties of different flow units and provinces (Carter et al., 2009; Campbell and Morgan, 2018). Such investigations have extended beyond volcanic edifices and volcanic plains and have shed new light on the other possible volcanic deposits within the Medusa Fossae Formation (Campbell and Morgan, 2018; Campbell et al., 2018).

Combined SAR/Sounder studies at higher frequencies than MARSIS/SHARAD can build on previous studies in order to examine the stratigraphically youngest volcanic units, including the products of explosive eruptions. It has been suggested that Martian volcanic activity transitioned from explosive to effusive eruption styles between the Noachian to Hesperian/Amazonian (Mouginis-Mark et al., 2022), but the possible detection of pyroclastics, only thousands of years old (Horvath et al., 2021), challenge this concept. Instead, pyroclastic material may be easily eroded, redeposited and buried on Mars (Morgan et al., 2015). Leveraging lunar studies, polarimetric SAR analysis, and dielectric sounder estimates would provide a new means to search for potential young pyroclastics.

GEOSPHERE SCIENCE TOPIC 1

PAYLOADS

CORE PAYLOAD

The I-MIM core payload addresses all of the scientific objectives related to recent geological processes. The combination of polarimetric SAR and sounding capability provide a powerful tool for probing the upper meter(s) of the surface at spatial resolutions of 10s of meters (e.g., as described in Section 2.2.1). Near-surface fine-scale layering in polar deposits can be measured, which would likely elucidate climate change over time scales of kyr to Myr, and buried ice can be identified in many geologic scenarios in the mid latitudes. Knowledge of properties of these buried ice deposits place strong limits on past climatic models and are crucial for human resource planning. Volcanic flow textures can be investigated at centimeters- to meter-scales and relative ages potentially assigned based on their roughness. Constraints on the impurity content of ices (Rivera-Valentín et al., 2022) and composition of volcanic materials can also be provided.

HIGH-PRIORITY, POTENTIAL COMPLEMENTARY PAYLOAD OPTIONS

VHF Sounder

The addition of a VHF sounder to the I-MIM payload would provide additional depth of penetration into the subsurface, bridging a gap in capability between the MRO SHARAD instrument and the core payload's L-band system. This provides added scientific value to exploration of the RZ (and rest of the surface) by increasing the potential to characterize the presence of ice that is either buried at greater depth or by thicker/more attenuating overburden. In concert with doing so, it would provide useful additional constraints on the dielectric properties of overburden material. A VHF sounder would have similar benefits for addressing objectives related to volcanic and regolith processes that have shaped the recent past.

High-resolution Stereo Imager

High-resolution imaging (and derived stereo topography) can further I-MIM's science goals through the study of exposed PLD and mid-latitude ice layers; ice-exposing impacts; and, lava-flow texture and superposition relationships.

OTHER POTENTIAL SUPPLEMENTAL PAYLOADS OF INTEREST

VIS-IR Spectrometer

An imaging spectrometer would provide thermal/compositional information that could complement currently available data (e.g., THEMIS and CRISM) and provide key insight into surface and near-surface environments connected to features observed at radar wavelengths.

Passive Radiometry Capability for Radar Systems Implemented (L-band, VHF, C-band)

Passive microwave energy emitted from the surface can provide important and unique information about its thermal and physical properties. Based on Mars 2020 RIMFAX data, an L-band radiometer could sense temperature variations at depths of up to 15 meters (Siegler et al., 2022). A VHF channel radiometer would sense to depths of up to 50 meters and the combination of the two channels would provide capability to identify variations resulting from subsurface temperature gradients due to regolith thermal properties changes (such as increased thermal conductivity due to thick layers of pore-filling ice) and/or changes in geothermal heat flux. With a C-band channel, direct measurement of the microwave loss tangent is possible, through its modulation of the diurnal brightness temperature amplitude (Feng et al., 2020; Siegler et al., 2020). This diurnal amplitude can vary as a function of mineralogy (e.g., ilmenite, hematite, magnetite) and density.

GEOSPHERE SCIENCE TOPIC 3
PROCESSES THAT SHAPE THE DISTANT PAST

GEO 3.1
Crater Ejecta Emplacement & Degradation

Impact cratering is ubiquitous across the Solar System, yet our current understanding of ejecta emplacement processes is still underway. Models of impact ejecta emplacement and a resulting continuous ejecta blanket were originally derived from lunar crater and nuclear explosion studies (Roberts, 1966; Oberbeck, 1975). However, an increasing number of morphologic observations of craters on Earth and Mars show evidence for layered ejecta (Osinski et al., 2011; Tornabene et al., 2012; Sacks et al., 2022) with melt on top of continuous ejecta blankets. Martian classification of single, double, and multiple layered ejecta (Barlow et al., 2000; Barlow et al., 2005; Barlow, 2015) suggests that a mixture of depositional processes is at play. Possible ejecta emplacement processes on Mars have included layered dry grain flows (e.g., Barnouin-Jha et al., 2005), atmospheric interaction (e.g., Barnouin-Jha et al., 1999) and incorporation of volatiles from target rocks (e.g., Tornabene et al., 2012). Double layered ejecta is most common in the northern plains of Mars, where evidence for extensive water-ice deposits has been detected and may act as the volatile resulting in layered ejecta (Osinski et al., 2011). Although these types of craters have not been observed on the Moon, radar and thermal data have proven useful in identifying buried ejecta, melt deposits, and ejecta of differing grain sizes (Neish et al., 2014; Ghent et al., 2016). HiRISE and THEMIS observations have revealed low nighttime temperature haloes in association with a wide variety of craters proposed to be fine-grained ejecta emplaced by atmospheric entrainment by vapor plume expansion winds (Ghent et al., 2010).

GEO 3.2
Sedimentation and Stratigraphy

Aeolian sediment transport, deposition and erosion are active processes spanning Mars' history and continue to alter the surface of Mars. This process, along with mass wasting, lava or ejecta emplacement, or airfall deposition can efficiently lead to the burial and preservation of landforms. For example, evidence for buried lithified ancient sand dunes was found exposed within Melas Chasma, Valles Marineris (Chojnacki et al., 2020), clusters of mounds interpreted to be buried early Noachian impact crater structures overlain by Mawrth material were found in southern Chryse Planitia (McNeil et al., 2021), and fluvial systems were found underlying ejecta from the Late Noachian-Early Hesperian Jones Crater east of Southern Margaritifer Terra (Mangold et al., 2012). Synthetic aperture radar has shown to be a particularly useful instrument for detecting buried landforms, such as paleochannels in arid regions dominated by aeolian sediments on Earth (e.g., McCauley et al., 1982; Abdelkareem et al., 2020; Monika et al., 2022) (Figure 5.14).

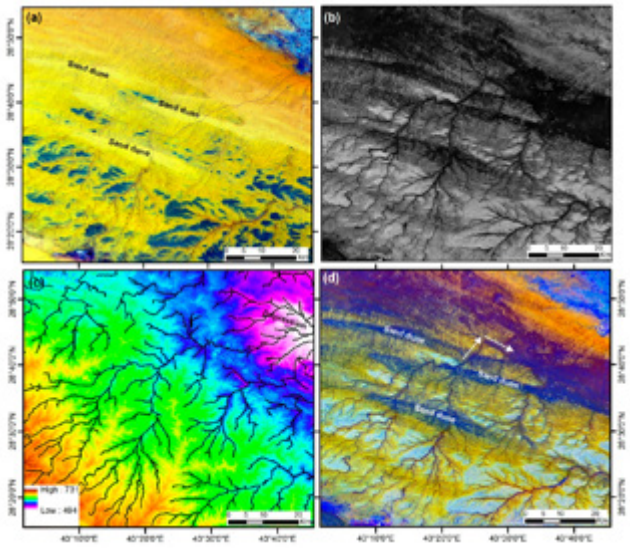

Figure 5.14 Buried drainage network in Wadi Riman/Batin in Saudi Arabia revealed using VIS-NIR and SAR data. (a) Landsat Operational Land Imager (OLI) revealing sediments dominating the surface. (b) ALOS/PALSAR L-band image revealing buried paleochannels trending to the north-east. Dark regions represent depressions. (c) SRTM DEM with 30 m spatial resolution. (d) Fused ALSO/PALSAR-Landsat-8 OLI data revealing paleochannels and local depressions. From Abdelkareem et al., 2020.

Other buried or subsurface features, such as lava tubes (Section 5.3.1, Topic 1.4), crater floors, volcanic fissures or lava flows, glacial crevasses, and alluvial and fluvial deposits could potentially be revealed using an orbital SAR/sounder instrument. Crucial information regarding geologic processes on Mars can be revealed by locating buried landforms and understanding their physical properties and conditions that led to its formation and preservation.

GEO 3.3
Unique Radar Terrains

A large region in portions of the Amazonis and Elysium Planitiae display unusual signatures in Earth-based and orbital radar data sets. These are mostly associated with the enigmatic Medusae Fossae Formation (MFF) (e.g., Kerber and Head, 2010). These geologic units appear to be composed primarily of friable deposits that have been severely eroded in places into landforms such as yardangs (Bradley et al., 2002). The formation processes and ages of the MFF are in debate. Numerous processes have been proposed, including volcanic, aeolian, paleo-polar, or others involving ice.

Age estimates range from Hesperian to late Amazonian. Much of the MFF terrain corresponds to the so-called "radar stealth" terrain, which has little to no discernible backscattered echo in several Earth-based data sets (e.g., Muhleman et al., 1991; Butler, 1994; Edgett et al., 1997; Harmon et al., 2012). This lack of echo indicates the near surface is homogeneous and likely rock-free (Harmon et al., 2012). At the longer wavelengths of the MARSIS and SHARAD sounders, signals are observed to penetrate 100s of m to several km to reflect off underlying units, or in some cases, multiple reflecting interfaces (Watters et al., 2007; Carter et al., 2009). Travel time and attenuation signatures in sounding data indicate a real dielectric permittivity consistent with both low density geologic materials and water ice, or some combination of the two (Watters et al., 2007; Campbell et al., 2021). An enhanced hydrogen signature in neutron spectrometer data was interpreted to indicate the presence of water ice in the upper meter (Wilson et al., 2018).

GEO 3.4
Noachian Climate and Ice

Climate conditions during the Noachian are much less certain relative to the rest of Mars' history. Valley networks and open-basin lakes are common features in Noachian terrain, indicating a warmer and wetter climate than present-day Mars (e.g., Craddock and Howard, 2002). However, it is unclear what the direct cause and duration of fluvial activity on the surface of Mars was during the Noachian. Climate simulations predict a cold and icy early Mars that was able to support an extensive late Noachian ice sheet referred to as the Late Noachian Icy Highlands (Wordsworth et al., 2013; Fastook and Head, 2015). Yet, little geomorphic evidence of glaciation has been associated with Noachian terrain. Eskers recording basal melting of an extensive ancient ice sheet (e.g., Scanlon et al. 2018) in the south polar Dorsa Argentea Formation have been reported (Kress and Head, 2015; Butcher et al. 2016). In addition, it has been proposed that a subset of valley networks are subglacial channel networks formed by largely cold-based polythermal glacial systems (Grau Galofre et al., 2020).

However, valley networks in Noachian terrain have been proposed to be largely attributed to top-down melting of ancient ice sheets rather than subglacial drainage (Fastook and Head, 2015); others argue the valley networks were formed during transient periods of precipitation and/or by groundwater activity (e.g., Craddock and Howard, 2002; Shi et al. 2022). Their mechanism of formation could have varied regionally, and multiple mechanisms could have operated in a given location over time. Continued search for and analysis of glacial and fluvial features in the Noachian Highlands with high resolution imagery, and potentially SAR imaging of buried features will improve our understanding of Noachian climate history.

GEOSPHERE SCIENCE TOPIC 3

PAYLOADS

CORE PAYLOAD

The I-MIM core payload addresses all of the scientific objectives related to geological processes in the more distant past. Similar to Topic 2, the combination of polarimetric SAR and sounding capability provide unique and valuable information for each of the subtopics described. Polarimetric information can be used to map ejecta blankets and impact melt deposits laterally and vertically and determine their wavelength-scale roughness (Campbell, 2012; Neish et al., 2014; 2017b; Yingling, 2020). L-band SAR data has successfully been used on Earth to detect and analyze buried paleochannels in arid desert environments (e.g., McCauley et al., 1982; Monika et al., 2022). And has been proposed for the study of near-surface volcanic structures, lava flow textures and emplacement, and MFF structures on Mars (Mouginis-Mark et al., 2022). High resolution SAR imaging can resolve the detailed distribution of stealth materials, and place them in context with existing image, spectral and topographic data. Higher resolution L-band information on the presence and distribution of ice in more ancient environments will complement the deeper low-resolution subsurface imaging of MARSIS and SHARAD.

HIGH-PRIORITY, POTENTIAL COMPLEMENTARY PAYLOAD OPTIONS

VHF Sounder

Similar to the previous topic, the addition of a VHF sounder to the I-MIM payload would provide capability that fills a gap between the MRO SHARAD instrument and the core payload's L-band system. This provides added value for all of the science discussed with respect to geologic processes that shape the more distant past, especially as these processes affect the surface to greater depths.

High-resolution Stereo Imager

The addition of a high-resolution imager to the I-MIM core payload would provide useful information for addressing all processes described for this topic. Key, though, would be information it could provide on the geomorphology of impact crater ejecta, impact melts, and fluvial features at scales approaching the wavelength (and resolution) of the core payload L-band SAR.

OTHER POTENTIAL SUPPLEMENTAL PAYLOAD OF INTEREST

C-Band SAR

A C-band SAR system would complement the L-band and VHF systems, providing a broad wavelength space with which to probe near surface properties. In the context of this topic it would provide useful information on wavelength scale roughness variations of impact crater ejecta (and impact melt) and important constraints on both the depth to buried landforms and the thickness/physical properties of unique radar terrains.

VIS-IR Spectrometer

As discussed with Topic 2, an imaging spectrometer would provide thermal/compositional information that could complement currently available data (e.g., THEMIS and CRISM) and provide key insight into surface and near-surface environments connected to features observed at radar wavelengths.

5.2.2 Summary for the Geosphere Theme

The I-MIM core payload can address a variety of important topics related to geologic processes on Mars. These include the ability to characterize present day weathering and erosion rates, constrain rates of ice/glacial flow, provide higher fidelity information on polar and mid-latitude ice deposits, examine the stratigraphy of recent volcanic flows, address questions regarding the emplacement and degradation of impact crater deposits, reveal buried geologic landforms, characterize the properties of unique radar terrains, and to build on our understanding of the early climate conditions on Mars. Addressing these processes provides a broader context for the ROs and has relevance to future human exploration and science goals defined by the community.

High-priority payload additions provide important support for addressing supplemental science objectives with the core payload and are uniquely suited for some additional science. A VHF sounder would provide depth resolution and penetration that bridges a critical gap between the core payload and current sounders at Mars. A high-resolution imager would provide key information on surface geomorphology at spatial scales that complement the capability of the core payload and would have capability, in concert with context information potentially provided by a supplemental imaging spectrometer, to constrain present day cratering rates. Other supplemental payload options such as an imaging spectrometer, a C-band SAR, and passive radiometry capability for flown radar systems would allow the I-MIM mission to address additional science goals.

A rich tapestry of features resulting from geologic processes on Mars . *Credit: NASA/JPL-Caltech/MSSS*

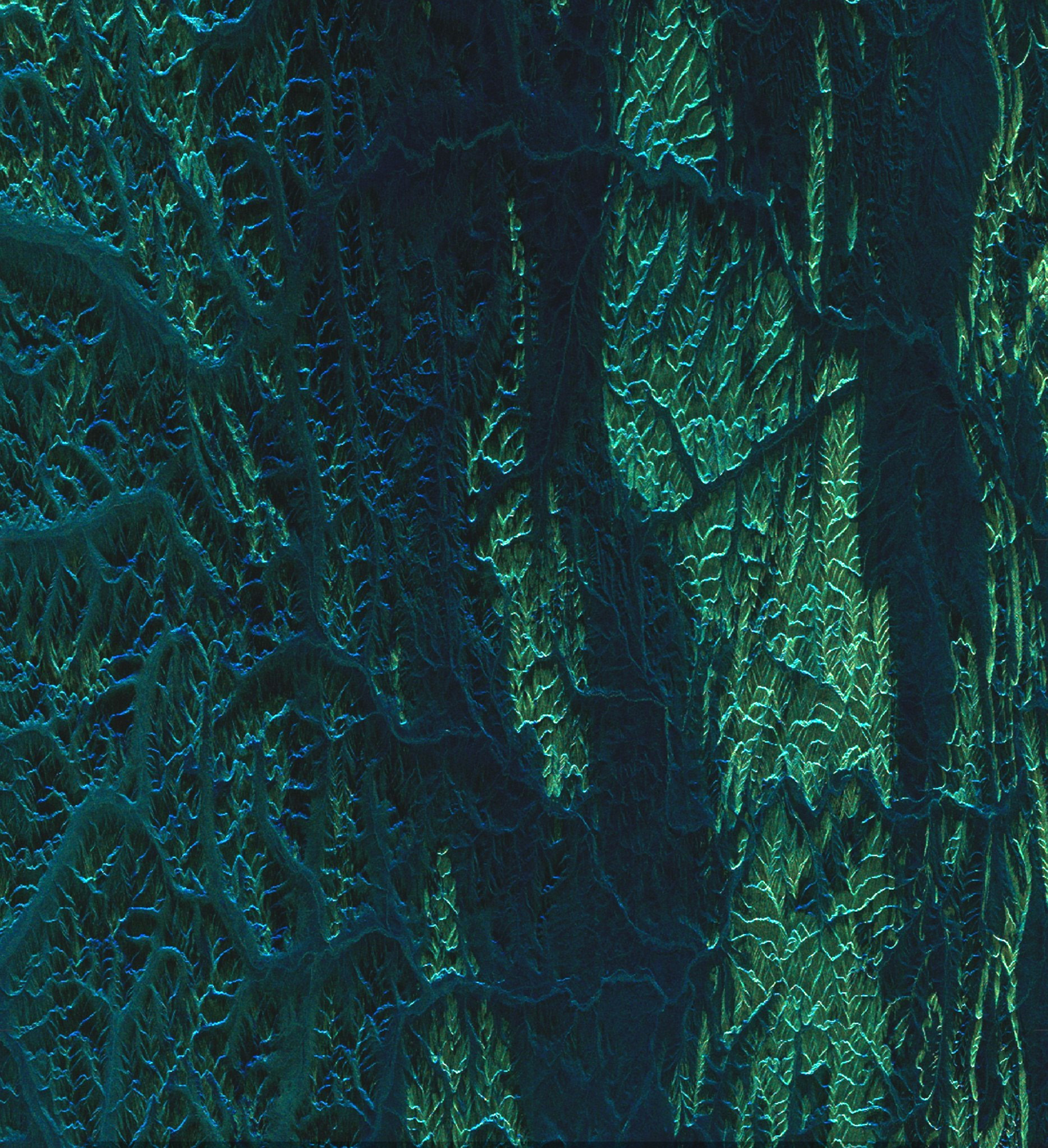

Example of a synthetic aperture radar image over Tombstone National Park, Canada, which has known buried ice deposits. Yellow-green indicates an area of potential ice (both exposed and subsurface), and blue indicates return from the surface.

Credit: RADARSAT Constellation Mission Imagery © Government of Canada (2022). RADARSAT is an official mark of the Canadian Space Agency.

5.3 SUPPLEMENTAL SCIENCE: HABITABILITY THEME

Mars is the only world other than Earth within the Sun's habitable zone. As a result, one of the driving questions in planetary science is whether Mars has evidence of past or present life. If any lifeforms native to Mars do exist, they must be protected from any contamination from Earth life (and vice versa) in order to study them properly.

As shown in the Science Traceability Matrix (Section 5.4) and in Table 5.3 below, the MDT Habitability Group established two organizing topics that I-MIM can address regarding Martian habitability:

1. Enable the search for past and present habitable environments; and,
2. Protect Martian and terrestrial life.

The Habitability Group identified seven specific topics that address the two top-level themes listed above. Six of these topics have aspects that are achievable with the core payload, and one has aspects that are only achievable with an additional payload.

The Habitability Group also considered how the capabilities of the core payload would contribute to the habitability-related science topics, as well as potential high-priority complementary payloads identified by the MDT (VHF Sounder and High-resolution Stereo Imager). Members also considered other potential supplemental payloads of value, should they become possible with communications relay and greater mass delivery per the I-MIM mission support objectives (MSO 1, MSO-2).

Table 5.3 Overview of Habitability Group High-priority Science Topics

TASK 3 HABITABILITY GROUP – HIGH-PRIORITY SCIENCE TOPICS	
HAB TOPIC 1	**Enable the Search for Past and Present Habitable Environments**
HAB 1.1	Presence of Liquid Brines
HAB 1.2	Global Distribution & Nature of Ice
HAB 1.3	Past Fluvial & Glaciofluvial Activity
HAB 1.4	Subsurface Void Detection
HAB 1.5	Geochemical Signatures of Habitability
HAB TOPIC 2	**Protect Martian & Terrestrial Life**
HAB 2.1	Planetary Protection
HAB 2.2	Human Health Hazards

5.3.1 HABITABILITY GROUP: Scientific Foundations & Payloads

HABITABILITY SCIENCE TOPIC 1

ENABLE THE SEARCH FOR PAST & PRESENT HABITABLE ENVIRONMENTS

The goal for this theme is to identify habitable environments on Mars. All life as we know it requires essential elements such as carbon, an energy source, and a water solvent. This theme primarily involves locating past and present regions where these ingredients may be found.

HAB 1.1
Presence Of Liquid Brines

Mars is predicted to have conditions favorable to the formation of meta-stable brines at or near the surface. Identifying and characterizing those regions have implications for (1) understanding the current habitability of Mars; and, (2) assessing the risk related to planetary protection, since a brine might be a vector for imported biological contamination (see Habitability Topic 2.1 below). Pure liquid water is not currently stable on the surface of Mars, but briny solutions are expected to form through deliquescence at or near the surface (Zorzano et al., 2009; Nuding et al., 2014). Indirect signatures of widespread and genuine Martian brines through geomorphic evidence are still highly debated (e.g., McEwen et al. 2011; Dundas et al., 2017), but transient droplets were observed on the Phoenix lander struts (Rennó et al., 2009).

Deliquescence is the process of water-vapor absorption by salt crystals. It is triggered when both the temperature and relative humidity meets a threshold dependent of the type of salts involved (Rivera-Valentín et al., 2022). At the surface, the eutectic of calcium perchlorate brines (which have the lowest-known eutectic temperature of 198 K) is met down to 50° latitude in the Northern hemisphere. Surface brines are predicted to be both diurnal and seasonal as they would freeze and/or effloresce with the amplitude and pace of Mars' thermo-hygrometric cycle. Below the diurnal thermal skin depth (> 30 cm deep), conditions for liquid brines are suspected to be more stable against daily variations through the Northern late-spring to summer season (Kreslavsky, 2022). The presence of an underlying ice table could provide a longer stability period through the fall season by offering enhanced stability against vertical diffusive vapor exchange (see Figure 5.15). Reliable meta-stable brine detection and ice depth measurement will bolster efforts to understand brine formation and stability, and hence, the habitability of the Martian near-surface.

CORE PAYLOAD

Liquid water is bright and specular at radar frequencies (e.g., Rutishauser et al., 2018; Grima et al., 2016), making it a distinguishable reflector or scatterer suitable for SAR and radar sounding investigations. The capability of the core payload in terms of penetration and vertical resolution matches the depth range where major thermodynamical processes related to the formation and stability of brines are expected to occur (see Figure 5.15).

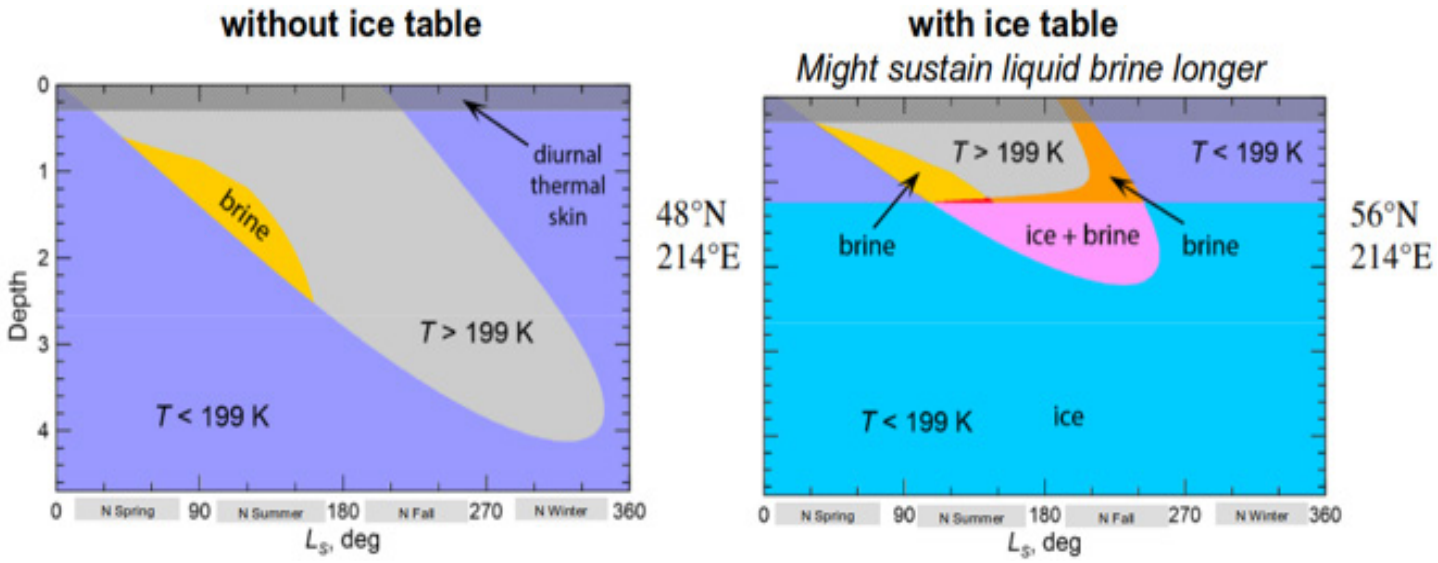

Figure 5.15 Predicted depth (seasonal thermal skin depth ~ meters) and season for deliquescence to occur and form a calcium perchlorate brine at Mars without (left) and with (right) a shallow ice slab. From Kreslavsky (2022).

HIGH-PRIORITY, POTENTIAL COMPLEMENTARY PAYLOAD OPTION

VHF Sounder

The detection of brine solutions on Mars with radar (Orosei et al., 2018) is ambiguous since other non-liquid conductive materials can also produce bright reflections (Smith et al., 2021; Bierson et al., 2021; Grima et al., 2022). A VHF radar sounder would provide additional data to help confirm a radiometric detection through its frequency-dependent signature.

OTHER POTENTIAL SUPPLEMENTAL PAYLOAD OF INTEREST

Radiometer

To discriminate liquid brines from other materials, time-series observations would highlight the seasonality of the detections. A multi-frequency (GHz) radiometer is a powerful instrument that would enable independent verification of the presence of a brine from its microwave emissions (Colliander et al., 2022).

HAB 1.2
Global Distribution & Nature of Ice

Many areas on Mars do not have liquid water today, but rather provide evidence of past or present water ice. These regions may have been habitable in the past or may become habitable in the future. It is therefore important to identify the locations where ice exists (or existed) on Mars, in both the shallow subsurface (< 10 m) or the deep subsurface (> 10 m).

A variety of observations indicate that that mid-to-high latitude soils on Mars are ice-rich in the top few meters. These observations include GRS/NS hydrogen abundance measurements (Boynton et al., 2002; Feldman et al., 2004; Mellon et al., 2004); direct observations of tabular slabs of ice beneath soil at the Phoenix landing site (Smith et al., 2009) and other mid-latitude locations (Dundas et al., 2018); measurements of soil thermal properties revealed by TES temperature observations (Bandfield and Feldman, 2008); CO_2 defrosting dates (Vincendon et al., 2010); and, spectroscopic detections of water ice beneath a dry regolith layer revealed by fresh impacts

between 39–64°N (Byrne et al., 2009). Recent findings combining MRO's Shallow Radar (SHARAD) data with morphological and other geophysical measurements suggest that near-surface ice may be present to at least 30° latitude in both hemispheres, with sporadic occurrences of relict ground ice at even more equatorward latitudes (Morgan et al., 2021). Ground ice is currently stable in the upper meter on Mars polewards of ~60° latitude (Mellon et al., 2004; Mellon and Jakosky, 1995; Schorghofer and Aharonson, 2005) and is widespread in both hemispheres (Boynton et al., 2002; Feldman et al., 2004), especially on cold, pole-facing slopes (Aharonson and Schorghofer, 2006; Conway and Balme, 2014).

Evidence exists that excess water-ice emplaced by airfall on Mars during high-obliquity "ice ages" in the recent past is still present at middle latitudes (~30–60°). These deposits are protected by a sedimentary lag deposit, which buries the ice beneath the level of interannual thermal instability that could bring it above the frost point (Head et al., 2003; Kostama et al., 2006; McKay et al., 1998; Mustard et al., 2001). Over geological time, this ice will likely return, via sublimation, to the poles in response to obliquity shifts (Mellon and Jakosky, 1993).

An extensive ice-rich deposit, present in both hemispheres and sometimes called the latitude dependent mantle (LDM), has been interpreted as a massive ice and dust/sediment deposit that was emplaced during the past ~2–4 My by airfall (e.g., Head et al., 2003) and likely also influenced by vapor deposition of pore ice (Mellon and Jakosky, 1993) and ice lensing (Fisher, 2005). Putative debris-covered glaciers in the mid latitudes, termed viscous flow features (VFF), are also thought to have formed by airfall and subsequent burial millions to hundreds of millions of years ago (e.g., Baker and Carter, 2019b, Hepburn et al. 2020).

In places, the covering sedimentary deposits may themselves contain ice (e.g., pore ice and/or ice lenses), emplaced after the ice deposits they overlie (e.g., Pathare et al., 2018). These different ice emplacement mechanisms have the potential to emplace pore ice and excess ice in the upper 10 m of the subsurface. Some of this ice could have formed habitable environments, and might preserve evidence of habitable environments today.

Deep water-ice-rich environments on Mars (>10 m depth) are also potentially habitable. While the surface of Mars is thought to have been intermittently habitable in its ancient past (Carr and Head 2015; Wordsworth et al. 2015; Wordsworth et al. 2016), subsurface environments are comparatively stable and offer protection from radiation below several meters depth (Hassler et al. 2014). Furthermore, the highest concentrations of subsurface biomass on Earth are found at rock-ice interfaces in sediment-rich ice due to the abundance of physical and chemical gradients that enable diffusive flux and chemical redox (Onstott et al. 2019).

The Martian mid latitudes contain vast deposits of shallow subsurface water-ice (< 10 m depth) that is thought to be a porous, often layered mixture of excess water-ice and lithics (Bramson et al. 2015, Stuurman et al. 2016). Given the expected redox gradients associated with dust/ice interfaces, features such as mid-latitude VFFs (putative debris-covered glaciers), water-ice deposits in Arcadia and Utopia Planitia, and the LDM are attractive targets for astrobiological investigations.

The basal layers of glacial ice, englacial layers containing entrained lithics (some of which may outcrop at the surface)(Butcher et al., 2021; Levy et al., 2021), and contacts between ice and covering debris are likely to have redox interfaces and are worthy targets for biomass characterization. This is especially true in areas where there is evidence of past meltwater, for example in the form of supraglacial valleys, eskers, streamlined bedforms, and subglacial grooves (Figure 5.16) (e.g., Fassett et al., 2010; Gallagher and Balme, 2015; Hubbard et al., 2011; Gallagher et al., 2021).

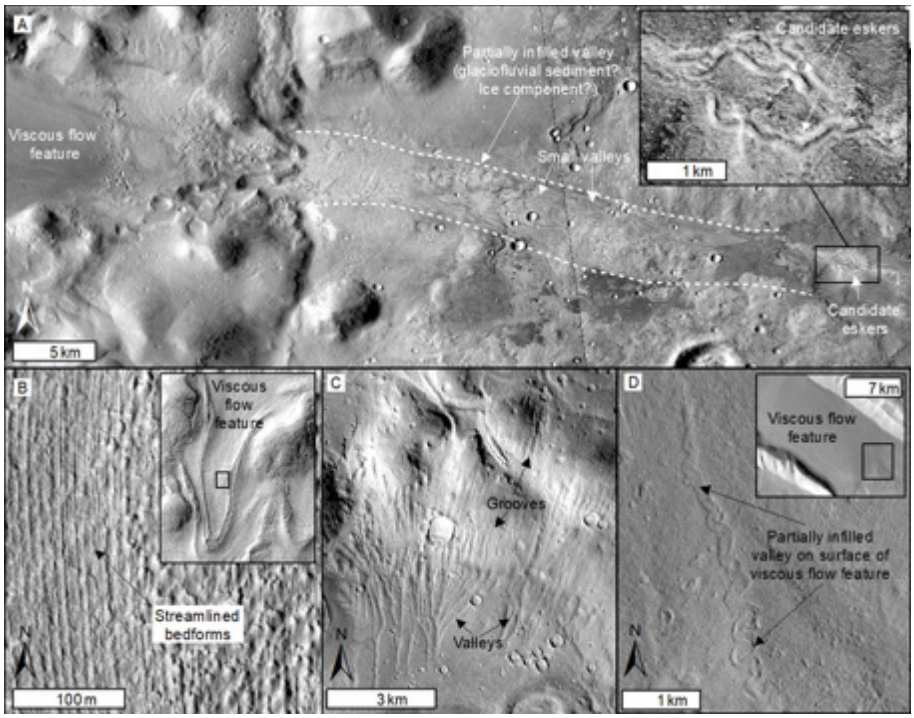

Figure 5.16 Examples of landform evidence for past meltwater production at the beds (A–C) and surfaces (D) of ice deposits on Mars. Features identified by: A. Gallagher and Balme, 2015; B. Hubbard et al., 2011; C. Gallagher et al., 2021; D. Fassett et al., 2010.

CORE PAYLOAD

The core radar payload will likely detect the depth-to-water-ice table at mid-to-high latitudes, but with an expected penetration depth of <10 m, it may not detect the top of the water-ice table at mid-to-low latitudes (≤ 45°). It is useful for characterizing the stratigraphy of shallow ice deposits, but cannot likely resolve internal or basal layers of deep mid-latitude ice. However, roughness signatures of lithic layers outcropping at the surface (which could source from basal and/or englacial positions) could be detectable in SAR imaging. Thus, the core sounder payload will be critical for characterizing the habitability of shallow ice deposits at mid-to-high latitudes.

HIGH-PRIORITY, POTENTIAL COMPLEMENTARY PAYLOAD OPTIONS

VHF Sounder

A VHF radar sounder (30–300 MHz) is absolutely necessary to characterize deeper ice (> 10 m). While the core radar payload will likely detect the top of the water-ice table in the mid-to-high latitudes, it is unlikely that it will detect the internal or basal layers of mid-latitude ice.

Resolving internal dust/ice layers in mid-latitude ice will be key for identifying areas of maximum astrobiological potential due to their relationship with past climate cycling and the history of liquid water stability on Mars, as well as their abundance of redox gradients.

High-resolution Stereo Imager

A HiRISE-scale imager would provide context for radar investigations of deep ice. HiRISE-class stereo imagery may be important for generating the stratigraphic profiles needed for dielectric permittivity inversions in areas with surface expression of internal ice/dust layers. Without a geologic model of the subsurface, it is challenging to invert for the electrical properties of the subsurface.

HAB 1.3
Past Fluvial & Glaciofluvial Activity

The I-MIM SAR would have the potential to solve a number of major questions related to the role that liquid water has played in the origins of various Martian landforms. This contribution can inform an understanding of the evolution of Mars' climate, water cycle, and the potential nature and distribution of past habitable environments. As an example, alluvial fans are widespread across the surface of Mars, and many appear to have experienced active deposition well into the Amazonian (e.g., Grant et al., 2012; 2014; Grant and Wilson, 2011, 2019; Wilson et al., 2021). Nevertheless, little is known about their stratigraphy, bulk properties, and age that all reflect depositional processes over time. As another example, the origins of widespread inter- and intra-crater plains materials remain ambiguous (e.g., Grant et al. 2009; Irwin et al., 2013; Wilson et al., 2022; Weitz et al., 2022). They often lack diagnostic features associated with volcanic, aeolian, water-lain, or other deposits.

Landform evidence suggests that some existing ice deposits on Mars produced meltwater at their beds (Figure 5.16A–C) and surfaces (Figure 5.16D) in the past (e.g., Fassett et al., 2010; Hubbard et al., 2011; Gallagher and Balme, 2015; Butcher et al., 2017, 2021). Evidence also exists for melting of past ice deposits (including larger ice sheets) that existed at various times through Mars' geologic history (e.g., Banks et al., 2009; Scanlon et al., 2015; Butcher et al., 2016; Gallagher et al., 2021).

It follows that glaciofluvial processes could have contributed to the origin and/or evolution of some deposits for which deposition and modification histories remain ambiguous. The existence of landforms indicative of glacial meltwater production on Mars suggests that meltwater could also have been produced elsewhere, but in volumes that were insufficient to generate landforms identifiable from orbit.

On Earth, microbial life exists on, within, and beneath glaciers and ice sheets, in extreme conditions such as those in dark subglacial lakes (Christner et al., 2014) and in cold-based polar glaciers (Montross et al., 2014). It may even be viable within hypersaline subglacial lakes (Rutishauser et al., 2018). Of particular interest for the search for habitable environments on Mars are those past meltwater environments where ice is (or was) in contact with rock or impurities (e.g., Stibal et al., 2012; Montross et al., 2014; Garcia-Lopez and Cid, 2017; Rutishauser et al., 2018). Potential habitats include (1) contacts between ice and surficial dust/debris cover; (2) basal ice and the ice-bed contact, or bed environments now exposed by ice retreat; and (3) interfaces between ice and included debris/impurities.

CORE PAYLOAD

Many landforms that record past fluvial and glaciofluvial activity are partially buried by later deposits (e.g., Figure 5.16D). I-MIM's core payload could reveal additional landforms that are completely buried in the shallow subsurface (top few meters). It can also provide information regarding the stratigraphy and sedimentology of the uppermost 5–10 meters of fans, plains, and other deposits over lateral scales of tens-to-hundreds of meters to reveal diagnostic properties of emplacement processes and evolution. Many relevant landforms at Mars' surface are visible at the imaging resolutions of MRO Context Camera (6 m/pixel) and Mars Express High Resolution Stereo Camera (15 m/pixel). Therefore, high-resolution (5 m) and spotlight (1.5 m) SAR imaging modes are suitable for investigating shallow buried landforms.

I-MIM would be best suited to image surfaces beneath dry materials, which could include formerly ice-rich deposits (e.g., desiccated portions of the LDM) that have lost much of their ice content. Coupled with sounder propagation/reflection models, the I-MIM radar in sounder mode should be able to define the stratigraphy and sedimentology of interbeds within the upper 5–10 m of the overburden, though resolving multiple, closely spaced, and/or thin beds (relative to the radar wavelength) may be problematic. The same methods used to characterize the occurrence of interbeds could be used to evaluate orientation of any beds.

HIGH-PRIORITY, POTENTIAL COMPLEMENTARY PAYLOAD OPTIONS

High-Resolution Stereo Imager

A high-resolution imager with stereo collection capabilities would enhance the characterization of landscapes influenced by past liquid water. For example, HiRISE-scale imaging (~0.25 m/pixel) has revealed landform evidence of glacial meltwater production (Figure 5.16B) that was not discernible at ~6 m/pixel CTX imaging scale (Hubbard et al., 2011). Meter-scale DEMs from stereo imaging greatly enhance our ability to scrutinize the origins of landforms on Mars (e.g., Banks et al., 2009; Butcher et al., 2020), and to model the evolution of small ice masses (e.g., Brough et al., 2016).

VHF Sounder

A VHF sounder capable of penetrating to greater depths than the core payload would also enhance the characterization of features such as fans, plains materials and other sediment deposits, constraining their deeper stratigraphy and thickness.

HAB 1.4
Subsurface Void Detection

Two scales of subsurface voids are of interest for habitability: "human-scale" (meters in size or larger) and "microbe-scale" (millimeters in size or smaller). Human-scale subsurface voids (such as lava-tube systems, basaltic caves, karstic caves, etc.) could offer natural environmentally stable infrastructure for human exploration. Underground caves have already been detected on Mars through satellite imagery (Wyrick et al., 2004; Cushing et al., 2007) and provide unique environments for crewed exploration. By virtue of being underground, caverns are protected from solar radiation and micrometeorite bombardment by meters to tens of meters of rock, depending on the ceiling thickness. This protection is suitable for establishing human presence, as well as for protecting biosignatures from degradation.

Underground atmosphere conditions are also more stable than the surface, without daily fluctuations in temperature and humidity. The stable subsurface temperatures also make subterranean voids promising sites for water-ice. Some terrestrial caves are known to harbor ice year-round, despite annual temperatures being above freezing (e.g., Arisa Cava and Mauna Loa ice cave, Hawai'i (Teehera et al. 2017)). In addition to water-ice, stable humidity also creates prominent environments for secondary mineral precipitation as at the void-wall interface. Secondary sulphates, carbonates, oxides, and silicates formed may provide both nutrients for microbial life as well as diverse materials for *in-situ* resource utilization (Polyak and Provencia, 2006; Lévéillé and Datta, 2010).

Currently, no known microbial life on Earth can survive the extreme radiation, cold, and dryness on the surface of Mars. However, it has long been considered that small voids in the ice-cemented areas on Mars could potentially support active microbial ecosystems and/or contain biosignature remnants of past micro-organisms. Hundreds of microbial strains have been isolated, identified, and archived from analogous high Arctic and Antarctic research sites, many capable of growth at sub-zero temperatures. Such microorganisms include the Arctic permafrost isolate *Planococcus halocryophilus*, capable of growing in a media containing 18% salt at -15°C, and maintaining metabolic activity down to at least -25°C (Mykytczuk et al., 2013). In the Canadian High Arctic, a viable microbial ecosystem inhabits Lost Hammer spring, a hypersaline (25% salinity), subzero (-5°C), anaerobic environment, where anaerobic methanotrophic, methanogenic, and sulfur-cycling metabolisms have been detected (Niederberger et al., 2010; Magnuson et al., 2022). In all the above examples, these environments require the formation of subzero, liquid brine pockets that create habitable niches, including ice-rich permafrost. The salts in essence act as freezing point depressants, creating subzero liquid habitats for microbial ecosystems.

CORE PAYLOAD

Thus far, large (human-scale) subsurface caverns are identified through pit craters and skylights on Mars (Cushing, 2012). Skylights are places where the cavern roof has collapsed, revealing part of the cave structure beneath. However, ground-penetrating radar is a known method of detecting m-scale subsurface voids on Earth (e.g., Miyamoto et al., 2005), and would provide a novel way of detecting caves on Mars. Analog work has been done to determine the scale and resolution of caves that can be detected using a radar sounder in a Martian context (e.g., Esmaeili et al., 2020). It is likely that the radar sounder on I-MIM could identify large caves (> 30 m) located a few meters under the surface but would have difficulty identifying small caves (< 30 m) buried under several meters of rock. The core payload could also constrain the rock porosity, which is key to understanding the number of micron-scale voids present in the Martian subsurface. However, the resultant measurement of the dielectric constant is ambiguous, unless coupled with a spectrometer capable of constraining the composition of the rock and its thermal inertia.

HIGH-PRIORITY, POTENTIAL COMPLEMENTARY PAYLOAD OPTION

VHF Sounder

A VHF radar sounder would be able to detect human-scale subsurface voids to greater depths than is possible with the core payload. When used in combination with the core payload, it would have a higher likelihood of detecting these regions on Mars.

OTHER POTENTIAL SUPPLEMENTAL PAYLOAD OF INTEREST

VNIR/TIR Spectrometer

A VNIR and TIR spectrometer with 10s of meters spatial resolution would provide information about the composition and thermal inertia of Martian rocks. This would provide constraints needed to convert the dielectric constant measurements provided by the radar sounder into a rock porosity measurement, useful for assessing the density of micron-scale voids.

HAB 1.5
Geochemical Signatures of Habitability

Life as we know it requires a water solvent. Hydrated minerals and minerals that are the result of alteration by interaction of a parent mineral with liquid water are evident in many areas on Mars (e.g., Mustard et al., 2008). Some examples of hydrated minerals found on Mars include alunite, jarosite, kaolinite, chlorite, and gypsum (e.g., Wernicke and Jakosky, 2021). Valles Marineris and the Noachian terrains to its south show much evidence of water interaction with surface material both geomorphologically (e.g., evidence of run-off and ground-water sapping to produce valley structures) and mineralogically (e.g., significant color variegation in spectra and broad-band color imaging). For example, color observations indicate that the phyllosilicates found in Her Desher Vallis are pervasive and ubiquitous in the area, pointing to a period when liquid water was active and modifying its basaltic bedrock (Buczkowski et al., 2014). Ground-water sapping is the current leading hypothesis for the production of Her Desher Vallis rather than surface flow, pointing to significant reserves of past or present subsurface water or ice. The indications of significant past water prompt two large-scale questions. First, is that subsurface water accessible to future crewed missions to Mars? Second, could past life have been transported into the sub-surface and preserved in some form as water migrated downwards?

Life also requires chemical energy and bio-essential elements. One promising geological setting that can provide both of them is hydrothermal systems (e.g., Martin and Russell, 2003). High-temperature water-rock interactions can provide reductants (e.g., H_2) and bio-essential elements (e.g., Fe) in upwelling hydrothermal fluids, and oxidants can be supplied from the surface and atmosphere (e.g., CO_2 and SO_4). On Mars, hydrothermal environments could have locally appeared at the surface on crater floors (e.g., Michalski et al., 2017) and potential mud-volcanoes (e.g., de Pablo and Komatsu, 2009). In particular,

domes and cones found on Mars (e.g., in Utopia Planitia, within the reconnaissance zone of I-MIM: de Pablo and Komatsu, 2009) might be mud-volcanoes; however, other possibilities (e.g., pingos and tuff cones) cannot be ruled out based on orbital images (Dundas and McEwen, 2010). The subsurface structures of the cones and domes (e.g., upwelling structure or ground ice) would provide critical insights into their origins. If these cones are mud-volcanoes, they could be a science target for future (potentially human) missions that aim to investigate habitability and to seek potential biosignatures. If these are pingos, they could be used as an in-situ resource for human missions.

CORE PAYLOAD

The core payload cannot adequately constrain the geochemical signatures of habitable environments. However, it could address the origin of upwelling structures, which may contain bio-essential elements. If cones and domes in Utopia Planitia are mud-volcanoes, upwelling hydrothermal fluids can be seen as vertical vein structures that cut the sedimentary strata. On the other hand, if they are pingos, the reflector at the interface between rocks and ground ice can be seen in the subsurface structure. This makes them distinguishable by SAR and radar sounding investigations. The capability of the core payload in terms of penetration and vertical resolution matches the depth range (several meters) of the subsurface structures expected for mud-volcanoes and pingos.

OTHER POTENTIAL SUPPLEMENTAL PAYLOADS OF INTEREST

Spectral Imager

To identify hydrated minerals on Mars, a high spatial resolution spectral imager (< 4 m resolution) is needed (either multi-band or hyperspectral, from 800 nm to 3 µm). A combination of a shallow radar and high spatial resolution spectral imaging would establish if a relationship between surface mineralogy and sub-surface water ice exists at low latitudes on Mars. Given the data volume requirements for high spatial resolution instruments, previously identified sites of high mineralogical diversity could be used as specific sites for investigation with a shallow radar.

Infrared Camera on Potential Demo Lander

If Agency partners include a lander with the I-MIM orbiter, an infrared camera onboard a demo lander would provide information on the occurrence of secondary minerals and salts in the stratigraphy near the landing site.

HABITABILITY SCIENCE TOPIC 2
PROTECT MARTIAN & TERRESTRIAL LIFE

Habitability Theme 2 seeks strategies to protect the cross-contamination of lifeforms on Earth and Mars and protect astronauts from the potential ill effects of living on another world.

HAB 2.1
Planetary Protection

The "special regions" on Mars are defined as sites in which Earth life could propagate (Beaty et al., 2006; Rummel et al., 2014). Special regions have T > 255 K and water activity (a_w) > 0.6, which are the currently known limits for the propagation of life on Earth. To prevent forward contamination by humans or their spacecraft, stringent cleaning protocols are required in order to access these regions. Therefore, identifying special regions on Mars before landing humans and/or their equipment near them is important. One key knowledge gap is how much human-derived materials can saltate and diffuse in the atmosphere around the human habitation site. Understanding that would determine how large of an area, including the special region and surrounding area, might need protection from contamination by humans and their equipment. Knowledge on the frequency and velocity at which the contaminants adhering to dust particles are transported to the surrounding areas due to the saltation would become important.

CORE PAYLOAD

Water activity (a_w) for ice and brines in equilibrium with ice is a function of temperature (Koop, 2002). The I-MIM core payload is largely insensitive to brine chemistry, but if brines are detected based on radar properties at a given depth, the temperature of those ices/brines can be modeled or measured (with a passive radiometer included as an add-on instrument).

This modeling would constrain the range of eutectic solutions that could be liquid at those temperatures (Starinsky and Katz, 2003; Tang and Munkelwitz, 1993). Knowing the subsurface temperature distribution will allow for the determination of where special regions exist. It will also allow for the determination of where human disturbances to the soil profile could produce a special region (e.g., by warming a region with imported equipment).

OTHER POTENTIAL SUPPLEMENTAL PAYLOAD OF INTEREST

Dust Counter & Anemometer on Potential Demo Lander

If Agency partners include a lander with the I-MIM orbiter, an onboard dust counter and anemometer would provide the critical wind speed for sand saltation. The frequency of dust-particle saltation is important for understanding forward contamination by humans and the speed and range of their diffusion in the atmosphere.

HAB 2.2
Human Health Hazards

It is necessary to constrain aspects of the Martian environment that could pose hazards to the health of human explorers. These include:

1. Potential biotic and abiotic contaminants in ice and other materials;
2. Terrain hazards; and,
3. Hazards associated with dust and related atmospheric processes.

Note that the RO-3 Group extensively cover aspects of landing-site safety (Section 3.4). The Habitability Group specifically focused on hazards to astronauts after their spacecraft has landed safely on Mars.

Several contaminants may be present in ice on Mars that would be dangerous for human consumption. Filtration and desalination of in-situ ice deposits may be minimum requirements for ensuring astronaut safety. Other impurities in the ice, such as solid

particulates, local concentrations of deuterium, or possible biological components may also need to be considered. These contaminants and impurities may be transferred to crops grown in local soil, so the safety of both the water and food supply would need to be considered.

Terrain hazards include rocks, rough surfaces, slopes and topographic processes such as rock/ice fall. They pose direct risks of injury and indirect risks to human health via potential damage to equipment or infrastructure upon which humans will rely for mobility, shelter, life support, and landing/launch safety. Slopes and roughness over various length scales pose challenges for mobility. For example, fields of cobble-to-boulder-sized clasts would be hazardous to traverse on foot and potentially impassable for a rover.

Fine-grained deposits such as dust could also be difficult to traverse due to sinkage and could also obscure hazardous shallow surfaces beneath. A slope or outcrop might be considered to pose a hazard if material could fall from any height that could cause injury. An analog for this potential hazard is evidence of rock/ice fall from ice-exposing scarps in Mars' mid latitudes, likely explained by scarp retreat due to ice sublimation (e.g., Dundas et al., 2017). The hazard posed by a given outcrop will depend on factors such as outcrop height and slope, grain size, material cohesion, ice content, the sublimation of that ice, and the nature of sampling/ISRU techniques.

Considering potential hazards generated by mission activity on the surface is critical. For example, landing or operating missions in ice-rich environments poses risks of subsidence, and outcrops (of ice or rock) could be destabilized by activity at/near them. Mission activity could also disturb dust deposits and add to the natural dust loading of the local atmosphere. Dust could pose hazards for human health and the function of life-support systems if it is able to compromise seals on spacesuits, equipment, and shelter. It also acts to reduce the optical depth of the atmosphere, potentially reducing visibility and light to unsafe levels.

CORE PAYLOAD

I-MIM's anchor payload has the potential to reveal astronaut mobility hazards in the near subsurface, such as rough surfaces or rock fields buried by thin deposits of dust. The primary payload can also constrain the concentration of contaminants in the ice (as described in detail in RO-1 Parameter 4), by observing the radar reflectivity as a function of depth in the top 10 m.

HIGH-PRIORITY, POTENTIAL COMPLEMENTARY PAYLOAD OPTION

High-Resolution Stereo Imager

Mobility hazards present around the landing site could be characterized by a high-resolution (< 1 m) stereo imager. An imager of this resolution could identify topographic and roughness hazards, and constrain the meter-scale slopes in the surrounding region.

OTHER POTENTIAL SUPPLEMENTAL PAYLOADS OF INTEREST

Dust Sensor & Camera On Potential Demo Lander

If Agency partners include a lander with the I-MIM orbiter, an onboard dust sensor and camera could constrain the dust particle size and optical depth at the landing site. These observations would be complementary to the orbital imaging recommended by the Atmosphere group (Section 5.1).

5.3.2 Summary for the Habitability Theme

The I-MIM core payload can address many important topics related to the current and past habitability of Mars. These include locating ice and brines that may serve as present-day habitable environments, characterizing the fluvial and/or glaciofluvial environments that might have hosted life in the past, and identifying subsurface habitats in the form of human-scale and microbe-scale voids in the substrate. The core payload also addresses issues of importance to planetary protection and the health of future astronauts.

With the addition of other high-priority payloads – namely, a VHF sounder and a high-resolution (< 1 m) stereo imager – these topics can be constrained to a higher fidelity than is possible with the core payload alone.

Other supplemental payloads such as a high spatial resolution spectral imager, a passive radiometer, and/or a lander with an onboard dust counter, anemometer, and camera would allow the I-MIM mission to address additional science goals.

5.4 SCIENCE TRACEABILITY MATRIX

The Science Traceability Matrix (STM) summarizes the results of the above MDT studies of science investigations that could be conducted with the anchor radar payload and complementary or supplementary instruments. The STM begins with the major theme areas identified in the three groups discussed above. For each investigation, within those theme areas, the STM summarizes the properties to constrain, the measurable parameters, the scale/resolution/accuracy required, and the instrumental capabilities needed.

Many space Agencies, decadal documents, and community priority documents have themes related to the future of Mars exploration. The theme areas reported above and in the STM are consistent with the themes identified by these Agencies in strategic documents listed in Section 2 and in additional materials provided to the MDT (see also Appendix A).

For example, goals from the Italian Space Agency (ASI) include searching for traces of past and present life on Mars and validating technologies, such as those related to ISRU, to prepare for the sustainable human exploration of Mars. These ASI goals are tied into both to their involvement in Artemis/Moon to Mars efforts and prior highly successful Mars radar studies with MARSIS and SHARAD.

The top priority investigation of the Canadian Space Agency (CSA) is the development of radar and its deployment on missions to map planetary surfaces. Their radar development was tied to the Next Mars Orbiter Mission (NEMO), and the CSA retained appropriations tied to an ice-mapping mission despite NASA's discontinuation of it. Their interest, experience, and technology readiness also builds on their long history of Earth-based radar studies (e.g., Radarsat). The CSA's goals also include the documentation of processes that have shaped planetary surfaces and the origin/distribution of volatiles.

Both Japan's Strategic Mars Exploration Program (JSMEP) plan and JAXA's participation in Artemis have led JAXA to prioritize goals related to addressing questions of water on Mars, including a late 2020s ice-mapping orbiter focused on distribution and inventory of water. JAXA also has goals to expand in areas related to human activities, habitable subsurface environments, and the acquisition of new technologies.

Within NASA, multiple cross-Agency, interdisciplinary, and intergenerational reports have identified the importance of water ice for future exploration plans including the Moon to Mars paradigm. Additionally, within the United States, MEPAG and the decadal survey conducted by the National Academies define priorities within the Mars planetary science community. Recent reports from both of these bodies have endorsed the concept of an ice-mapping radar as a precursor for human missions and the pursuit of high-priority science investigations (U.S. Decadal Survey, 2022; MEPAG NEX-SAG, 2015).

Goals of the Netherlands Space Office (NSO) are tied to human spaceflight and planetary science, such as the question "Are there other planets that could sustain life?" The NSO goals are also tied into further development of the Dutch space sector, and feed into their contribution of solar panels on Orion and additional technology contributions for international collaborations in human/robotic spaceflight.

ATMOSPHERE PARAMETER 1 SURFACE-ATMOSPHERE INTERACTIONS

ATMO 1.1 Surface/Subsurface Volatile Inventory & Variability

	MEASURABLE PARAMETER(S)	SCALE / RESOLUTION / ACCURACY	CAPABILITIES NEEDED*	
Seasonal Water & CO_2 Ice Cap hickness Ice Cap Thickness	Surface Deformation & Interferometric Decorrelation	Horizontal Resolution: 30 meter Vertical Resolution: 1 cm (change detection) Frequency: Ls ~20 degree intervals during the year	✓	InSAR
Seasonal Water & CO_2 Ice Cap Thickness	Surface Reflectivity	Horizontal Resolution: 100 meter Frequency: Ls ~20 degree intervals during the year	✓	SAR Sounder Mode
Seasonal Water & CO_2 Ice Cap hickness	Backscatter Coefficients & Polarizations	Horizontal Resolution: 100 meter Frequency: Ls ~20 degree intervals during the year	✓	PolSAR
Near-surface Ice Abundance	Same as GEO 2.2 and HAB 1.2	Same as GEO 2.2 and HAB 1.2	✓	SAR Tomography & SAR Sounder Mode
Presence of & Depth to Ice Table	Same as GEO 2.2 and HAB 1.2	Same as GEO 2.2 and HAB 1.2	✓	SAR Sounder Mode & PolSAR & Tomography
Fine Characterization of Polar Layered Deposits	Same as GEO 2.1	Same as GEO 2.1	✓	SAR Sounder Mode
	Same as GEO 2.1	Same as GEO 2.1	1	VHF Radar Sounder
	Same as GEO 2.1	Same as GEO 2.1	2	Hi-res Stereo Imager
Subsurface Water-ice Content	Radar Reflectivity as a Function of Depth	Horizontal Resolution: ~100 m to observe RSL site; ~1 m to resolve single RSL	✓	SAR Tomography, SAR Sounder Mode, or Both
Change in Topography Caused RSL Debris Flow	InSAR Differential Images	Horizontal Resolution: ~100 m to observe RSL site; ~1 m to resolve single RS	✓	InSAR
Surface Materials (wet or dry)	Surface Reflectivity & Polarization	Horizontal Resolution: ~100 m to observe RSL site; ~1 m resolution to resolve single RSL	✓	PolSAR
Albedo Change	Visible Images	Horizontal Resolution: ~100 m to observe RSL site; ~1 m to resolve single RSL	2	Hi-res Stereo Imager
Surface Temperature Change	Thermal Emission	Horizontal Resolution: ~100 m to observe RSL site; ~1 m to resolve single RSL	+	*Thermal Imager*

* ✓ L-band Radar Addresses (green)
1,2 High Priority Complementary Instruments Identified in Task 1 (blue)
\+ *Potential Supplemental Instrument (P = priority)*
++ *Potential Supplemental on Additional Platform, if implemented*

ATMOSPHERE PARAMETER 1 SURFACE-ATMOSPHERE INTERACTIONS

ATMO 1.2 Recurring Slope Lineae & Variability (See also GEO 1.1, 1.2)

PROPERTY TO CONSTRAIN	MEASURABLE PARAMETER(S)	SCALE / RESOLUTION / ACCURACY	CAPABILITIES NEEDED*	
Subsurface Water-Ice Content	Radar Reflectivity as a Function of Depth	Horizontal Resolution: ~100 m to observe RSL site; ~1 m to resolve single RSL	✓	SAR Tomography, SAR Sounder Mode, or Both
Change in Topography Caused by RSL Debris Flow	InSAR Differential Images	Horizontal Resolution: ~100 m to observe RSL site; ~1 m to resolve single RSL	✓	InSAR
Surface Materials (Wet or Dry)	Surface Reflectivity & Polarization	Horizontal Resolution: ~100 m to observe RSL site; ~1 m resolution to resolve single RSL	✓	PolSAR
Albedo Change	Visible Images	Horizontal Resolution: ~100 m to observe RSL site; ~1 m to resolve single RSL	2	Hi-res Stereo Imager
Surface Temperature Change	Thermal Emission	Horizontal Resolution: ~100 m to observe RSL site; ~1 m to resolve single RSL	+	*Thermal Imager*

* ✓ L-band Radar Addresses (green); 1,2 High Priority Complementary Instruments Identified in Task 1 (blue); + *Potential Supplemental Instrument (P = priority)*; ++ *Potential Supplemental on Additional Platform, if implemented*

The following cannot be accomplished by the anchor payload, but are captured given Agency partner interests in atmospheric science, the expertise of the MDT, and the potential for augmentations within mission boundaries.

ATMOSPHERE PARAMETER 1 SURFACE-ATMOSPHERE INTERACTIONS

ATMO 1.3 Near-surface Atmospheric Conditions

PROPERTY TO CONSTRAIN	MEASURABLE PARAMETER(S)	SCALE / RESOLUTION / ACCURACY	CAPABILITIES NEEDED*	
Water Vapor Abundance	Line Profiles of H_2O & Its Isotopologies	Altitude Range: 0–50+ km Spatial Resolution: ~4 deg latitude × 2–8 km vertical Precision: <10 ppmv (choice of frequency dependent)	+ P1	Sub-mm Sounder
	IR Absorption by Water Vapor		+ P2a	TIR Atmospheric Limb Sounder
	In situ Water Vapor Abundance	Range: 0–3000 pp Precision: <1 ppm	++	On Potential Demo Lander: Tunable Laser Spectrometer
D/H Ratio	In situ D/H Ratio	Range: 0–7000 ‰ Precision: δD <500‰	+ P1	Sub-mm Sounder
Wind Speed	Doppler Shift of Rotational Lines of CO, H_2O & the Isotopologies	Altitude Range: 0–50 km+ Spatial Resolution: ~4 deg latitude × 6–8 km vertical Precision: 10-15 m/s (parameters tradeable)	++	On Potential Demo Lander: Tunable Laser Spectrometer
	Doppler Shift of Dust Aerosol Measured by Backscatter at 1064 nm	Spatial Resolution: ~2 deg latitude × 2 km vertical Wind Error: < 5 m/s	+ P1	Sub-mm Sounder
	Wind Velocity	Range: 0–100 m/s Accuracy: 1 m/s	+	Doppler Lidar
Dust & Ice Aerosol Abundance	IR Absorption for Ice & Dust Aerosols	Altitude Range: 0–10 km Spatial Resolution: ~4 deg latitude Precision: 10-5 above 5 km for dust and ice	++	On Potential Demo Lander: Anemometer
	In situ Dust Number Density	Range: 0–109/m^3 Precision: 106/m^3	+ P2a	TIR Atmospheric Limb Sounder
Surface Temperature Change	Thermal Emission	Range: 130–320 K Accuracy: 2 K, Lat: 85°N - 85°S, 10 km resolution	++	On Potential Demo Lander: Dust Counter
	In situ Temperature	Range: 50–350 K Precision: 1	+	TIR Spectrometer
Surface Pressure	NIR Absorption from 1900-2100 nm	Range: 150–1500 Pa Accuracy: 1 Pa or 5%	++	On Potential Demo Lander: Multi-thermometer
	In situ Pressure		+	Mini-near Infrared Spectrometer
	Carrier Wave Frequency Shift in Radio Beam		++	On Potential Demo Lander: Barometer

* ✓ L-band Radar Addresses (green) 1,2 High Priority Complementary Instruments Identified in Task 1 (blue) + *Potential Supplemental Instrument (P = priority)* ++ *Potential Supplemental on Additional Platform, if implemented*

Most of the following cannot be accomplished by the anchor payload, but are captured given Agency partner interests in atmospheric science, the expertise of the MDT, and the potential for augmentations within mission boundaries.

ATMOSPHERE PARAMETER 2 ATMOSPHERIC & AERONOMIC STRUCTURE & PROCESSES

ATMO 2.1 Ionospheric Irregularities, Space Weather & Crustal Magnetic Field Effects on the Upper Atmosphere (1 of 3)

PROPERTY TO CONSTRAIN	MEASURABLE PARAMETER(S)	SCALE / RESOLUTION / ACCURACY	CAPABILITIES NEEDED*	
Total Electron Content	Signal Attenuation, Phase Distortion, Propagation Delay	Scale: Sub-km to 100s of km Ionospheric Irregularities Resolution: ~300 m Fresnel-scale Density Irregularities in InSAR Image	✓	InSAR
Ionospheric Density	Total Electron Content	Scale: Sub-km to 100s of km Ionospheric Irregularities Resolution: ~300 m Fresnel-scale Density Irregularities in InSAR Image	✓	SAR InSAR
		Significant improvement in TEC Accuracy and Calibration	1	VHF Radar Sounder
Albedo Change	Carrier Wave Frequency Shift in Radio Beam Passing through Ionosphere	Range: 0-3 ± 0.05 × 105 cm^{-3} Altitude: 100–200 ± 5 km	++	*Radio Occultation (Spacecraft-Spacecraft)*
Context: Airglow Brightness	Maps of Airglow for Monitoring Atmospheric Waves & TEC	Limb & Nadir Imaging: at 297 nm and/or 557.7 nm	+ *P2b*	*UV/Visible Imager*
Aurora & Airglow Distribution	Brightness	CO_2+ UVD : at 289 nm O: 557 nm [& optionally 630 nm, 1 nm/pix(R=800)] Orbital Requirements: SZA > 120 degrees Wide Latitudinal Coverage: >[-50,50] degrees	+ *P2b*	*UV/Visible Imager*
Solar Energetic Particles & Precipitating Electrons	Energetic Electron & Ion Flux	Electron Energy: 0.01–200 keV dE/E: 30%	+	*Energetic Particle Detector*
Precipitating Suprathermal Electrons & Precipitating Electrons (Context)	Suprathermal Electron Flux	Electron Energy: 0.01–200 keV dE/E: 30%	+	*Electron Analyzer*
Ion Composition	Mass-separated Ion Density	Mass Resolution: M/dM>3000 Density Range: >103 [cm^{-3}]	+	*Ion Mass Spectrometer*
Ionospheric Wind	In-situ 2D Map of the O+ Velocity	Vertical Velocity Res: < 20 m/s with: Density Range: 100–105 [cm^{-3}]	+	*RPA and Ion Drift Meter*

* ✓ L-band Radar Addresses (green) + *Potential Supplemental Instrument (P = priority)*
1,2 High Priority Complementary Instruments Identified in Task 1 (blue) ++ *Potential Supplemental on Additional Platform, if implemented*

The following cannot be accomplished by the anchor payload, but are captured given Agency partner interests in atmospheric science, the expertise of the MDT, and the potential for augmentations within mission boundaries.

ATMOSPHERE PARAMETER 2 ATMOSPHERIC & AERONOMIC STRUCTURE & PROCESSES

ATMO 2.1 Ionospheric Irregularities, Space Weather & Crustal Magnetic Field Effects on the Upper Atmosphere (2 of 3)

PROPERTY TO CONSTRAIN	MEASURABLE PARAMETER(S)	SCALE / RESOLUTION / ACCURACY	CAPABILITIES NEEDED*	
Magnetic Field	Magnetic Field	Magnetic Field Range: ±2000 nT Accuracy: 0.5 nT	+	*Magnetometer*
Space Weather Conditions Change in Topography Space Weather Conditions	Solar Wind Speed, Density, & Temperature	Speed: 200–2000 ± 25 km/s Density: 1–50 ± 0.5 cm^{-3} T: 10-50 ± 2 eV	++	*Space Weather Package on Potential High-altitude Relay Orbiter:* *Solar Wind Ion & Solar Energetic Particle (SEP) Detectors*
	Interplanetary Magnetic Field Vector	Range: 0–200 nT Per-axis Accuracy: 0.5 nT Cadence: 1 s	++	*Space Weather Package on Potential High-altitude Relay Orbiter:* *Magnetometer*
Wind Fields	Doppler Shift of Rotational Lines of CO & Its Isotopologues	Altitude Range: 10–110 km Spatial Resolution: ~4 deg latitude × 6–8 km vertical Precision: 10–15 m/s (parameters tradeable; see text)	+ P1	*Sub-mm Sounder*
	Doppler Shift of Dust Aerosol Measured by Backscatter at 1064 nm	Spatial Range: Near Surface - 35 km Spatial Resolution: ~2 deg latitude × 2 km vertical Wind Error: < 5 m/s (higher altitudes achievable under some conditions; see text)	+	*Doppler Lidar*
	Absorption by Dust at IR Wavelengths	Spatial Range: 5–120 km Spatial Resolution: <10 km horizontal × <5 km vertical Wind Accuracy: < 5 m/s	+	*TIR Atmospheric Imager*
Water Vapor (Geographic & Altitude Profiles)	Line Profiles of H_2O & Its Isotopologues	Altitude Range: 0–110 km Spatial Resolution: ~4 deg latitude × 2-8 km vertical Precision: <10 ppmv (choice of frequency dependent)	+ P1	*Sub-mm Sounder*
	Absorption by Water Vapor in IR	Spatial Range: 0–30 km Spatial Resolution: ~4 deg latitude × 2 km vertical Precision: 10 ppm below 20 km	+ P2a	*TIR Atmospheric Limb Sounder*

* ✓ L-band Radar Addresses (green) + *Potential Supplemental Instrument (P = priority)*
1,2 High Priority Complementary Instruments Identified in Task 1 (blue) ++ *Potential Supplemental on Additional Platform, if implemented*

The following cannot be accomplished by the anchor payload, but are captured given Agency partner interests in atmospheric science, the expertise of the MDT, and the potential for augmentations within mission boundaries.

ATMOSPHERE PARAMETER 2 ATMOSPHERIC & AERONOMIC STRUCTURE & PROCESSES

ATMO 2.1 Ionospheric Irregularities, Space Weather & Crustal Magnetic Field Effects on the Upper Atmosphere (3 of 3)

PROPERTY TO CONSTRAIN	MEASURABLE PARAMETER(S)	SCALE / RESOLUTION / ACCURACY	CAPABILITIES NEEDED*	
Temperature & Pressure: Geographic & Altitude Profiles	Line Profiles of CO & Its Isotopologues	Spatial Range: 0–110 km Spatial Resolution: ~4 deg latitude × <10 km vertical Precision: 1-6 K (metrics altitude- & frequency-dependent)	+ P1	Sub-mm Sounder
Water Vapor (Geographic & Altitude Profiles)	Absorption of IR Wavelengths	Spatial Range: 0–110 km Spatial Resolution: ~4 deg latitude × <10 km vertical Precision: 1-6 K (metrics altitude- & frequency-dependent)	+ P2a	TIR Atmospheric Limb Sounder
	Interplanetary Magnetic Field Vector	Range: 0–200 nT Per-axis Accuracy: 0.5 nT Cadence: 1 s	+ P1	Sub-mm Sounder
Ozone Abundance	Line Profile of Thermally Emitted Radiation from the Rotational Line of O_3	Altitude Range: 0–60+ km Spatial Resolution: ~8 deg latitude × <8 km vertical Precision: 10~100 ppbv (altitude, frequency dependent)	+ P1	Sub-mm Sounder
Atmospheric Waves	Radiance from the Upper Atmosphere at 289 nm and 557 nm	Horizontal Resolution: 20 km Vertical Resolution: 1 nm Spectral resolution: 5 km Orbital Requirements: SZA > 120 degrees Wide Latitudinal Coverage: >[-50,50] degrees	+ P2b	UV/Visible Imager
Aerosol Abundance	Absorption in IR for Water & Dust Aerosols	Spatial Range: 0–110 km Spatial Resolution: ~4 deg latitude × 5 km vertical Precision: Better than 1e-4 km^{-1} above 5 km for dust and ice	+ P2a	TIR Atmospheric Limb Sounder
	Backscatter of Dust Aerosols & Cross-polarized Backscatter of Water-ice Aerosols	Spatial Range: 0–40 km Spatial Resolution: 2 deg latitude × 2 km altitude Relative Error: < 10% for dust and for water-ice in N. spring (other seasons/conditions > 10%)	+	Lidar

* ✓ L-band Radar Addresses (green) + *Potential Supplemental Instrument (P = priority)*
1,2 High Priority Complementary Instruments Identified in Task 1 (blue) ++ *Potential Supplemental on Additional Platform, if implemented*

The following cannot be accomplished by the anchor payload, but are captured given Agency partner interests in atmospheric science, the expertise of the MDT, and the potential for augmentations within mission boundaries.

ATMOSPHERE PARAMETER 2 ATMOSPHERIC & AERONOMIC STRUCTURE & PROCESSES

ATMO 2.2 Structure, Dynamics, Vertical Coupling, & Loss to Space

PROPERTY TO CONSTRAIN	MEASURABLE PARAMETER(S)	SCALE / RESOLUTION / ACCURACY	CAPABILITIES NEEDED*	
Water-related Ions	Density & Temperature of Water-related Ions (Separation of CO_2 & H_2O-related Species)	Mass Resolution: M/dM > 3000 Density Range: >103 [cm^{-3}]	+	*Ion Mass Spectrometer*
	Line Profiles of CO & Its Isotopologues	Temperature Range: 300–20000 [K]	+	*RPA & Ion Drift Meter*
Oxygen Ion Motion	In-situ 2D Map of the O+ Density & Velocity	Vertical Velocity Res: < 20 m/s Mass Resolution: M/dM > 40 Density Range: 100-105 [cm^{-3}]	+	*RPA & Ion Drift Meter* *Ion Mass Spectrometer*
Elemental & Isotopic Abundance (To Elucidate Past Atmosphere)	Isotopic Abundance in the Upper Atmosphere	Mass Resolution: M/dM > 3000	+	*High-res Mass Spectrometer*
	Neon Elemental & Isotopic Abundance in the Lower Atmosphere	Min: ^{20}Ne (Major Isotope) Abundance within Factor of 3 Uncertainty Full: ^{20}Ne Abundance within Factor of 2 Uncertainty & ^{20}Ne/^{22}Ne Ratio with Uncertainty < 10% Extra: ^{20}Ne/^{22}Ne Ratio with Uncertainty < 1%	++	*On Potential High-altitude Relay Orbiter: Ne-Ar Separation Mass Spectrometer*
Water Vapor Column Abundance (3D Maps - lat, long, local time)	Absorption by Water Vapor in IR	Range: 20%, local time res: 0.5h Accuracy: 5–400 pr. µm Latitude Range: 60°S – 60°N Horizontal Resolution: 100 km	++	*On Potential High-altitude Relay Orbiter In Meteorological Package: Nadir Mini-IR spectrometer*
Temperature (4D Maps - lat, long, local time, altitude)	CO_2 Absorption of IR Wavelengths	Range: 100–300 K Accuracy: 2° K, Local Time Res: 0.5h Latitude Range: 60°S – 60°N Horizontal Resolution: 100 km	+ *P1*	*Sub-mm Sounder*
Surface Meteorological Conditions	Temperature, Pressure, Wind, Water Vapor, Dust & Ice Density	Same as Atmosphere 1.3	++	*On Potential Demo Lander: Meteorological Package & Tunable Laser Spectrometer*

* ✓ L-band Radar Addresses (green) 1,2 High Priority Complementary Instruments Identified in Task 1 (blue) + *Potential Supplemental Instrument (P = priority)* ++ *Potential Supplemental on Additional Platform, if implemented*

GEOLOGY 1 GEOSPHERE PROCESSES THAT SHAPE THE PRESENT

GEO1.1 Mobile Sediments, Mass Wasting, & Seasonal Changes (See also ATMO 1.1, 1.2)

PROPERTY TO CONSTRAIN	MEASURABLE PARAMETER(S)	SCALE / RESOLUTION / ACCURACY	CAPABILITIES NEEDED*	
Surface Changes	Interferometric Decorrelation	cm-scale	✓	InSAR
Surface Changes	Horizontal Displacement	m-scale	1	Hi-res Stereo Imager
Surface Geomorphology	Reflectance (I/F)	Spatial Resolution: 10s of cm-scale Vertical Precision: m-scale	1	Hi-res Stereo Imager
Surface Changes	Interferometric Decorrelation	Mass Resolution: 10s of mm-scale	+	*InSAR (C-Band)*

GEO 1.2 Flowing Ice (See also ATMO 1.2)

PROPERTY TO CONSTRAIN	MEASURABLE PARAMETER(S)	SCALE / RESOLUTION / ACCURACY	CAPABILITIES NEEDED*	
Surface Changes	Interferometric Decorrelation	cm-scale	✓	InSAR
Surface Geomorphology	Reflectance (I/F)	Spatial Resolution: 10s of cm-scale Vertical Precision: m-scale	1	Hi-res Stereo Imager
Surface Changes	Interferometric Decorrelation	Mass Resolution: 10s of mm-scale	+	*InSAR (C-Band)*

GEO 1.3 Present Cratering Rates

PROPERTY TO CONSTRAIN	MEASURABLE PARAMETER(S)	SCALE / RESOLUTION / ACCURACY	CAPABILITIES NEEDED*	
Surface Geomorphology	Interferometric Decorrelation	Spatial Resolution: 10s of cm-scale	1	Hi-res Stereo Imager
Surface Changes; Compositional or Thermal Differences	Reflectance (I/F)	Spatial Resolution: 10s of cm-scale	+	*Spectrometer (VNIR/TIR Wavelengths)*

* ✓ L-band Radar Addresses (green)
1,2 High Priority Complementary Instruments Identified in Task 1 (blue)
\+ *Potential Supplemental Instrument (P = priority)*
++ *Potential Supplemental on Additional Platform, if implemented*

GEOLOGY 2 GEOSPHERE PROCESSES THAT SHAPED THE RECENT PAST

GEO 2.1 Polar Deposits (PLDs and CO_2)

PROPERTY TO CONSTRAIN	MEASURABLE PARAMETER(S)	SCALE / RESOLUTION / ACCURACY	CAPABILITIES NEEDED*	
Permittivity Contrasts	Echo Time Delay	Penetration: 10s of meters Vertical Resolution: meter-scale	✓	SAR Sounder Mode
Scattering Properties	Backscatter Coefficient	Spatial Resolution: 10s of cm-scale	✓	Polarimetric SAR
Permittivity Contrasts	Echo Time Delay	Penetration: 100s of meters Vertical Resolution: meter-scale	1	VHF Radar Sounder
Surface Geomorphology	Reflectance (I/F)	Spatial Resolution: < m-scale Vertical Precision: meter-scale	2	Hi-res Stereo Imager
Mineralogy/Thermal Inertia	Reflectance (I/F)/Emissivity	Spatial Resolution: 10s of m-scale	+	*Spectrometer (VNIR/TIR wavelengths)*
Temperature with Depth	Emissivity (Brightness Temperature)	Radiometric Accuracy: 0.1 K	+	*Passive Radiometer (L-band, VHF, and/or C-Band)*

* ✓ L-band Radar Addresses (green); 1,2 High Priority Complementary Instruments Identified in Task 1 (blue); + *Potential Supplemental Instrument (P = priority)*; ++ *Potential Supplemental on Additional Platform, if implemented*

GEOLOGY 2 GEOSPHERE PROCESSES THAT SHAPED THE RECENT PAST

GEO 2.2 Mid-latitude Ice

PROPERTY TO CONSTRAIN	MEASURABLE PARAMETER(S)	SCALE / RESOLUTION / ACCURACY	CAPABILITIES NEEDED*	
Permittivity Contrasts	Echo Time Delay	Penetration: Up to 10 meters Vertical Resolution: meter-scale	✓	SAR Sounder Mode
Scattering Properties	Backscatter Coefficient	Spatial Resolution: 10s of meters	✓	Polarimetric SAR
Permittivity Contrasts	Echo Time Delay	Penetration: 10s of meters Vertical Resolution: meter-scale	1	*VHF Radar Sounder*
Surface Geomorphology	Reflectance (I/F)	Spatial Resolution: < m-scale Vertical Precision: meter-scale	2	*Hi-res Stereo Imager*
Mineralogy/Thermal Inertia	Reflectance (I/F)/Emissivity	Spatial Resolution: 10s of m-scale	+	*Spectrometer (VNIR/TIR wavelengths)*
Temperature with Depth	Emissivity (Brightness Temperature)	Radiometric Accuracy: 0.1 K	+	*Passive Radiometer (L-band, VHF, and/or C-Band)*

* ✓ L-band Radar Addresses (green); 1,2 High Priority Complementary Instruments Identified in Task 1 (blue); + *Potential Supplemental Instrument (P = priority)*; ++ *Potential Supplemental on Additional Platform, if implemented*

GEOLOGY 2 GEOSPHERE PROCESSES THAT SHAPED THE RECENT PAST

GEO 2.3 Recent Volcanism (Texture, Stratigraphy & Composition)

PROPERTY TO CONSTRAIN	MEASURABLE PARAMETER(S)	SCALE / RESOLUTION / ACCURACY	CAPABILITIES NEEDED*	
Scattering Properties	Backscatter Coefficient	Spatial Resolution: 10s of meters	✓	Polarimetric SAR
Permittivity Contrasts	Echo Time Delay	Penetration: meter-scale Vertical Resolution: meter-scale	✓	SAR Sounder Mode
Permittivity Contrasts	Echo Time Delay	Penetration: 10s of meters Vertical Resolution: meter-scale	1	VHF Radar Sounder
Surface Geomorphology	Reflectance (I/F)	Spatial Resolution: < m-scale Vertical Precision: meter-scale	2	Hi-res Stereo Imager
Mineralogy/Thermal Inertia	Reflectance (I/F)/Emissivity	Spatial Resolution: 10s of meters	+	*Spectrometer (VNIR/TIR wavelengths)*

* ✓ L-band Radar Addresses (green); 1,2 High Priority Complementary Instruments Identified in Task 1 (blue); + *Potential Supplemental Instrument (P = priority)*; ++ *Potential Supplemental on Additional Platform, if implemented*

GEOLOGY 3 GEOSPHERE PROCESSES THAT SHAPED THE DISTANT PAST

GEO 3.1 Crater Ejecta Emplacement & Degradation

PROPERTY TO CONSTRAIN	MEASURABLE PARAMETER(S)	SCALE / RESOLUTION / ACCURACY	CAPABILITIES NEEDED*	
Scattering Properties	Backscatter Coefficient	Spatial Resolution: 10s of meters	✓	Polarimetric SAR
Permittivity Contrasts	Echo Time Delay	Penetration: meter-scale Vertical Resolution: 10s of meters	✓	SAR Sounder Mode
Permittivity Contrasts	Echo Time Delay	Penetration: 10s of meters Vertical Resolution: meter-scale	1	VHF Radar Sounder
Surface Geomorphology	Reflectance (I/F)	Spatial Resolution: < m-scale Vertical Precision: meter-scale	2	Hi-res Stereo Imager
Scattering Properties	Backscatter Coefficient	Spatial Resolution: 10s of meters	+	*SAR (C-Band)*
Mineralogy/Thermal Inertia	Reflectance (I/F)/Emissivity	Spatial Resolution: 10s of meters	+	*Spectrometer (VNIR/TIR Wavelengths)*

GEO 3.2 Sedimentation & Stratigraphy (including Buried Landforms)

PROPERTY TO CONSTRAIN	MEASURABLE PARAMETER(S)	SCALE / RESOLUTION / ACCURACY	CAPABILITIES NEEDED*	
Permittivity Contrasts	Echo Time Delay	Penetration: meter-scale Vertical Resolution: meter-scale	✓	SAR Sounder Mode
Scattering Properties	Backscatter Coefficient	Spatial Resolution: 10s of meters	✓	Polarimetric SAR
Permittivity Contrasts	Echo Time Delay	Penetration: 10s of meters Vertical Resolution: meter-scale	1	VHF Radar Sounder
Scattering Properties	Backscatter Coefficient	Spatial Resolution: 10s of meters	+	*SAR (C-Band)*

* ✓ L-band Radar Addresses (green)
1,2 High Priority Complementary Instruments Identified in Task 1 (blue)
\+ *Potential Supplemental Instrument (P = priority)*
++ *Potential Supplemental on Additional Platform, if implemented*

GEOLOGY 3 GEOSPHERE PROCESSES THAT SHAPED THE DISTANT PAST

GEO 3.3 Unique Radar Terrains (MFF, Stealth Regions, etc.)

PROPERTY TO CONSTRAIN	MEASURABLE PARAMETER(S)	SCALE / RESOLUTION / ACCURACY	CAPABILITIES NEEDED*	
Permittivity Contrasts	Echo Time Delay	Penetration: meter-scale Vertical Resolution: meter-scale	✓	SAR Sounder Mode
Scattering Properties	Backscatter Coefficient	Spatial Resolution: 10s of meters	✓	Polarimetric SAR
Permittivity Contrasts	Echo Time Delay	Penetration: 10s of meters Vertical Resolution: meter-scale	1	VHF Radar Sounder
Scattering Properties	Backscatter Coefficient	Spatial Resolution: 10s of meters	✓	SAR Sounder Mode

GEO 3.4 Noachian Climate and Ice

PROPERTY TO CONSTRAIN	MEASURABLE PARAMETER(S)	SCALE / RESOLUTION / ACCURACY	CAPABILITIES NEEDED*	
Scattering Properties	Backscatter Coefficient	Spatial Resolution: 10s of meters	✓	Polarimetric SAR
Permittivity Contrasts	Echo Time Delay	Penetration: 10s of meters Vertical Resolution: meter-scale	✓	SAR Sounder Mode
Surface Geomorphology	Reflectance (I/F)	Spatial Resolution: < m-scale	2	Hi-res Stereo Imager
Permittivity Contrasts	Echo Time Delay	Penetration: 10s of meters Vertical Resolution: meter-scale	1	VHF Radar Sounder

* ✓ L-band Radar Addresses (green)
1,2 High Priority Complementary Instruments Identified in Task 1 (blue)
\+ *Potential Supplemental Instrument (P = priority)*
++ *Potential Supplemental on Additional Platform, if implemented*

HABITABILITY 1 ENABLE THE SEARCH FOR PAST & PRESENT HABITABLE ENVIRONMENTS

HAB 1.1 Presence of Liquid Brines

PROPERTY TO CONSTRAIN	MEASURABLE PARAMETER(S)	SCALE / RESOLUTION / ACCURACY	CAPABILITIES NEEDED*	
Brine Depth & Distribution (top 10 m)	Distance to Top of Ice Layer, Subsurface Reflections, & SAR Radar Backscatter (top 10 m)	Vertical Penetration: top few meters to 10 meter Horizontal Resolution: meters to 10s of meters Vertical Resolution: meter scale	✓	SAR SAR Sounder Mode
Brine Depth & Distribution (top 100 m)	Distance to Top of Ice Layer, Subsurface Reflections, & SAR Radar Backscatter (top 100 m)		1	VHF Radar Sounder
Seasonal Variability of Brines	Temperature of Top of Ice Layer	Horizontal Resolution: 10s of meters	+	Passive Radiometer

HAB 1.2 Global Distribution & Nature of Ice

PROPERTY TO CONSTRAIN	MEASURABLE PARAMETER(S)	SCALE / RESOLUTION / ACCURACY	CAPABILITIES NEEDED*	
Depth to Top of Ice Table (top 10 m)	Stratigraphy of Near Subsurface (top 10 m)	Vertical: m-scale Lateral: 100s of meters to kms	✓	SAR Sounder Mode
Radar Reflectivity as a Function of Depth (top 100 m)	Dielectric Constant as a Function of Depth (top 100 m)	Vertical Resolution: 1–2 m subsurface to depths of 10–100 m	1	VHF Radar Sounder
Distribution of Massive Ice Deposits & Near-surface Geomorphology	SAR imaging	Spatial Resolution: 10s of meters	✓	SAR
Surface Geomorphology	Optical Imaging	Spatial Resolution: meter-scale	2	Hi-res Stereo Imager
Subsurface Stratigraphy	Grain Size, Layer Thickness & Bedding Orientation	Vertical: m-scale (up to 10 m) Lateral: 100s of meters Orientation: < 1° over kilometers laterally	✓	SAR Sounder Mode
Near-surface Geomorphology	Thickness & Ice Content of Covering Deposits	Spatial Resolution: 10 meters	✓	SAR
Surface Geomorphology	Optical Imaging	Spatial Resolution: meter-scale	2	Hi-res Stereo Imager

* ✓ L-band Radar Addresses (green)
1,2 High Priority Complementary Instruments Identified in Task 1 (blue)
\+ *Potential Supplemental Instrument (P = priority)*
++ *Potential Supplemental on Additional Platform, if implemented*

HABITABILITY 1 ENABLE THE SEARCH FOR PAST & PRESENT HABITABLE ENVIRONMENTS

HAB 1.3 Past Fluvial & Glaciofluvial Activity

PROPERTY TO CONSTRAIN	MEASURABLE PARAMETER(S)	SCALE / RESOLUTION / ACCURACY	CAPABILITIES NEEDED*	
Subsurface Stratigraphy	Grain Size, Layer Thickness & Bedding Orientation	Vertical: m-scale (up to 10 m) Lateral: 100s of meters Orientation: <1° over kilometers laterally	✓	SAR Sounder Mode
Near-surface Geomorphology	Thickness & Ice Content of Covering Deposits	Spatial Resolution: 10 meters	✓	SAR
Surface Geomorphology	Optical Imaging	Spatial Resolution: meter-scale	2	Hi-res Stereo Imager

HAB 1.4 Subsurface Void Detection

PROPERTY TO CONSTRAIN	MEASURABLE PARAMETER(S)	SCALE / RESOLUTION / ACCURACY	CAPABILITIES NEEDED*	
Subsurface Vertical Profile (top 10 m)	Radar Reflectivity as a Function of Depth (Top 10 m)	Vertical Resolution: m-scale Spatial Resolution: 10s of m scale	✓	SAR Sounder Mode
Subsurface Vertical Profile (top 100 m)	Radar Reflectivity as a Function of Depth (Top 100 m)	Vertical Resolution: 1–2 m subsurface to depths of 10–100 m	1	VHF Radar Sounder
Rock Porosity, Density, & Ice Content (ambiguous)	Dielectric Constant (Top 10 m)	Vertical Resolution: m-scale Spatial Resolution: 10s of m scale	✓	SAR Sounder Mode
Rock Porosity, Density, & Ice Content (constrained)	Composition of Surface Rocks & Thermal Inertia	Spectral Features: 800 nm – 3 micron wavelength range & TIR channels Spatial Resolution: 10s of m scale	+	*Spectrometer (VNIR/TIR wavelengths)*

HAB 1.5 Geochemical Signatures of Habitability

PROPERTY TO CONSTRAIN	MEASURABLE PARAMETER(S)	SCALE / RESOLUTION / ACCURACY	CAPABILITIES NEEDED*	
Subsurface Vertical Profile of Putative Mud Volcanoes	Radar Reflectivity as a Function of Depth (Top 10 m)	Vertical Resolution: m-scale Spatial Resolution: 10s of m scale	✓	SAR Sounder Mode
Surface Composition	Spectral Features in the 800 nm to 3 micron Wavelength Range	Spatial Resolution: optimize < 4 m; could be multi-band or hyperspectral; SNR	++	*VNIR Spectrometer*

* ✓ L-band Radar Addresses (green)
1,2 High Priority Complementary Instruments Identified in Task 1 (blue)
\+ *Potential Supplemental Instrument (P = priority)*
++ *Potential Supplemental on Additional Platform, if implemented*

HABITABILITY 2 PROTECT MARTIAN & TERRESTRIAL LIFE

HAB 2.1 Planetary Protection

PROPERTY TO CONSTRAIN	MEASURABLE PARAMETER(S)	SCALE / RESOLUTION / ACCURACY	CAPABILITIES NEEDED*	
Scattering Properties	Water Activity, Depth to Top of Ice, Ice Contaminants	Vertical Penetration: top 10s of meters Horizontal Resolution: meters to 10s of meters	✓	SAR Sounder Mode (needs thermal model)
Permittivity Contrasts	Water Activity, Depth to Top of Ice, Ice Contaminants		+	*Passive Radiometer* *(no thermal model)*
Permittivity Contrasts	Water Activity	Detect Shallow Ice: < 1 thermal skin depth Horizontal Resolution: 10s of meters	+	*TIR Imager*
Surface Geomorphology	Surface Detection of Dust (Number Density & Particle Size) & Their Relationship to Local Wind Velocity	Dust (0.5–50 μm): 105–108 particle/m^3 for every min Wind Velocity: ~1 m/sec	++	–

HAB 2.2 Human Health Hazards

PROPERTY TO CONSTRAIN	MEASURABLE PARAMETER(S)	SCALE / RESOLUTION / ACCURACY	CAPABILITIES NEEDED*	
Ice Contaminants	Radar Reflectivity as a Function of Depth (top 10 m)	Vertical Resolution: m-scale Spatial Resolution: 10s of m scale	✓	SAR Sounder Mode
Mobility Challenges	Slope, Topographic, and Roughness Hazards & Rock Size Distribution	Spatial Resolution: <10 m scale	✓	SAR
Permittivity Contrasts	Slope, Topographic, and Roughness Hazards & Rock Size Distribution	Spatial Resolution: centimeter to meter-scale	2	Hi-res Stereo Imager
Dust Hazards	Dust Particle Size, Optical Depth at Landing Site	Dust (0.5–50 μm): 105–108 particle/m^3 for every min.	++	–

* ✓ L-band Radar Addresses (green) + *Potential Supplemental Instrument (P = priority)*
1,2 High Priority Complementary Instruments Identified in Task 1 (blue) ++ *Potential Supplemental on Additional Platform, if implemented*

5.5 SUMMARY OF SUPPLEMENTAL SCIENCE OBJECTIVES & TRACEABILITY

The MDT's second task was to assess the range of scientific investigations that could be conducted with the anchor radar payload. The team also assessed the value added to scientific investigations if one or both complementary instruments identified in Task 1 were included. In addition, the team examined options for supplemental instruments that could provide synergistic or augmented capabilities to address outstanding scientific questions. The investigations and at their associated instrumental measurement details are summarized in the Science Traceability Matrix (STM; Section 5.4). Three scientific theme areas were identified for the subgroups' studies: Atmosphere, and Geosphere, and Habitability.

The MDT Atmosphere Group found that the anchor radar payload can address three major atmospheric science topics of wide interest: surface/subsurface volatile inventory and variability, recurring slope lineae, and upper atmospheric processes, especially ionospheric irregularities. Atmospheric science would further benefit from either or both of the MDT-identified complementary payloads (VHF sounder and a high-resolution imager). In addition, several supplemental payloads could contribute vital information about past and present climatology, weather, and space weather. The group developed a prioritized list of such instruments, with the three highest priority being: sub-millimeter sounder, thermal infrared (TIR) atmospheric limb sounder, and UV and VIS imager.

The MDT Geosphere Group established three organizing topics that categorize processes that have shaped: (1) the present day, (2) the recent past, and (3) the more distant past. The group identified the interferometric SAR (InSAR) capabilities of the anchor radar payload as being especially suited to addressing present day processes acting on scales of centimeters to meters. These include sediment mobility, mass wasting, seasonal cycles, and glacial flow, all important drivers of landscape evolution. For the recent (kyr to Myr) past, the group found the anchor payload broadly addresses all of the identified scientific objectives related to geologic processes acting over these timescales. These include polar to mid-latitude ice-related processes, and recent volcanism. For more ancient processes, the group again found the anchor radar payload to be highly capable in addressing such processes as crater formation and degradation, buried landforms, unique radar terrains (e.g., “stealth”) and Noachian climate and ice. The group found that a VHF sounder would provide depth resolution and penetration that bridges a critical gap between the core payload and current sounders at Mars for geological investigations. A high-resolution imager would provide key information on surface geomorphology at spatial scales that complement the capability of the core payload.

The MDT Habitability Group established two organizing topics that I-MIM can address regarding Martian habitability: 1) Enable the search for past and present habitable environments; and, 2) Protect Martian and terrestrial life. The group found that the anchor radar payload can address many important topics related to current and past habitability, including locating ice and brines that may serve as present-day habitable environments, characterizing the fluvial and/or glaciofluvial environments that might have hosted life in the past, and identifying subsurface habitats in the form of human-scale and microbe-scale voids in the substrate. With the addition of the complementary payloads, these topics can be constrained to a higher fidelity than is possible with the core payload alone. Other supplemental payloads such as a high spatial resolution spectral imager, a passive radiometer, and/or a lander with an onboard dust counter, anemometer, and camera were identified to support science investigations related to habitability.

Polygonal terrain suggesting Martian mid-latitude ice.

Credit: NASA/JPL-Caltech/UArizona

6 OPERATIONS CONCEPT & STRATEGIES

The MDT was directed in its charter to carry out a third task:

> *"…[T]he MDT will additionally provide a model concept of operations (e.g., orbit altitude, local solar time, timing dedicated to data collection etc.) that reflects mission goals, objectives, requirements, and MDT findings, with supporting information from the mission's engineering teams about the primary mission (e.g., launch, arrival, duration) and I-MIM spacecraft/payload capabilities."*

The MDT used the following approach to undertake Task 3:

1. Use as a starting point the mission design provided by the mission concept team;
2. Assess the high-level Concept of Operations (ConOps) model provided by the mission team;
3. Accept or modify elements of the provided mission design to optimize accomplishment of the Task 1 Reconnaissance Objectives; document justification;
4. Determine deltas to the ConOps that would improve RO achievement with the complementary payloads (onboard or as free flyers) from Task 1:
   - VHF Sounder to complete sub-surface coverage
   - Hi-res Imager to obtain single and stereo detailed coverage
5. Consider additional ConOps changes needed and/or desired for Task 2 objectives, with:
   - L-band SAR/Sounder only;
   - L-band with complementary instrument(s) in item 4, and,
   - Add-on instrument(s) proposed in Task 2.

Section 6.1 provides an overview, including assumptions.

Section 6.2 focuses primarily on a Concept of Operations for a threshold mission that carries ONLY the primary payload.

Section 6.3 provides a broad overview of the ConOps in the event Agency partners can accommodate MDT-identified high-priority complementary instruments: a VHF Sounder and a High-resolution Stereo Imager.

More detailed ConOps considerations for each follow in Sections 6.4 and 6.5, respectively.

Section 6.6 briefly addresses the potential for supplemental payloads.

Section 6.7 provides summary tables of coverage estimates for each phase, payload, and mode.

Section 6.8 provides a summary of the Task 3 chartered activity.

The Task 3 team comprised 21 MDT members and a mission technical support team.

6.1 BACKGROUND

Human and robotic missions to Mars have been the subject of many detailed studies by several national space Agencies over the last 40 years. These studies include a variety of overarching mission objectives that tend to drive the concept of operations for a particular study. To date, no space Agency studying human missions to Mars has committed to any particular scenario or set of objectives to the point of setting mission requirements. However, accessing a source of *in situ* water for both scientific investigation and as a resource for use by the astronauts is a frequently discussed feature of most human Mars mission studies. Consequently, an important data set that will influence where and how human missions will be carried out depends on determining the location of accessible water (assumed to be in the form of subsurface ice) and details regarding the characteristics of the ice deposit. I-MIM's core payload (with potential augmentation, as discussed elsewhere) can fill important missing data, particularly in revealing the near subsurface (i.e., roughly the top 10 meters) constituents and associated physical properties. To acquire the necessary critical dataset, the I-MIM Project should place a high priority on initially collecting near-surface mapping data (at low to medium resolution) to support planners of future robotic and human surface missions. An I-MIM Reconnaissance Zone (RZ) can be pre-defined covering an area where both subsurface ice can be expected and crewed landings are feasible. The next priority should be to identify and gather higher resolution data for a select number of targeted areas of interest (TAI), as defined by RO-3. For human mission planning, this means sampling TAI ranging from those characterized by largely featureless surface terrain with uniform subsurface properties to those with complex surface terrain and intricate subsurface profiles. Gathering data from TAI that span this range will be central to assessments of future human Mars missions, especially to understand the safety, costs, and benefits associated with conducting surface operations at each type of site.

6.1.1 ConOps Assumptions

CONOPS ASSUMPTIONS FOR THE RECONNAISSANCE ZONE

The Reconnaissance Zone (RZ) delineates areas of highest priority for subsurface ice mapping by the I-MIM core payload, as defined by the multilateral mission Concept Team in the I-MIM Reconnaissance Objectives provided to the MDT. The intent is to identify the most equatorward, ice-rich candidate locations for human exploration (see RO-3) in the Martian mid-latitudes where human missions are more operationally viable. The RZ is based on results from the Mars Subsurface Water Ice Mapping (SWIM) team, as well as other factors (e.g., elevation masks for human-class landings, latitude limits within the mid-latitudes, etc.). The SWIM team has been using data from thermal and neutron spectrometers, imagers, an altimeter, and radar sounders onboard Mars orbiters to map buried ice in the Martian mid-latitudes (Morgan et al., 2021; Putzig and Morgan et al., 2022 In Press).

For each data set, the team has established methods to assign values of ice consistency, which may extend between -1 and 1. A value of -1 indicates that the data are wholly inconsistent with the presence of ice, a value of 0 indicates that the data are equivocal to the presence of ice, and a value of 1 indicates that the data are wholly consistent with the presence of ice. The team established sets of equations to produce composite ice-consistency values across all datasets. A preliminary equation weights the datasets equally and is applied over all depths (Morgan et al. 2021). A later set of equations weights the datasets differently and is applied over three depth zones (Putzig et al., 2022, In Press). In the latter case, the weightings are based on the dataset sensing depths relative to the depth zones of interest.

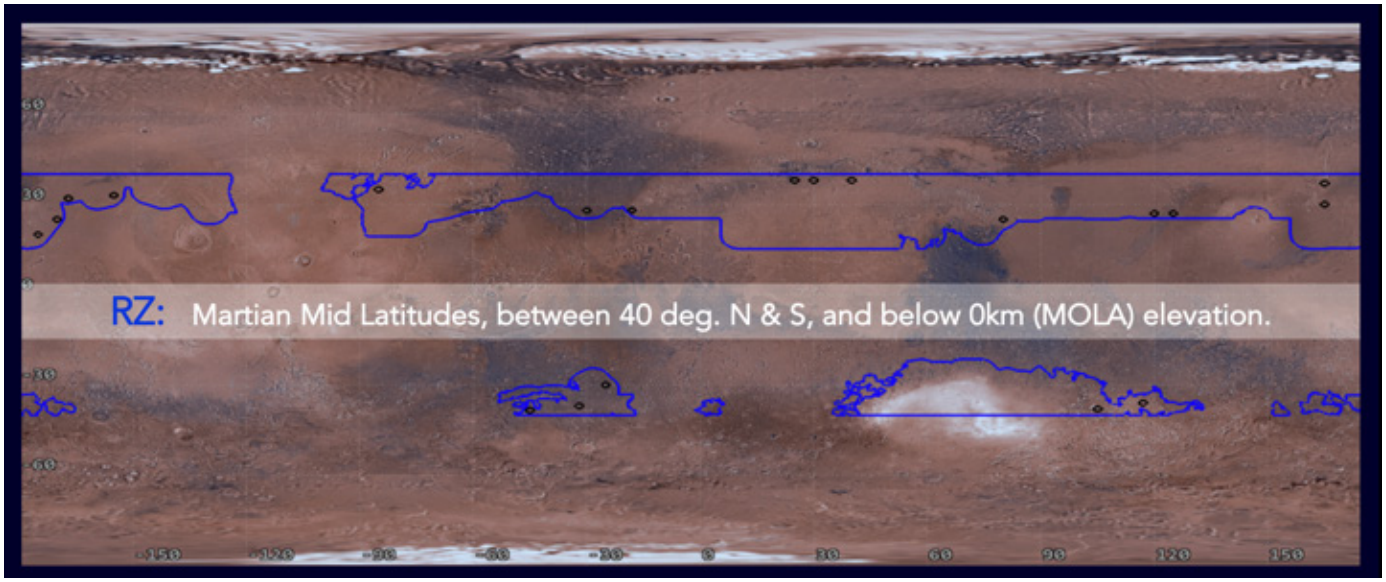

Figure 6.1 The Reconnaissance Zone (RZ) is outlined in blue. Black circles, not necessarily to scale, are randomly placed to simulate eventual identification of Targeted Areas of Interest (TAI); illustrated only for depicting the conceptual "survey then select" I-MIM strategy for locating candidate sites for human exploration.

Given the expected performances of the I-MIM core payload, the mission team chose the SWIM composite ice consistency map for the 1–5 m depth zone as the basis of the RZ map. The mission team set the bounds of the RZ using a lower threshold value of 0 in the SWIM map. SWIM mapping extends to 60° latitude in each hemisphere and to an elevation of +1 km above the Martian datum (areoid), but the mission team set the RZ more restrictively to between ±40° latitude and 0 km maximum elevation to account for engineering constraints for human missions. Areas of higher latitude and elevation exceed notional limits of environmental conditions likely acceptable for initial architectures for human missions to Mars.

Finally, in determining the RZ's extent, the mission team excluded regions in the south smaller than 100 km in diameter given they unlikely have sufficient size for human-exploration needs.

The Task 3 Group used the above description of the RZ to create a model Concept of Operations. The survey of the RZ is highest priority in the early part of the mission. The MDT worked under the assumption the RZ needs to be mapped with ≥95% coverage by the low-resolution (30 m) SAR to fulfil the objectives.

An estimated ~4 Tbit of downlinked data volume is required to reach 95% coverage of the RZ as currently defined. The total data volume could be reduced with judicious data acquisition; however, without knowledge of the final orbit and repeat periods, too many variables exist for a more accurate estimation.

CONOPS ASSUMPTIONS FOR TARGETED AREAS OF INTEREST (TAI)

RO-3 calls for detailed, high-resolution maps of "targeted areas of interest" (TAI) within the surveyed RZ that have adequate (RO-1) and accessible (RO-2) water ice and address the four I-MIM RO-3 criteria (human-led surface science, human-class landing and launch, ISRU, and civil engineering) for characterizing locations for future human exploration.

Limitations on the Description of TAI

The MDT does not set a pre-determined number, size, or coverage percentage target for the TAI, but a total number in the range of 5–25 would appear to be reasonable. The Task 3 Group acknowledges that Mars may provide numerous locations of various sizes

suitable for human exploration. The MDT assumes that TAI, on average, are circular with a nominal radius of 50 km. The Task 3 Group leaves defining these quantities more specifically to future work, especially during a Phase A study for application at the conclusion of the Phase 1 Concept of Operations described below, when the 30-meter SAR reconnaissance is (nearly) complete.

Note that high-resolution data are not likely to be needed for the entire area inside each TAI: some TAI could need as little as 5% of the area mapped to draw a conclusion about its utility for planning purposes, while others could need the full 100% depending on the complexity and suitability of the region.

Potential Pre-arrival Selection of a Limited Set of TAI

TAI are candidate locations for human exploration that would be subject to detailed characterization in a second phase of the I-MIM mission, per the four RO-3 criteria at minimum (in brief, human-led surface science, human-class landing/launch, ISRU, and civil engineering), as articulated in Section 4.4 and in the RTM. Ideally, these sites would be selected after the completion of the RZ survey. However, that plan is likely inefficient given necessary operational planning. This inefficiency could be mitigated by exercising characterization (high-resolution) SAR modes and radar sounding during the initial phase and by using present knowledge and datasets to pre-select a small number of promising TAI for ice access. Such data sets include the SWIM maps; HiRISE and CTX imagery; and, THEMIS, CRISM, and other relevant Mars datasets, including ground-truth data from past/present robotic missions (e.g., RIMFAX). Such a catalog of candidate TAI could drive initial I-MIM operational orbit trajectory planning and payload targeting procedure development during Phase A. Acquisition of a small number of TAI in the first mission phase would support data pipeline procedure development and validation in preparation for the mission's second phase.

CONOPS ASSUMPTIONS FOR THE L-BAND RADAR

The L-band radar is the anchor payload for the mission. It has two modes that offer different performance and capability as outlined in Table 6.1.

Other resolutions are available for this instrument concept, but the MDT focuses on these for this report. The data in the SAR modes can be combined if multiple passes over a site are obtained to produce InSAR and tomography products at the cost of increased data volume (assumptions: factor of 2 InSAR; factor of 10 for tomography). The total data volume available will constrain areal coverage of the latter products. The nadir sounder mode is also available for assessing vertical profiles of the substrate.

Table 6.1 ConOps Assumptions for I-MIM Anchor Payload

SAR MODE	MAIN PHASE OF USE	RESOLUTION (M)	DATA GENERATION RATE (MBPS)
Low-res SAR (raw)	1 (RZ)	30	42
Low-res SAR (processed)	1 (RZ)	30	8
High-res SAR	2 (TAI)	5	333
High-res SAR	2 (TAI)	3	400
Sounder	2 (TAI)	3	7.2

6.1.2 Suggested Principles for I-MIM ConOps

The ConOps discussions produced the following guiding principles:

- Defining a threshold mission that could be achieved within a minimum amount of time would be desirable. The potential for difficulties/failures with the spacecraft and payload in the near-Martian environment suggests that obtaining the highest possible scientific return in an initial phase should be a priority, without interfering with the ability to meet the requirements-driving reconnaissance objectives, per the Agency-provided assumptions in the MDT Charter.
- The Reconnaissance Zone (RZ) survey is the highest priority early in the mission and would be achieved in an initial phase (Phase 1 – Broad Survey Phase).
- A "Detailed Characterization Phase (Phase 2) for Target Areas of Interest (TAI) would be reached via a transition from Phase 1 in terms of operation.
  - By focusing on low-resolution surveys of the RZ before selection and detailed mapping of TAI, the chances of missing exciting locations during the prime mission and potentially using up available bandwidth focused on intractable candidate locations for human exploration is reduced. Furthermore, should the mission fail during the prime mission, the important widespread reconnaissance would have a higher chance of completion, providing full context for subsequent decision making.
- The duration of the Phase 1 should have sufficient margins to be robust.
  - Solar conjunction may remove up to four weeks from normal data-acquisition operations. Given that the arrival date is unknown, the timing of any conjunction with respect to the phases is also unknown. Consequently, operational planning and the timing of the phase transition should be robust against a reduction of downlink. (The MDT notes that the telecom system planned by ASI should minimize losses around conjunction.)
  - In general, the spacecraft and operations should probably be robust against 3–7 days of communication (downlink/uplink) loss. Commanding on a weekly basis based around a longer-term plan that covers the repeat cycle appears to be a workable approach.
- A small percentage (5–10%) of the low-resolution mode SAR used to map the RZ should be returned in raw form for continued calibration purposes, with the remainder used in a mode with data processed onboard. Phase 1 should also allocate small amounts of time/data volume to high-resolution SAR and sounder modes and complementary payloads to allow verification of operational and ground data analysis systems prior to entrance into the second phase and to support acquisition of time-sensitive, seasonal targets of opportunity.
  - All instrument modes and approaches should be exercised early in the mission to ensure correct operation/commanding of those modes and to provide data sets that can be used to improve and/or refine data collection, reduction, and analysis tools, even if the most prolific use of those modes might occur later in the mission.
  - A prime mission duration of 1 Mars year would be typical. However, this timeframe would require that high-priority seasonal targets be acquired (although not necessarily downlinked) within Phase 1.
- The MDT found that total data volumes (over one Mars year corresponding to a typical prime mission duration) constrain surface coverage in high-resolution modes,

particularly when including potential complementary and supplementary payloads.

- The L-band Radar is capable of generating far more data than can be downlinked even in the most optimistic scenario. This capability may well be true for the MDT-identified, high-priority complementary payloads as well. Hence, the data volume available to the payloads needs to be allocated at values that reflect their contributions to the mission objectives. Total data volume over a fixed period is a precious resource that can be easily consumed by operation of both the L-band Radar and the complementary payloads in their highest resolution modes. Optimization of data usage (including compression, optimum selection of modes, and careful targeting) is necessary, suggesting that significant planning effort should be allocated prior to arrival at Mars.
- The data downlink rate from the spacecraft can change by more than an order of magnitude depending upon the Earth-Mars distance. A large onboard storage device capable of holding data for up to two years should be considered, but usage (and hence sizing of the storage) is strongly dependent upon the acquisition strategy.

Managing the content of this storage would be an important task. The approach and sizing of the storage should be part of a Phase A study. High-priority science targets that can only be acquired during low data downlink periods (e.g., time-sensitive seasonal targets) may also provide a justification for significant onboard data storage capacity.

6.1.3 Mission Phasing

The Task 3 Group produced the following notional top-level timeline:

Table 6.2 Concept of Operations Top-level Timeline based upon an initial date for Mars Orbit Insertion defined to be T0 ("time zero")

ACTIVITY	COMPLETION DATE	NOTES
Mars Orbit Insertion (MOI)	T0	Per Definition
In-orbit Spacecraft Commissioning	T0+2 w	–
Period of aerobraking or solar-electric propulsion to reach final orbit (if required)	T1	T1–T0 is Unknown, but might be on the order of 6 months by analogy with Odyssey and MRO
Final Orbit Spacecraft Check-Out	T1+1 w	–
Payload Commissioning and Entry into Primary Mission	T1+2w = T2	–
Broad Survey Phase (Phase 1)	T2+10 mos. = T3	Beginning of Primary Science Phase (See Section 6.1.6)
Detailed Characterization Phase (Phase 2)	T3+12 mos.	1 Mars Year in Orbit Completed
TOTAL DURATION OF THE PRIMARY SCIENCE PHASE		22 MONTHS

6.1.4 Orbit Considerations

The orbit inclination in the Mars reference frame can be set during orbit insertion, but is normally difficult to change through maneuvers because of the associated large delta-V. The inclination defines the extent of latitudinal coverage.

For the Reconnaissance Objectives, the inclination may not need to be higher than 45°. This inclination would cover the RZ with the SAR and would provide the maximum amount of time directly above the RZ for observations. Because of data-volume limitations (even in the best-case scenarios), time directly above the RZ is not a limiting factor and does not affect the recommendations for orbital characteristics. Similarly, time-of-day for observations is a non-issue for the L-band radar. Lower inclination orbits, however, compromise total scientific return by eliminating mid- to high-latitude science, and the associated long eclipse durations give rise to power, thermal control, and telecommunications issues.

The importance of high-latitude studies is a common theme in discussions of the scientific output from I-MIM and therefore quasi-polar (high inclination) orbits are preferred. A satellite orbit is Sun-synchronous if the orbital plane is near-polar and the altitude is such that the satellite passes over the equator at constant local time. A satellite in this orbit about Mars shifts its orbital plane by ~0.6°/Earth day maintaining the local time at the equatorial crossing. Sun-synchronous and asynchronous orbits have both been used at Mars. NASA's Mars Reconnaissance Orbiter (MRO) uses a Sun-synchronous orbit held at 3PM ± 30 minutes for the dayside equatorial pass. ESA's ExoMars Trace Gas Orbiter (TGO) is on an asynchronous orbit with the spacecraft passing over different local times according to a repeat cycle of about 35 days. Table 6.3 itemizes various advantages and disadvantages.

Table 6.3 Advantages and Disadvantages of Sun-synchronous and Asynchronous Orbits

	SUN-SYNCHRONOUS (MRO-LIKE; 3 PM)	ASYNCHRONOUS (TGO-LIKE)
Spacecraft Considerations	Near-terminator Sun-synchronous orbits are advantageous for power and telecommunications.	–
L-band Radar	The orbit synchronicity is irrelevant for L-band radar as solar illumination of the surface is not required and diurnal ionospheric effects are likely small in this frequency range. The same applies to the VHF sounder in the complementary payload.	
Imager(s)	▪ Near-constant illumination. ▪ If 3 PM is chosen, this is ideal for shadow definition and associated surface hazard identification. ▪ If 3 PM is chosen, there is no access to low phases limiting color (mineralogical) definition and the range of phase angles for determination of surface properties is limited.	▪ Occasional terminator orbits with poor data quality. ▪ Occasional midday crossings of the equator region with resulting high color (mineralogical) definition. ▪ Surfaces can be observed over a large range of phase angle.

The emphasis on safety and hazard avoidance with a potential optical remote-sensing payload (one of the two highest priority potential augmentations identified by the MDT) suggests that a 3 PM Sun-synchronous orbit is preferable. If no optical remote-sensing payload is onboard, then near-terminator Sun-synchronous orbits would still be preferred because they are advantageous to the spacecraft.

It should be apparent that low-altitude, quasi-circular (low-eccentricity) orbits are preferred because they produce high-resolution data that are more uniform in resolution over the orbit. The L-band radar can accommodate for altitude differences by changing the roll angle; the sounding mode is unaffected in resolution by altitude. However, both modes suffer from performance loss with increasing altitude. It should be noted that MGS, Odyssey, MRO, and TGO reached their respective orbits using aerobraking. The need for aerobraking or solar-electric powered orbit changes and their respective implications for the mission (duration, properties of the initial orbit, spacecraft resilience to dynamic pressure, calibration/commissioning during/before aerobraking, etc.) should be assessed.

A satellite is in an exact orbital resonance (R:D) when the spacecraft performs exactly R revolutions with respect to its ascending node, while the planet (Mars) rotates exactly D times with respect to the precessing orbital plane. In an orbital resonance, the ground tracks are exactly the same after R nodal revolutions and D nodal days (e.g., Bezděk et al., 2010). Resonant orbits (sometimes called repeat orbits) have important advantages for I-MIM. In particular, they can support acquisition of InSAR data because the geometry of the observations can be defined well in advance and can be in the optimum configuration. A fully resonant orbit is ideal for InSAR. However, disadvantages exist in that targets between the ground tracks may require a spacecraft roll – particularly at equatorial latitudes for quasi-polar orbits for any accommodated complementary payload elements – and the resonant nature of the orbit implies that such targets would never be in the optimum geometry. These can be accommodated by setting SAR acquisition during instrument programming.

Two approaches to the operation of a spacecraft at Mars are illustrated by contrasting approaches taken by TGO and MRO. In the case of TGO, the spacecraft orbit is controlled to "fly-the-plan." In other words, small orbit correction maneuvers (OCMs) are made once a week (unless the orbit drift is insignificant within a specified tolerance, in which case the OCM is skipped) in order to keep the spacecraft on a long-term plan for the orbit evolution. In the case of MRO, the orbit drifts and frequent orbit updates are provided to the planners even relatively late in the planning process. There are potentially other solutions.

I-MIM Reconnaissance Objectives call for full coverage of both the RZ and specific high-resolution coverage of selected TAI within it (i.e., candidate locations for human exploration). The ability to have a clear plan of when those TAI will be acquired suggests that "flying-the-plan" may be the more efficient approach. A resonant (repeat) orbit could be implemented, but with the possibility of allowing the spacecraft to perform a temporary controlled drift once coverage in a specific repeat orbit completes. The cost in terms of fuel may be small, while gains can be expected elsewhere from avoiding more intensive parts of the planning cycle arising from uncontrolled orbit drift. This concept should, however, be traded against the financial costs associated with planning and executing weekly maneuvers.

Preliminary work in the model provided to the MDT centered around a 55-day repeat cycle. However, the Task 3 Group noted that, given full freedom, a repeat cycle that is a multiple of 7 days (e.g., 48 or 56 days) could have advantages in that each cycle covers the same "real estate" and cycles can be planned with that in mind according to a fixed working week on Earth. This input supports the idea that key sites can be acquired in the optimum way through long-term prediction. The Task 3 Group noted that an MRO-like orbit with a 56-day repeat cycle (cf. MRO 17-day cycle and TGO 35-day cycle) implies a semi-major axis of 3652 km (roughly 256 km over datum). This cycle duration also implies a mean ground-track separation of 29 km at the equator and hence a mean roll angle to "fill-in" coverage between ground-tracks of ±3.2 deg if a perfectly resonant orbit is implemented, easily accommodated by the anchor payload.

6.1.5 Spacecraft Capabilities/Constraints Affecting Operations

An incomplete list of the capabilities of the spacecraft according to the current baseline is given in Table 6.4. The table illustrates the roll rates, the pointing performance, and the total power available to the SAR payload. The MDT notes that several other items under study and as yet undefined may constrain the operations (e.g., transmission rates within the spacecraft). The MDT recommends that when I-MIM enters Phase A, a study of the spacecraft power consumption should be made to evaluate potential constraints.

Table 6.4 Baseline Spacecraft Capabilities

ITEM	PERFORMANCE	COMMENT/IMPLICATIONS
Method of Approach to Final Orbit		Chemical and electric propulsion methods of reaching final orbit are still being addressed in a trade study.
Max. Roll Rate	0.43 deg/s	It takes ~195 sec from nadir to 44.4 deg off-nadir pointing, excluding settling time.
Settling (tranquilization) Time	TBD	Settling time is not yet evaluated, because flexible parameters of the SAR's reflector and boom (dominant contributors to spacecraft vibration) are not available yet. Settling time is expected to be comparable to attitude maneuver time.
Spacecraft Stability	0.01 deg/s	Current requirement (= 0.0083 deg/sec) from I-MIM to support the high-resolution imaging.
Max. Roll Angle from Nadir for Routine Ops	44.4 deg	This performance is assumed.
Absolute Pointing Error (APE)	deg (3σ)	The APE for the SAR reflector (LDR) needs to be evaluated, considering both misalignment between the spacecraft body and LDR and the structural vibration of LDR and boom.
Absolute Pointing Knowledge (APK) (after the fact)	0.03 deg (3σ)	Same as for APE.
Maximum Power required for SAR	761 W (w/o margin)	The spacecraft can provide this power for the period of time specified as the observation duty cycle (Latitude: ±25 to 40 deg).
Maximum Power Required for Comms	816 W (w/o margin)	N/A

The MDT recommends that, when I-MIM enters Phase A, the mission team should study spacecraft power consumption to evaluate further any operational constraints.

6.1.6 Coverage and Data Volume Simulations for I-MIM

The I-MIM Concept Team ran (and provided to the MDT) Systems ToolKit (STK) simulations to provide estimates of the SAR 30 m mode coverage of the RZ (and the corresponding data volume). Originally, similar models estimated that 6 months would be needed to complete >95% coverage of the Reconnaissance Zone; the new simulations checked this estimate in greater detail and with two different operational scenarios. The downlink data rate in the model varies with the Mars-Earth distance, with a reference value of 1.88 Mbps at a distance of 1.5 AU. It should be noted that solar conjunction can only affect one of the two phases in any nominal 1 Mars Year primary mission and that, in the studied case, conjunction would occur in Phase 1. The model made no allowance for the expected step-wise decrease in data rate with increasing Earth-Mars distance. Estimates of downlink data volumes assume direct-to-Earth (DTE) communication, with no limit on available Deep Space Network (DSN).

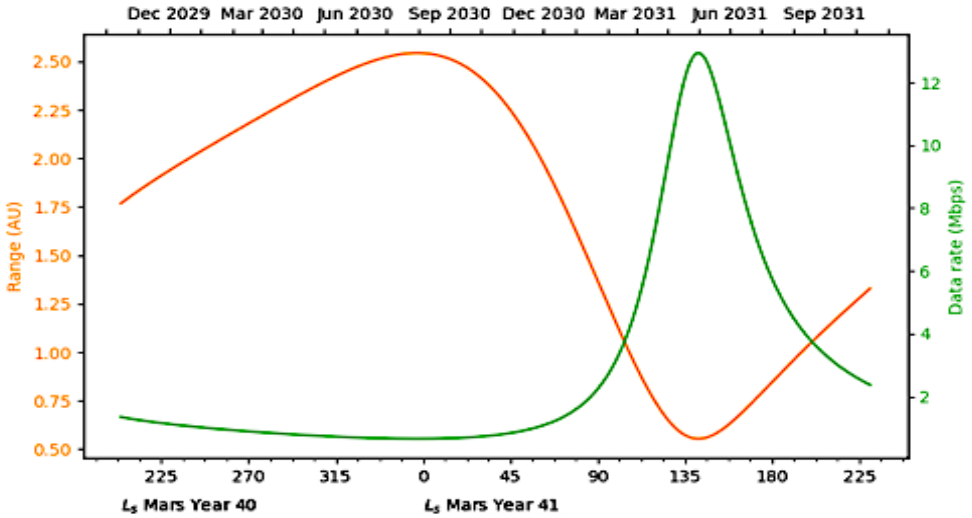

Figure 6.2 Variation in data rate with Earth-Mars distance strongly depends on the Earth-Mars distance. The plot, provided to the MDT by the I-MIM mission team, shows this variation assuming a nominal launch date in 2028.

The model did not include the nadir Sounder mode or the high-resolution imaging approaches. For optimization, the model acquired SAR data only if the orbiter had not previously imaged at least 10% of a pass over the RZ. Results are given in Table 6.5.

Note that higher coverage percentages can be obtained (to nearly 100 % within 6 months) if the optimization procedure is relaxed (i.e., higher total coverage comes at the expense of more repeated coverage which implies higher data volume usage).

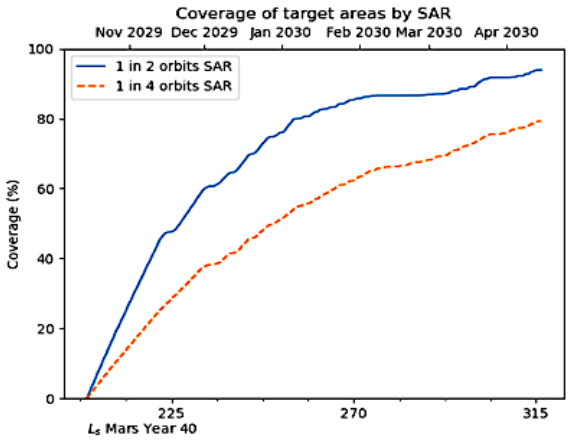

Figure 6.3 Coverage of the RZ by the SAR as a function of time with the two concepts of operation.

Table 6.5 Coverage and Data Volumes

	SAR 30 M ON 1 OF 2 ORBITS	SAR 30 M ON 1 OF 4 ORBITS
Coverage % (Recon Zone)	93.88%	79.25%
SAR 30 m Total On Time	9283 min	6430 min
Data Volume Acquired	557 GB	386 GB

Figures 6.4 and 6.5 illustrate the build-up of coverage of the RZ. The model plots show significant amounts of data volume can be available, even in the scenarios for additional data transmission from other SAR modes or complementary payloads. The speed of acquiring the required coverage of the RZ is not driven by the downlink data volume, but by the orbital coverage of the RZ. In the first concept, where the SAR is used every other orbit, the 95% coverage requirement is almost achieved within a 6-month period, while the alternative concept of operation still reaches ~80% in the required period. Nonetheless, this indicates that the RZ can be covered to the required level quickly and that, if additional data from other modes or payloads are required, then they can be accommodated without having a major impact on the time for RZ mapping if observations are well-planned.

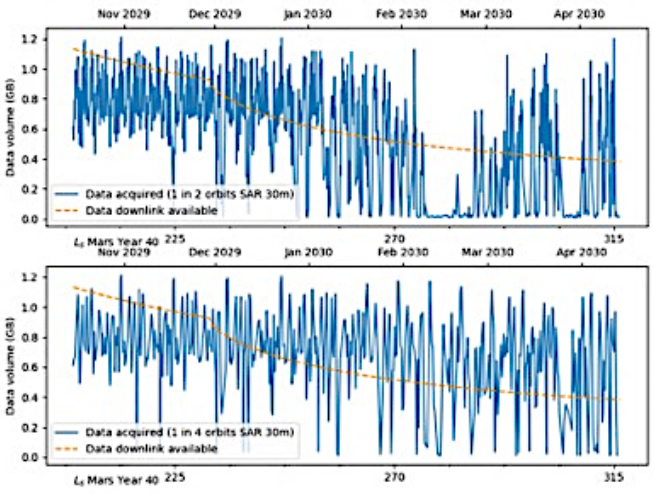

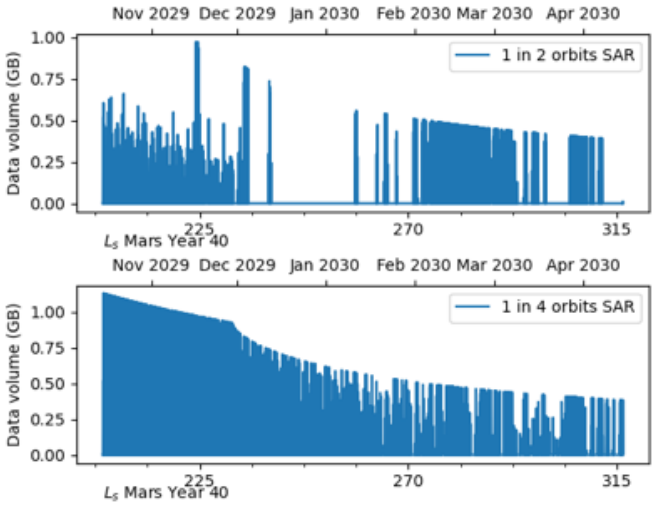

Figure 6.4 (Left) Data volume acquired by SAR 30 m mode and downlink volume available, per orbit
Figure 6.5 (Right) Unused downlink data volume per orbit

The two basic concepts of operation probably represent end-members. A more sophisticated scheme can be envisaged. For example, the first concept may be the nominal case, but with a minor fraction of time operating in the second conceptual scheme to obtain higher resolution data. In order to provide flexibility and margin on meeting the 95% coverage requirement, the MDT found that 10 months should be sufficient to complete RZ mapping (Phase 1) at this 95% level and, given that this value includes sufficient margin to be robust, the duration should allow a small number of other activities that could support a smooth and efficient transition to Phase 2. An earlier transition to Phase 2 is desirable if the mapping requirements and the operational planning allows. The Task 3 Group noted the need for three key payload calibration activities described in the background materials supplied by the mission Concept Team, but assume that negligible data will be required for these activities.

6.1.7 Operational Profile for the SAR

The Task 3 Group based the operational profile of the SAR on data allocation (including InSAR, tomography etc.). The MDT finds that the mission should have two phases:

Phase 1. Broad Survey Phase

Phase 2. Detailed Characterization Phase

The following assumes a Primary Mission (PM) of one Mars year (per the Agency-provided assumptions in the MDT Charter) and allocates data volumes for the various instruments/experiments based on discussed priorities, including a priority to provide human mission planners with as much relevant data early in the mission as possible. This priority for early reconnaissance has two major benefits, among others.

First, this approach gives time early in the mission to identify RO-3 TAI for more detailed exploration during Phase 2. Data returned from mapping the Reconnaissance Zone (RZ) will provide knowledge of locations with high Circular Polarization Ratio (CPR) that, when combined with sounder data, can be used to assess where ice is present and accessible for human-led ice sampling, water-ice-related ISRU, and civil engineering (e.g., for use in construction and additive manufacturing) and where the surface might best support human-class landings and launches. Naturally, the distribution can also be used to constrain models of the origin of the detected ice.

As discussed previously, the MDT recommends having some small number of TAI identified before arrival. That will partially use the remaining 20% data allocation, with other remaining data volume being used for seasonal targets. An approach to defining these early TAI is discussed below, with final definition (including number and distribution) to be made at an appropriate time (e.g., before Mars Orbit Insertion). In general, when the I-MIM spacecraft reaches its operational orbit and begins mapping the RZ with 30-meter resolution SAR (Phase 1), the mission team will likely have opportunities to exercise other procedures (e.g., when the spacecraft is following previously mapped ground tracks), data pipelines, and instruments, if implemented. Those opportunities would likely benefit the I-MIM Project in preparing for subsequent detailed characterization (Phase 2), which would use the full suite of SAR approaches and those of any additional instruments at high resolution. The benefit of practice during Phase 1 means that, when Phase 2 begins in earnest, the team would be ready to take on this shift in emphasis.

Using a catalog of pre-selected targets as “practice” during Phase 1 would actually contribute to achieving I-MIM objectives in that further characterizing sites pre-selected on the basis of RO-3 criteria and science potential would contribute to research goals and mission success. Such a catalog would also benefit the mission in that it would permit early, preliminary analyses that might inform the need for continued investigation of a particular site and/or assign priorities in Phase 2 targeting decisions. During Phase 2 operations, a now refined catalog of TAI for human Mars mission planning and for scientific investigations would be available for I-MIM targeting.

Observation planning will be necessary and an operations team will be needed to optimize the scientific return. The degree to which this work can be done in advance (prior to the start of the prime mission) should be the subject of further study.

6.2 CONOPS CONCEPT 1 (CC1)

PRIMARY ANCHOR PAYLOAD ONLY

6.2.1 CC1: Broad Survey Phase 1

The highest priority for Phase 1 is to acquire the data necessary to define a set of TAI that will be targeted in Phase 2. Within Phase 1, allocating 80% of the returned data to the 30-meter resolution SAR mode should ensure that all useful passes over the RZ can be downlinked with sufficient margin (see Section 6.1.6). Phase 1 RZ mapping should last 10 months or until 95% coverage of the RZ with this data set has been acquired, whichever comes first.

This plan includes sufficient margin to deal with unexpected delays and optimization of observing strategies. Some of the data returned to Earth in this mode should be unprocessed, for short-term and long-term calibration purposes. With the set point of 80% of the returned data allocated to the 30-meter SAR observations, and a flexible duration with a singular goal, the number of degrees of freedom for modeling data acquisition is reduced, making modeling more tractable in a Phase A study. By fixing the transition at 95% spatial coverage of the RZ with 30-meter SAR data, it is possible to model the total data returned in that mode and model the various possible durations that may be affected by downlink rate. The total data volume dedicated to RZ coverage has only one variable, based on the degree of overlapping permitted for the observations. If this value is decided in a Phase A study, then it is possible to estimate the data allocation for the 30-meter SAR mode and use that to budget for the other modes and payloads, while acknowledging uncertainties arising from ground station allocation, instrument and spacecraft anomalies, etc.

Requirements-driving Reconnaissance Objectives

In support of RO-1 and RO-2, Phase 1 (the Broad Survey Phase) should focus primarily on collecting 30-meter-per-pixel SAR data throughout the identified Reconnaissance Zone (RZ). Data volumes, including onboard storage and data transmission back to Earth, should be heavily weighted towards these 30-meter data, to the level of 80% of the available bandwidth: 75% for data processed onboard and 5% for SLC data that has not been processed. The latter will support the validation of the onboard processing. As noted above, Phase 1 has been allocated 10 months including margins, or until ≥95% of the RZ is covered at least once with 30-meter SAR data. If this 95% threshold is reached before 10 months, then Phase 2 can begin immediately. However, the MDT recognizes that the transition may require operational planning such that it cannot be arbitrarily initiated at any time. Acknowledging that the final ~5% of a RZ survey would require waiting for favorable ground tracks and antenna pointings, the MDT finds that the value of transitioning from Phase 1 to Phase 2 before 100% coverage of the RZ is evident.

Science Targets of Opportunity

During Phase 1, seasons on Mars will advance. Season-specific observations (i.e., those that can only be acquired once during a single Mars Year primary mission) should be given priority when possible in this phase. For example, the mission team should trade-off acquiring high- resolution InSAR measurements of the growth or retreat of a seasonal cap against other high-resolution SAR observations of TAI when there is no impact on requirements-driving reconnaissance.

Onboard Storage for Later Downlink

Given the option for sufficient onboard storage, it may be possible to collect important data during a period with low downlink and then send it back after 1) Phase 1 is complete, and/or 2) downlink is more favorable. In these circumstances, the orbiter can make important seasonal observations without competing for downlink.

Initial Exercise of Specific Modes

In order to provide in-flight data sets for validation of data acquisition and on-ground data processing for high-resolution and sounding modes, a small number of data sets should be acquired based on pre-selected sites.

6.2.2 CC1: Detailed Characterization Phase 2

Phase 2 is the detailed phase of the mission, in which the higher resolution radar modes and intensive radar sounding share the available bandwidth. The duration of Phase 2 is the remaining portion of the PM, or one Mars Year minus the duration of Phase 1 (nominally 12 months, but longer if the transition from Phase 1 can be accomplished earlier). At the conclusion of Phase 1, Phase 2 should provide detailed characterization of TAI to make RO-3 required measurements and enable additional science investigations per SSO-1 (in brief, near-global coverage) and SSO-2 (high-value science observations of opportunity).

The Task 3 Group prioritizes four groups of activities for acquisition and downlink priority (although not necessarily data volume).

Priority 1
Finalize RZ Survey

Acknowledging that the final ~5% of a RZ survey would require waiting for favorable ground tracks and antenna pointing that would deviate from the primary mission, transitioning from Phase 1 to Phase 2 before 100% coverage of the RZ is achieved is sensible. Thus, the first priority of Phase 2 should be to complete the 100% coverage of the RZ. It is expected that <10% of the data volume needs to be allocated for these 30 m SAR observations. Of that 10%, some part should again be dedicated to downlinking SLC data in order to maintain calibration and validation ability.

Priority 2
Characterize Pre-arrival-selected TAI

To fulfill RO-3, the second priority for Phase 2 is to complete any remaining need for high-resolution mapping (SAR and imagery) and radar sounding of the previously identified TAI.

Priority 3
Characterize Newly Identified TAI

To fulfill RO-3, the third priority for Phase 2 is to begin collecting data over the TAI selected based on Phase 1 results.

Priority 4
High-value Science Observations of Opportunity

To enable the supplemental science (MDT Task 2), the final priority for Phase 2 is to collect science targets of opportunity, such as observations of seasonal processes, geology outside of the RZ, habitability targets, and polar terrains. These observations should be guided by the priority topics defined by the MDT in Task 2, as further detailed by the mission reconnaissance/science team should the mission proceed to Phase A. These data need not be returned immediately, and onboard storage can be used to buffer low downlink rates if necessary. The total data return allocation for observations other than the 30 m SAR mode is ~90%. A notional breakdown of the 90% for the detailed phase could be as follows: 60% for high-resolution SAR mapping (explicitly including repeat passes for InSAR and tomography) and 30% would be allocated to sounder mapping.

The MDT did not discuss the value of a global (or larger area than the RZ) low-resolution mapping by the SAR. The relative priority has thus not been set, but could be re-discussed when finalizing the operations plan.

The different phases and the different assumption on payloads imply certain coverage estimates for each payload/mode. Table 6.6 can be used to determine the number of TAI that can be studied, the effective area to be covered by the imager, and the effective ground-track length to be covered by the sounders.

Table 6.6 Concept 1 Summary

CONCEPT 1	PHASE 1	RZ BROAD SURVEY PHASE	
INSTRUMENT - SAR			
MODE	**DATA ALLOCATION**	**ESTIMATED AREAL COVERAGE**	**# TAI COVERED (HIGH RES ONLY)**
SAR (mod res) Raw[4]	5%	2.11 10^6 km^2	–
SAR (low res) Processed	75%	166.2 10^6 km^2	–
Over-subscription to Allow for Overheads etc.[5]	–	7.9	–
SAR (high res)	5%	0.29 10^6 km^2	37
InSAR	8%	0.16 10^6 km^2	20
Tomography[6]	2%	0.0079 10^6 km^2	1
Sounder[7]	5%	0.41 10^6 km^2	–
Equivalent Circumferences of Mars[8]	–	19.2	–
Calibration[9]	0%	–	–
TOTAL	**100% (~19.7 TB)**	–	–

[4] The engineering team expects around a few scenes (~5) at 1000 km per scene every month to be dedicated to calibration. However, the science may require more observations for scientific validation of the compressed data. The areal coverage given here assumes around 1.5% areal coverage of uncompressed data for scientific validation.
[5] The over-subscription factor here indicates that, from a data volume perspective, the data allocation to the RZ mapping can be reduced. The time to map is dominated by the time taken to get the observations and not by the data volume needed.
[6] The area given here does not imply that the targets chosen for detailed tomography observation will be completed by the end of Phase 1. Some areas may not have been completed. The value given here is an equivalent area if the observation had been completed.
[7] The path length for which sounder data is obtained is converted into a unit of circumferences of Mars to give a more physically intuitive impression of the total coverage.
[8] The path length for which sounder data is obtained is converted into a unit of circumferences of Mars to give a more physically intuitive impression of the total coverage
[9] While calibration data are essential, they are assumed to consume negligible data volume for this estimate.

CONCEPT 1	PHASE 2	TAI DETAILED CHARACTERIZATION PHASE

INSTRUMENT - SAR

MODE	DTA ALLOCATION	ESTIMATED AREAL COVERAGE	# TAI COVERED (HIGH RES ONLY)
SAR (low res) Raw	2%	1.01 10^6 km^2	–
SAR (low res) Processed	8%	212.7 10^6 km^2	–
SAR (high res)	10%	0.71 10^6 km^2	90
InSAR	26%	0.61 10^6 km^2	78
Tomography[10]	24%	0.113 10^6 km^2	14
Sounder	30%	2.95 10^6 km^2	–
Equivalent Circumferences of Mars	–	138.6	–
Calibration	0%	–	–
TOTAL[11]	100% (~23.6TB)	-	-

[10] The allocation to tomographic observations might be a little high; some further study should focus on the exact coverage necessary.

[11] 2.25 Mbps average assumed with 8h/day downlink to give 64.8 Gbit/day. 1 TAI of 100 km in radius = 0.0314 106 km^2. The InSAR value in Phase 1 (Concept 1) implies ~5 TAI. The InSAR value in Phase 2 implies ~18-19 TAI without overhead while 3 TAI can be covered with full tomography in Phase 2. For the sounders, a distance has been given and converted to the number of circumferences of Mars the value implies to allow a simple 1st order estimate of the grid spacing implied by the allocated data volume. No overheads assumed.

6.3 CONOPS CONCEPT 2 (CC2)

Primary Anchor Payload + Complementary Payload(s)

Concept 2 assumes the additional payloads of a VHF Sounder and a High-Resolution Stereo Imager; both are covered in more detail in Sections 6.4 and 6.5, respectively. The top priority of Phase 1 remains the acquisition of the data from the RZ that is necessary to define a set of TAI that would be targeted in Phase 2. The main difference between CC1 and CC2 is that data allocations are needed to support the complementary payloads, while maintaining the high priority mapping of the RZ and the detailed studies of TAI.

6.3.1 CC2: Broad Survey Phase

Phase 1 (the Broad Survey Phase) in CC2 maintains the RZ 30 m SAR mapping in full, but takes ~1/3 of the remaining data volume from the high-resolution pre-selected TAI and uses it for the VHF sounder and high-resolution stereo imager in order to begin their science missions. The two payloads would use this allocation to support the observation of the TAI and acquire seasonal targets that are not available during the rest of the prime mission.

Similar to Concept 1, to make RO-1 and RO-2 measurements, 30 m-resolution SAR coverage of the RZ is the highest priority. Data volumes, including onboard storage and data transmission back to Earth, should be heavily weighted towards these 30 m data to the level of 80% of the available bandwidth: 75% for data processed onboard and 5% for SLC data that has not been processed.

Of the remaining 20% data allocation, the suggested splitting of data allocations is 10% to high-resolution SAR, 5% to the imager, and 5% to the sounders. Based on average data rates, this plan would imply ~100 imaged sites of 6 km × 50 km (a typical HiRISE footprint) within Phase 1. This coverage is considered an absolute minimum to address seasonal opportunities (see below) and again justifies the potential need for significant onboard storage.

6.3.2 CC2: Detailed Characterization Phase 2

Phase 2 is the detailed phase of the mission, in which the higher resolution radar modes, intensive radar sounding, and imagery should share the available bandwidth, along with any additional payloads. The duration of Phase 2 will be maintained so that main difference to CC1 is additional data allocated to the complementary payloads at the expense of high resolution SAR data over TAI.

Priority 1
Finalize RZ Survey

Phase 2 should be a detailed investigation phase and begin after the conclusion of Phase 1. Thus, the first priority of Phase 2 should be to complete the 100% coverage of the RZ and follows the approach for CC1.

Priority 2
Characterize TAI

The second priority for Phase 2 is to complete any remaining need for high-resolution mapping (SAR and imagery) and radar sounding of the TAI, assuming that the number and size of the pre-selected TAI do not significantly impact the acquisition of the TAI determined in Phase 1 RZ mapping.

Priority 3
Characterize New TAI

The third priority for Phase 2 is to begin collecting data over the identified TAI based on the Phase 1 results.

Priority 4
High-value Science Observations of Opportunity

The final priority for Phase 2 is to collect science targets of opportunity. These data need not be returned immediately, and onboard storage can hold them until downlink rates are favorable. The total data return allocation for observations other than the 30 m SAR mode is ~90%.

The breakdown of the 90% for the detailed phase should be as follows: 30% for high-resolution SAR mapping (explicitly including repeat passes for InSAR and tomography); 30% for sounder mapping. (either with L-band exclusively or L-band and VHF); and, 30% for high-resolution imagery.

The different phases and the different assumption on payloads imply certain coverage estimates for each payload/mode. Table 6.5 can be used to determine the number of TAI that can be studied, the effective area to be covered by the imager, and the effective ground-track length to be covered by the sounder. Table 6.7 provides a summary of ConOps Concept 2.

Table 6.7 Concept 2 Summary

CONCEPT 2	PHASE 1	RZ BROAD SURVEY PHASE	
INSTRUMENT - SAR			
MODE	DATA ALLOCATION	ESTIMATED AREAL COVERAGE	# TAI COVERED (HIGH RES ONLY)
SAR (low res) Raw	5%	2.11 10^6 km^2	–
SAR (low res) Processed	75%	166.2 10^6 km^2	–
Over-subscription to Allow for Overheads	–	7.9	–
SAR (high res)	5%	0.29 10^6 km^2	37
InSAR	4%	0.079 10^6 km^2	10
Tomography	1%	0.0039 10^6 km^2	0.5
Sounder	3%	0.25 10^6 km^2	–
SAR (low res) Processed	–	11.5	–
Calibration	0%	–	–
INSTRUMENT - VHF SOUNDER	2%	0.051 10^6 km^2	–
Equivalent Circumferences of Mars	–	2.4	–
INSTRUMENT - STEREO HIGH-RESOLUTION IMAGER	5%	0.049 106 km^2	–
TOTAL	**100%**	–	–

CONCEPT 2 PHASE 2 TAI DETAILED CHARACTERIZATION PHASE

INSTRUMENT - SAR

MODE	DATA ALLOCATION	ESTIMATED AREAL COVERAGE	# TAI COVERED (HIGH RES ONLY)
SAR (low res) Raw	2%	1.00 10^6 km^2	–
SAR (low res) Processed	8%	212.7 10^6 km^2	–
SAR (high res)	4%	0.28 10^6 km^2	36
InSAR	13%	0.31 10^6 km^2	39
Tomography	13%	0.061 10^6 km^2	7
Sounder	15%	1.48 10^6 km^2	–
Equivalent Circumferences of Mars	–	69.3	–
Calibration	0%	–	–
INSTRUMENT - VHF SOUNDER	15%	0.46 10^6 km^2	–
Equivalent Circumferences of Mars	–	21.4	–
INSTRUMENT - STEREO HIGH-RESOLUTION IMAGER	30%	0.35 10^6 km^2	–
TOTAL	100%	–	–

6.4 CONOPS FOR VHF SOUNDER

In the event the Agency partners are able to include this MDT-identified, high-priority potential augmentation, the following provides a concept of operations for the addition of a VHF Sounder to the primary anchor payload.

6.4.1 VHF Sounder Background

A subsurface radar sounder is a nadir-operating instrument, meaning that it produces science data from the nadir direction regardless of the direction in which the radar signal is transmitted and received. Of course, the maximum gain is obtained when the radar antenna is pointed straight to nadir for the duration of the data acquisition. The following discussion assumes, therefore, that the VHF Sounder's directional antenna would always be nadir-looking in a standard orbit and its mounting point on the spacecraft would be based on the most convenient operational scenario for sounder operations. Per that assumption, an operational interaction between the main SAR modes and the VHF Sounder would exist, even if the two instruments are not operated at the same time.

The radar transmit a linear frequency modulated pulse, or “chirp” (a signal resulting from sweeping the carrier frequency range in a very short time) and receive its echo immediately (Rank 0 operations) or after transmitting a second pulse (Rank 1 operations). The preference would be Rank 1 operations, because it improves the along track resolution of the data by a factor of two. At the operating frequencies of the VHF Sounder, higher rank operations are not envisaged.

6.4.2 Operational Characteristics

For the purposes of this MDT ConOps model (deriving the data volume and other operational characteristics), the VHF Sounder would conceptually have a single main operational mode with:

- a baseline Rank parameter;
- a baseline Pulse Repetition Frequency (PRF) value;
- an engineering Receive Window (RxWin) duration value;
- an engineering echo Sampling Rate (SRate) value;
- a baseline sample Resolution (Res) value; and,
- a variable echoes Pre-summing (Pre) value.

Baseline values are considered the nominal ones for this MDT ConOps model, but in the real instrument, each of them would be selectable to cater to different operating conditions (e.g., substantial changes in the orbit shape). Engineering values are fixed during the design phase of the instrument (in principle, it could be possible to adjust them as well in a small range).

During nominal operations, the instrument would be kept indefinitely in a low power, stand-by mode. For each acquisition (corresponding to a ground track segment that crosses a target area of interest), the instrument would transition to an operational mode in which radar pulses (“chirps”) are transmitted, receive echoes, and are processed in a very limited way. At the end of the acquisition, the duration of which is proportional to the length of the ground track segment of interest, the instrument would transition back to the stand-by mode.

The current concept does not foresee an internal buffer memory for acquisition. Therefore, sampled echoes would be streamed to the spacecraft data storage in real-time. However, echo pre-summing processing would be performed by the sounder. In order to acquire the echoes from the subsurface, the receive window would be opened (start of sampling

time) just before the arrival to the receiver of the first surface return, and kept open for the duration needed to capture the returns at the maximum useful depth. Since the receive window would be a fixed parameter, its "positioning" in time after the associated transmitted pulse requires knowledge of the distance between the spacecraft and the surface. This distance is variable due to the shape of the orbit (known to a high degree of accuracy) and surface topography.

Figure 6.6 Concept of Operations for the VHF Sounder

ACQUISITION DURATION

The minimum observation time is driven by the needs of the algorithms that will process the data on the ground. For the purposes of this MDT ConOps model, this minimum duration can be set at 20 seconds (s). Considering at least 5 s of lead time before the start of an observation, and another 5 s of trailing time to compensate for minor inaccuracies on orbital position knowledge (an error that typically manifests along track with a delay in the overflight of a latitude of interest), the total minimum observation time can be set to 30 s. For the proposed orbit this corresponds to ~95 km along track. The maximum duration depends exclusively on data allocations (in onboard storage and downlink).

For the purpose of this MDT ConOps model, the single, longest, data acquisition pass relates to the shape of the Reconnaissance Zone sections. Each active orbit will cross the RZ 4 times for a maximum total acquisition time of 20 minutes (m).

Considering the shape and the constraints related to the Reconnaissance Zone, as defined for the purposes of I-MIM's MDT, the distribution of total acquisition durations per orbit ranges from 7 minutes to 20 minutes (the period of an MRO-like orbit is 112 minutes).

Near-global coverage for supplemental scientific studies is of interest for many investigations. Observations of polar zones may have acquisition durations of less than 15 minutes per polar region. Those observations are not a factor in the above, which only considers the potential VHF Sounder in the context of improving measurements to meet reconnaissance objectives.

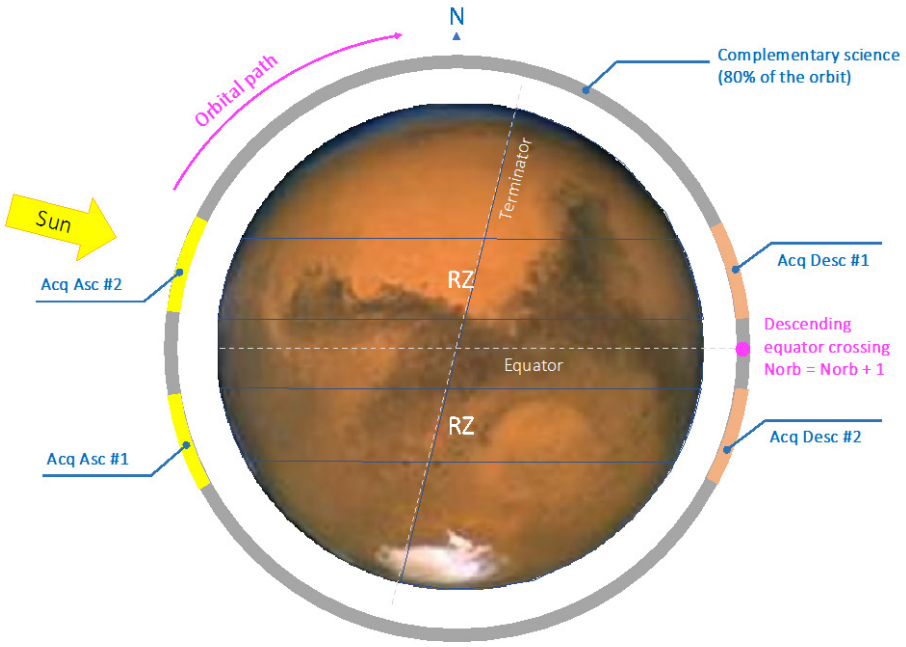

Figure 6.7 Schematic Showing Acquisition Opportunities over the Reconnaissance Zone

6.4.3 Data Volume Estimates

The following estimates assume an MRO-like orbit, which is close to the orbit proposed above. A more realistic approach must include some overhead associated with the data. A detailed calculation has been made and shows that the overall overhead can be estimated to be < 1.5% of the total data volume of sounder science data. This overhead is not included in the estimates.

DATA VOLUME FIGURES

The following numerical model (developed from an ASI-provided reference model for the MDT-proposed VHF Sounder) provides ideal PRF (pulse repetition frequency) values for varying orbital altitudes.

In the end, a fixed value could be chosen for the entire mission. The PRF value directly affects the data rates.

For the purpose of this MDT ConOps model, two values are suitable for an MRO-like orbit (Figure 6.8).

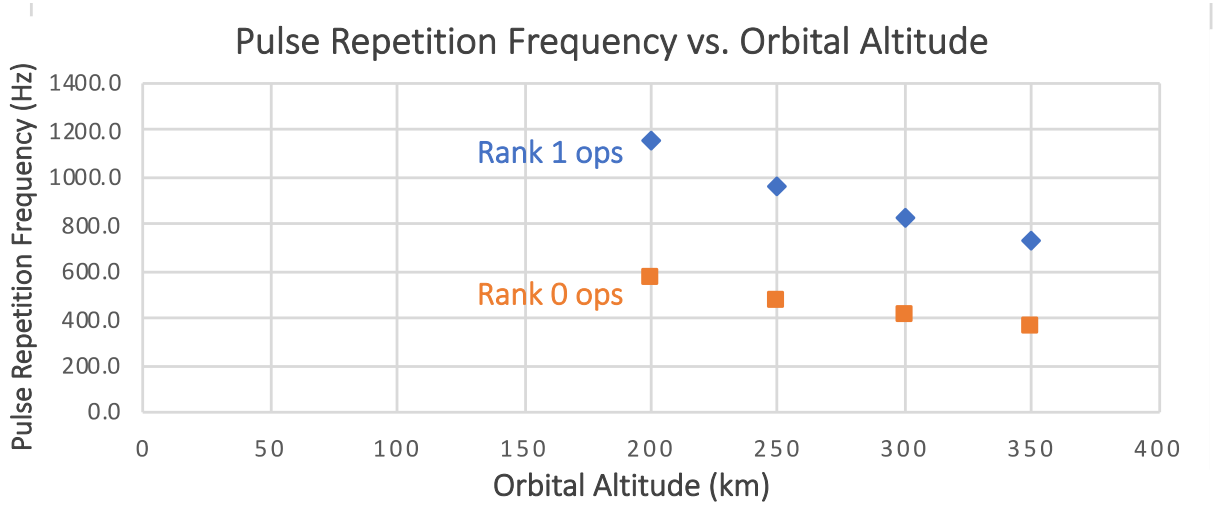

Figure 6.8 Two PRF Values Suitable for an MRO-like orbit

DATA VOLUME FIGURES

The conservative value chosen for this MDT ConOps model is 965 Hz, which provides a likely maximum value because an orbit lower than 250 km in altitude is not considered probable. For both the selected and alternate (PRF) values, the amount of data produced by the radar in megabits per second (Mbps) is shown in Table 6.9. These values have been obtained for the following operating conditions:

- Receive Window = 115 μs
- Sampling Rate = 1/35 MHz
- Sample Resolution = 8 bits

Table 6.9 Data rates in Mbps for two PRF values and four pre-summing settings

	PreSUM = 1	PreSUM = 2	PreSUM = 4	PreSUM = 8
PRF = 965 Hz	93.26	46.63	23.31	11.66
PRF = 832 Hz	*80.33*	*40.17*	*20.08*	*10.04*

DATA VOLUME FOR OPERATIONAL SCENARIOS

Two main operational scenarios regarding I-MIM's mission provide mission-level, data-volume estimates:

- Scenario 1
  Coverage of the Reconnaissance Zone (two bands of latitude, one for each hemisphere)
- Scenario 2
  Detailed coverage and study of target areas of interest within the Reconnaissance Zone

The VHF Sounder would mainly be used in:

Scenario 1:

To complement the main L-band radar instrument when sounding profiles are needed for those areas in which the L-band sounder mode does not penetrate deeply enough in the subsurface to assess fully ice deposits or site stratigraphy.

SCENARIO 1

The maximum acquisition duration over both RZ bands (two acquisitions on the northern RZ band, and two acquisitions on the southern RZ band) is 20 minutes. Assuming that the TAI for a single VHF Sounder pass is limited to only one acquisition over a given RZ latitude band, paralleling a previous observation of the L-band Sounder Mode, this acquisition would be ~4 minutes in duration.

Table 6.10 shows the total Data Volume (DV) for such acquisitions. The total DV for them is estimated assuming that 50% of Sounder Mode acquisitions will need these complementary VHF Sounder acquisitions.

From SHARAD's experience, the ideal pre-summing values for this scenario are assumed to be 4 and 8 for resultant data volumes shown in Table 6.10:

Table 6.10 Data Volumes for Scenario 1

	PreSUM = 4	PreSUM = 8
Total DV per Acquisition (4 min)	5.595 Gbit	2.797 Gbit

The assumed data production rate here is 23 Mbps.

Scenario 2:

To perform a full mapping of a target area of interest in order to provide a detailed stratigraphic model, three-dimensional volumes of the subsurface, and additional dielectric properties of the regolith.

SCENARIO 2

Full mapping with the VHF Sounder of a TAI takes into account the size of the Fresnel zone, which, for the scope of this ConOps model, is assumed for an operating frequency of 100 MHz. Therefore, it is about 1.3 km wide. The ideal full coverage of the TAI would be obtained with 75 acquisitions. That definitely requires a drifting orbit to be able to cover a (relatively) small target area of interest in many weeks of operations (in a 14-day period, no more than two ground tracks are expected to cross the same TAI).

The duration of the overflight of a TAI is about 53 s. Adding 10 s at each end to take into account some overfly timing uncertainties would give a conservative value of about 75 s for each pass over a TAI. Assuming 75 passes, a very conservative total acquisition time is 75 * 75 = 5625 s, dispersed over many months of operations. The total, very conservative, DV produced for each TAI, assuming operations at pre-summing 1 and 2 is:

Table 6.11 Data Volumes for Scenario 2

	PreSUM = 1	PreSUM = 2
Total DV per Single Pass over TAI (75 s)	6.994 Gbit	3.497 Gbit
Total DV per Full TAI coverage (5625 s)	524.6 Gbit	262.3 Gbit

These real worst-case values do not take into account that the geometry of the TAI may require fewer acquisitions or even shorter durations. The minimum spacing to consider the TAI fully covered (controlled by the Fresnel zone size) can also be relaxed somewhat.

This model also assumes parallel observations; in reality, intersecting observations (some acquired during the ascending portion of the orbit, some during the descending) would be more convenient (particularly for producing 3D volumes) and would produce sufficient coverage as well.

ADDITIONAL FACTORS AFFECTING THE DATA VOLUME

The VHF Sounder DV figures contain implicit margins because of the different worst-case conditions selected. Most likely, it would be possible to make improvements (that is, reduce the DV figures) by adjusting the following parameters:

- PRF Good variability exists between the two theoretical extremes; PRF is also conditioned by the orbit shape and other radar factors.
- Pre-summing Value As shown in the different tables.
- Sample Resolution could be reduced to 6 or even 4 bits. MRO/SHARAD is also equipped with this feature, but it has never been used on a routine basis.
- On-board Processing to Reduce the Data Volume Different techniques for this strategy exist (with some heritage from MEX/MARSIS), and new ones can be devised. Usually, they reduce the processing options on ground, but the operational concept of the mission might allow repeated passes without on-board processing when more accuracy or flexibility are needed.

Certain combinations of these parameters might produce substantial benefits in terms of data-volume reduction.

6.5 CONOPS FOR HIGH-RESOLUTION IMAGER

In the event the Agency partners are able to include this MDT-identified, high-priority potential augmentation, the following provides a concept of operations for the addition of a high-resolution stereo imager to the anchor radar payload.

6.5.1 Background

High-resolution imaging has led to rapid advances in our understanding of where subsurface ice is located and its nature. Ice-exposing impacts (at latitudes as low as 35°N) map out the distribution of clean (visibly bright) subsurface ice within decimeters of the surface. Ice-exposing scarps in the mid latitudes illustrate cross-sections of icy deposits that are decameters thick, shallowly buried, relatively pure, and layered. Measurements of polygonal fracturing have been used to constrain the presence and depth of subsurface ice. Thermokarst landforms such as scallops and expanded craters are characterized by high-resolution stereo DTMs and illuminate a history of ice loss. They also demonstrate that subsurface ice that exceeds available pore space remains in terrain adjacent to these features. High-resolution stereo topography has also been used with radar data to constrain dielectric constants in Arcadia and Utopia Planitiae, and argue for the presence of decameters-thick extensive ice sheets in those locations.

Safety assessments for human-class landing require image resolutions of a few decimeters. Sub-meter-scale boulders pose a threat to landing spacecraft. Quantifying the abundance of these hazards requires at least HiRISE-scale resolution. Such images also produce meter-scale DTMs that characterize slope distributions used to assess safety.

The MDT notes that high-resolution imaging also supports human-led science, ISRU, and civil engineering. High-resolution imaging to continue these investigations and characterize I-MIM TAI is recommended by the MDT as a complementary payload.

6.5.2 Operational Characteristics

To characterize how such an instrument would be integrated into the I-MIM mission, it is necessary to make some assumptions about its capabilities. Assumptions are:

- I-MIM will be in an MRO-like orbit: low eccentricity, low altitude, and sun-synchronous. This closely agrees with the MDT's expected orbit for the mission (see above).
- The local mean solar time (LMST) of the equator-crossing should be around 15:00 LMST following the HiRISE experience. The core payload has fairly loose constraints on this, while the spacecraft power profile would be best in a terminator orbit. The MRO-type orbit is an excellent compromise.

HiRISE-class resolution is required to extend past investigations in meaningful ways, to address issues of landing-site safety (1 µrad IFOV; 25–30 cm/pixel from an MRO-like orbit), and to characterize TAI for human-led surface science, ISRU, and civil engineering;

- Multiple colors (4) are required to distinguish icy material from bright non-icy material following the experience with the CaSSIS imager on TGO; and,
- Stereo will be achieved with independent observations on separate orbits. This compromise limits the volume and mass of the imager.

Advances in technology overcome several obstacles related to acquiring these data. HiRISE images are rarely longer than 25 km; however, modern CMOS TDI detectors can be run at full resolution for several minutes at a time, yielding single images long enough to traverse a TAI. Color coverage can extend across the entire image strip (only the central 20% was covered on HiRISE), which obviates the need for multiple overlapping images to generate color coverage. The field of view can be modestly increased from 5 to 6.1 km, which reduces the number of separate observations to cover a given area. An MRO-like orbit with the repeat cycle proposed herein would provide 25.6 cm/px for a 1 µrad/px design. Data are acquired at 12 bits/pixel (with improved radiometry and SNR over HiRISE), and down-sampled to 8-bit through on-board look-up tables. The limited downlink available to I-MIM requires compression to be implemented. The Task 2 Habitability Group assesses that 10:1 wavelet compression yields acceptable impacts to image quality, but a study should confirm negligible impact to the quality of stereo solutions.

Sufficient time exists in the I-MIM mission to acquire the required quantity of high-resolution image data. A TAI will typically be at a latitude of about 40 and notionally might be about 100 km in diameter. With an MRO-like orbit, at least one opportunity will be available per week to image a TAI. Spacecraft rolls allow for considerable fine-tuning of image locations, so coverage gaps can be readily filled. Even in the end-member situation where 100% coverage of the TAI were desired, it would only take 17 parallel images (or 34 for stereo coverage) with an average image length of 76 km. Stereo color coverage in this end-member case can thus be completed in 34 weeks (comfortably within the I-MIM primary mission) as all TAI can be covered concurrently. In reality, only a

fraction of each TAI is likely to need high-resolution image coverage as noted above.

The Task 3 Group considered whether such a high-resolution imager would be compatible with the SAR concept, and whether a free-flying element for the imager alone would be preferable. The Task 3 Group noted that stability of the platform or the ability to determine the jitter of the platform is of critical importance as HiRISE has demonstrated. The present requirement would be of the order of 0.0083 deg/s. Note that the settling times are given above.

While a dedicated free flyer for a large imaging system has been demonstrated (e.g., ESA's recent CHEOPS), the Task 3 Group is not aware of a small independent spacecraft carrying such a high-resolution system. The MDT recommends a system study that focuses on accommodation and pointing requirements. If on the same platform, a trade-off could be made against the potential for interference by the SAR's radiated emissions.

6.5.3 Data Volume Estimates

Data volumes associated with high-resolution imaging are large. However, with careful prioritization of targets by the I-MIM reconnaissance/science team, it would consume a reasonable fraction of the mission's total downlink. Each square kilometer imaged in color and stereo (one 4-band observation and one 1-band observation) requires 0.96 Gb, which can be reduced to 64 Mb through conversion to 8 bits and compression. For the purposes of generating a model ConOps in this Task 3 study, a notional 100 km-diameter TAI has an area of 7854 km^2, corresponding to 500 Gb. With careful targeting, only a fraction (estimated to be 20%) of each TAI need be imaged (corresponding to 100 Gb) to validate that a TAI is worth keeping under consideration.

The mission anticipates that several dozen TAI might be identified, resulting in several Tb of imaging data. The Task 2 Habitability Group estimate 5 Tb in total. Data rates from I-MIM to Earth vary strongly in response to Earth-Mars distance, but average 64.8 Gb/day or 42.8 Tb over one Martian year (a typical length for a Mars orbiter's primary mission). Thus, for the imaging campaign described above, the high-resolution imager requires 12% of the mission's total downlink. This figure is within the allocated budget discussed in the next sub-section, and hence there is margin against this potential requirement. Downlink is the primary limitation on the area covered by high-resolution imaging – any increases to available downlink can easily be utilized by the instrument. That said, the MDT Task 3 Group recognizes that the Agency partners have not determined the area of a TAI, and may wish to establish different assumptions or a ConOps that could be further developed by the mission's planned reconnaissance/science team should I-MIM proceed to a mission-formulation phase.

A high-resolution imager could acquire its observations while minimizing impacts to the operations of the core payload. The core payload may operate in either SAR or sounder mode, with different spacecraft roll values; however, in either case, the imager would likely view different terrain, so coordinated observations between the two instruments may not have to be considered. Much of the data acquisition by the core payload may be conducted on the night side and in the winter hemisphere of the day side, precisely where poor illumination precludes the best quality imaging. Thus, disruption to core payload operation is likely to be minimal and restricted to dayside observations in the summer hemisphere. In those cases, small variations in SAR incidence angle can be tolerated, allowing the spacecraft to make small rolls and to target sites for imaging while the SAR is operating. Larger rolls to complete stereo pairs (especially in smooth areas where larger convergence angles are required) will necessitate the suspension of SAR observations for approximately 20 minutes (based on MRO roll performance). This would not be an issue if SAR coverage is already at 100% for the imager target.

DATA VOLUME FIGURES

It is apparent that the high-resolution SAR modes can consume much more data than can be downlinked with the DTE communications link. A trade-off between mission duration, increased ground station coverage, mission cost/complexity, and the scientific benefit of the acquired data (linking to the STM) was not possible within the time available to the MDT. The need for a solution such as using the large deployable reflector for downlink appears strong. A more detailed assessment of the data acquisition strategy to justify this need should be made.

A crude estimate of the coverage in each mode is given in the following table. Note that no overhead or loss is assumed. The footnotes to the tables attempt to clarify the assumptions made.

Table 6.12 Coverage Estimate for All Modes

MODE/INSTRUMENT	COVERAGE PER UNIT DATA VOLUME
SAR (low-res)	2143 km^2/Gbit
SAR (low-res, processed)	11250 km^2/Gbit
SAR (hi-res)[12]	200 km^2/Gbit
InSAR	100 km^2/Gbit
Tomography	20 km^2/Gbit
Sounder	420 km^2/Gbit (along-track)
Potential VHF sounder	20 km^2/Gbit (along-track; pre-summing 1)
Potential Imager	15.6 km^2/Gbit (4 color, 1 bps)

[12] Exact value slightly depends on profile of acquisition. 150 km^2/Gbits would be more on the conservative side, while 200 km^2/Gbit is a more optimistic scenario with relatively long high-resolution strips acquired.

6.6 CONOPS FOR ADDITIONAL POTENTIAL AUGMENTATIONS

Primary Anchor Payload + Complementary Payload(s) + Potential Supplemental Payloads

In the event the Agency partners are able to include additional augmentations per the intent of the two Mission Support Objectives (in brief, a mass-delivery capability for integrated payloads and/or piggybacks/rideshares and a communications relay capability to support the additional data volume), the following provides broad inputs on ConOps considerations. However, given these potential payloads are multiple and less defined, the Task 3 Group did not examine ConOps for them in any detail.

Phase 1

Depending on the full set of instruments, the proposed breakdown discussed in Section 6.2 will need to be re-opened. The MDT notes that in Phase 1, the data budget for any additional instrument should come from the 20% allocated to non-30-m SAR modes.

Phase 2

If additional payloads are added to the mission complement, the MDT notes that:

- the mission team must assign appropriate/ adequate data volume within the prime mission, thereby influencing the rate and total data return from the core and complementary payloads;
- the construction of a final payload by any selection team must evaluate the consequences (particularly on the total data volume returned) of a specific selection; and,
- instruments may have very different requirements in terms of data volume and evaluation of the respective needs would be necessary and traded against the needs of the primary and complementary payloads.

6.7 SUMMARY OF CONCEPT OF OPERATIONS

The nominal orbit profile of I-MIM (high inclination, ~255 km altitude, Sun-synchronous at 3 PM) seems compatible with currently known constraints and the main scientific objectives. The MDT did not assess the approach to this final orbit (e.g., aerobraking), but conducting calibration activities before reaching the final orbit in an aerobraking scenario would help optimize the data return in the prime mission.

The MDT recommends a two-phase approach to mission operations within the prime mission. The first phase (Phase 1) should focus on the mapping of the Reconnaissance Zone (RZ) with complementary data at high resolution to support a smooth transition to the second phase (Phase 2), which provides detailed observations of Targeted Areas of Interest (TAI).

Phase 1 of I-MIM's Primary Mission should focus on collecting 30 meter-per-pixel SAR data throughout the identified RZ, in support of Reconnaissance Objectives. Phase 1 RZ mapping should last 10 months or until 95% coverage of the RZ with this data set has been acquired, whichever comes first. In all variations of Phase 1 studied so far, the data allocation is more than sufficient to complete 30 m SAR mapping of the RZ within the duration of Phase 1, being more strongly related to the coverage required. Sufficient margin is also evident in the scenario studied.

In support of RO-3, an efficient approach for characterizing the TAI is a controlled repeat cycle that is a multiple of 7 days, allowing long-term prediction. A small number of TAI should be identified prior to arrival for early targeting to facilitate the Phases 1–2 transition and provide some early data on potentially interesting targets.

The prime mission is set to one Mars year. As a consequence, and in support of supplemental science investigations, season-specific observations (i.e., those that can only be acquired once during a single Mars Year primary mission) should be given priority when possible.

For example, the mission team should strongly consider acquiring high-resolution InSAR measurements of the growth or retreat of a seasonal cap in place of other high-resolution SAR observations of the TAI when the impact or risk to meeting mission requirements is low.

The MDT perceived total data volumes (over the Mars year) as constraining, particularly in Phase 2 when including the high-resolution SAR modes (i.e., InSAR, tomography, etc.), and potential complementary and supplementary payloads. Careful planning and optimization of the observing strategy is necessary. An appropriate operations plan should be put in place prior to Mars Orbit Insertion.

The construction of the observing strategy should consider the need for "human mission site characterization" and the operations concept and flight teams should have the appropriate expertise. In general, however, it appears highly likely that I-MIM's main goals can be addressed within the nominal 1 Mars year, although a more detailed linking between the science traceability matrix and the required data volume should be initiated in the next phase.

Impact revealing previously buried near-surface ground ice.

Credit: NASA/JPL-Caltech/UArizona

7 SUMMARY OF FINDINGS

The findings of the I-MIM Reconnaissance/Science Measurement Definition Team are listed below. Additional summary descriptions for each can be found in the Executive Summary and in the MDT-Task-related sections (i.e., Sections 4–6).

TASK 1: Requirements-driving Reconnaissance Objectives

FINDING 1

Most of the high-priority reconnaissance objectives can be met with the currently scoped radar instrument.

FINDING 2

The combination of SAR, sounder, and polarimetric capabilities is unique and powerful to accomplish the ice mapping needed to pave the way for the human exploration of Mars.

FINDING 3

The core payload would have a high likelihood of finding ice deposits that could be readily accessed in situ (within the top few meters and not covered with large rocks).

FINDING 4

Two high-value complementary instruments identified by the MDT could be optimized to aid in strengthening I-MIM's ability to achieve its reconnaissance objectives: a VHF sounder and a high-resolution imager with stereo capabilities.

TASK 2: Supplemental Science

FINDING 5

A broad suite of additional high-priority scientific investigations can be accomplished with the anchor radar payload, including multiple themes of interest to the international Mars science community: atmospheric science, geology, and habitability.

FINDING 6

The complementary instruments identified by the MDT for ice reconnaissance (VHF sounder and visible imager) would significantly enhance I-MIM's scientific impact.

FINDING 7

I-MIM could increase its scientific impact by making supplemental measurements with additional instruments and/or platforms, which could also be optimized to fill remaining high-priority gaps in meeting the reconnaissance objectives.

- Surface temperature measurements would provide high benefit to science and ice reconnaissance.
- Measurements of winds and atmospheric profiles of temperature, water vapor, and trace gases would advance the understanding of ice-related and other atmospheric processes.
- Surface compositional information would greatly enhance geological and habitability investigations.

TASK 3: Concept of Operations

FINDING 8

The MDT developed a feasible concept of operations for a nominal mission timeframe of one Mars year, split into two phases. The first phase (10 months) would be dedicated primarily to acquiring 30 m SAR coverage of the Reconnaissance Zone. In the second phase, the mission would perform targeted observations to obtain high-resolution SAR imaging and sounding of areas of interest, including new targets identified in the first phase.

FINDING 9

The mission as conceived is achievable within the provided constraints of consumables such as power and data volume, but I-MIM's reconnaissance and science investigations could be more easily and fully accomplished with increased capabilities for downlinking data to Earth, especially if additional instruments are provided.

In summary, the International Mars Ice Mapper (I-MIM) mission concept represents an opportunity to observe Mars in a new way and to acquire essential information needed for the first human visitors. The mission's capabilities would enable unique new science covering a broad range of international science priorities, in addition to the primary goal of reconnaissance for human missions.

The anchor radar payload is a highly capable investigative tool for addressing both the reconnaissance objectives for human exploration and broader science investigations of Mars. Both the reconnaissance and science objectives could be more comprehensively achieved with the addition of carefully selected additional instruments, as described in this report. A model concept of operations shows that the major mission objectives could be readily met in a single Mars year.

Based on these findings, the MDT concludes that the Agency partners should continue to pursue development of the I-MIM mission as a key element in the future exploration of Mars.

The MDT-defined reconnaissance and science investigations align with and advance the Agency partners' goals for the future human and robotic exploration of Mars.

Appendix A. ALIGNMENT WITH STRATEGIC AGENCY DOCUMENTS

RECONNAISSANCE OBJECTIVES

OBJECTIVE	PARAMETER	2023–2032 DECADAL SURVEY SCIENCE QUESTION SUBTOPICS* (UNITED STATES)	MEPAG SCIENCE GOALS 2020 (UNITED STATES)	ASI (ITALY)	CSA (CANADA)	JAXA (JAPAN)	NSO (NETHERLANDS)
RECONNAISSANCE GOAL	All Below.	Moon-to-Mars and Artemis Accords + individual strategic plans for the future human-robotic exploration of Mars					
RO-1 Location & Extent of Near-surface Ice	▪ Ice Presence ▪ Ice Concentration ▪ Lateral Extent & Continuity of Ice ▪ Non-ice Constituents in the Matrix	Precursor for ice sampling/ice coring (first listed human-facilitated investigation; Decadal, Survey, Table 19.1)	GOAL I A2, B2 GOAL II A2, B1, B2, C2 GOAL III A1, A3, A4 GOAL IV A3, B4, C2, D1	6.1, 6.2B-D, 7.1	PAT-01 PAT-04 PGGP-01 PGGP-02 PGGP-03 AB-04	GOAL 1.2A–C GOAL 2.1, 2.2	See Habitability. Robotic exploration and human spaceflight goals.
RO-2 Geotechnical Characteristics of the Overburden	▪ Overburden Properties ▪ Surface Characteristics	Precursor for human facilitated geology (second-listed human-facilitated investigation) and some network stations (third-listed human-facilitated science investigation)	GOAL I A2, B2 GOAL II A2 GOAL III A2, A3, A4 GOAL IV A3, B4, C2, D1	6.2B-D	PAT-01 PGGP-01 PGGP-03	GOAL 1.2A–C	Robotic exploration and human spaceflight goals.
RO-3 Characterization of Candidate Sites for Human Exploration	▪ RO-1 & RO-2 above + ▪ Post-landing Mars Science ▪ Post-landing Environmental Science for Human Mission Planning	Precursor for ice sampling/ice coring (first listed human-facilitated science investigation)	GOAL I A2 (RO-3A) GOAL IV A3 (RO-3B, D) GOAL IV B4 (RO-3C, D) GOAL IV C2 (RO-3C, D)	6.1, 6.2, 6.3, 7.1	PAT-01 PAT-03 PGGP-01 PGGP-02 PGGP-03	GOAL 1.2A-C GOAL 2.1, 2.2	Robotic exploration and human spaceflight goals.

*The RTM and STM parameters and the work of the MDT address the following decadal findings, among others, and could continue to be pursued should the mission continue to a formulation phase during which time the Agency partners intend to form a mission reconnaissance/science team
"With engagement of the scientific community in measurement definition, iMIM has the potential to be a pathfinding example of how Mars human exploration objectives can simultaneously advance high priority science questions related to Mars climate and how scientific expertise can help successfully realize human exploration objectives for ISRU."
"International participation in human programs has the benefit of (i) spreading the cost out over a larger number of participating entities and making it more affordable to each, (2) providing wider participation of scientists, engineers, and the public from different countries and cultures, and (3) enhancing international cooperation in peaceful endeavors."

ATMO 1 SURFACE-ATMOSPHERE INTERACTIONS

INVESTIGATION	PROPERTY TO CONSTRAIN	2023–2032 DECADAL SURVEY SCIENCE QUESTION SUBTOPICS (UNITED STATES)	MEPAG SCIENCE GOALS 2020 (UNITED STATES)	ASI (ITALY)	CSA (CANADA)	JAXA (JAPAN)	NSO (NETHERLANDS)
ATMO 1.1 Surface/Subsurface Volatile Inventory and Variability (See also GEO 2.1, 2.2, and Hab 1.2)	▪ Seasonal Water & CO_2 Ice Cap Thickness ▪ Near-surface Ice Abundance ▪ Presence of & Depth to Ice Table ▪ Fine Characterization of Polar Layered Deposits	5.3, 5.4, 5.5, 5.6 6.2, 6.3, 6.4	GOAL I A2 GOAL II A1, A2, B1, B2, C2 GOAL III A1, A4 GOAL IV A1, B4, C2	6.2A-E	PAT-01 PGGP-01 PGGP-02 PGGP-03	GOAL 1.2A-D GOAL 2.1	See Habitability.
ATMO 1.2 Recurring Slope Lineae (See also GEO 1.1, 1.2)	▪ Subsurface ▪ Water-ice Content Change in Topography Caused by RSL Debris Flow ▪ Surface Materials (wet or dry) ▪ Albedo Change ▪ Surface Temperature Change	5.3, 5.4, 5.5, 5.6 6.2, 6.4	GOAL I A2 GOAL II A2 GOAL III A1	6.2D, 6.2E	PAT-01 PGGP-01 PGGP-03	GOAL 1.2C	-
ATMO 1.3 Near-surface Atmospheric Conditions	▪ Water Vapor Abundance ▪ D/H Ratio ▪ Wind Speed ▪ Dust & Ice Aerosol Abundance ▪ Surface Temperature ▪ Surface Pressure	5.3, 5.4, 5.5, 5.6 6.2, 6.3, 6.4	GOAL II A1, A2 GOAL III A1 GOAL IV A1, A3, B3, B4	6.2E	PAT-01 PAT-03	GOAL 1.2C GOAL 1.2D	-

ATMO 2 ATMOSPHERIC & AERONOMIC STRUCTURE & PROCESSES

INVESTIGATION	PROPERTY TO CONSTRAIN	2023-2032 DECADAL SURVEY SCIENCE QUESTION SUBTOPICS (UNITED STATES)	MEPAG SCIENCE GOALS 2020 (UNITED STATES)	ASI (ITALY)	CSA (CANADA)	JAXA (JAPAN)	NSO (NETHERLANDS)
ATMO 2.1 Ionospheric Irregularities, Space Weather & Crustal Magnetic Field Effects on the Upper Atmosphere	▪ Total Electron Content ▪ Ionospheric Density ▪ Context: Airglow Brightness ▪ Aurora & Airglow Distribution ▪ Solar Energetic Particles & Precipitating Electrons (Context) ▪ Precipitating ▪ Suprathermal Electrons & Precipitating Electrons (Context) ▪ Ion Composition ▪ Ionospheric Wind ▪ Magnetic Field ▪ Space Weather Conditions	6.1, 6.2, 6.3, 6.4, 6.5, 6.6	GOAL II A4, C2 GOAL IV B1	6.2D, E	PSE-01 PSE-02	GOAL 1.2D	-
ATMO 2.2 Structure, Dynamics, Vertical Coupling, & Loss to Space	▪ Wind Fields ▪ Water Vapor ▪ Temperature & Pressure ▪ Ozone Abundance ▪ Atmospheric Waves ▪ Aerosol Abundance ▪ Water-related Ions ▪ Oxygen Ion Motion ▪ Elemental & ▪ Isotopic Abundance ▪ Water Vapor Column ▪ Abundance ▪ Temperature ▪ Surface ▪ Meteorological Conditions	6.1, 6.2, 6.3, 6.4, 6.5, 6.6	GOAL II A4, B3, C1 GOAL IV A1, B3	6.2D	PAT-01 PAT-02 PAT-03 PAT-04	GOAL 1.2D	-

GEO 1 GEOSPHERE PROCESSES THAT SHAPE THE PRESENT

INVESTIGATION	PROPERTY TO CONSTRAIN	2023–2032 DECADAL SURVEY SCIENCE QUESTION SUBTOPICS (UNITED STATES)	MEPAG SCIENCE GOALS 2020 (UNITED STATES)	ASI (ITALY)	CSA (CANADA)	JAXA (JAPAN)	NSO (NETHERLANDS)
GEO 1.1 Mobile Sediments, Mass Wasting, & Seasonal Changes (See also ATMO 1.2)	▪ Surface Changes ▪ Surface Geomorphology	5.4, 5.6	GOAL I A2 GOAL II A2 GOAL III A2, A4 GOAL IV A3, B2, B3, B4	6.2C, D	PGGP-01 PGGP-03 PAT-01	GOAL 1.2A, C, D	-
GEO 1.2 Flowing ice	▪ Surface Changes ▪ Surface Geomorphology	4.4, 5.4, 5.6	GOAL I A2 GOAL II A2 GOAL III A2 GOAL III A4	6.2C	PGGP-01 PGGP-02 PGGP-03 PAT-01	GOAL 1.2C	-
GEO 1.3 Present Cratering Rates	▪ Surface Geomorphology ▪ Surface Changes; Compositional or Thermal Differences	4.1-4.4	GOAL III A4	6.2C	PGGP-01 PGGP-05	GOAL 1.2A, D	-

GEO 2 GEOSPHERE PROCESSES THAT SHAPED THE RECENT PAST

INVESTIGATION	PROPERTY TO CONSTRAIN	2023–2032 DECADAL SURVEY SCIENCE QUESTION SUBTOPICS (UNITED STATES)	MEPAG SCIENCE GOALS 2020 (UNITED STATES)	ASI (ITALY)	CSA (CANADA)	JAXA (JAPAN)	NSO (NETHERLANDS)
GEO 2.1 Polar Deposits (PLDs and CO_2)	▪ Permittivity Contrasts ▪ Scattering Properties ▪ Surface Geomorphology ▪ Mineralogy/Thermal Inertia ▪ Temperature with Depth	5.4, 5.5, 6.2, 6.4	GOAL II A2, B1, C2 GOAL III A1, A2, A3	6.2C, D	PGGP-01 PGGP-03 PAT-01	GOAL 1.2A–C	-
GEO 2.2 Mid-latitude Ice	▪ Permittivity Contrasts ▪ Scattering Properties ▪ Surface Geomorphology ▪ Mineralogy/Thermal Inertia ▪ Temperature with Depth	5.4, 5.5, 6.2, 6.4	GOAL I A2 GOAL II A2, B2, C2 GOAL III A1-A4 GOAL IV A3, B4, C2, D1, D2	6.1, 6.2B-D, 7.1	PGGP-01 PGGP-02 PGGP-03 PAT-01	GOAL 1.2A–C GOAL 2.1, 2.2	See Habitability. Human spaceflight goals.
GEO 2.3 Recent Volcanism (Texture, Stratigraphy & Composition)	▪ Scattering Properties ▪ Permittivity Contrasts ▪ Surface Geomorphology ▪ Mineralogy/Thermal Inertia	5.2, 5.3	GOAL III A3, A4	6.2C, D	PGGP-01 PGGP-04	GOAL 1.2A, B	-

GEO 3 GEOSPHERE PROCESSES THAT SHAPED THE RECENT PAST

INVESTIGATION	PROPERTY TO CONSTRAIN	2023–2032 DECADAL SURVEY SCIENCE QUESTION SUBTOPICS (UNITED STATES)	MEPAG SCIENCE GOALS 2020 (UNITED STATES)	ASI (ITALY)	CSA (CANADA)	JAXA (JAPAN)	NSO (NETHERLANDS)
GEO 3.1 Crater Ejecta Emplacement & Degradation	▪ Scattering Properties ▪ Permittivity Contrasts ▪ Surface Geomorphology ▪ Mineralogy/Thermal Inertia	4.3, 4.4, 5.4	GOAL III A3, A4	6.2C	PGGP-01 PGGP-05	GOAL 1.2A, B	–
GEO 3.2 Sedimentation & Stratigraphy (including buried landforms)	▪ Permittivity Contrasts ▪ Scattering Properties	5.4	GOAL III A2, A4	6.2B-D	PGGP-01	GOAL 1.2A, B	–
GEO 3.3 Unique Radar Terrains (MFF, Stealth Regions, etc.)	▪ Permittivity Contrasts ▪ Scattering Properties	5.3, 5.4	GOAL III A2, A4	6.2C	PGGP-01 PGGP-03	GOAL 1.2A, B	–
GEO 3.4 Noachian Climate and Ice	▪ Scattering Properties ▪ Permittivity Contrasts ▪ Surface Geomorphology	5.4, 6.2, 10.3	GOAL I A2 GOAL II C2 GOAL III A3, A4	6.2B-E	PGGP-01 PGGP-03	GOAL 1.2A–C	–

HAB 1 ENABLE THE SEARCH FOR PAST & PRESENT HABITABLE ENVIRONMENTS

INVESTIGATION	PROPERTY TO CONSTRAIN	2023–2032 DECADAL SURVEY SCIENCE QUESTION SUBTOPICS (UNITED STATES)	MEPAG SCIENCE GOALS 2020 (UNITED STATES)	ASI (ITALY)	CSA (CANADA)	JAXA (JAPAN)	NSO (NETHERLANDS)
HAB 1.1 Presence of Liquid Brines	▪ Brine Depth and Distribution (top 10 m) ▪ Brine Depth and Distribution (top 100 m) ▪ Seasonal Variability of Brines	10.1, 10.2, 10.3, 10.6, 10.7	GOAL I A2, B2 GOAL II C2 GOAL III A1 GOAL IV D1	6.2B-D	PGGP-01 PGGP-03	GOAL 1.2B,C	Answers to questions such as "How did life on Earth come to be?" and "Are there other planets in the universe that could sustain life?"
HAB 1.2 Global Distribution & Nature of Ice	▪ Depth to Top of Ice Table (top 10 m) ▪ Radar Reflectivity as a Function of Depth (top 100 m) ▪ Distribution of Massive Ice Deposits & Near-surface Geomorphology ▪ Surface Geomorphology	10.1, 10.2, 10.3, 10.6, 10.7	GOAL I A2, B2 GOAL II C2 GOAL II A1, B2, C2 GOAL III A1, A3, A4	6.2B-D	PGGP-01 PGGP-02 PGGP-03	GOAL 1.2A-D	Same as for Hab 1.1.
HAB 1.3 Past Fluvial & Glaciofluvial Activity	▪ Subsurface Stratigraphy ▪ Near-surface Geomorphology ▪ Surface Geomorphology	10.1, 10.2, 10.3, 10.6, 10.7	GOAL I A2, B2 GOAL II B2, C2 GOAL III A1-4	6.2B–D	PGGP-01 PGGP-03	GOAL1.2A-C	Same as for Hab 1.1.
HAB 1.4 Subsurface Void Detection	▪ Subsurface Vertical Profile (top 10 m) ▪ Subsurface Vertical Profile (top 100 m) ▪ Rock Porosity, Density, & Ice Content (ambiguous) ▪ Rock Porosity, Density, & Ice Content (constrained)	10.1, 10.2, 10.7	GOAL III A4	6.2B-D	PGGP-01	GOAL 1.2A, B	Same as for Hab 1.1.
HAB 1.5 Geochemical Signatures of Habitability	▪ Surface Composition ▪ Subsurface Vertical Profile of Putative Mud Volcanoes	10.1, 10.2, 10.7	GOAL I B2	6.2A, B	AB-03	GOAL 1.3	Same as for Hab 1.1.

HAB 2 PROTECT MARTIAN & TERRESTRIAL LIFE

INVESTIGATION	PROPERTY TO CONSTRAIN	2023-2032 DECADAL SURVEY SCIENCE QUESTION SUBTOPICS (UNITED STATES)	MEPAG SCIENCE GOALS 2020 (UNITED STATES)	ASI (ITALY)	CSA (CANADA)	JAXA (JAPAN)	NSO (NETHERLANDS)
HAB 2.1 Planetary Protection	HAB 1.2A Ice Temperature HAB 1.2B Dust Loading & Movement	Addresses finding that "NASA has not yet developed a planetary protection plan and related research activities specifically tailored to understand and mitigate the risk of forward and back contamination from human missions to Mars on timescales consistent with the earliest plausible human missions."	GOAL IV D1, D2	6.2B, 7.1	PAT-04 AB-04	GOAL 1.2C, D GOAL 2.3 GOAL 3	-
HAB 2.2 Human Health Hazards	▪ Depth to Top of Ice Table (top 10 m) ▪ Radar Reflectivity as a Function of Depth (top 100 m) ▪ Distribution of Massive Ice Deposits & Near-surface Geomorphology ▪ Surface Geomorphology	10.1, 10.2, 10.3, 10.6, 10.7	GOAL IV B4, D1	6.2B-E, 6.3, 7.1	PGGP-03 PAT-04 SH-01, SH-03	GOAL 2.2	Technologies supporting human spaceflight.

The MDT had access to Agency priorities as a framing context, but developed the RTM and STM independently. With finalization of those, an initial analysis of alignments between the high-level community-defined parameters and multilateral Agency science and human-exploration priorities is depicted above, with references below. The identified matches may not depict all possible connections and may either fully or partially address the stated Mars strategic research aim. The Agencies and a future I-MIM reconnaissance/science team should analyze further if the mission proceeds to Phase A.

ASI | Strategic Vision Document for Space

ASI Goals for the Robotic Exploration of the Solar System:

6.1 To develop instrumentation for exploration - parallels language in 7.1, focused on human exploration of the Moon/Mars

- Consolidate and enhance Italian capabilities in future robotic solar-system-exploration missions by participating in Martian and lunar missions in preparation for future and sustained human exploration missions (including technologies for human health) - parallels language in 7.1, focused on human exploration of the Moon/Mars
  - Validate new technologies to prepare for the sustainable human exploration of the Moon and Mars (smart landers, autonomous navigation systems, subsurface drilling, image recognition, in situ resource utilization, cubesat free flyers for exploration and communication in deep space)
  - Develop intelligent robots that respond to external stimuli and are made of conformable, flexible materials

6.2 To sustain Italian leadership in solar system exploration

- Support the participation of the scientific and industrial community in solar-system-exploration missions, exoplanet research, and the use of related data and scientific returns, in collaboration with other international partners, primarily ESA and NASA

Major Research Areas (RA) as provided by ASI to the MDT (enumeration derived for the purpose of this report only):

1. Search for traces of past and present life on Mars
2. Interior Structure/Subsurface Investigation
3. Surface Mapping
   - Morphology
   - Geology/composition
   - Volcanism
   - Global Tectonics
4. Atmosphere
   - Dust Composition
   - Habitat/Environment
   - Exosphere
   - Magnetosphere
5. Sub-Surface Sampling & Characterization [Precursor]
6. Physics [Potential Radio Science]
   - General Relativity
   - Gravity field
   - Geophysics

6.3 To support development of enabling technologies

- Ensure the national technological capacity necessary for robotic exploration of the solar system, while promoting opportunities for industry

Canadian Space Agency | Planetary Science Priorities

Astrobiology

AB-03

Accessing the Subsurface for Astrobiology - below the harsh surface radiation environment of Mars, Europa and other astrobiology targets

AB-04

Accessing Special Regions - areas of Mars where temperature and availability of liquid water are believed most favourable for life

Planetary Atmospheres

PAT-01

Understand Mars Surface-Atmosphere Interactions -the present-day cycle of water on Mars

PAT-02

Understand the Chemistry of Planetary Atmospheres

PAT-03

Constrain the Dynamics of Planetary Atmospheres - winds and weather

PAT-04

Understand Atmospheric and Exospheric Aerosols - dust in climate and storms

Planetary Geology, Geophysics and Prospecting

PGGP-01

Document the geological record and processes that have shaped the surface of the terrestrial planets, their moons, icy satellites and asteroids

Top Priority Investigation: Development of radar and its deployment on missions to map planetary surfaces

PGGP-02

Determine the Resource Potential of the Moon Mars and Asteroids

PGGP-03

Understand the origin and distribution of volatiles on the terrestrial planets and their moons asteroids and comets

Understanding the emplacement and dynamics of subsurface ice on Mars

PGGP-04

Determine the interior structure and properties of the terrestrial planets and their moons, icy satellites and asteroids

PGGP-05

Understand the impact, threat and hazards posed by impact events on the Earth and other solar system bodies

Planetary Space Environment

PSE-01

Understand the role of magnetic fields, plasma and atmosphere-ionosphere dynamics on the history and evolution of planets and other solar-system bodies

PSE-02

Understand and characterize the plasma processes that shape the heliosphere and drive planetary and interplanetary space weather and related effects which create hazards to space exploration

Science and Space Health

SH-01

Better understand the risks to living organisms of radiation exposure beyond low-Earth orbit and develop effective countermeasures

SH-02

Better understand biological and physiological changes that occur in reduced gravity environments and to develop effective countermeasures

SH-03

Develop a more integrated understanding of the biological and physiological effects of the space environment and develop integrated countermeasures

JAXA | Japan Strategic Mars Exploration Plan (JSMEP)

Note: the following comes from information about JSMEP provided to the MDT. The content is drawn directly, but the enumeration is established for the purpose of the above Agency alignment table in this appendix.

JSMEP starts with a Martian moon's sample return mission (MMX: Martian Moons Explorer) in 2024–2029, followed by a Mars orbiter (MO) in later 2020s and a Mars lander/rover (ML/R) mission in early 2030s. JSMEP's goals are:

GOAL 1: Address questions of water on Mars:

GOAL 1.1: Origin and Delivery (MMX)

GOAL 1.2: Distribution and Inventory (I-MIM)

- Objective 1.2A Global Mapping & Landing Site Selection (including ground ice as a resource and site for science investigation)
- Objective 1.2B Radar Observation of the Subsurface World
- Objective 1.2C Circulation and Storage of Water and Volatiles
- Objective 1.2D Monitoring of Space and Surface Environment (space weather, weather, aqueous environment)

Addressed if augmentation

GOAL 1.3: Chemical Evolution (future rover)

GOAL 2: Ensure the expansion of the areas of human activities by exploring the habitable subsurface world

- Objective 2.1 Ground Ice as a Resource
- Objective 2.2 Human Landing Site Characterization
- Objective 2.3 Planetary Protection [precursor]

GOAL 3: Acquire key technologies including EDL (entry-descent-landing) with aerodynamic control, drilling and sampling on the surface, deep space telecommunication, **transportation to/from the Mars orbit, and planetary protection.**

Addressed if augmentation

NASA | 2023-2032 Decadal Survey

The MDT work was nearly complete when the preliminary Decadal Survey was released (May 2022). The following is an early attempt to match MDT results with decadal priorities that the mission can further study in the future.

4.1 How Have Planetary Bodies Collisionally and Dynamically Evolved throughout Solar System History?

I-MIM-related Strategic Decadal Research includes studies of impact structures that have been potentially erased by geologic processes to constrain early impact populations striking Mars. Subtopic questions are not directly relevant, as they largely focus on planetesimals and small bodies; studying the unrevealed subsurface could indirectly address the above topic.

4.2 How Did Impact Bombardment Vary with Time and Location in the Solar System?

I-MIM-related Strategic Decadal Research includes studies that help determine the absolute age of a Martian basin or well-defined surface and use them to calibrate the timing of early Martian bombardment. Relevant subtopic questions relate to late heavy bombardment and derived chronologies for the timing of major geological and geophysical events, including when recorded history begins. They also consider the current impact flux and changes in that flux over billions of years.

4.3 How Did Collisions Affect the Geological, Geophysical, and Geochemical Evolution and Properties of Planetary Bodies?

I-MIM-related Strategic Decadal Research includes studies of the nature and global distribution of hydrothermal deposits in large Martian craters that may have been habitable zones. Relevant subtopic questions consider how impacts have influenced the physical evolution of Mars, whether they expose interior compositions, the formation and evolution of impact-driven hydrothermal systems, delivery of volatile and non-volatile materials and variation in the impact process.

4.4 How Do the Physics and Mechanics of Impacts Produce Disruption of and Cratering on Planetary Bodies?

I-MIM-related Strategic Decadal Research includes determining how impact physics and mechanics changes at different impact sites by mapping those sites with high-resolution remote sensing images and how impacts affected oceans and ices on Mars by characterizing Martian surface conditions, including the existence of water or ice. Relevant subtopic questions consider impact process variations based on projective/Mars properties and impact parameters.

5.2 How Have the Interiors of Solid Bodies Evolved?

I-MIM-related Strategic Decadal Research relates to the timing and flux of volcanism on Mars and studies of remanent crust magnetization on Mars. Relevant subtopic questions relate to internal processes controlling surface topography and tectonic features and how and where hydrothermal/geothermal processes have modified surfaces. Relevant subtopic questions relate to post accretion mechanisms, processes controlling magnetic fields, and the physical consequences of cooling on the crust.

5.3 How Have Surface/Near-Surface Characteristics and Compositions of Solid Bodies Been Modified by, and Recorded, Interior Processes?

I-MIM-related Strategic Decadal Research focuses on the identification and classification of modern and ancient volcanic and tectonic landforms on Mars and on providing fundamental constrains on lithospheric properties such as the thickness of the deforming layer. Relevant subtopic questions relate to internal processes controlling surface topography.

5.4 How Have Surface Characteristics and Compositions of Solid Bodies Been Modified by, and Recorded, Surface Processes and Atmospheric Interactions?

I-MIM-related Strategic Decadal Research includes characterizing weathering, habitability, the history of glaciation and erosion, planetary ice-regolith mixtures, and ice clathrates. Relevant subtopic questions relate to glacial and fluvial processes and regolith generation and transport, among others.

5.5 How Have Surface Characteristics and Compositions of Solid Bodies Been Modified by, and Recorded External Processes?

I-MIM-related Strategic Decadal Research includes investigating the effects of sublimation, space weathering and interior processes. Relevant subtopic questions relate to volatile deposition, sublimation, transport, and redeposition, and loss in the present and past, among others.

5.6 What Drives Active Processes Occurring in the Interiors and on the Surfaces of Solid Bodies?

I-MIM-related Strategic Decadal Research includes constraining the rate of active surface changes on Mars related to dune migration, mass movements, sedimentation, or ice sublimation using long-term, repeat-pass strategies. Relevant subtopic questions include investigations of active sedimentary and regolith processes, among others.

6.1 How Do Solid-Body Atmospheres Form and What Was Their State During and Shortly after Accretion?

I-MIM-related Strategic Decadal Research includes constraining the earliest stages of atmospheric evolution on Mars, deriving the sources of exospheric volatiles by measuring the distribution, composition, and abundance of surface volatiles. It also includes understanding the initial states of planetary atmospheres by developing models coupled to processes such as

delivery, loss of volatiles from impacts, chemistry, dynamics, and atmospheric escape due to both thermal and non-thermal escape mechanisms. Relevant subtopic questions includes the role of the space environment in liberating volatiles.

6.2 What Processes Govern the Evolution of Planetary Atmospheres and Climates Over Geologic Timescales?

I-MIM-related Strategic Decadal Research includes constraining the timing of Martian climate transitions and Martian atmospheric evolution processes and determining how and why Mars's climate has changed over orbital time scales by performing radar mapping of the polar layered terrain and by making in situ measurements of their structure and composition (thickness of layers, dust content, and isotope ratios) and their local meteorology (including volatile and dust fluxes). It also includes studying surface-exchange processes. Relevant subtopic questions include the nature of the early Martian climate, orbital forcing (including obliquity and eccentric changes) governing climate change, and surface volatile redistribution on modern Mars.

6.3 What Processes Drive the Dynamics and Energetics of Atmospheres on Solid Bodies?

I-MIM-related Strategic Decadal Research includes:

- determining drivers of atmospheric dynamics and energetics, lower-upper atmosphere coupling, spatio-temporal thermal and wind measurements over multiple annual cycles on Mars;
- studying how the surface is coupled to the main atmosphere by measuring the transport of heat, momentum, volatiles, and dust through the planetary boundary layer on bodies with collisional atmospheres such as Mars;
- exploring the cause of variability in Martian dust storms and hence climate in relationship to dust;
- determining how aerosols influence atmospheric dynamics and energetics on diurnal, seasonal, and multi-annual timescales on Mars (dust and clouds);
- understanding ion-neutral drag on upper atmospheric circulation by performing in situ measurements of ion and neutral winds, as well as ion electron densities, plasma distribution functions, and magnetic fields on Mars; and,
- exploring connections among the solar wind, magnetic fields, and the neutral atmosphere/ exosphere.

Relevant subtopic questions relate to what controls the onset, evolution, and annual variability of dust storms on Mars.

6.4 How Do Planetary Surfaces and Interiors Influence and Interact with Their Host Atmospheres?

I-MIM-related Strategic Decadal Research involves investigations of how and where stable water ice deposits form on Mars by measuring their distribution through radar and spectroscopic mapping from orbit, and by measuring the ice vertical distribution, volatile fluxes, and environmental drivers at the surface. It also includes determinations of the way in which dust lifting and sand motion are linked to the state of the near-surface Martian atmosphere and inferences about near-surface wind patterns and environmental conditions based on seasonal and annual variations captured by high-resolution imaging of Mars. Relevant subtopic questions relate to the way in which major constituents in planetary atmospheres drive the formation, evolution, and stability of polar caps and other reservoirs over seasonal times scales, as well as the way in which these reservoirs drive volatile transport and generate winds resulting in aeolian activity. They also include how minor constituents in the Martian atmosphere drive the distribution of surface and near-surface volatiles such as water ice on Mars.

6.5 What Processes Govern Atmospheric Loss to Space?

I-MIM-related Strategic Decadal Research includes studies of the flow of energy and escaping gases through collisional atmospheres such as that of Mars to diagnose lower-upper atmosphere coupling; the way in which escaping ions influence the magnetospheric current systems by performing multi-point measurements in induced magnetospheres (e.g., Mars); and the relationship between the loss of volatiles and the effects of magnetic fields. Relevant subtopic questions include how the presence or absence of magnetic fields influence the escape of gases, how atmospheric dynamics such as Martian dust storms affect the escape of gases, and considerations of what processes controlling the trace gas composition in the Martian atmosphere.

6.6 What Chemical and Microphysical Processes Govern the Clouds, Hazes, Chemistry and Trace Gas Composition of Solid Body Atmospheres?

I-MIM-related Strategic Decadal Research includes investigations of the microphysical parameters that influence the formation of clouds in the Martian atmosphere. Relevant subtopic questions involve how the nature of the ionosphere affects the structure and composition of exospheres and cloud formation and composition.

10.1 What Is "Habitability"?

I-MIM-related Strategic Decadal Research includes characterizing known and candidate modern habitable environments on Mars, as well as the character, timing, and nature of past habitable environments. Relevant subtopic questions relate to environmental characteristics required for habitability and its sustainability, change, and loss.

10.2 Where Are or Were the Solar System's Past or Present Habitable Environments?

I-MIM-related Strategic Decadal Research considers the extent of present and former habitable environments in the solar system, including determining the past and present existence and distribution of liquid water and the evolution of the Martian climate. Relevant subtopic questions consider what terrestrial planetary bodies reveal about habitable environments.

10.3 Water Availability: What Controls the Amount of Available Water on a Body Over Time?

I-MIM-related Strategic Decadal Research includes establishing whether liquid water is present on Mars today in the subsurface through ice and geophysical measurements that probe the upper crust. It also focuses on determining the distribution, history, and processes driving the availability of ice and liquid water on Mars over time, including mapping stratigraphy, sounding of the subsurface, and models for geomorphic features and climate processes. Relevant subtopic questions consider initial constraints on liquid water inventories and subsequent controls.

10.5 What Is the Availability of Nutrients and Other Inorganic Ingredients to Support Life?

I-MIM-related Strategic Decadal Research includes characterizing candidate current and ancient habitable environments on Mars, the impact of seasonal cycles in the Martian atmosphere, and observations of the behavior of aerosols, trace gas and isotope abundances, and meteorology. Subtopic questions are more related to inventories, forms, and distribution of life-supporting elements.

10.6 What Controls the Energy Available for Life?

I-MIM-related Strategic Decadal Research includes determining the geophysical parameters that control past and present material fluxes in rocky subsurfaces (e.g., porosity, permeability), including change detection. Relevant subtopic questions consider geophysical processes determining and governing available energy sources.

10.7 What Controls the Continuity or Sustainability of Habitability?

I-MIM-related Strategic Decadal Research relates to the nature, timing, and processes controlling past habitable environments on Mars, the frequency and effects of impacts on local and planetary habitability, and understanding the rates and styles of recycling surface materials. Relevant subtopic questions relate to both endogenous and exogenous controls on the continuity of habitability.

[Indirect contributions to Exoplanets topic, per the above]

12.4 Impacts and Dynamics
12.5 Solid Body Interiors and Surfaces
12.6 Atmosphere and Climate Evolution on Solid Bodies
12.11 Dynamic Habitability

NASA | MEPAG

GOAL I LIFE

I A2 Investigate the nature and duration of habitability near the surface and in the deep subsurface.

I B2 Constrain the surface, atmosphere, and subsurface processes through which organic molecules could have formed and evolved over Martian history.

GOAL II CLIMATE

II A1 Characterize the dynamics, thermal structure, and distributions of dust, water, and carbon dioxide in the lower atmosphere.

II A2 Constrain the processes by which volatiles and dust exchange between surface and atmospheric reservoirs.

II A4 Characterize the state and controlling processes of the upper atmosphere and magnetosphere.

II B1 Determine the climate record of the recent past that is expressed in geomorphic, geological, glaciological, and mineralogical features of the polar regions.

II B2 Determine the record of the climate of the recent past that is expressed in geomorphic, geological, glaciological, and mineralogical features of low- and mid-latitudes.

II B3 Determine how the chemical composition and mass of the atmosphere has changed in the recent past.

II C1 Determine how the chemical composition and mass of the atmosphere have evolved from the ancient past to the present.

II C2 Find and interpret surface records of past climates and factors that affect climate.

GOAL III GEOLOGY

III A1 Identify and characterize past and present water and other volatile reservoirs.

- III A1.1 Determine the modern extent and volume of liquid water and hydrous minerals within the crust.
- III A1.2 Identify the geologic evidence for the location, volume, and timing of ancient water reservoirs.
- III A1.3 Determine the subsurface structure and age of the Polar Layered Deposits (PLD) and identify links to climate.
- III A1.4 Determine how the vertical and lateral distribution of surface ice and ground ice has changed over time.
- III A1.5 Determine the role of volatiles in modern dynamic surface processes, correlate with records of recent climate change, and link to past processes and landforms.

III A2 Document the geologic record preserved in sediments and sedimentary deposits.

- III A2.1 Constrain the location, volume, timing, and duration of past hydrologic cycles that contributed to the sedimentary and geomorphic record.

III A3 Constrain the magnitude, nature, timing, and origin of ancient environmental transitions.

III A4 Determine the nature and timing of construction and modification of the crust.

III A4.7. Develop a planet-wide model of Mars evolution through global and regional mapping efforts.

GOAL IV PREPARE FOR HUMANS

IV A1 Determine the aspects of the atmospheric state that affect orbital capture and EDL for human scale missions to Mars.

IV A3 Assess landing-site characteristics and environment related to safe landing of human-scale landers.

- IV B1 Assess risks to crew health and performance by: (1) characterizing in detail the ionizing radiation environment at the martian surface and (2) determining the possible toxic effects of martian dust on humans

IV B2 Characterize the surface particulates that could affect engineering performance and lifetime of hardware and infrastructure.

IV B3 Assess the climatological risk of dust storm activity in the human exploration zone at least one year in advance of landing and operations.

IV B4 Assess landing-site characteristics and environment related to safe operations and trafficability within the possible area to be accessed by elements of a human mission.

IV C2 Characterize potentially extractable water resources to support ISRU for long-term human needs.

- IV C2.1 Identify a set of candidate water resource deposits that have the potential to be relevant for future human exploration.
- IV C2.2 Prepare high spatial resolution maps of … water ice at or within a few meters of the surface that include the information needed to design and operate an extraction and processing system with adequate cost, risk, and performance.

IV D1 Determine the martian environmental niches that meet the definition of "Special Region" at the human landing site and inside of the exploration zone. [Precursor – IV D1.1 "locations and characteristics of natural or potential spacecraft-induced Special Regions"]

IV D4 Determine the astrobiological baseline of the human landing site prior to human arrival

- *IV D4.1 Determine characteristics of the Mars atmosphere, surface, and sub-surface environments that constitute the astrobiological baseline of the landing site prior to the introduction of terrestrial bio-material.*

NSO | Space Activities (2020)

THEMES

Planetary Science

- Answers to questions such as "How did life on Earth come to be?" and "Are there other planets in the universe that could sustain life?"

Human Spaceflight (e.g., solar panels on Orion)

AIMS

Develop the Dutch Space Sector

- Focus on developing those technologies in which the Netherlands has leading capabilities (e.g., solar panels)

Coordinate National and International Space Programs

- Stimulate successes in space through knowledge networks
- Contribute Dutch technologies that support international collaboration in human and robotic spaceflight
- Maintain leadership roles and participation in international missions and space-related organizations

From additional information provided to the MDT:

NSO Alignment with Agency Goals for Future Mars Exploration

- Netherlands Solar Arrays (with Airbus Defence and Space Netherlands)
- Active in all missions and markets (single satellites, small and large constellations, smallsat arrays, and traditional large arrays)
- Moon/Mars Human/Robotic Connection: Providing Solar Panels for the Orion/Artemis Service Module (NASA/ESA) and Exomars (ESA)

I-MIM Opportunity in the Context of NSO goals

- Support development effort for new solar arrays concept
- Demonstrate very high power density (W/m^2, W/m^3) Flexible Compact Solar Array with concise requirements in deep space
- International cooperation and networking
- Fostering commercial opportunities in the space sector

Appendix B. ACRONYMS

ASI	Agenzia Spaziale Italiana (Italian Space Agency)
CaSSIS	Colour and Stereo Surface Imaging System
CBOE	Coherent Back-scatter Opposition Effect
CCF	Concentric Crater Fills
CIMR	Copernicus Imaging Microwave Radiometer [Mission]
CMOS TDI	Complementary Metal-oxide Semiconductor Time Delay and Integration
CONOPS	Concept of Operations
CPR	Circular Polarization Ratio
CRISM	Compact Reconnaissance Imaging Spectrometer for Mars
CTX	Context Camera
DSN	Deep Space Network
DTM	Digital Terrain Model
DV	Data Volume
GLF	Glacier-like Forms
HiRISE	High Resolution Imaging Science Experiment
HRMS	High-resolution ion/neutral Mass Spectrometer
ICE-SAG	Ice and Climate Evolution Science Analysis Group
I-MIM	International Mars Ice Mapper
ISRU	In Situ Resource Utilization
InSAR	Interferometric SAR
JAXA	Japan Aerospace Exploration Agency
JSMEP	Japan Strategic Mars Exploration Program
LDA	Lobate Debris Aprons
LDM	Latitude Dependent Mantle
LVF	Lineated Valley Fill
MARSIS	Mars Advanced Radar for Subsurface and Ionosphere Sounding
MEPAG	Mars Exploration Program Assessment Group
MEX	Mars Express
MGS	Mars Global Surveyor
MOLA	Mars Orbiter Laser Altimeter
MRO	Mars Reconnaissance Orbiter
NASA	National Aeronautics and Space Administration
NEX-SAG	Next [Mars] Orbiter Science Analysis Group
NSO	Netherlands Space Office
OCM	Orbit Correction Maneuvers
PLD	Polar Layered Deposits
POLSAR	Polarimetric SAR
PRF	Pulse Repetition Frequency
PRI	Pulse Repetition Intervals
RSM	RADARSAT Constellation Mission
RF	Radio Frequency
RIMFAX	Radar Imager for Mars' Subsurface Experiment
RSL	Recurring Slope Lineae
SAR	Synthetic Aperture Radar
SCET	Spacecraft Event Time
SEP	Solar Electric Propulsion
SEP	Solar Energetic Particles
SHARAD	Shallow Subsurface Radar

SLC	Single Look Complex
SMAP	Soil Moisture Active Passive [Mission]
SNR	Signal to Noise Ratio
STK	Systems Tool Kit
SWIM	Subsurface Water Ice Mapping
TEC	Total Electron Content
TGO	Trace Gas Orbiter
THEMIS	Thermal Emission Imaging System
TIR	Thermal Infrared
TRN	Terrain Relative Navigation
UV-VIS	UltraViolet-Visible
VFF	Viscous Flow Features
VHF	Very High Frequency
VIS-IR	Visible-Infrared

Appendix C. REFERENCES

Abdelkareem, M., Abdalla, F., Mohamed, S. Y., & El-Baz, F. (2020). Mapping paleohydrologic features in the arid areas of Saudi Arabia using remote-sensing data. *Water*, *12*(2), 417. https://doi.org/10.3390/w12020417

Abalakin, V. K., Bursa, M., Davies, M. E., de Bergh, C., Lieske, J. H., Oberst, J., ... & Thomas, P. C. (2002). Report of the IAU/IAG working group on cartographic coordinates and rotational elements of the planets and satellites: 2000. *Celestial Mechanics and Dynamical Astronomy*, *82*(1), 83-111. https://doi.org/10.1023/A:1013939327465

Abotalib, A. Z., & Heggy, E. (2019). A deep groundwater origin for recurring slope lineae on Mars. *Nature geoscience*, *12*(4), 235-241. https://doi.org/10.1038/s41561-019-0327-5

Abshire, J. B., Smith, M.D., Cremons, D.R., Guzewich, S.D., Sun, X., Yu, A., & Hovis, F. (2022, June 14-17). MARLI: Mars LIDAR for measuring global wind and aerosol profiles from orbit, 7th Mars Atmosphere Modeling and Observations Conference. Paris, France. http://dx.doi.org/10.1117/12.2325408

Aharonson, O., Schorghofer, N., & Gerstell, M. F. (2003). Slope streak formation and dust deposition rates on Mars. *Journal of Geophysical Research: Planets*, *108*(E12). https://doi.org/10.1029/2003JE002123

Aharonson, O., Zuber, M. T., Smith, D. E., Neumann, G. A., Feldman, W. C., & Prettyman, T. H. (2004). Depth, distribution, and density of CO_2 deposition on Mars. *Journal of Geophysical Research: Planets, 109* (E5). https://doi.org/10.1029/2003JE002223

Aharonson, O., & Schorghofer, N. (2006). Subsurface ice on Mars with rough topography. *Journal of Geophysical Research: Planets*, *111*(E11). https://doi.org/10.1029/2005JE002636

Alwarda, R., & Smith, I. B. (2021). Stratigraphy and volumes of the units within the massive carbon dioxide ice deposits of Mars. *Journal of Geophysical Research: Planets, 126*(5), e2020JE006767. https://doi.org/10.1029/2020JE006767

Aoki, S., Nakagawa, H., Sagawa, H., Giuranna, M., Sindoni, G., Aronica, A., & Kasaba, Y. (2015). Seasonal variation of the HDO/H_2O ratio in the atmosphere of Mars at the middle of northern spring and beginning of northern summer. *Icarus, 260*, 7-22. https://doi.org/10.1016/j.icarus.2015.06.021

Aoki, S., Vandaele, A. C., Daerden, F., Villanueva, G. L., Liuzzi, G., Thomas, I. R., ... & NOMAD team. (2019). Water vapor vertical profiles on Mars in dust storms observed by TGO/NOMAD. *Journal of Geophysical Research: Planets*, *124*(12), 3482-3497. https://doi.org/10.1029/2019JE006109

Archinal, B. A., Acton, C. H., A'hearn, M. F., Conrad, A., Consolmagno, G. J., Duxbury, T., ... & Williams, I. P. (2018). Report of the IAU working group on cartographic coordinates and rotational elements: 2015. *Celestial Mechanics and Dynamical Astronomy*, *130*(3), 1-46. https://doi.org/10.1007/s10569-017-9805-5

Arvidson, R. E., Anderson, R. C., Bartlett, P., Bell III, J. F., Blaney, D., Christensen, P. R., ... & Wilson, J. (2004a). Localization and physical properties experiments conducted by Spirit at Gusev Crater. *Science*, *305*(5685), 821-824. https://doi.org/10.1126/science.1099922

Arvidson, R. E., Anderson, R. C., Bartlett, P., Bell III, J. F., Christensen, P. R., Chu, P., ... & Wilson, J. (2004b). Localization and physical property experiments conducted by Opportunity at Meridiani Planum. *Science*, *306*(5702), 1730-1733. https://doi.org/10.1126/science.1104211

Arvidson, R., Adams, D., Bonfiglio, G., Christensen, P., Cull, S., Golombek, M., ... & Tamppari, L. (2008). Mars Exploration Program 2007 Phoenix landing site selection and characteristics. *Journal of Geophysical Research: Planets*, *113*(E3) https://doi.org/10.1029/2007JE003021

Baker, D. M., & Carter, L. M. (2019a). Probing supraglacial debris on Mars 1: Sources, thickness, and stratigraphy. *Icarus*, *319*, 745-769. https://doi.org/10.1016/j.icarus.2018.09.001

Baker, D. M., & Carter, L. M. (2019b). Probing supraglacial debris on Mars 2: Crater morphology. *Icarus*, *319*, 264-280. https://doi.org/10.1016/j.icarus.2018.09.009

Bandfield, J. L. (2007). High-resolution subsurface water-ice distributions on Mars. *Nature*, 447(7140), 64–67. https://doi.org/10.1038/nature05781

Bandfield, J. L., & Feldman, W. C. (2008). Martian high latitude permafrost depth and surface cover thermal inertia distributions. *Journal of Geophysical Research: Planets*, *113*(E8). https://doi.org/10.1029/2007JE003007

Banfield, D., Colaprete, A., Cook, A., Mauro, D., Bookbinder, J., Maryatt, B., … & Cassell, A. (2022, June28-Jul 1). A Mars network mission addressing climate and surface processes. [Abstract #7017]. In *Optimizing Planetary In-Situ Surface-Atmosphere Interaction Investigations Workshop*. Retrieved from: https://www.hou.usra.edu/meetings/planetinsitu2022/pdf/7017.pdf

Banks, M. E., Lang, N. P., Kargel, J. S., McEwen, A. S., Baker, V. R., Grant, J. A., ... & Strom, R. G. (2009). An analysis of sinuous ridges in the southern Argyre Planitia, Mars using HiRISE and CTX images and MOLA data. *Journal of Geophysical Research: Planets*, *114*(E9). https://doi.org/10.1029/2008JE003244

Barlow, N. G. (2005). A review of Martian impact crater ejecta structures and their implications for target properties. *Large meteorite impacts III, 384*, 433-442. https://doi.org/10.1130/0-8137-2384-1.433

Barlow, N. G. (2015). Characteristics of impact craters in the northern hemisphere of Mars. *Large Meteorite Impacts and Planetary Evolution IV, 518*, 31-63. https://doi.org/10.1130/2015.2518(03)

Barlow, N. G., Boyce, J. M., Costard, F. M., Craddock, R. A., Garvin, J. B., Sakimoto, S. E., ... & Soderblom, L. A. (2000). Standardizing the nomenclature of Martian impact crater ejecta morphologies. *Journal of Geophysical Research: Planets, 105*(E11), 26733-26738. https://doi.org/10.1029/2000JE001258

Barnouin-Jha, O. S., Baloga, S., & Glaze, L. (2005). Comparing landslides to fluidized crater ejecta on Mars. *Journal of Geophysical Research: Planets*, *110*(E4), 1-22. https://doi.org/10.1029/2003JE002214

Barnouin-Jha, O. S., Schultz, P. H., & Lever, J. H. (1999). Investigating the interactions between an atmosphere and an ejecta curtain: 2. Numerical experiments. *Journal of Geophysical Research: Planets*, *104*(E11), 27117-27131. https://doi.org/10.1029/1999JE001026

Beaty, D., Buxbaum, K., Meyer, M., Barlow, N., Boynton, W., Clark, B., Deming, J., Doran, P.T., Edgett, K., Hancock, S. (2006). Findings of the Mars special regions science analysis group. *Astrobiology* 6, 677–732. https://doi.org/10.1089/ast.2006.6.677

Beaty, D.W., Mueller, R.P., Bussey, D.B., Davis, R.M., Hays, L.E., Hoffman, S.J., & Zbinden, E. (2016). Some strategic considerations related to the potential use of water resource deposits on Mars by future human explorers. ASCE Earth and Space Conference, Orlando, FL Retrieved from https://trs.jpl.nasa.gov/handle/2014/46054

Becerra, P., Sori, M. M., & Byrne, S. (2017). Signals of astronomical climate forcing in the exposure topography of the North Polar Layered Deposits of Mars. *Geophysical Research Letters, 44*(1), 62-70. https://doi.org/10.1002/2016GL071197

Belyaev, D. A., Fedorova, A. A., Trokhimovskiy, A., Alday, J., Montmessin, F., Korablev, O. I., ... & Shakun, A. V. (2021). Revealing a high water abundance in the upper mesosphere of Mars with ACS onboard TGO. *Geophysical Research Letters*, *48*(10), e2021GL093411. https://doi.org/10.1029/2021GL093411

Bezděk, A., Klokočník, J., Kostelecký, J., Floberghagen, R., & Gruber, C. (2009). Simulation of free fall and resonances in the GOCE mission. *Journal of Geodynamics, 48*(1), 47-53. https://doi.org/10.1016/j.jog.2009.01.007

Bierson, C. J., Phillips, R. J., Smith, I. B., Wood, S. E., Putzig, N. E., Nunes, D., & Byrne, S. (2016). Stratigraphy and evolution of the buried CO_2 deposit in the Martian south polar cap. *Geophysical Research Letters*, *43*(9), 4172-4179. https://doi.org/10.1002/2016GL068457

Bierson, C. J., Tulaczyk, S., Courville, S. W., & Putzig, N. E. (2021). Strong MARSIS radar reflections from the base of Martian south polar cap may be due to conductive ice or minerals. *Geophysical Research Letters*, *48*(13). https://doi.org/10.1029/2021GL093880

Black, G. J., Campbell, D. B., & Nicholson, P. D. (2001a). Icy Galilean satellites: Modeling radar reflectivities as a coherent backscatter effect. *Icarus*, *151*(2), 167-180. https://doi.org/10.1006/icar.2001.6616

Black, G. J., Campbell, D. B., & Ostro, S. J. (2001b). Icy Galilean satellites: 70 cm radar results from Arecibo. *Icarus*, *151*(2), 160-166. https://doi.org/10.1006/icar.2001.6615

Bockheim, J. G., Campbell, I. B., & McLeod, M. (2007). Permafrost distribution and active-layer depths in the McMurdo Dry valleys, Antarctica. *Permafrost and periglacial processes*, *18*(3), 217-227. https://doi.org/10.1002/ppp.588

Boynton, W. V., Feldman, W. C., Squyres, S. W., Prettyman, T. H., Bruckner, J., Evans, L. G., ... & Shinohara, C. (2002). Distribution of hydrogen in the near surface of Mars: Evidence for subsurface ice deposits. *science*, *297*(5578), 81-85. https://doi.org/10.1126/science.1073722

Bradley, B. A., Sakimoto, S. E., Frey, H., & Zimbelman, J. R. (2002). Medusae Fossae formation: new perspectives from Mars global surveyor. *Journal of Geophysical Research: Planets, 107*(E8), 2-1. https://doi.org/10.1029/2001JE001537

Bramson, A. M., Byrne, S., & Bapst, J. (2017). Preservation of Mid-Latitude Ice Sheets on Mars. Journal of Geophysical Research: Planets, 112, 11, 2250–2266. https://doi.org/10.1002/2017JE005357

Bramson, A. M., Byrne, S., Putzig, N. E., Sutton, S., Plaut, J. J., Brothers, T. C., & Holt, J. W. (2015). Widespread excess ice in Arcadia Planitia, Mars. *Geophysical Research Letters*, *42*(16), 6566-6574. https://doi.org/10.1002/(ISSN)1944-8007

Bridges, N., Geissler, P., Silvestro, S., & Banks, M. (2013). Bedform migration on Mars: Current results and future plans. *Aeolian Research*, *9*, 133-151. https://doi.org/10.1016/j.aeolia.2013.02.004

Brooks, C. L., Romashkova, E. A., Deahn, M. C., Williams, N. R., Golombek, M. P., Calef, F. J., ... & Morris, M. M. (2022). Quantifying Rock Detectability and Refining Candidate Landing and Sample Tube Depot Sites for Mars Sample Return. *LPI Contributions*, *2678*, 2772. Retrieved from: https://ui.adsabs.harvard.edu/abs/2022LPICo2678.2772B/abstract

Brough, S., Hubbard, B., & Hubbard, A. (2016). Former extent of glacier-like forms on Mars. *Icarus*, *274*, 37-49. https://doi.org/10.1016/j.icarus.2016.03.006

Buczkowski, D., Ackiss, S., Seelos, K., Murchie, S., Seelos, F., Malaret, E., & Hash, C. (2014, April). Her Desher and Nirgal Vallis phyllosilicates: Pedogenesis or groundwater sapping?. In *European Planetary Science Congress* (Vol. 9, pp. EPSC2014-523). Retrieved from: https://ui.adsabs.harvard.edu/abs/2014EPSC....9..523B/abstract

Buhler, P. B., Ingersoll, A. P., Piqueux, S., Ehlmann, B. L., & Hayne, P. O. (2020). Coevolution of Mars's atmosphere and massive south polar CO_2 ice deposit. *Nature Astronomy*, *4*(4), 364-371. https://doi.org/10.1038/s41550-019-0976-8

Buhler, P. B., & Piqueux, S. (2021). Obliquity-Driven CO2 Exchange Between Mars' Atmosphere, Regolith, and Polar Cap. *Journal of Geophysical Research: Planets, 126*(5), e2020JE006759. https://doi.org/10.1029/2020JE006759

Bussey, B., & Hoffman, S. J. (2016, March). Human Mars landing site and impacts on Mars surface operations. In *2016 IEEE Aerospace Conference* (pp. 1-21). IEEE. https://doi.org/10.1109/AERO.2016.7500775

Butcher, F. E.G., Arnold, N.S., Conway, S.J., Berman, D.C., Davis, J.M., Balme, M.R. (2021). Potential for sampling of subglacial and englacial environments in Mars' mid latitudes, without deep drilling. [Abstract #1231]. In *52nd Lunar and Planetary Science Conference*. Retrieved from: https://www.hou.usra.edu/meetings/lpsc2021/pdf/1231.pdf

Butcher, F. E., Balme, M. R., Conway, S. J., Gallagher, C., Arnold, N. S., Storrar, R. D., ... & Hagermann, A. (2020). Morphometry of a glacier-linked esker in NW Tempe Terra, Mars, and implications for sediment-discharge dynamics of subglacial drainage. *Earth and Planetary Science Letters*, *542*, 116325. https://doi.org/10.1016/j.epsl.2020.116325

Butcher, F. E., Balme, M. R., Gallagher, C., Arnold, N. S., Conway, S. J., Hagermann, A., & Lewis, S. R. (2017). Recent basal melting of a mid-latitude glacier on Mars. *Journal of Geophysical Research: Planets*, *122*(12), 2445-2468. https://doi.org/10.1002/2017JE005434

Butcher, F. E., Conway, S. J., & Arnold, N. S. (2016). Are the dorsa argentea on mars eskers?. *Icarus*, *275*, 65-84. https://doi.org/10.1016/j.icarus.2016.03.028

Butler, B.J. (1994). 3.5-cm radar investigation of Mars and Mercury: Planetological implications. Dissertation (Ph.D.), California Institute of Technology. doi:10.7907/MSRK-FF90. https://resolver.caltech.edu/CaltechTHESIS:01252013-144953787

Byrne, S., Zuber, M. T., & Neumann, G. A. (2008). Interannual and seasonal behavior of Martian residual ice-cap albedo. *Planetary and Space Science*, *56*(2), 194-211. https://doi.org/10.1016/j.pss.2006.03.018

Byrne, S., & Ingersoll, A. P. (2003). A sublimation model for Martian south polar ice features. *Science*, *299*(5609), 1051-1053. https://doi.org/10.1126/science.1080148

Byrne, S., Dundas, C. M., Kennedy, M. R., Mellon, M. T., McEwen, A. S., Cull, S. C., ... & Seelos, F. P. (2009). Distribution of mid-latitude ground ice on Mars from new impact craters. *science*, *325*(5948), 1674-1676. https://doi.org/10.1126/science.1175307

Calvin, W. M., James, P. B., Cantor, B. A., & Dixon, E. M. (2015). Interannual and seasonal changes in the north polar ice deposits of Mars: Observations from MY 29–31 using MARCI. *Icarus, 251*, 181-190. https://doi.org/10.1016/j.icarus.2014.08.026

Calvin, W. M., & Titus, T. N. (2008). Summer season variability of the north residual cap of Mars as observed by the Mars Global Surveyor Thermal Emission Spectrometer (MGS-TES*). Planetary and Space Science, 56*(2), 212-226. https://doi.org/10.1016/j.pss.2007.08.005

Campbell, B. A. (2012). High circular polarization ratios in radar scattering from geologic targets. *Journal of Geophysical Research: Planets, 117*(E6). https://doi.org/10.1029/2012JE004061

Campbell, B. A., (2016). Planetary Geology with Imaging Radar: Insights from Earth-based Lunar Studies, 2001–2015. *Publications of the Astronomical Society of the Pacific, 128*, 964. https://doi.org/10.1088/1538-3873/128/964/062001

Campbell, B., Carter, L., Phillips, R., Plaut, J., Putzig, N., Safaeinili, A., ... & Orosei, R. (2008). SHARAD radar sounding of the Vastitas Borealis Formation in Amazonis Planitia. *Journal of Geophysical Research: Planets*, *113*(E12). https://doi.org/10.1029/2008JE003177

Campbell, B. A., & Morgan, G. A. (2018). Fine-scale layering of Mars polar deposits and signatures of ice content in nonpolar material from multiband SHARAD data processing. *Geophysical Research Letters*, *45*(4), 1759-1766. https://doi.org/10.1002/2017GL075844

Campbell, B. A., Watters, T. R., & Morgan, G. A. (2021). Dielectric properties of the Medusae fossae formation and implications for ice content. *Journal of Geophysical Research: Planets*, *126*(3). https://doi.org/10.1029/2020JE006601

Carr, M. H., & Head, J. W. (2015). Martian surface/near-surface water inventory: Sources, sinks, and changes with time. *Geophysical Research Letters*, *42*(3), 726-732. https://doi.org/10.1002/2014GL062464

Carter, L. M., Campbell, B. A., Holt, J. W., Phillips, R. J., Putzig, N. E., Mattei, S., ... & Egan, A. F. (2009). Dielectric properties of lava flows west of Ascraeus Mons, Mars. *Geophysical Research Letters*, *36*(23). https://doi.org/10.1029/2009GL040749

Chaffin, M. S., Kass, D. M., Aoki, S., Fedorova, A. A., Deighan, J., Connour, K., ... & Korablev, O. I. (2021). Martian water loss to space enhanced by regional dust storms. *Nature Astronomy*, *5*(10), 1036-1042. https://doi.org/10.1038/s41550-021-01425-w

Chamberlain, M. A., & Boynton, W. V. (2007). Response of Martian ground ice to orbit-induced climate change. *Journal of Geophysical Research: Planets, 112*(E6). https://doi.org/10.1029/2006JE002801

Chojnacki, M., Fenton, L. K., Weintraub, A. R., Edgar, L. A., Jodhpurkar, M. J., & Edwards, C. S. (2020). Ancient Martian aeolian sand dune deposits recorded in the stratigraphy of Valles Marineris and implications for past climates. *Journal of Geophysical Research: Planets*, *125*(9). https://doi.org/10.1029/2020JE006510

Christensen, P., & Moore, H. J. (1992). The Martian surface layer. In H.H. Kieffer, B.M. Jakosky, C.W. Snyder, M.S. Matthews (Eds.), *Mars* (pp. 686-729). University of Arizona Press, Space Science Series. https://doi.org/10.2307/j.ctt207g59v

Christensen, P. R. (1986). The spatial distribution of rocks on Mars. *Icarus*, *68*(2), 217-238. https://doi.org/10.1016/0019-1035(86)90020-5

Christner, B. C., Priscu, J. C., Achberger, A. M., Barbante, C., Carter, S. P., Christianson, K., ... & Vick-Majors, T. J. (2014). A microbial ecosystem beneath the West Antarctic ice sheet. *Nature*, *512*(7514), 310-313. https://doi.org/10.1038/nature13667

Colaprete, A., Cook, A., Mauro, D., Bookbinder, J., Maryatt, B., Wilson, J., ... & Cassell, A. (2022). Aeolus: A Mars Climate Mission. LPI Contributions, 2678, 2663. Retrieved from: https://www.hou.usra.edu/meetings/lpsc2022/pdf/2663.pdf

Colaprete, A., & Jakosky, B. M. (1998). Ice flow and rock glaciers on Mars. *Journal of Geophysical Research: Planets, 103*(E3), 5897-5909. https://doi.org/10.1029/97JE03371

Colliander, A., Mousavi, M., Marshall, S., Samimi, S., Kimball, J. S., Miller, J. Z., ... & Burgin, M. (2022). Ice Sheet Surface and Subsurface Melt Water Discrimination Using Multi-Frequency Microwave Radiometry. *Geophysical Research Letters*, *49*(4). https://doi.org/10.1029/2021gl096599

Contu, S., Meschini, A., & Rigato, R. (2019). Development status of Large Reflectors at TAS-I. *In 2019 IEEE Indian Conference on Antennas and Propogation (InCAP)* (pp. 1–4). IEEE. https://doi.org/10.1109/InCAP47789.2019.9134515

Conway, S. J., & Balme, M. R. (2014). Decameter thick remnant glacial ice deposits on Mars. *Geophysical Research Letters*, *41*(15), 5402-5409. https://doi.org/10.1002/2014GL060314

Costard, F. M., & Kargel, J. S. (1995). Outwash plains and thermokarst on Mars. *Icarus, 114*(1), 93-112. https://doi.org/10.1006/icar.1995.1046

Craddock, R. A., & Howard, A. D. (2002). The case for rainfall on a warm, wet early Mars. *Journal of Geophysical Research: Planets*, *107*(E11), 21-1. https://doi.org/10.1029/2001JE001505

Craig, D. A., Troutman, P., & Herrmann, N. (2015). Pioneering space through the evolvable Mars campaign. In *AIAA Space 2015 Conference and Exposition* (p. 4409). https://doi.org/10.2514/6.2015-4409

Cramer, A. G., Withers, P., Elrod, M. K., Benna, M., & Mahaffy, P. R. (2020). Effects of the 10 September 2017 Solar Flare on the Density and Composition of the Thermosphere of Mars. *Journal of Geophysical Research: Space Physics*, *125*(10) https://doi.org/10.1029/2020JA028518

Crosta, G. B., De Blasio, F. V., & Frattini, P. (2018). Global scale analysis of Martian landslide mobility and paleoenvironmental clues. *Journal of Geophysical Research: Planets*, *123*(4), 872-891. https://doi.org/10.1002/2017JE005398

Cushing, G. E. (2012). Candidate cave entrances on Mars. *Journal of Cave and Karst Studies*, *74*(1), 33-47. http://dx.doi.org/10.4311/2010EX0167R

Cushing, G. E., Titus, T. N., Wynne, J. J., & Christensen, P. R. (2007). THEMIS observes possible cave skylights on Mars. *Geophysical Research Letters, 34*(17). https://doi.org/10.1029/2007GL030709

Cutts, J. A., & Lewis, B. H. (1982). Models of climate cycles recorded in Martian polar layered deposits. *Icarus, 50*(2-3), 216-244. https://doi.org/10.1016/0019-1035(82)90124-5

Daubar, I. J., Banks, M. E., Schmerr, N. C., & Golombek, M. P. (2019). Recently formed crater clusters on Mars. *Journal of Geophysical Research: Planets*, *124*(4), 958-969. https://doi.org/10.1029/2018JE005857

Daubar, I. J., McEwen, A. S., Byrne, S., Kennedy, M. R., & Ivanov, B. (2013). The current martian cratering rate. *Icarus*, *225*(1), 506-516. https://doi.org/10.1016/j.icarus.2013.04.009

Davila, A. F., Duport, L. G., Melchiorri, R., Jaenchen, J., Valea, S., de Los Rios, A., ... & Wierzchos, J. (2010). Hygroscopic salts and the potential for life on Mars. *Astrobiology*, *10*(6), 617-628. https://doi.org/10.1089/ast.2009.0421

de Pablo, M. Á., & Komatsu, G. (2009). Possible pingo fields in the Utopia basin, Mars: Geological and climatical implications. *Icarus*, *199*(1), 49-74. https://doi.org/10.1016/j.icarus.2008.09.007

Delaloye, R., Strozzi, T., Lambiel, C., Barboux, C., Mari, S., Stocker, A., ... & Raetzo, H. (2010, June). The contribution of InSAR data to the early detection of potentially hazardous active rock glaciers in mountain areas. In *Proceedings of the ESA Living Planet Symposium, Bergen (Norway)* (Vol. 28). Retrieved from: https://ui.adsabs.harvard.edu/abs/2010ESASP.686E.119D/abstract

Diniega, S., Bramson, A. M., Buratti, B., Buhler, P., Burr, D. M., Chojnacki, M., ... & Widmer, J. M. (2021). Modern Mars' geomorphological activity, driven by wind, frost, and gravity. *Geomorphology*, *380*, 107627. https://doi.org/10.1016/j.geomorph.2021.107627

Diniega, S., Byrne, S., Bridges, N. T., Dundas, C. M., & McEwen, A. S. (2010). Seasonality of present-day Martian dune-gully activity. *Geology*, *38*(11), 1047-1050. https://doi.org/10.1130/G31287.1

Diniega, S., Hansen, C. J., Allen, A., Grigsby, N., Li, Z., Perez, T., & Chojnacki, M. (2019). Dune-slope activity due to frost and wind throughout the north polar erg, Mars. *Geological Society, London, Special Publications*, *467*(1), 95-114. https://doi.org/10.1144/sp467.6

Diniega, S., Hansen, C. J., McElwaine, J. N., Hugenholtz, C. H., Dundas, C. M., McEwen, A. S., & Bourke, M. C. (2013). A new dry hypothesis for the formation of Martian linear gullies. *Icarus*, *225*(1), 526-537. https://doi.org/10.1016/j.icarus.2013.04.006

Dundas, C. M. (2020). An aeolian grainflow model for martian recurring slope lineae. *Icarus*, *343*, 113681. https://doi.org/10.1016/j.icarus.2020.113681

Dundas, C. M., Becerra, P., Byrne, S., Chojnacki, M., Daubar, I. J., Diniega, S., ... & Valantinas, A. (2021). Active Mars: A dynamic world. *Journal of Geophysical Research: Planets*, *126*(8). https://doi.org/10.1029/2021JE006876

Dundas, C. M., Bramson, A. M., Ojha, L., Wray, J. J., Mellon, M. T., Byrne, S., ... & Holt, J. W. (2018). Exposed subsurface ice sheets in the Martian mid-latitudes. *Science*, *359*(6372), 199-201. https://doi.org/10.1126/science.aao1619

Dundas, C. M., Byrne, S., McEwen, A. S., Mellon, M. T., Kennedy, M. R., Daubar, I. J., & Saper, L. (2014). HiRISE observations of new impact craters exposing Martian ground ice. *Journal of Geophysical Research: Planets, 119*(1), 109-127. https://doi.org/10.1002/2013JE004482

Dundas, C. M., Diniega, S., Hansen, C. J., Byrne, S., & McEwen, A. S. (2012). Seasonal activity and morphological changes in Martian gullies. *Icarus*, *220*(1), 124-143. https://doi.org/10.1016/j.icarus.2012.04.005

Dundas, C. M., Diniega, S., & McEwen, A. S. (2015). Long-term monitoring of martian gully formation and evolution with MRO/HiRISE. *Icarus*, *251*, 244-263. https://doi.org/10.1016/j.icarus.2014.05.013

Dundas, C. M., & McEwen, A. S. (2010). An assessment of evidence for pingos on Mars using HiRISE. *Icarus*, *205*(1), 244-258. https://doi.org/10.1016/j.icarus.2009.02.020

Dundas, C. M., McEwen, A. S., Chojnacki, M., Milazzo, M. P., Byrne, S., McElwaine, J. N., & Urso, A. (2017). Granular flows at recurring slope lineae on Mars indicate a limited role for liquid water. *Nature Geoscience*, *10*(12), 903-907. https://doi.org/10.1038/s41561-017-0012-5

Dundas, C. M., McEwen, A. S., Diniega, S., Hansen, C. J., Byrne, S., & McElwaine, J. N. (2019). The formation of gullies on Mars today. *Geological Society, London, Special Publications*, *467*(1), 67-94. https://doi.org/10.1144/SP467.5

Edgett, K. S., Butler, B. J., Zimbelman, J. R., & Hamilton, V. E. (1997). Geologic context of the Mars radar "Stealth" region in southwestern Tharsis. *Journal of Geophysical Research: Planets, 102*(E9), 21545-21567. https://doi.org/10.1029/97JE01685

Entekhabi, D., Njoku, E. G., O'Neill, P. E., Kellogg, K. H., Crow, W. T., Edelstein, W. N., ... & Van Zyl, J. (2010). The soil moisture active passive (SMAP) mission. *Proceedings of the IEEE, 98*(5), 704-716. https://doi.org/10.1109/JPROC.2010.2043918

Esmaeili, S., Kruse, S., Jazayeri, S., Whelley, P., Bell, E., Richardson, J., ... & Young, K. (2020). Resolution of lava tubes with ground penetrating radar: The TubeX project. *Journal of Geophysical Research: Planets*, *125*(5), e2019JE006138. https://doi.org/10.1029/2019JE006138

Fanara, L., Gwinner, K., Hauber, E., & Oberst, J. (2020). Present-day erosion rate of north polar scarps on Mars due to active mass wasting. *Icarus*, *342*, 113434. https://doi.org/10.1016/j.icarus.2019.113434

Fassett, C. I., Dickson, J. L., Head, J. W., Levy, J. S., & Marchant, D. R. (2010). Supraglacial and proglacial valleys on Amazonian Mars. *Icarus*, *208*(1), 86-100. https://doi.org/10.1016/j.icarus.2010.02.021

Fastook, J. L., & Head, J. W. (2014). Amazonian mid-to high-latitude glaciation on Mars: Supply-limited ice sources, ice accumulation patterns, and concentric crater fill glacial flow and ice sequestration. *Planetary and Space Science*, *91*, 60-76. https://doi.org/10.1016/j.pss.2013.12.002

Fastook, J. L., & Head, J. W. (2015). Glaciation in the Late Noachian Icy Highlands: Ice accumulation, distribution, flow rates, basal melting, and top-down melting rates and patterns. *Planetary and Space Science, 106*, 82-98.

Fedorova, A. A., Montmessin, F., Korablev, O., Luginin, M., Trokhimovskiy, A., Belyaev, D. A., ... & Wilson, C. F. (2020). Stormy water on Mars: The distribution and saturation of atmospheric water during the dusty season. *Science*, *367*(6475), 297-300. https://www.science.org/doi/10.1126/science.aay9522

Feldman, W. C., Boynton, W. V., Tokar, R. L., Prettyman, T. H., Gasnault, O., Squyres, S. W., ... & Reedy, R. C. (2002). Global distribution of neutrons from Mars: Results from Mars Odyssey. *Science, 297*(5578), 75-78. https://doi.org/10.1126/science.1073541

Feldman, W. C., Pathare, A., Maurice, S., Prettyman, T. H., Lawrence, D. J., Milliken, R. E., & Travis, B. J. (2011). Mars Odyssey neutron data: 2. Search for buried excess water ice deposits at nonpolar latitudes on Mars. *Journal of Geophysical Research: Planets, 116*(E11). https://doi.org/10.1029/2011JE003806

Feldman, W. C., Prettyman, T. H., Maurice, S., Plaut, J. J., Bish, D. L., Vaniman, D. T., ... & Tokar, R. L. (2004). Global distribution of near-surface hydrogen on Mars. *Journal of Geophysical Research: Planets*, *109*(E9). https://doi.org/10.1029/2003JE002160

Feng, J., Siegler, M. A., & Hayne, P. O. (2020). New constraints on thermal and dielectric properties of lunar regolith from LRO diviner and CE-2 microwave radiometer. *Journal of Geophysical Research: Planets*, *125*(1). https://doi.org/10.1029/2019JE006130

Fergason, R. L., Kirk, R. L., Cushing, G., Galuszka, D. M., Golombek, M. P., Hare, T. M., ... & Redding, B. L. (2017). Analysis of local slopes at the InSight landing site on Mars. *Space Science Reviews*, *211*(1), 109-133. https://doi.org/10.1007/s11214-016-0292-x

Fisher, D. A. (2005). A process to make massive ice in the martian regolith using long-term diffusion and thermal cracking. *Icarus*, *179*(2), 387-397. https://doi.org/10.1016/j.icarus.2005.07.024

Flynn, G. J. (1997). The contribution by interplanetary dust to noble gases in the atmosphere of Mars. *Journal of Geophysical Research: Planets*, *102*(E4), 9175-9182. https://doi.org/10.1029/96JE03883

Focardi, P., Spencer, M. W., & Piepmeier, J. R. (2016). SMAP instrument antenna, on orbit performance validation & verification. In 2016 *IEEE International Symposium on Antennas and Propagation (APSURSI)* (pp. 1371-1372). IEEE.

French, H. (2013). *The Periglacial Environment* (3rd ed.). Wiley. https://www.wiley.com/en-us/The+Periglacial+Environment%2C+3rd+Edition-p-9781118684948

Furuya, M., Suzuki, T., Maeda, J., & Heki, K. (2017). Midlatitude sporadic-E episodes viewed by L-band split-spectrum InSAR. *Earth, Planets and Space*, *69*(1), 1-10. https://doi.org/10.1186/s40623-017-0764-6

Gallagher, C., & Balme, M. (2015). Eskers in a complete, wet-based glacial system in the Phlegra Montes region, Mars. *Earth and Planetary Science Letters*, *431*, 96-109. https://doi.org/10.1016/j.epsl.2015.09.023

Gallagher, C., Butcher, F. E., Balme, M., Smith, I., & Arnold, N. (2021). Landforms indicative of regional warm based glaciation, Phlegra Montes, Mars. *Icarus*, *355*. https://doi.org/10.1016/j.icarus.2020.114173

Ganesh, I., Carter, L. M., & Smith, I. B. (2020). SHARAD mapping of Arsia Mons caldera. *Journal of Volcanology and Geothermal Research, 390*, 106748. https://doi.org/10.1016/j.jvolgeores.2019.106748

Garcia-Lopez, E., & Cid, C. (2017). Glaciers and ice sheets as analog environments of potentially habitable icy worlds. *Frontiers in microbiology*, *8*, 1407. https://doi.org/10.3389%2Ffmicb.2017.01407

Ghent, R. R., Carter, L. M., Bandfield, J. L., Udovicic, C. T., & Campbell, B. A. (2016). Lunar crater ejecta: Physical properties revealed by radar and thermal infrared observations. *Icarus*, *273*, 182-195. https://doi.org/10.1016/j.icarus.2015.12.014

Ghent, R. R., Gupta, V., Campbell, B. A., Ferguson, S. A., Brown, J. C. W., Fergason, R. L., & Carter, L. M. (2010). Generation and emplacement of fine-grained ejecta in planetary impacts. *Icarus*, *209*(2), 818-835. https://doi.org/10.1016/j.icarus.2010.05.005

Giardini, D., Lognonné, P., Banerdt, W. B., Pike, W. T., Christensen, U., Ceylan, S., ... & Yana, C. (2020). The seismicity of Mars. *Nature Geoscience*, *13*(3), 205-212. https://doi.org/10.1038/s41561-020-0539-8

Golombek, M. P., Arvidson, R. E., Bell, J. F., Christensen, P. R., Crisp, J. A., Crumpler, L. S., ... & Zurek, R. W. (2005). Assessment of Mars Exploration Rover landing site predictions. *Nature*, *436*(7047), 44-48. https://doi.org/10.1038/nature03600

Golombek, M. P., Cook, R. A., Moore, H. J., & Parker, T. J. (1997). Selection of the Mars Pathfinder landing site. *Journal of Geophysical Research: Planets*, *102*(E2), 3967-3988. https://doi.org/10.1029/96JE03318

Golombek, M., Grant, J., Kipp, D., Vasavada, A., Kirk, R., Fergason, R., ... & Watkins, M. (2012a). Selection of the Mars Science Laboratory landing site. *Space science reviews*, *170*(1), 641-737. https://doi.org/10.1007s11214-012SPAC875R1

Golombek, M. P., Grant, J. A., Parker, T. J., Kass, D. M., Crisp, J. A., Squyres, S. W., ... & Rice Jr, J. W. (2003a). Selection of the Mars Exploration Rover landing sites. *Journal of Geophysical Research: Planets*, *108*(E12), 8072. https://doi.org/10.1029/2003JE002074

Golombek, M., Grott, M., Kargl, G., Andrade, J., Marshall, J., Warner, N., ... & Banerdt, W. B. (2018). Geology and physical properties investigations by the InSight lander. *Space Science Reviews*, *214*(5), 1-52. https://doi.org/10.1007/s11214-018-0512-7

Golombek, M. P., Haldemann, A. F. C., Forsberg-Taylor, N. K., DiMaggio, E. N., Schroeder, R. D., Jakosky, B. M., ... & Matijevic, J. R. (2003b). Rock size-frequency distributions on Mars and implications for Mars Exploration Rover landing safety and operations. *Journal of Geophysical Research: Planets*, *108*(E12), 8086-8109. https://doi.org/10.1029/2002JE002035

Golombek, M. P., Haldemann, A. F. C., Simpson, R. A., Fergason, R. L., Putzig, N. E., Arvidson, R. E., ... & Mellon, M. T. (2008a). Martian surface properties from joint analysis of orbital, Earth-based, and surface observations. In J. F. Bell III (Ed.), *The martian surface-composition, mineralogy, and physical properties* (pp. 468-497). https://doi.org/10.1017/CBO9780511536076.022

Golombek, M. P., Huertas, A., Marlow, J., McGrane, B., Klein, C., Martinez, M., ... & Cheng, Y. (2008b). Size-frequency distributions of rocks on the northern plains of Mars with special reference to Phoenix landing surfaces. *Journal of Geophysical Research: Planets*, *113*(E3). https://doi.org/10.1029/2007JE003065

Golombek, M., Huertas, A., Kipp, D., & Calef, F. (2012b). Detection and characterization of rocks and rock size-frequency distributions at the final four Mars Science Laboratory landing sites. *International Journal of Mars Science and Exploration*, *7*, 1-22. DOI:10.1555/mars.2012.0001 Retrieved from: http://www.marsjournal.org/contents/2012/0001/files/golombek_mars_2012_0001.pdf

Golombek, M., Kass, D., Williams, N., Warner, N., Daubar, I., Piqueux, S., ... & Pike, W. T. (2020a). Assessment of InSight landing site predictions. *Journal of Geophysical Research: Planets*, *125*(8). https://dx.doi.org/10.1029/2020JE006502

Golombek, M., Kipp, D., Warner, N., Daubar, I. J., Fergason, R., Kirk, R. L., ... & Banerdt, W. B. (2017). Selection of the InSight landing site. *Space Science Reviews*, *211*(1), 5-95. https://doi.org/10.1007/s11214-016-0321-9

Golombek, M. P., Trussell, A., Williams, N., Charalambous, C., Abarca, H., Warner, N. H., ... & Deen, R. (2021). Rock Size-Frequency Distributions at the InSight Landing Site, Mars. *Earth and Space Science*, *8*(12). https://doi.org/10.1029/2021EA001959

Golombek, M., Williams, N., Grip, H., Tzanetos, T., Balaram, J., Maki, J., ... & Bell, J. (2022). Mars Helicopter, Ingenuity: Operations and Initial Results. *LPI Contributions*, *2678*, 2156. Retrieved from: https://ui.adsabs.harvard.edu/abs/2022LPICo2678.2156G/abstract

Golombek, M., Williams, N., Warner, N. H., Parker, T., Williams, M. G., Daubar, I., ... & Sklyanskiy, E. (2020b). Location and setting of the Mars InSight lander, instruments, and landing site. *Earth and Space Science*, *7*(10). https://doi.org/10.1029/2020EA001248

Gomba, G., Parizzi, A., De Zan, F., Eineder, M., & Bamler, R. (2016). Toward operational compensation of ionospheric effects in SAR interferograms: The split-spectrum method. *IEEE Transactions on Geoscience and Remote Sensing*, *54*(3), 1446-1461. https://doi.org/10.1109/TGRS.2015.2481079

Grant, J. A., Golombek, M. P., Grotzinger, J., et al., (2011), The science process for selecting landing sites for the Mars Science Laboratory. *Planetary and Space Science*, *59*(11-12), 1114–1127. https://doi.org/10.1016/j.pss.2010.06.016

Grant, J. A., Golombek, M. P., Parker, T. J., Crisp, J. A., Squyres, S. W., & Weitz, C. M. (2004). Selecting landing sites for the 2003 Mars Exploration Rovers. *Planetary and Space Science*, *52*(1-3), 11-21. https://doi.org/10.1016/j.pss.2003.08.011

Grant, J. A., Golombek, M. P., Wilson, S. A., Farley, K. A., Williford, K. H., & Chen, A. (2018). The science process for selecting the landing site for the 2020 Mars rover. *Planetary and Space Science*, *164*, 106-126. https://doi.org/10.1016/j.pss.2018.07.001

Grant, J. A., & Schultz, P. H. (1990). Gradational epochs on Mars: Evidence from west-northwest of Isidis Basin and Electris. *Icarus, 84*(1), 166-195. https://doi.org/10.1016/0019-1035(90)90164-5

Grant, J. A., & Wilson, S. A. (2011). Late alluvial fan formation in southern Margaritifer Terra, Mars. *Geophysical Research Letters*, *38*(8). https://doi.org/10.1029/2011GL046844

Grant, J. A., & Wilson, S. A. (2012). A possible synoptic source of water for alluvial fan formation in southern Margaritifer Terra, Mars. *Planetary and Space Science*, *72*(1), 44-52. https://doi.org/10.1016/j.pss.2012.05.020

Grant, J. A., & Wilson, S. A. (2019). Evidence for late alluvial activity in Gale crater, Mars. *Geophysical Research Letters*, *46*(13), 7287-7294. https://doi.org/10.1029/2019GL083444

Grant, J.A., Wilson, S.A., Fortezzo, C.M., and Clark, D.A. (2009). Geologic map of MTM-20012 and -25012 quadrangles, Margaritifer Terra region of Mars: U.S. Geological Survey Scientific Investigations Map 3041, 1:500,000. https://doi.org/10.3133/sim3041

Grant, J. A., Wilson, S. A., Mangold, N., Calef III, F., & Grotzinger, J. P. (2014). The timing of alluvial activity in Gale crater, Mars. *Geophysical Research Letters*, *41*(4), 1142-1149. https://doi.org/10.1002/2013GL058909

Grant, J. A., Wilson, S. A., Noe Dobrea, E., Fergason, R. L., Griffes, J. L., Moore, J. M., & Howard, A. D. (2010b). HiRISE views an enigmatic deposit in the Electris region of Mars. *Icarus, 205*, 53-63. https://doi.org/10.1016/j.icarus.2009.04.009

Grau Galofre, A., Jellinek, A. M., & Osinski, G. R. (2020). Valley formation on early Mars by subglacial and fluvial erosion. *Nature Geoscience, 13*(10), 663-668. https://doi.org/10.1038/s41561-020-0618-x

Gray, A. L., Mattar, K. E., Vachon, P. W., Bindschadler, R., Jezek, K. C., … & Crawford, J. P. (1998, July). InSAR results from the RADARSAT Antarctic Mapping Mission data: estimation of glacier motion using a simple registration procedure. In *IGARSS'98. Sensing and Managing the Environment. 1998 IEEE International Geoscience and Remote Sensing. Symposium Proceedings.(Cat. No. 98CH36174)* (Vol. 3, pp. 1638-1640). IEEE. DOI: 10.1109/IGARSS.1998.691662 Retrieved from: https://ieeexplore.ieee.org/document/691662

Grima, C. (2014a). Comments on "An inversion of planetary rough surface permittivity from radar sounder observations". *IEEE Antennas and Wireless Propagation Letters*, *13*, 1812-1813. https://doi.org/10.1109/LAWP.2014.2329414

Grima, C., Greenbaum, J. S., Lopez Garcia, E. J., Soderlund, K. M., Rosales, A., Blankenship, D. D., & Young, D. A. (2016). Radar detection of the brine extent at McMurdo Ice Shelf, Antarctica, and its control by snow accumulation. *Geophysical Research Letters*, *43*(13), 7011-7018. https://doi.org/10.1002/2016GL069524

Grima, C., Kofman, W., Herique, A., Orosei, R., & Seu, R. (2012). Quantitative analysis of Mars surface radar reflectivity at 20 MHz. *Icarus*, *220*(1), 84-99. https://doi.org/10.1016/j.icarus.2012.04.017.

Grima, C., Kofman, W., Mouginot, J., Phillips, R. J., Hérique, A., Biccari, D., ... & Cutigni, M. (2009). North polar deposits of Mars: Extreme purity of the water ice. *Geophysical Research Letters*, *36*(3), L03203. https://doi.org/10.1029/2008GL036326

Grima, C., Mouginot, J., Kofman, W., Hérique, A., & Beck, P. (2022). The Basal Detectability of an Ice-Covered Mars by MARSIS. *Geophysical Research Letters*, *49*(2). https://doi.org/10.1029/2021gl096518

Grima, C., Schroeder, D. M., Blankenship, D. D., & Young, D. A. (2014b). Planetary landing-zone reconnaissance using ice-penetrating radar data: Concept validation in Antarctica. *Planetary and Space Science*, *103*, 191-204. https://doi.org/10.1016/j.pss.2014.07.018

Grimm, R. E., Harrison, K. P., Stillman, D. E., & Kirchoff, M. R. (2017). On the secular retention of ground water and ice on Mars. *Journal of Geophysical Research: Planets*, *122*(1), 94-109. https://doi.org/10.1002/2016JE005132

Grotzinger, J. P., Sumner, D. Y., Kah, L. C., Stack, K., Gupta, S., Edgar, L., ... & Sirven, J. B. (2014). A habitable fluvio-lacustrine environment at Yellowknife Bay, Gale Crater, Mars. *Science*, *343*(6169), 1242777. https://doi.org/10.1126/science.1242777.

Grotzinger, J. P., Gupta, S., Malin, M. C., Rubin, D. M., Schieber, J., Siebach, K., ... & Wilson, S. A. (2015). Deposition, exhumation, and paleoclimate of an ancient lake deposit, Gale crater, Mars. *Science*, *350*(6257), aac7575. https://doi.org/10.1126/science.aac7575

Hansen, C. J., Thomas, N., Portyankina, G., McEwen, A., Becker, T., Byrne, S., ... & Mellon, M. (2010). HiRISE observations of gas sublimation-driven activity in Mars' southern polar regions: I. Erosion of the surface. *Icarus*, 205(1), 283-295. https://doi.org/10.1016/j.icarus.2009.07.021

Hapke, B. (1990). Coherent backscatter and the radar characteristics of outer planet satellites, *Icarus, 88*, 407–417. https://doi.org/10.1016/0019-1035(90)90091-M

Harmon, J. K., Nolan, M. C., Husmann, D. I., & Campbell, B. A. (2012). Arecibo radar imagery of Mars: The major volcanic provinces. *Icarus*, *220*(2), 990-1030. https://doi.org/10.1016/j.icarus.2009.07.021

Harmon, J. K., Perillat, P. J., & Slade, M. A. (2001). High-resolution radar imaging of Mercury's north pole. *Icarus*, *149*(1), 1-15. https://doi.org/10.1006/icar.2000.6544

Hartmann, W. K. (2005). Martian cratering 8: Isochron refinement and the chronology of Mars. *Icarus, 174*(2), 294-320. https://doi.org/10.1016/j.icarus.2004.11.023

Hartmann, W. K., & Daubar, I. J. (2017). Martian cratering 11. Utilizing decameter scale crater populations to study Martian history. *Meteoritics & Planetary Science, 52*(3), 493-510. https://doi.org/10.1111/maps.12807

Hassler, D. M., Zeitlin, C., Wimmer-Schweingruber, R. F., Ehresmann, B., Rafkin, S., Eigenbrode, J. L., ... & Berger, G. (2014). Mars' surface radiation environment measured with the Mars Science Laboratory's Curiosity rover. *Science*, *343*(6169), 1244797. DOI: 10.1126/science.1244797

Havivi, S., Amir, D., Schvartzman, I., August, Y., Maman, S., Rotman, S. R., & Blumberg, D. G. (2018). Mapping dune dynamics by InSAR coherence. *Earth Surface Processes and Landforms*, *43*(6), 1229-1240. https://doi.org/10.1002/esp.4309

Head, J. W., Marchant, D. R., Dickson, J. L., Kress, A. M., & Baker, D. M. (2010). Northern mid-latitude glaciation in the Late Amazonian period of Mars: Criteria for the recognition of debris-covered glacier and valley glacier landsystem deposits. *Earth and Planetary Science Letters*, *294*(3-4), 306-320. https://doi.org/10.1016/j.epsl.2009.06.041

Head, J. W., Mustard, J. F., Kreslavsky, M. A., Milliken, R. E., & Marchant, D. R. (2003). Recent ice ages on Mars. *Nature*, *426*(6968), 797-802. https://doi.org/10.1038/nature02114

Head, J. W., Neukum, G., Jaumann, R., Hiesinger, H., Hauber, E., Carr, M., ... & Van Gasselt, S. (2005). Tropical to mid-latitude snow and ice accumulation, flow and glaciation on Mars. *Nature, 434*(7031), 346-351. https://doi.org/10.1038/nature03359

Hecht, M. H., Kounaves, S. P., Quinn, R. C., West, S. J., Young, S. M., Ming, D. W.,... & Smith, P. H. (2009). Detection of perchlorate and the soluble chemistry of martian soil at the Phoenix lander site. *Science*, *325*(5936), 64-67. https://doi.org/10.1126/science.1172466

Heet, T. L., Arvidson, R. E., Cull, S. C., Mellon, M. T., & Seelos, K. D. (2009). Geomorphic and geologic settings of the Phoenix Lander mission landing site. *Journal of Geophysical Research: Planets*, *114*(E1). https://doi.org/10.1029/2009JE003416

Hepburn, A. J., Ng, F. S. L., Livingstone, S. J., Holt, T. O., & Hubbard, B. (2020). Polyphase mid-latitude glaciation on Mars: Chronology of the formation of superposed glacier-like forms from crater-count dating. *Journal of Geophysical Research: Planets*, *125*(2). https://doi.org/10.1029/2019JE006102

Herkenhoff, K. E., & Plaut, J. J. (2000). Surface ages and resurfacing rates of the polar layered deposits on Mars. *Icarus*, *144*(2), 243-253. https://doi.org/10.1006/icar.1999.6287

Hibbard, S. M., Williams, N. R., Golombek, M. P., Osinski, G. R., & Godin, E. (2021). Evidence for widespread glaciation in Arcadia Planitia, Mars. *Icarus*, *359*, 114298. https://doi.org/10.1016/j.icarus.2020.114298

Hoffman, S. J., Andrews, A., Joosten, B. K., & Watts, K. (2017, March). A water rich Mars surface mission scenario. In *2017 IEEE Aerospace Conference* (pp. 1-21). IEEE. https://doi.org/10.1109/AERO.2017.7943911

Holt, J. W., Safaeinili, A., Plaut, J. J., Head, J. W., Phillips, R. J., Seu, R., ... & Gim, Y. (2008). Radar sounding evidence for buried glaciers in the southern mid-latitudes of Mars. *Science*, *322*(5905), 1235-1238. https://doi.org/10.1126/science.1164246

Horvath, D. G., Moitra, P., Hamilton, C. W., Craddock, R. A., & Andrews-Hanna, J. C. (2021). Evidence for geologically recent explosive volcanism in Elysium Planitia, Mars. *Icarus*, *365*, 114499. https://doi.org/10.1016/j.icarus.2021.114499.

Hu, R. (2019). Predicted diurnal variation of the deuterium to hydrogen ratio in water at the surface of Mars caused by mass exchange with the regolith. *Earth and Planetary Science Letters*, *519*, 192-201. https://doi.org/10.1016/j.epsl.2019.05.017

Hubbard, B., Milliken, R. E., Kargel, J. S., Limaye, A., & Souness, C. (2011). Geomorphological characterisation and interpretation of a mid-latitude glacier-like form: Hellas Planitia, Mars. *Icarus*, *211*(1), 330-346. https://doi.org/10.1016/j.icarus.2010.10.021

Hvidberg, C. S., Fishbaugh, K. E., Winstrup, M., Svensson, A., Byrne, S., & Herkenhoff, K. E. (2012). Reading the climate record of the Martian polar layered deposits. *Icarus, 221*(1), 405-419. https://doi.org/10.1016/j.icarus.2012.08.009

Irwin III, R. P., & Grant, J. A. (2013). Geologic map of MTM-15027,-20027,-25027, and-25032 quadrangles, Margaritifer Terra region of Mars. *US Geological Survey Scientific Investigations Map*, *3209*. https://doi.org/10.3133/sim3209

Jaeger, W. L., Keszthelyi, L. P., Skinner Jr, J. A., Milazzo, M. P., McEwen, A. S., Titus, T. N., ... & Kirk, R. L. (2010). Emplacement of the youngest flood lava on Mars: A short, turbulent story. *Icarus, 205*(1), 230-243. https://doi.org/10.1016/j.icarus.2009.09.011

Jakosky, B. M. (2019). The CO_2 inventory on Mars. *Planetary and Space Science, 175*, 52-59. https://doi.org/10.1016/j.pss.2019.06.002

Jakosky, B. M., & Farmer, C. B. (1982). The seasonal and global behavior of water vapor in the Mars atmosphere: Complete global results of the Viking atmospheric water detector experiment. *Journal of Geophysical Research: Solid Earth, 87*(B4), 2999-3019. https://doi.org/10.1029/JB087iB04p02999

Jakosky, B. M., Grebowsky, J. M., Luhmann, J. G., Connerney, J., Eparvier, F., Ergun, R., ... & Yelle, R. (2015). MAVEN observations of the response of Mars to an interplanetary coronal mass ejection. *Science*, *350*(6261). DOI: 10.1126/science.aad0210

Jakosky, B.M., Slipski, M., Benna, M., Mahaffy, P., Elrod, M., Yelle, R., Stone, S., Alsaeed, N., (2017). Mars' atmospheric history derived from upper-atmosphere measurements of $^{38}Ar/^{36}Ar$. *Science, 355*(6332), 1408–1410. https://doi.org/10.1126/science.aai7721

JeongAhn, Y., & Malhotra, R. (2015). The current impact flux on Mars and its seasonal variation. *Icarus*, *262*, 140-153. https://doi.org/10.1016/j.icarus.2015.08.032

Jolitz, R. D., Dong, C. F., Rahmati, A., Brain, D. A., Lee, C. O., Lillis, R. J., ... & Jakosky, B. M. (2021). Test particle model predictions of SEP electron transport and precipitation at Mars. *Journal of Geophysical Research: Space Physics*, *126*(8). https://doi.org/10.1029/2021JA029132

Kang, Y., Zhao, C., Zhang, Q., Lu, Z., & Li, B. (2017). Application of InSAR techniques to an analysis of the Guanling landslide. *Remote sensing*, *9*(10), 1046. https://doi.org/10.3390/rs9101046

Kedar, S., Panning, M. P., Smrekar, S. E., Stähler, S. C., King, S. D., Golombek, M. P., ... & Banerdt, W. B. (2021). Analyzing low frequency seismic events at Cerberus Fossae as long period volcanic quakes. *Journal of Geophysical Research: Planets*, *126*(4). https://doi.org/10.1029/2020JE006518

Kerber, L., & Head, J.W. (2010). The age of the Medusae Fossae Formation: Evidence of Hesperian emplacement from crater morphology, stratigraphy, and ancient lava contacts. *Icarus, 206*(2), 669-684. https://doi.org/10.1016/j.icarus.2009.10.001

Kieffer, H. H., Christensen, P. R., & Titus, T. N. (2006). CO_2 jets formed by sublimation beneath translucent slab ice in Mars' seasonal south polar ice cap. *Nature*, *442*(7104), 793-796. https://doi.org/10.1038/nature04945

Kieffer, H. H., & Titus, T. N. (2001). TES mapping of Mars' north seasonal cap. *Icarus, 154*(1), 162-180. https://doi.org/10.1006/icar.2001.6670

Kilic, L., Prigent, C., Aires, F., Boutin, J., Heygster, G., Tonboe, R. T., ... & Donlon, C. (2018). Expected performances of the Copernicus Imaging Microwave Radiometer (CIMR) for an all-weather and high spatial resolution estimation of ocean and sea ice parameters. *Journal of Geophysical Research: Oceans, 123*(10), 7564-7580. https://doi.org/10.1029/2018JC014408

Kirk, R. L., Howington-Kraus, E., Rosiek, M. R., Anderson, J. A., Archinal, B. A., Becker, K. J., ... & McEwen, A. S. (2008). Ultrahigh resolution topographic mapping of Mars with MRO HiRISE stereo images: Meter-scale slopes of candidate Phoenix landing sites. *Journal of Geophysical Research: Planets*, *113*(E3). https://doi.org/10.1029/2007JE003000

Kleinböhl, A., Schofield, J. T., Abdou, W. A., Irwin, P. G., & De Kok, R. J. (2011). A single-scattering approximation for infrared radiative transfer in limb geometry in the Martian atmosphere. *Journal of Quantitative Spectroscopy and Radiative Transfer*, *112*(10). https://doi.org/10.1016/j.jqsrt.2011.03.006

Kleinböhl, A., Friedson, A. J., & Schofield, J. T. (2017). Two-dimensional radiative transfer for the retrieval of limb emission measurements in the Martian atmosphere. *Journal of Quantitative Spectroscopy and Radiative Transfer*, *187*, 511-522. https://doi.org/10.1016/j.jqsrt.2016.07.009

Kleinböhl, A., Schofield, J. T., Kass, D. M., & McCleese, D. J. (2016, October). The Advanced Mars Climate Sounder (AMCS)-A Proven Atmospheric Profiler for Future Mars Orbiters. In *3rd International Workshop on Instrumentation for Planetary Mission* (Vol. 1980, p. 4066). Retrieved from: https://ui.adsabs.harvard.edu/abs/2016LPICo1980.4066K/abstract

Koop, T. (2002). The water activity of aqueous solutions in equilibrium with ice. *Bulletin of the Chemical Society of Japan*, *75*(12), 2587-2588. https://doi.org/10.1246/bcsj.75.2587

Kostama, V. P., Kreslavsky, M. A., & Head, J. W. (2006). Recent high-latitude icy mantle in the northern plains of Mars: Characteristics and ages of emplacement. *Geophysical Research Letters*, *33*(11). https://doi.org/10.1029/2006GL025946

Kowalewski, D. E., Marchant, D. R., Levy, J. S., & Head, J. W. (2006). Quantifying low rates of summertime sublimation for buried glacier ice in Beacon Valley, Antarctica. *Antarctic Science*, *18*(3), 421-428. https://doi.org/10.1017/S0954102006000460

Kowalewski, D. E., Marchant, D. R., Head III, J. W., & Jackson, D. W. (2012). A 2D model for characterising first-order variability in sublimation of buried glacier ice, Antarctica: Assessing the influence of polygon troughs, desert pavements and shallow subsurface salts. *Permafrost and Periglacial Processes*, *23*(1), 1-14. https://doi.org/10.1002/ppp.731

Kreslavsky, M. A. (2022). Seasonal Brine Formation in Shallow Subsurface on Mars. LPI Contributions, 2678, 2628. https://www.hou.usra.edu/meetings/lpsc2022/pdf/2628.pdf

Kreslavsky, M. A., & Head III, J. W. (2002). Mars: Nature and evolution of young latitude-dependent water-ice-rich mantle. Geophysical Research Letters, 29(15), 14-1. https://doi.org/10.1029/2002GL015392

Kreslavsky, M. A., Head, J. W., & Marchant, D. R. (2008). Periods of active permafrost layer formation during the geological history of Mars: Implications for circum-polar and mid-latitude surface processes. *Planetary and Space Science*, *56*(2), 289-302. https://doi.org/10.1016/j.pss.2006.02.010

Kress, A. M., & Head, J. W. (2015). Late Noachian and early Hesperian ridge systems in the south circumpolar Dorsa Argentea Formation, Mars: Evidence for two stages of melting of an extensive late Noachian ice sheet. *Planetary and Space Science*, *109*, 1-20. https://doi.org/10.1016/j.pss.2014.11.025

Kumar, P. S., Krishna, N., Lakshmi, K. P., Raghukanth, S. T. G., Dhabu, A., & Platz, T. (2019). Recent seismicity in Valles Marineris, Mars: Insights from young faults, landslides, boulder falls and possible mud volcanoes. *Earth and Planetary Science Letters*, *505*, 51-64. https://doi.org/10.1016/j.epsl.2018.10.008

Kurokawa, H., Kuroda, T., Aoki, S., & Nakagawa, H. (2022). Can we constrain the origin of Mars' recurring slope lineae using atmospheric observations?. *Icarus*, *371*, 114688. https://doi.org/10.1016/j.icarus.2021.114688

Kurokawa, H., Miura, Y. N., Sugita, S., Cho, Y., Leblanc, F., Terada, N., & Nakagawa, H. (2021). Mars' atmospheric neon suggests volatile-rich primitive mantle. *Icarus*, *370*, 114685. https://doi.org/10.1016/j.icarus.2021.114685

Lacelle, D., Davila, A. F., Fisher, D., Pollard, W. H., DeWitt, R., Heldmann, J., ... & McKay, C. P. (2013). Excess ground ice of condensation–diffusion origin in University Valley, Dry Valleys of Antarctica: Evidence from isotope geochemistry and numerical modeling. *Geochimica et Cosmochimica Acta*, *120*, 280-297. https://doi.org/10.1016/j.gca.2013.06.032

Lalich, D. E., Holt, J. W., & Smith, I. B. (2019). Radar reflectivity as a proxy for the dust content of individual layers in the Martian north polar layered deposits. *Journal of Geophysical Research: Planets*, *124*(7), 1690-1703. https://doi.org/10.1029/2018JE005787

Langlais, B., Thébault, E., Houliez, A., Purucker, M. E., & Lillis, R. J. (2019). A new model of the crustal magnetic field of Mars using MGS and MAVEN. *Journal of Geophysical Research: Planets*, *124*(6), 1542-1569. https://doi.org/10.1029/2018JE005854

Laskar, J., Levrard, B., & Mustard, J. F. (2002). Orbital forcing of the Martian polar layered deposits. Nature, 419(6905), 375-377. https://doi.org/10.1038/nature01066

Leask, E. K., Ehlmann, B. L., Dundar, M. M., Murchie, S. L., & Seelos, F. P. (2018). Challenges in the search for perchlorate and other hydrated minerals with 2.1-μm absorptions on Mars. *Geophysical research letters*, *45*(22), 12-180. https://doi.org/10.1029/2018GL080077

Lee, C. O., Jakosky, B. M., Luhmann, J. G., Brain, D. A., Mays, M. L., Hassler, D. M., ... & Halekas, J. S. (2018). Observations and impacts of the 10 September 2017 solar events at Mars: An overview and synthesis of the initial results. *Geophysical Research Letters*, *45*(17), 8871-8885. https://doi.org/10.1029/2018GL079162

Lefort, A., Russell, P. S., & Thomas, N. (2010). Scalloped terrains in the Peneus and Amphitrites Paterae region of Mars as observed by HiRISE. Icarus, 205(1), 259-268. https://doi.org/10.1016/j.icarus.2009.06.005

Leinss, S., & Bernhard, P. (2021). TanDEM-X: Deriving InSAR height changes and velocity dynamics of great aletsch glacier. *IEEE Journal of Selected Topics in Applied Earth Observations and Remote Sensing*, *14*, 4798-4815. doi: 10.1109/JSTARS.2021.3078084

Léveillé, R. J., & Datta, S. (2010). Lava tubes and basaltic caves as astrobiological targets on Earth and Mars: a review. *Planetary and Space Science*, *58*(4), 592-598. https://doi.org/10.1016/j.pss.2009.06.004

Levrard, B., Forget, F., Montmessin, F., & Laskar, J. (2007). Recent formation and evolution of northern Martian polar layered deposits as inferred from a Global Climate Model. *Journal of Geophysical Research: Planets*, *112*(E6). https://doi.org/10.1029/2006JE002772

Levy, J. S., Fassett, C. I., Head, J. W., Schwartz, C., & Watters, J. L. (2014). Sequestered glacial ice contribution to the global Martian water budget: Geometric constraints on the volume of remnant, midlatitude debris-covered glaciers. Journal of Geophysical Research: Planets, 119(10), 2188-2196. https://doi.org/10.1002/2014JE004685

Levy, J. S., Fassett, C. I., Holt, J. W., Parsons, R., Cipolli, W., Goudge, T. A., ... & Armstrong, I. (2021). Surface boulder banding indicates Martian debris-covered glaciers formed over multiple glaciations. *Proceedings of the National Academy of Sciences*, *118*(4). https://doi.org/10.1073/pnas.2015971118

Levy, J., Head, J., & Marchant, D. (2009). Thermal contraction crack polygons on Mars: Classification, distribution, and climate implications from HiRISE observations. *Journal of Geophysical Research: Planets*, *114*(E1). https://doi.org/10.1029/2008JE003273

Lillis, R. J., Mitchell, D., Montabone, L., Heavens, N., Harrison, T., Stuurman, C., ... & Tripathi, A. (2021). MOSAIC: A Satellite Constellation to Enable Groundbreaking Mars Climate System Science and Prepare for Human Exploration. The Planetary Science Journal, 2(5), 211. https://doi.org/10.3847/PSJ/ac0538

Lucchitta, B. K. (1984). Ice and debris in the fretted terrain, Mars. Journal of Geophysical Research: Solid Earth, 89(S02), B409-B418. https://doi.org/10.1029/JB089iS02p0B409

Magnuson, E., Altshuler, I., Fernández-Martínez, M. Á., Chen, Y. J., Maggiori, C., Goordial, J., & Whyte, L. G. (2022). Active lithoautotrophic and methane-oxidizing microbial community in an anoxic, sub-zero, and hypersaline High Arctic spring. *The ISME Journal*, 1-11. https://doi.org/10.1038/s41396-022-01233-8

Mahaffy, P. R., Webster, C. R., Cabane, M., Conrad, P. G., Coll, P., Atreya, S. K., ... & Mumm, E. (2012). The sample analysis at Mars investigation and instrument suite. *Space Science Reviews*, *170*(1), 401-478. https://doi.org/10.1007/s11214-012-9879-z

Malin, M. C., Bell III, J. F., Cantor, B. A., Caplinger, M. A., Calvin, W. M., Clancy, R. T., ... & Wolff, M. J. (2007). Context camera investigation on board the Mars Reconnaissance Orbiter. *Journal of Geophysical Research: Planets*, *112*(E5). https://doi.org/10.1029/2006JE002808

Malin, M. C., Edgett, K. S., Posiolova, L. V., McColley, S. M., & Dobrea, E. Z. N. (2006). Present-day impact cratering rate and contemporary gully activity on Mars. *science*, *314*(5805), 1573-1577. https://doi.org/10.1126/science.1135156

Mangold, N. (2005). High latitude patterned grounds on Mars: Classification, distribution and climatic control. *Icarus*, *174*(2), 336-359. https://doi.org/10.1016/j.icarus.2004.07.030

Mangold, N., Adeli, S., Conway, S., Ansan, V., & Langlais, B. (2012). A chronology of early Mars climatic evolution from impact crater degradation. *Journal of Geophysical Research: Planets*, *117*(E4). https://doi.org/10.1029/2011JE004005

Mangold, N., Allemand, P., Duval, P., Geraud, Y., & Thomas, P. (2002). Experimental and theoretical deformation of ice–rock mixtures: Implications on rheology and ice content of Martian permafrost. *Planetary and Space Science, 50*(4), 385-401. https://doi.org/10.1016/S0032-0633(02)00005-3

Mangold, N., Maurice, S., Feldman, W. C., Costard, F., & Forget, F. (2004). Spatial relationships between patterned ground and ground ice detected by the Neutron Spectrometer on Mars. *Journal of Geophysical Research: Planets, 109*(E8). https://doi.org/10.1029/2004JE002235

Martin, W., & Russell, M. J. (2003). On the origins of cells: a hypothesis for the evolutionary transitions from abiotic geochemistry to chemoautotrophic prokaryotes, and from prokaryotes to nucleated cells. *Philosophical Transactions of the Royal Society of London. Series B: Biological Sciences*, *358*(1429), 59-85. https://doi.org/10.1098/rstb.2002.1183

Martínez, G. M., Newman, C. N., Vicente-Retortillo, D., Fischer, E., Renno, N. O., Richardson, M. I., ... & Vasavada, A. R. (2017). The modern near-surface Martian climate: a review of in-situ meteorological data from Viking to Curiosity. *Space Science Reviews*, *212*(1), 295-338. https://doi.org/10.1007/s11214-017-0360-x

Marty, B. (2012). The origins and concentrations of water, carbon, nitrogen and noble gases on Earth. *Earth and Planetary Science Letters*, *313*, 56-66. https://doi.org/10.1016/j.epsl.2011.10.040

Massé, M., Conway, S. J., Gargani, J., Patel, M. R., Pasquon, K., Mcewen, A., ... & Jouannic, G. (2016). Transport processes induced by metastable boiling water under Martian surface conditions. *Nature Geoscience*, *9*(6), 425-428. https://doi.org/10.1038/ngeo2706

Massonnet, D., & Feigl, K. L. (1998). Radar interferometry and its application to changes in the Earth's surface. Reviews of Geophysics, 36(4), 441-500. https://doi.org/10.1029/97RG03139

McCauley, J. F., Schaber, G. G., Breed, C. S., Grolier, M. J., Haynes, C. V., Issawi, B., ... & Blom, R. (1982). Subsurface valleys and geoarcheology of the eastern Sahara revealed by shuttle radar. *Science*, *218*(4576), 1004-1020. https://doi.org/10.1126/science.218.4576.1004

McCleese, D. J., Schofield, J. T., Taylor, F. W., Calcutt, S. B., Foote, M. C., Kass, D. M., ... & Zurek, R. W. (2007). Mars Climate Sounder: An investigation of thermal and water vapor structure, dust and condensate distributions in the atmosphere, and energy balance of the polar regions. *Journal of Geophysical Research: Planets*, *112*(E5). https://doi.org/10.1029/2006JE002790

McEwen, A. S., Eliason, E. M., Bergstrom, J. W., Bridges, N. T., Hansen, C. J., Delamere, W. A., ... & Weitz, C. M. (2007). Mars reconnaissance orbiter's high resolution imaging science experiment (HiRISE). *Journal of Geophysical Research: Planets*, *112*(E5). https://doi.org/10.1029/2005JE002605

McEwen, A. S., Ojha, L., Dundas, C. M., Mattson, S. S., Byrne, S., Wray, J. J., ... & Gulick, V. C. (2011). Seasonal flows on warm Martian slopes. *science*, *333*(6043), 740-743. https://doi.org/10.1126/science.1204816

McEwen, A. S., Dundas, C. M., Mattson, S. S., Toigo, A. D., Ojha, L., Wray, J. J., ... & Thomas, N. (2014). Recurring slope lineae in equatorial regions of Mars. *Nature geoscience*, *7*(1), 53-58. https://doi.org/10.1038/ngeo2014

McKay, C. P. (2009). Snow recurrence sets the depth of dry permafrost at high elevations in the McMurdo Dry Valleys of Antarctica. *Antarctic Science*, *21*(1), 89-94. https://doi.org/10.1017/S0954102016000572

McKay, C. P., Mellon, M. T., & Friedmann, E. I. (1998). Soil temperatures and stability of ice-cemented ground in the McMurdo Dry Valleys, Antarctica. *Antarctic Science*, *10*(1), 31-38. https://doi.org/10.1017/s0954102098000054

McNeil, J. D., Fawdon, P., Balme, M. R., & Coe, A. L. (2021). Morphology, morphometry and distribution of isolated landforms in southern Chryse Planitia, Mars. *Journal of Geophysical Research: Planets*, *126*(5). https://doi.org/10.1029/2020JE006775

Mellon, M. T. (1997). Small-scale polygonal features on Mars: Seasonal thermal contraction cracks in permafrost. *Journal of Geophysical Research: Planets*, *102*(E11), 25617-25628. https://doi.org/10.1029/97JE02582

Mellon, M. T., Arvidson, R. E., Sizemore, H. G., Searls, M. L., Blaney, D. L., Cull, S., ... & Zent, A. P. (2009). Ground ice at the Phoenix landing site: Stability state and origin. *Journal of Geophysical Research: Planets, 114*(E1). https://doi.org/10.1029/2009JE003417

Mellon, M. T., Feldman, W. C., & Prettyman, T. H. (2004). The presence and stability of ground ice in the southern hemisphere of Mars. *Icarus*, *169*(2), 324-340. https://doi.org/10.1016/j.icarus.2003.10.022

Mellon, M. T., & Jakosky, B. M. (1993). Geographic variations in the thermal and diffusive stability of ground ice on Mars. *Journal of Geophysical Research: Planets*, *98*(E2), 3345-3364. https://doi.org/10.1029/92JE02355

Mellon, M. T., & Jakosky, B. M. (1995). The distribution and behavior of Martian ground ice during past and present epochs. *Journal of Geophysical Research: Planets*, *100*(E6), 11781-11799. https://doi.org/10.1029/95JE01027

Mellon, M. T., Mckay, C. P., & Heldmann, J. L. (2014). Polygonal ground in the McMurdo Dry Valleys of Antarctica and its relationship to ice-table depth and the recent Antarctic climate history. Antarctic Science, 26(4), 413-426. https://doi.org/10.1017/S0954102013000710

MEPAG ICE-SAG. (2019). Report from the ice and climate evolution science analysis group (ICE-SAG). Mars Exploration Program Analysis Group (MEPAG). Retrieved from https://mepag.jpl.nasa.gov/reports/ICESAG_Report_FINAL.pdf

MEPAG NEX-SAG. (2015). Report from the next orbiter science analysis group (NEX-SAG). Mars Exploration Program Analysis Group (MEPAG). Retrieved from: https://mepag.jpl.nasa.gov/reports/NEX-SAG_draft_v29_FINAL.pdf

Michalski, J. R., Dobrea, E. Z. N., Niles, P. B., & Cuadros, J. (2017). Ancient hydrothermal seafloor deposits in Eridania basin on Mars. *Nature communications*, *8*(1), 1-10. doi.org/10.1038/ncomms15978

Mishchenko, M. I. (1992). The angular width of the coherent backscatter opposition effect: An application to icy outer planet satellites, *Astrophysics and Space Science, 194*(2), 327–333, https://doi.org/10.1007/BF00644001

Miyamoto, H., Haruyama, J. I., Kobayashi, T., Suzuki, K., Okada, T., Nishibori, T., ... & Masumoto, K. (2005). Mapping the structure and depth of lava tubes using ground penetrating radar. *Geophysical research letters*, *32*(21). https://doi.org/10.1029/2005GL024159

Möhlmann, D. T. F. (2011). Latitudinal distribution of temporary liquid cryobrines on Mars. *Icarus*, *214*(1), 236-239. https://doi.org/10.1016/j.icarus.2011.05.006

Monika, Govil, H., & Thakur, M. (2022). Contribution of L band SAR data for identification of buried/paleochannels in Jaisalmer region of Rajasthan, India. *Advances in Space Research*. https://doi.org/10.1016/j.asr.2022.03.036

Montross, S., Skidmore, M., Christner, B., Samyn, D., Tison, J. L., Lorrain, R., ... & Fitzsimons, S. (2014). Debris-rich basal ice as a microbial habitat, Taylor Glacier, Antarctica. *Geomicrobiology Journal*, *31*(1), 76-81. https://doi.org/10.1080/01490451.2013.811316

Morgan, G. A., Campbell, B. A., Carter, L. M., Plaut, J. J., & Phillips, R. J. (2013). 3D reconstruction of the source and scale of buried young flood channels on Mars. *Science*, *340*(6132), 607-610. https://doi.org/10.1126/science.1234787

Morgan, G. A., Campbell, B. A., Carter, L. M., & Plaut, J. J. (2015). Evidence for the episodic erosion of the Medusae Fossae Formation preserved within the youngest volcanic province on Mars. *Geophysical Research Letters*, *42*(18), 7336-7342. https://doi.org/10.1002/2015GL065017

Morgan, G. A., Putzig, N. E., Perry, M. R., Sizemore, H. G., Bramson, A. M., Petersen, E. I., ... & Campbell, B. A. (2021). Availability of subsurface water-ice resources in the northern mid-latitudes of Mars. *Nature Astronomy*, *5*(3), 230-236. https://doi.org/10.1038/s41550-020-01290-z

Motohka, T., Kankaku, Y., Miura, S., & Suzuki, S. (2019, July). ALOS-4 L-band SAR mission and observation. In *IGARSS 2019-2019 IEEE International Geoscience and Remote Sensing Symposium* (pp. 5271-5273). IEEE. DOI: 10.1109/IGARSS.2019.8898169

Mouginis-Mark, P. J., Zimbelman, J. R., Crown, D. A., Wilson, L., & Gregg, T. K. (2022). Martian volcanism: Current state of knowledge and known unknowns. *Geochemistry*, 125886. https://doi.org/10.1016/j.chemer.2022.125886

Mouginot, J., Pommerol, A., Kofman, W., Beck, P., Schmitt, B., Herique, A., ... & Plaut, J. J. (2010). The 3–5 MHz global reflectivity map of Mars by MARSIS/Mars Express: Implications for the current inventory of subsurface H_2O. *Icarus*, *210*(2), 612-625. https://doi.org/10.1016/j.icarus.2010.07.003.

Muhleman, D.O., Berge, G.L. (1991). Observations of Mars, Uranus, Neptune, Io, Europa, Ganymede, and Callisto at a wavelength of 2.66mm, *Icarus, 92,* 263-272, https://doi.org/10.1016/0019-1035(91)90050-4

Mustard, J. F., Cooper, C. D., & Rifkin, M. K. (2001). Evidence for recent climate change on Mars from the identification of youthful near-surface ground ice. *Nature*, *412*(6845), 411-414. https://doi.org/10.1038/35086515

Mustard, J. F., Murchie, S. L., Pelkey, S. M., Ehlmann, B. L., Milliken, R. E., Grant, J. A., ... & Wolff, M. (2008). Hydrated silicate minerals on Mars observed by the Mars Reconnaissance Orbiter CRISM instrument. *Nature*, *454*(7202), 305-309. https://doi.org/10.1038/nature07097

Mykytczuk, N., Foote, S. J., Omelon, C. R., Southam, G., Greer, C. W., & Whyte, L. G. (2013). Bacterial growth at−15 C; molecular insights from the permafrost bacterium Planococcus halocryophilus Or1. *The ISME journal*, *7*(6), 1211-1226. https://doi.org/10.1038/ismej.2013.8

NASA (2021, September). HEOMD Strategic Campaign Operations Plan for Exploration (SCOPE). *HEOMD-007*, DAA #20210022080 Retrieved from https://ntrs.nasa.gov/api/citations/20210022080/downloads/HEOMD-007%20HEO%20SCOPE%20-%2009-28-2021%20NTRS.pdf

NASA (2022, January). "Reference Surface Activities for Crewed Mars Mission Systems and Utilization. *HEOMD-415*, DAA #20220000589 Retrieved from https://ntrs.nasa.gov/citations/20220000589

Neish, C. D., Laflèche, É. A., & Patterson, G. W. (2021, March). Physical Properties of Lunar Impact Melt Deposits. In *52nd Lunar and Planetary Science Conference* (No. 2548, p. 1589). Retrieved from: https://www.hou.usra.edu/meetings/lpsc2021/pdf/1589.pdf

Neish, C. D., Hamilton, C. W., Hughes, S. S., Nawotniak, S. K., Garry, W. B., Skok, J. R., ... & Heldmann, J. L. (2017a). Terrestrial analogues for lunar impact melt flows. *Icarus*, *281*, 73-89. https://doi.org/10.1016/j.icarus.2016.08.008

Neish, C. D., Herrick, R. R., Zanetti, M., & Smith, D. (2017b). The role of pre-impact topography in impact melt emplacement on terrestrial planets. *Icarus*, *297*, 240-251. https://doi.org/10.1016/j.icarus.2017.07.004

Neish, C. D., Madden, J., Carter, L. M., Hawke, B. R., Giguere, T., Bray, V. J., ... & Cahill, J. T. S. (2014). Global distribution of lunar impact melt flows. *Icarus*, *239*, 105-117. https://doi.org/10.1016/j.icarus.2014.05.049

Newman, C. E., Lewis, S. R., & Read, P. L. (2005). The atmospheric circulation and dust activity in different orbital epochs on Mars. *Icarus, 174*(1), 135-160. https://doi.org/10.1016/j.icarus.2004.10.023

Niederberger, T. D., Perreault, N. N., Tille, S., Lollar, B. S., Lacrampe-Couloume, G., Andersen, D., ... & Whyte, L. G. (2010). Microbial characterization of a subzero, hypersaline methane seep in the Canadian High Arctic. *The ISME journal*, *4*(10), 1326-1339. https://doi.org/10.1038/ismej.2010.57

Nowicki, S. A., & Christensen, P. R. (2007). Rock abundance on Mars from the thermal emission spectrometer. *Journal of Geophysical Research: Planets*, *112*(E5). https://doi.org/10.1029/2006JE002798

Nuding, D., Rivera-Valentin, E. G., Davis, R. D., Gough, R. V., Chevrier, V. F., & Tolbert, M. A. (2014). Deliquescence and efflorescence of calcium perchlorate: An investigation of stable aqueous solutions relevant to Mars. *Icarus*, *243*, 420-428. https://doi.org/10.1016/j.icarus.2014.08.036

Nunes, D. C., Smrekar, S. E., Fisher, B., Plaut, J. J., Holt, J. W., Head, J. W., ... & Phillips, R. J. (2011). Shallow Radar (SHARAD), pedestal craters, and the lost Martian layers: Initial assessments. *Journal of Geophysical Research: Planets, 116*(E4). https://doi.org/10.1029/2010JE003690

Oberbeck, V. R. (1975). The role of ballistic erosion and sedimentation in lunar stratigraphy. *Reviews of Geophysics*, *13*(2), 337-362. https://doi.org/10.1029/RG013i002p00337

Onstott, T. C., Ehlmann, B. L., Sapers, H., Coleman, M., Ivarsson, M., Marlow, J. J., ... & Niles, P. (2019). Paleo-rock-hosted life on Earth and the search on Mars: a review and strategy for exploration. *Astrobiology*, *19*(10), 1230-1262. https://doi.org/10.1089/ast.2018.1960

Orgel, C., Hauber, E., Gasselt, S., Reiss, D., Johnsson, A., Ramsdale, J. D., Smith, I., Swirad, Z. M., Séjourné, A., Wilson, J. T., Balme, M. R., Conway, S. J., Costard, F., Eke, V. R., Gallagher, C., Kereszturi, Á., Łosiak, A., Massey, R. J., Platz, T., … Teodoro, L. F. (2019). Grid mapping the Northern Plains of Mars: A new overview of recent water- and ice-related landforms in Acidalia Planitia. *Journal of Geophysical Research: Planets*, *124*(2), 454–482. https://doi.org/10.1029/2018je005664

Orosei, R., Lauro, S. E., Pettinelli, E., Cicchetti, A., Coradini, M., Cosciotti, B., ... & Seu, R. (2018). Radar evidence of subglacial liquid water on Mars. *Science*, *361*(6401), 490-493. https://doi.org/10.1126/science.aar7268

Osinski, G. R., Tornabene, L. L., & Grieve, R. A. (2011). Impact ejecta emplacement on terrestrial planets. *Earth and Planetary Science Letters*, *310*(3-4), 167-181. https://doi.org/10.1016/j.epsl.2011.08.012

Osterloo, M. M., Hamilton, V. E., Bandfield, J. L., Glotch, T. D., Baldridge, A. M., Christensen, P. R., ... & Anderson, F. S. (2008). Chloride-bearing materials in the southern highlands of Mars. *Science*, *319*(5870), 1651-1654 https://doi.org/10.1126/science.1150690

Owen, T., Biemann, K., Rushneck, D. R., Biller, J. E., Howarth, D. W., & Lafleur, A. L. (1977). The composition of the atmosphere at the surface of Mars. *Journal of Geophysical research*, *82*(28), 4635-4639. https://doi.org/10.1029/JS082i028p04635

Pathare, A. V., Feldman, W. C., Prettyman, T. H., & Maurice, S. (2018). Driven by excess? Climatic implications of new global mapping of near-surface water-equivalent hydrogen on Mars. *Icarus*, *301*, 97-116. https://doi.org/10.1016/j.icarus.2017.09.031

Petersen, E. I., Holt, J. W., & Levy, J. S. (2018). High ice purity of Martian lobate debris aprons at the regional scale: evidence from an orbital radar sounding survey in Deuteronilus and Protonilus Mensae. *Geophysical Research Letters*, *45*(21), 11-595-11,604. https://doi.org/10.1029/2018GL079759

Phillips, R. J., Davis, B. J., Tanaka, K. L., Byrne, S., Mellon, M. T., Putzig, N. E., ... & Seu, R. (2011). Massive CO_2 ice deposits sequestered in the south polar layered deposits of Mars. *Science*, *332*(6031), 838-841. DOI: 10.1126/science.1203091

Piqueux, S., Buz, J., Edwards, C. S., Bandfield, J. L., Kleinböhl, A., Kass, D. M., ... & Themis Teams. (2019). Widespread shallow water ice on Mars at high latitudesand midlatitudes. *Geophysical Research Letters*, *46*(24), 14290-14298. https://doi.org/10.1029/2019GL083947

Piqueux, S., Byrne, S., & Richardson, M. I. (2003). Sublimation of Mars's southern seasonal CO2 ice cap and the formation of spiders. *Journal of Geophysical Research: Planets, 108*(E8). https://doi.org/10.1029/2002JE002007

Piqueux, S., Kleinböhl, A., Hayne, P. O., Kass, D. M., Schofield, J. T., & McCleese, D. J. (2015). Variability of the Martian seasonal CO2 cap extent over eight Mars Years. *Icarus, 251*, 164-180. https://doi.org/10.1016/j.icarus.2014.10.045

Plaut, J. J., Safaeinili, A., Holt, J. W., Phillips, R. J., Head III, J. W., Seu, R., ... & Frigeri, A. (2009). Radar evidence for ice in lobate debris aprons in the mid-northern latitudes of Mars. *Geophysical Research Letters*, *36*(2). https://doi.org/10.1029/2008GL036379

Polkko, J., Hieta, M., Harri, A.-M., Tamppari, L., Martınez, G., Viu dez-Moreiras, D., … & MEDA team. (2022). Initial results of the relative humidity observations by MEDA instrument onboard the Mars 2020 Perseverance Rover. Submitted to *Journal of Geophysical Research: Planets*. Retrieved from: http://www-mars.lmd.jussieu.fr/paris2022/abstracts/poster_Hieta_Maria.pdf

Polsgrove, T. & Dwyer-Cianciolo, A. M. (2016). Human Mars Entry, Descent and Landing Architecture Study Overview. AIAA 2016-5494. *AIAA SPACE 2016*. https://doi.org/10.2514/6.2016-5494

Polsgrove, T. P., Thomas, H. D., Cianciolo, A. D., Collins, T., & Samareh, J. (2017). Mission and design sensitivities for human Mars landers using Hypersonic Inflatable Aerodynamic Decelerators. *IEEE Aerospace Conference*, 1-9, https://doi.org/10.1109/AERO.2017.7943887

Polyak, V. J., & Provencio, P. P. (2006). Protecting lava tube caves. In Hildreth-Werker, V., & J.C. Werker, (Eds.) *Cave Conservation and Restoration*. Huntsville, Alabama: National Speleological Society, pp. 133-140.

Portyankina, G., Hansen, C. J., & Aye, K. M. (2017). Present-day erosion of Martian polar terrain by the seasonal CO_2 jets. *Icarus*, *282*, 93-103. https://doi.org/10.1016/j.icarus.2016.09.007

Putzig, N. E., & Mellon, M. T. (2007a). Thermal behavior of horizontally mixed surfaces on Mars. *Icarus*, *191*(1), 52-67. https://doi.org/10.1016/j.icarus.2007.03.022

Putzig, N. E., & Mellon, M. T. (2007b). Apparent thermal inertia and the surface heterogeneity of Mars. *Icarus*, *191*(1), 68-94. https://doi.org/10.1016/j.icarus.2007.05.013

Putzig, N. E., Mellon, M. T., Kretke, K. A., & Arvidson, R. E. (2005). Global thermal inertia and surface properties of Mars from the MGS mapping mission. *Icarus*, *173*(2), 325-341. https://doi.org/10.1016/j.icarus.2004.08.017

Putzig, N.E., Morgan, G.A., Sizemore, H.G., Baker, D.M.H., Petersen, E.I., Pathare, A.V., …& Smith, I.B. (2022; In Press), Ice Resource Mapping on Mars. Chapter 16 in Badescu, V., Zacny, K., Bar-Cohen, Y. (Eds.), *Handbook of Space Resources*, Springer Nature Switzerland AG. Retrieved from: https://nathaniel.putzig.com/publications.htm

Putzig, N. E., Phillips, R. J., Campbell, B. A., Holt, J. W., Plaut, J. J., Carter, L. M., ... & Seu, R. (2009). Subsurface structure of Planum Boreum from Mars Reconnaissance Orbiter shallow radar soundings. *Icarus*, 204(2), 443-457.

Raack, J., Conway, S. J., Herny, C., Balme, M. R., Carpy, S., & Patel, M. R. (2017). Water induced sediment levitation enhances downslope transport on Mars. *Nature communications*, *8*(1), 1-10. https://doi.org/10.1038/s41467-017-01213-z

Ramsdale, J. D., Balme, M. R., Gallagher, C., Conway, S. J., Smith, I. B., Hauber, E., ... & Wilson, J. T. (2019). Grid Mapping the Northern Plains of Mars: Geomorphological, Radar, and Water-Equivalent Hydrogen Results From Arcadia Plantia. *Journal of Geophysical Research: Planets, 124*(2), 504-527. https://doi.org/10.1029/2018JE005663

Raney, R.K., Brisco, B., Dabboor, M., Mahdianpari, M. (2021). RADARSAT Constellation Mission's Operational Polarimetric Modes: A User-Driven Radar Architecture. *Canadian Journal of Remote Sensing, 47*, 1–16. https://doi.org/10.1080/07038992.2021.1907566

Raney, R.K., Cahill, J.T.S., Patterson, G.W., Bussey, D.B.J. (2012). The m-chi decomposition of hybrid dual-polarimetric radar data with application to lunar craters. *Journal of Geophysical Research: Planets, 117*. https://doi.org/10.1029/2011JE003986

Read, W. G., Tamppari, L. K., Livesey, N. J., Clancy, R. T., Forget, F., Hartogh, P., ... & Chattopadhyay, G. (2018). Retrieval of wind, temperature, water vapor and other trace constituents in the Martian Atmosphere. *Planetary and Space Science*, *161*, 26-40. https://doi.org/10.1016/j.pss.2018.05.004

Rennó, N. O., Bos, B. J., Catling, D., Clark, B. C., Drube, L., Fisher, D., ... & Young, S. M. (2009). Possible physical and thermodynamical evidence for liquid water at the Phoenix landing site. *Journal of Geophysical Research: Planets*, *114*(E1). https://doi.org/10.1029/2009JE003362

Rivera-Valentín, E. G., Meyer, H. M., Taylor, P. A., Mazarico, E., Bhiravarasu, S. S., Virkki, A. K., ... & Giorgini, J. D. (2022). Arecibo S-band Radar Characterization of Local-scale Heterogeneities within Mercury's North Polar Deposits. *The Planetary Science Journal*, *3*(3), 62. https://doi.org/10.3847/PSJ/ac54a0

Roberts, G. P., Matthews, B., Bristow, C., Guerrieri, L., & Vetterlein, J. (2012). Possible evidence of paleomarsquakes from fallen boulder populations, Cerberus Fossae, Mars. *Journal of Geophysical Research: Planets*, *117*(E2). https://doi.org/10.1029/2011JE003816

Roberts, W. A. (1966). Shock—A process in extraterrestrial sedimentology. *Icarus, 5*(1-6), 459-477. https://doi.org/10.1016/0019-1035(66)90059-5

Rodin, A., Vinogradov, I., Zenevich, S., Spiridonov, M., Gazizov, I., Kazakov, V., ... & Korablev, O. (2020). Martian multichannel diode laser spectrometer (M-dls) for in-situ atmospheric composition measurements on mars onboard exomars-2022 landing platform. *Applied Sciences*, *10*(24), 8805. https://doi.org/10.3390/app10248805

Rodriguez Sanchez-Vahamonde, C., & Neish, C. (2021). The Surface Texture of Martian Lava Flows as Inferred from Their Decimeter-and Meter-scale Roughness. *The Planetary Science Journal*, *2*(1), 15. http://dx.doi.org/10.3847/PSJ/abbfac Rouyet, L., Lauknes, T. R., Christiansen, H. H., Strand, S. M., & Larsen, Y. (2019). Seasonal dynamics of a permafrost landscape, Adventdalen, Svalbard, investigated by InSAR. *Remote Sensing of Environment*, *231*, 111236. https://doi.org/10.1016/j.rse.2019.111236

Rouyet, L., Lauknes, T. R., Christiansen, H. H., Strand, S. M., & Larsen, Y. (2019). Seasonal dynamics of a permafrost landscape, Adventdalen, Svalbard, investigated by InSAR. *Remote Sensing of Environment, 231*, 111236. https://doi.org/10.1016/j.rse.2019.111236

Rubin, M., Altwegg, K., Balsiger, H., Bar-Nun, A., Berthelier, J. J., Briois, C., ... & Wurz, P. (2018). Krypton isotopes and noble gas abundances in the coma of comet 67P/Churyumov-Gerasimenko. *Science advances*, *4*(7), eaar6297. https://doi.org/10.1126/sciadv.aar6297

Rummel, J. D., Beaty, D. W., Jones, M. A., Bakermans, C., Barlow, N. G., Boston, P. J., ... & Wray, J. J. (2014). A new analysis of Mars "special regions": findings of the second MEPAG Special Regions Science Analysis Group (SR-SAG2). *Astrobiology 14*, 887–968. https://doi.org/10.1089/ast.2014.1227

Russell, P., Thomas, N., Byrne, S., Herkenhoff, K., Fishbaugh, K., Bridges, N., ... & McEwen, A. (2008). Seasonally active frost-dust avalanches on a north polar scarp of Mars captured by HiRISE. *Geophysical Research Letters*, *35*(23). https://doi.org/10.1029/2008GL035790

Rutishauser, A., Blankenship, D. D., Sharp, M., Skidmore, M. L., Greenbaum, J. S., Grima, C., ... & Young, D. A. (2018). Discovery of a hypersaline subglacial lake complex beneath Devon Ice Cap, Canadian Arctic. *Science Advances*, *4*(4), eaar4353. https://doi.org/10.1126%2Fsciadv.aar4353

Sacks, L. E., Tornabene, L. L., Osinski, G. R., & Sopoco, R. (2022). Hargraves Crater, Mars: Insights into the internal structure of layered ejecta deposits. *Icarus*, *375*, 114854. https://doi.org/10.1016/j.icarus.2021.114854

Safaeinili, A., Kofman, W., Mouginot, J., Gim, Y., Herique, A., Ivanov, A. B., ... & Picardi, G. (2007). Estimation of the total electron content of the Martian ionosphere using radar sounder surface echoes. *Geophysical Research Letters*, 34(23). https://doi.org/10.1029/2007GL032154

Sakai, S., Seki, K., Terada, N., Shinagawa, H., Sakata, R., Tanaka, T., & Ebihara, Y. (2021). Effects of the IMF Direction on Atmospheric Escape From a Mars-like Planet Under Weak Intrinsic Magnetic Field Conditions. *Journal of Geophysical Research: Space Physics*, *126*(3), e2020JA028485. https://doi.org/10.1029/2020JA028485

Sakata, R., Seki, K., Sakai, S., Terada, N., Shinagawa, H., & Tanaka, T. (2020). Effects of an intrinsic magnetic field on ion loss from ancient Mars based on multispecies MHD simulations. *Journal of Geophysical Research: Space Physics*, *125*(2). https://doi.org/10.1029/2019JA026945

Sánchez–Cano, B., Blelly, P. L., Lester, M., Witasse, O., Cartacci, M., Orosei, R., ... & Kopf, A. J. (2019). Origin of the extended Mars radar blackout of September 2017. *Journal of Geophysical Research: Space Physics*, *124*(6), 4556-4568. https://doi.org/10.1029/2018JA026403

Sato, H., Kim, J. S., Otsuka, Y., Wrasse, C. M., Rodrigues de Paula, E., & Rodrigues de Souza, J. (2021). L-Band Synthetic Aperture Radar Observation of Ionospheric Density Irregularities at Equatorial Plasma Depletion Region. *Geophysical Research Letters*, *48*(16), e2021GL093541. https://doi.org/10.1029/2021GL093541

Savijärvi, H., Harri, A. M., & Kemppinen, O. (2016). The diurnal water cycle at Curiosity: Role of exchange with the regolith. *Icarus*, *265*, 63-69. https://doi.org/10.1016/j.icarus.2015.10.008

Scanlon, K. E., Head, J. W., Fastook, J. L., & Wordsworth, R. D. (2018). The Dorsa Argentea formation and the Noachian-Hesperian climate transition. *Icarus*, *299*, 339-363. https://doi.org/10.1016/j.icarus.2017.07.031

Scanlon, K. E., Head, J. W., & Marchant, D. R. (2015). Volcanism-induced, local wet-based glacial conditions recorded in the Late Amazonian Arsia Mons tropical mountain glacier deposits. *Icarus*, *250*, 18-31. https://doi.org/10.1016/j.icarus.2014.11.016

Schaefer, E. I., McEwen, A. S., & Sutton, S. S. (2019). A case study of recurring slope lineae (RSL) at Tivat crater: Implications for RSL origins. *Icarus*, *317*, 621-648. https://doi.org/10.1016/j.icarus.2018.07.014

Schmidt, F., Andrieu, F., Costard, F., Kocifaj, M., & Meresescu, A. G. (2017). Formation of recurring slope lineae on Mars by rarefied gas-triggered granular flows. *Nature Geoscience*, *10*(4), 270-273. https://doi.org/10.1038/ngeo2917

Schneider, N. M., Deighan, J. I., Jain, S. K., Stiepen, A., Stewart, A. I. F., Larson, D., ... & Jakosky, B. M. (2015). Discovery of diffuse aurora on Mars. *Science*, *350*(6261), aad0313. DOI: 10.1126/science.aad0313

Schneider, N. M., Jain, S. K., Deighan, J., Nasr, C. R., Brain, D. A., Larson, D., ... & Jakosky, B. M. (2018). Global aurora on Mars during the September 2017 space weather event. *Geophysical Research Letters*, *45*(15), 7391-7398. https://doi.org/10.1029/2018GL077772

Schneider, N. M., Milby, Z., Jain, S. K., Gérard, J. C., Soret, L., Brain, D. A., ... & Jakosky, B. M. (2021). Discrete Aurora on Mars: Insights into their distribution and activity from MAVEN/IUVS observations. *Journal of Geophysical Research: Space Physics*, 126(10), e2021JA029428. https://doi.org/10.1029/2021JA029428

Schon, S. C., Head, J. W., & Milliken, R. E. (2009). A recent ice age on Mars: Evidence for climate oscillations from regional layering in mid-latitude mantling deposits. *Geophysical Research Letters*, *36*(15). https://doi.org/10.1029/2009GL038554

Schorghofer, N. (2007). Dynamics of ice ages on Mars. *Nature*, *449*(7159), 192-194. https://doi.org/10.1038/nature06082

Schorghofer, N., & Aharonson, O. (2005). Stability and exchange of subsurface ice on Mars. *Journal of Geophysical Research: Planets*, *110*(E5). https://doi.org/10.1029/2004JE002350

Schorghofer, N., Aharonson, O., Gerstell, M. F., & Tatsumi, L. (2007). Three decades of slope streak activity on Mars. *Icarus*, *191*(1), 132-140. https://doi.org/10.1016/j.icarus.2007.04.026

Schorghofer, N., Aharonson, O., & Khatiwala, S. (2002). Slope streaks on Mars: Correlations with surface properties and the potential role of water. *Geophysical Research Letters*, *29*(23), 41-1–41-4. https://doi.org/10.1029/2002GL015889

Schorghofer, N., & Edgett, K. S. (2006). Seasonal surface frost at low latitudes on Mars. *Icarus*, 180(2), 321-334. https://doi.org/10.1016/j.icarus.2005.08.022

Schorghofer, N., & Forget, F. (2012). History and anatomy of subsurface ice on Mars. *Icarus*, 220(2), 1112-1120. https://doi.org/10.1016/j.icarus.2012.07.003

Seibert, N. M., & Kargel, J. S. (2001). Small-scale Martian polygonal terrain: Implications for liquid surface water. Geophysical Research Letters, 28(5), 899-902. https://doi.org/10.1029/2000GL012093

Séjourné, A., Costard, F., Swirad, Z. M., Łosiak, A., Bouley, S., Smith, I., ... & Platz, T. (2019). Grid mapping the Northern Plains of Mars: Using morphotype and distribution of ice-related landforms to understand multiple ice-rich deposits in Utopia Planitia. *Journal of Geophysical Research: Planets*, *124*(2), 483-503. https://doi.org/10.1029/2018JE005665

Seu, R., Phillips, R. J., Biccari, D., Orosei, R., Masdea, A., Picardi, G., ... & Nunes, D. C. (2007). SHARAD sounding radar on the Mars Reconnaissance Orbiter. *Journal of Geophysical Research: Planets*, *112*(E5). https://doi.org/10.1029/2006JE002745

Shi, Y., Zhao, J., Xiao, L., Yang, Y., & Wang, J. (2022). An arid-semiarid climate during the Noachian-Hesperian transition in the Huygens region, Mars: Evidence from morphological studies of valley networks. *Icarus*, *373*, 114789. https://doi.org/10.1016/j.icarus.2021.114789

Shoemaker, E. S., Carter, L. M., Garry, W. B., Morgan, G. A., & Plaut, J. J. (2022). New Insights Into Subsurface Stratigraphy Northwest of Ascraeus Mons, Mars, Using the SHARAD and MARSIS Radar Sounders. *Journal of Geophysical Research: Planets*, 127(6), e2022JE007210. https://doi.org/10.1029/2022JE007210

Sibille, L., Moses, R. W., Mueller, R. P., Viotti, M. A., Munk, M. M., & van Susante, P. J. (2021). Mars Reconnaissance: Civil Engineering Advances for Human Exploration. *Planetary/Astrobiology Decadal Survey Whitepapers*, *53*(4). Retrieved from: https://digitalcommons.mtu.edu/michigantech-p/15787

Siegler, M. A., Feng, J., Lucey, P. G., Ghent, R. R., Hayne, P. O., & White, M. N. (2020). Lunar titanium and frequency-dependent microwave loss tangent as constrained by the Chang'E-2 MRM and LRO diviner lunar radiometers. *Journal of Geophysical Research: Planets*, *125*(9), e2020JE006405. https://doi.org/10.1029/2020JE006405

Siegler, M. A., White, M. N., Brovoll, S., Hamran, S., Russell, P., Mellon, M., ... & Martinez, G. (2022). Passive Radiometry of Subsurface Temperatures Using the Mars 2020 Rimfax Instrument. *LPI Contributions*, *2678*, 1491. Retrieved from: https://www.hou.usra.edu/meetings/lpsc2022/pdf/1491.pdf

Silvestro, S., Chojnacki, M., Vaz, D. A., Cardinale, M., Yizhaq, H., & Esposito, F. (2020). Megaripple migration on Mars. *Journal of Geophysical Research: Planets*, *125*(8), e2020JE006446. https://doi.org/10.1029/2020JE006446

Sizemore, H. G., Mellon, M. T., Searls, M. L., Lemmon, M. T., Zent, A. P., Heet, T. L., ... & Keller, H. U. (2010). In situ analysis of ice table depth variations in the vicinity of small rocks at the Phoenix landing site. *Journal of Geophysical Research: Planets*, *115*(E1). https://doi.org/10.1029/2009JE003414

Slade, M. A., Butler, B. J., & Muhleman, D. O. (1992). Mercury radar imaging: Evidence for polar ice. *Science*, *258*(5082), 635-640. https://doi.org/10.1126/science.258.5082.635

Smith, I. B., Lalich, D. E., Rezza, C., Horgan, B. H. N., Whitten, J. L., Nerozzi, S., & Holt, J. W. (2021). A solid interpretation of bright radar reflectors under the Mars south polar ice. *Geophysical Research Letters*, *48*(15). https://doi.org/10.1029/2021gl093618

Smith, I. B., Schlegel, N. J., Larour, E., Isola, I., Buhler, P. B., Putzig, N. E., & Greve, R. (2022). Carbon dioxide ice glaciers at the south pole of Mars. *Journal of Geophysical Research: Planets, 127*(4), e2022JE007193. https://doi.org/10.1029/2022JE007193

Smith, P. H., Tamppari, L. K., Arvidson, R. E., Bass, D., Blaney, D., Boynton, W. V., ... & Zent, A. P. (2009). H_2O at the Phoenix landing site. *Science*, *325*(5936), 58-61. https://doi.org/10.1126/science.1172339

Smith, D. E., Zuber, M. T., Frey, H. V., Garvin, J. B., Head, J. W., Muhleman, D. O., ... & Sun, X. (2001a). Mars Orbiter Laser Altimeter: Experiment summary after the first year of global mapping of Mars. *Journal of Geophysical Research: Planets*, *106*(E10), 23689–23722. https://doi.org/10.1029/2000JE001364

Smith, D. E., Zuber, M. T., & Neumann, G. A. (2001b). Seasonal variations of snow depth on Mars. *Science, 294*(5549), 2141–2146. https://doi.org/10.1126/science.1066556

Sori, M. M., Byrne, S., Hamilton, C. W., & Landis, M. E. (2016). Viscous flow rates of icy topography on the north polar layered deposits of Mars. *Geophysical Research Letters*, *43*(2), 541-549. https://doi.org/10.1002/2015GL067298

Sori, M. M., Byrne, S., & Bramson, A. M. (2017). Present-day flow rates of mid-latitude glaciers on Mars. [Abstract 382]. *European Planetary Science Congress 2017*, *11*, 1-2. Retrieved from: https://meetingorganizer.copernicus.org/EPSC2017/EPSC2017-382.pdf

Sori, M.M., Becerra, P., Bapst, J., Byrne, S., & McGlasson, R. A. (2022), Orbital forcing of Martian climate revealed in a south polar outlier ice deposit, *Geophys. Res. Lett. 49*, e2021GL097450. https://doi.org/10.1029/2021GL097450

Souness, C., Hubbard, B., Milliken, R. E., & Quincey, D. (2012). An inventory and population-scale analysis of martian glacier-like forms. *Icarus, 217*(1), 243-255. https://doi.org/10.1016/j.icarus.2011.10.020

Speyerer, E. J., Povilaitis, R. Z., Robinson, M. S., Thomas, P. C., & Wagner, R. V. (2016). Quantifying crater production and regolith overturn on the Moon with temporal imaging. Nature, 538(7624), 215-218. https://doi.org/10.1038/nature19829

Squyres, S. W. (1978). Martian fretted terrain: Flow of erosional debris. *Icarus*, 34(3), 600-613. https://doi.org/10.1016/0019-1035(78)90048-9

Squyres, S. W. (1979). The distribution of lobate debris aprons and similar flows on Mars. *Journal of Geophysical Research: Solid Earth, 84*(B14), 8087-8096. https://doi.org/10.1029/JB084iB14p08087

Squyres, S. W., Arvidson, R. E., Bell Iii, J. F., Bruckner, J., Cabrol, N. A., Calvin, W., ... & Yen, A. (2004). The Opportunity rover's Athena science investigation at Meridiani Planum, Mars. *Science*, *306*(5702), 1698-1703. https://doi.org/10.1126/science.1106171

Starinsky, A., & Katz, A. (2003). The formation of natural cryogenic brines. *Geochimica et Cosmochimica Acta*, *67*(8), 1475-1484. https://doi.org/10.1016/S0016-7037(02)01295-4

Stibal, M., Šabacká, M., & Žárský, J. (2012). Biological processes on glacier and ice sheet surfaces. *Nature Geoscience*, *5*(11), 771-774. https://doi.org/10.1038/ngeo1611

Stillman, D. E., Bue, B. D., Wagstaff, K. L., Primm, K. M., Michaels, T. I., & Grimm, R. E. (2020). Evaluation of wet and dry recurring slope lineae (RSL) formation mechanisms based on quantitative mapping of RSL in Garni Crater, Valles Marineris, Mars. *Icarus*, *335*, 113420. https://doi.org/10.1016/j.icarus.2019.113420

Stillman, D. E., Grimm, R. E., & Dec, S. F. (2010). Low-Frequency Electrical Properties of Ice−Silicate Mixtures. *The Journal of Physical Chemistry B, 114*(18), 6065-6073. https://doi.org/10.1021/jp9070778

Stillman, D. E., Michaels, T. I., & Grimm, R. E. (2017). Characteristics of the numerous and widespread recurring slope lineae (RSL) in Valles Marineris, Mars. *Icarus*, *285*, 195-210. https://doi.org/10.1016/j.icarus.2016.10.025

Stillman, D. E., Michaels, T. I., Grimm, R. E., & Hanley, J. (2016). Observations and modeling of northern mid-latitude recurring slope lineae (RSL) suggest recharge by a present-day martian briny aquifer. *Icarus*, *265*, 125-138. https://doi.org/10.1016/j.Icarus.2015.10.007

Stillman, D. E., Michaels, T. I., Grimm, R. E., & Harrison, K. P. (2014). New observations of martian southern mid-latitude recurring slope lineae (RSL) imply formation by freshwater subsurface flows. *Icarus*, *233*, 328-341. https://doi.org/10.1016/j.icarus.2014.01.017

Stuurman, C. M., Osinski, G. R., Holt, J. W., Levy, J. S., Brothers, T. C., Kerrigan, M., & Campbell, B. A. (2016). SHARAD detection and characterization of subsurface water ice deposits in Utopia Planitia, Mars. *Geophysical Research Letters*, *43*(18), 9484-9491. https://doi.org/10.1002/(ISSN)1944-8007

Swindle, T. D., Caffee, M. W., & Hohenberg, C. M. (1986). Xenon and other noble gases in shergottites. *Geochimica et Cosmochimica Acta*, *50*(6), 1001-1015. https://doi.org/10.1016/0016-7037(86)90381-9

Tamppari, L. K., N. J. Livesey, W. Read, D. Banfield, B. et al. (2022, June). Testing the efficacy of a Mars submillimeter (submm) sounder for atmospheric measurements. [Abstract]. In *7th Mars Atmosphere Modeling and Observations Conference*. Retrieved from: http://www-mars.lmd.jussieu.fr/paris2022/abstracts/poster_Tamppari_Leslie.pdf

Tamppari, L., Livesey, N. J., Abshire, J. B., Colaprete, A., Diner, D. J., Feldman, S. M., ... & Spiers, G. D. (2018, December). An Assessment of Martian Atmospheric Wind Measurement Techniques: A Workshop Report. In *AGU Fall Meeting Abstracts* (Vol. 2018, pp. P43L-3916). Retrieved from: https://ui.adsabs.harvard.edu/abs/2018AGUFM.P43L3916T/abstract

Tang, I. N., & Munkelwitz, H. R. (1993). Composition and temperature dependence of the deliquescence properties of hygroscopic aerosols. *Atmospheric Environment. Part A. General Topics*, *27*(4), 467-473. https://doi.org/10.1016/0960-1686(93)90204-C

Teehera, K. B., Jungbluth, S. P., Onac, B. P., Acosta-Maeda, T. E., Hellebrand, E., Misra, A. K., ... & Schorghofer, N. (2018). Cryogenic minerals in Hawaiian lava tubes: a geochemical and microbiological exploration. *Geomicrobiology Journal, 35*(3), 227-241. https://doi.org/10.1080/01490451.2017.1362079

Tesson, P. A., Conway, S. J., Mangold, N., Ciazela, J., Lewis, S. R., & Mège, D. (2020). Evidence for thermal-stress-induced rockfalls on Mars impact crater slopes. *Icarus*, *342*. https://doi.org/10.1016/j.icarus.2019.113503

Thomas, N., Hansen, C. J., Portyankina, G., & Russell, P. S. (2010). HiRISE observations of gas sublimation-driven activity in Mars' southern polar regions: II. Surficial deposits and their origins. *Icarus*, *205*(1), 296-310. https://doi.org/10.1016/j.icarus.2009.05.030

Thomas, P. C., James, P. B., Calvin, W. M., Haberle, R., & Malin, M. C. (2009). Residual south polar cap of Mars: Stratigraphy, history, and implications of recent changes. *Icarus*, *203*(2), 352-375. https://doi.org/10.1016/j.icarus.2009.05.014

Thomas, P. C., Calvin, W., Cantor, B., Haberle, R., James, P. B., & Lee, S. W. (2016). Mass balance of Mars' residual south polar cap from CTX images and other data. *Icarus*, *268*, 118-130. https://doi.org/10.1016/j.icarus.2015.12.038

Thomas, P. C., Calvin, W. M., & James, P. B. (2020). Debris accumulations of CO_2 ice in the south polar residual cap of mars: Longevity and processes. *Icarus*, *341*. https://doi.org/10.1016/j.icarus.2020.113625

Thomas, P. C., Calvin, W. M., Gierasch, P., Haberle, R., James, P. B., & Sholes, S. (2013). Time scales of erosion and deposition recorded in the residual south polar cap of Mars. *Icarus*, *225*(2), 923-932. https://doi.org/10.1016/j.icarus.2012.08.038

Titus, T. N., Kieffer, H. H., & Christensen, P. R. (2003). Exposed water ice discovered near the south pole of Mars. *Science*, *299*(5609), 1048-1051. https://doi.org/10.1126/science.1080497

Toigo, A. D., Smith, M. D., Seelos, F. P., & Murchie, S. L. (2013). High spatial and temporal resolution sampling of Martian gas abundances from CRISM spectra. *Journal of Geophysical Research: Planets, 118*(1), 89-104. https://doi.org/10.1029/2012JE004147

Toon, O. B., Pollack, J. B., Ward, W., Burns, J. A., & Bilski, K. (1980). The astronomical theory of climatic change on Mars. *Icarus, 44*(3), 552-607. https://doi.org/10.1016/0019-1035(80)90130-X

Tornabene, L. L., Osinski, G. R., McEwen, A. S., Boyce, J. M., Bray, V. J., Caudill, C. M., ... & Mouginis-Mark, P. J. (2012). Widespread crater-related pitted materials on Mars: Further evidence for the role of target volatiles during the impact process. *Icarus*, *220*(2), 348-368. https://doi.org/10.1016/j.icarus.2012.05.022

Toups, L., Hoffman, S. J., & Watts, K. (2016, March). Mars surface systems common capabilities and challenges for human missions. In *2016 IEEE Aerospace Conference* (pp. 1-18). IEEE. Retrieved from: https://ntrs.nasa.gov/api/citations/20160001039/downloads/20160001039.pdf

Trent, D., Thomas, D., Samareh, J. A., & Dwyer Cianciolo, A. (2021). Mars Entry, Descent, Landing, and Ascent Systems Sensitivities to Landing Site and Atmospheric Dust. In *ASCEND 2021* (p. 4135). https://doi.org/10.2514/6.2021-4135

Vandaele, A. C., Korablev, O., Daerden, F., Aoki, S., Thomas, I. R., Altieri, F., ... & Rodionov, D. (2019). Martian dust storm impact on atmospheric H_2O and D/H observed by ExoMars Trace Gas Orbiter. *Nature*, *568*(7753), 521-525. https://doi.org/10.1038/s41586-019-1097-3

Villanueva, G. L., Mumma, M. J., Novak, R. E., Käufl, H. U., Hartogh, P., Encrenaz, T., Tokunaga, A., Khayat, A., & Smith, M. D. (2015). Strong water isotopic anomalies in the martian atmosphere: probing current and ancient reservoirs. *Science, 348*(6231):218-21. https://doi.org/10.1126/science.aaa3630

Villanueva, G. L., Liuzzi, G., Crismani, M. M. J., Aoki, S., Vandaele, A. C., Daerden, F., Smith, M. D., Mumma, M. J., Knutsen, E. W., Neary, L., Viscardy, S., Thomas, I. R., Lopez-Valverde, M. A., Ristic, B., Patel, M. R., Holmes, J. A., Bellucci, G., Lopez-Moreno, J. J., & NOMAD team. (2021). Water heavily fractionated as it ascends on Mars as revealed by ExoMars/NOMAD. *Science Advances, 7*, eabc8843. https://doi.org/10.1126/sciadv.abc8843

Vincendon, M., Forget, F., & Mustard, J. (2010). Water ice at low to midlatitudes on Mars. *Journal of Geophysical Research: Planets*, *115*(E10). https://doi.org/10.1029/2010JE003584

Viola, D., McEwen, A. S., Dundas, C. M., & Byrne, S. (2015). Expanded secondary craters in the Arcadia Planitia region, Mars: Evidence for tens of Myr-old shallow subsurface ice. *Icarus*, *248*, 190-204. https://doi.org/10.1016/j.icarus.2014.10.032

Wagstaff, K. L., Titus, T. N., Ivanov, A. B., Castaño, R., & Bandfield, J. L. (2008). Observations of the north polar water ice annulus on Mars using THEMIS and TES. *Planetary and Space Science, 56*(2), 256-265. https://doi.org/10.1016/j.pss.2007.08.008

Watters, T. R., Campbell, B., Carter, L., Leuschen, C. J., Plaut, J. J., Picardi, G., ... & Stofan, E. R. (2007). Radar sounding of the Medusae Fossae Formation Mars: Equatorial ice or dry, low-density deposits? *Science, 318*(5853), 1125-1128. https://doi.org/10.1126/science.1148112

Webster, C. R., Mahaffy, P. R., Atreya, S. K., Flesch, G. J., Mischna, M. A., Meslin, P. Y., ... & MSL Science Team. (2015). Mars methane detection and variability at Gale crater. *Science*, *347*(6220), 415-417. https://doi.org/10.1126/science.1261713

Webster, C. R., Mahaffy, P. R., Flesch, G. J., Niles, P. B., Jones, J. H., Leshin, L. A., ... & MSL Science Team. (2013). Isotope ratios of H, C, and O in CO_2 and H_2O of the Martian atmosphere. *Science*, *341*(6143), 260-263. https://doi.org/10.1126/science.1237961

Weiss, B. P., Fong, L. E., Vali, H., Lima, E. A., & Baudenbacher, F. J. (2008). Paleointensity of the ancient Martian magnetic field. *Geophysical Research Letters*, *35*(23). https://doi.org/10.1029/2008GL035585

Weitz, C. M., Wilson, S. A., Grant, J. A., and Irwin, R. P., III. (2022). Geologic map of western Ladon basin, Mars, MTM Quadrangles, -15032 and -20032, USGS Scientific Investigation Map, scale 1:1,000,000. In press.

Wernicke, L. J., & Jakosky, B. M. (2021). Martian hydrated minerals: A significant water sink. *Journal of Geophysical Research: Planets*, *126*(3). https://doi.org/10.1029/2019JE006351

Williams, K. E., Heldmann, J. L., McKay, C. P., & Mellon, M. T. (2018). The effects of snow and salt on ice table stability in University Valley, Antarctica. *Antarctic science*, *30*(1), 67-78. https://doi.org/10.1017/S0954102017000402

Wilson, S. A., J. A. Grant, K. K. Williams. (2022). Geologic map of Morava Valles and Margaritifer basin, Mars, MTM Quadrangles -10022 and -15022, U. S. Geol. Surv. Scientific Investigation Map 3489, scale 1:1,000,000.

Wilson, S. A., Morgan, A. M., Howard, A. D., & Grant, J. A. (2021). The global distribution of craters with alluvial fans and deltas on Mars. *Geophysical Research Letters*, *48*(4). https://doi.org/10.1029/2020GL091653

Wilson, J. T., Eke, V. R., Massey, R. J., Elphic, R. C., Feldman, W. C., Maurice, S., & Teodoro, L. F. (2018). Equatorial locations of water on Mars: Improved resolution maps based on Mars Odyssey Neutron Spectrometer data. *Icarus, 299*, 148-160. https://doi.org/10.1016/j.icarus.2017.07.028

Wordsworth, R. D. (2016). The climate of early Mars. *Annual Review of Earth and Planetary Sciences, 44*, 381-408.

Wordsworth, R., Forget, F., Millour, E., Head, J. W., Madeleine, J. B., & Charnay, B. (2013). Global modelling of the early martian climate under a denser CO_2 atmosphere: Water cycle and ice evolution. *Icarus, 222*(1), 1-19.

Wordsworth, R. D., Kerber, L., Pierrehumbert, R. T., Forget, F., & Head, J. W. (2015). Comparison of "warm and wet" and "cold and icy" scenarios for early Mars in a 3-D climate model. *Journal of Geophysical Research: Planets*, *120*(6), 1201-1219. https://doi.org/10.1002/2015JE004787

Wyrick, D., Ferrill, D. A., Morris, A. P., Colton, S. L., & Sims, D. W. (2004). Distribution, morphology, and origins of Martian pit crater chains. *Journal of Geophysical Research: Planets, 109*(E6). https://doi.org/10.1029/2004JE002240

Xiao, H., Stark, A., Schmidt, F., Hao, J., Su, S., Steinbrügge, G., & Oberst, J. (2022). Spatio-temporal level variations of the Martian Seasonal South Polar Cap from co-registration of MOLA profiles. *Journal of Geophysical Research: Planets.* https://doi.org/10.1029/2022JE007196

Yingling, W.A. (2020). Impact Melt-Bearing Deposits Around Martian Craters. MSc Thesis, The University of Western Ontario. Retrieved from https://www.hou.usra.edu/meetings/lpsc2020/pdf/2672.pdf

Zanetti, M., Hiesinger, H., Reiss, D., Hauber, E., & Neukum, G. (2010). Distribution and evolution of scalloped terrain in the southern hemisphere, Mars. *Icarus*, *206*(2), 691-706. https://doi.org/10.1016/j.icarus.2009.09.010

Zebker, H. A., Rosen, P., Hensley, S., & Mouginis-Mark, P. J. (1996). Analysis of active lava flows on Kilauea volcano, Hawaii, using SIR-C radar correlation measurements. *Geology*, *24*(6), 495-498. https://doi.org/10.1130/0091-7613(1996)024%3C0495:AOALFO%3E2.3.CO;2

Zorzano, M. P., Mateo-Martí, E., Prieto-Ballesteros, O., Osuna, S., & Renno, N. (2009). Stability of liquid saline water on present day Mars. *Geophysical Research Letters*, *36*(20). https://doi.org/10.1029/2009gl040315

Zhou, X., Chang, N. B., & Li, S. (2009). Applications of SAR Interferometry in Earth and Environmental Science Research. Sensors (Basel, Switzerland), 9(3), 1876–1912. https://doi.org/10.3390/s90301876

Zuber, M. T., Smith, D. E., Solomon, S. C., Abshire, J. B., Afzal, R. S., Aharonson, O., ... & Duxbury, T. C. (1998). Observations of the north polar region of Mars from the Mars Orbiter Laser Altimeter. *Science*, *282*(5396), 2053-2060. https://doi.org/10.1126/science.282.5396.2053

INTERNATIONAL MARS ICE MAPPER MISSION

The International Mars Ice Mapper (I-MIM) mission concept is being developed by a multilateral team of space agencies from five countries: Canada, Italy, Japan, the Netherlands, and the United States. I-MIM's primary goal is to map and to characterize accessible, near-surface (uppermost 10 m) water ice and its overburden in mid-to-low latitudes to support planning for the first potential human surface missions to Mars. To maximize return on investment in the mission, the Agencies are committed to additional scientific investigations planetwide, with priorities guided by the participating international scientific community, including this MDT.